

Three-point functions in the SU(2) sector at strong coupling

YOICHI KAZAMA[†] AND SHOTA KOMATSU[‡]

*Institute of Physics, University of Tokyo,
Komaba, Meguro-ku, Tokyo 153-8902 Japan*

Abstract

Extending the methods developed in our previous works ([1110.3949](#), [1205.6060](#)), we compute the three-point functions at strong coupling of the non-BPS states with large quantum numbers corresponding to the composite operators belonging to the so-called SU(2) sector in the $\mathcal{N} = 4$ super-Yang-Mills theory in four dimensions. This is achieved by the semi-classical evaluation of the three-point functions in the dual string theory in the $AdS_3 \times S^3$ spacetime, using the general one-cut finite gap solutions as the external states. In spite of the complexity of the contributions from various parts in the intermediate stages, the final answer for the three-point function takes a remarkably simple form, exhibiting the structure reminiscent of the one obtained at weak coupling. In particular, in the Frolov-Tseytlin limit the result is expressed in terms of markedly similar integrals, however with different contours of integration. We discuss a natural mechanism for introducing additional singularities on the worldsheet without affecting the infinite number of conserved charges, which can modify the contours of integration.

[†]kazama@hep1.c.u-tokyo.ac.jp

[‡]skomatsu@hep1.c.u-tokyo.ac.jp

Contents

1	Introduction	4
1.1	Introduction and motivation	4
1.2	Preview and the main result	6
1.2.1	The set-up	6
1.2.2	Evaluation of the contribution of the action	8
1.2.3	Evaluation of the contribution of the vertex operators	10
1.2.4	Final result for the three-point function	12
2	String in $EAdS_3 \times S^3$ and classical solutions	14
2.1	String in $EAdS_3 \times S^3$ spacetime	14
2.1.1	Preliminaries	14
2.1.2	Sigma model formulation	16
2.1.3	Pohlmeyer reduction for a string in S^3	19
2.2	One-cut finite gap solutions in S^3	21
2.2.1	Basic one-cut solution and “reconstruction” formula	21
2.2.2	One-cut solutions from multi-cut solutions	25
2.3	Some properties of the eigenvectors of the monodromy matrix	28
3	Structures of the action for the S^3 part	30
3.1	Contour integral representation of the action	30
3.2	WKB expansions of the auxiliary linear problem	36
3.3	The action in terms of the Wronskians	38
4	Structure of the contribution from the vertex operators	39
4.1	Basic idea and framework	39
4.2	Characterization of the gauge theory operators by symmetry properties	43
4.3	Wave functions for the S^3 part	47
4.3.1	Symmetry structure of the vertex operators and the classical solutions	47
4.3.2	Construction of the wave function for the right sector	50
4.3.3	Contribution of the left sector and complete wave function for the S^3 part	54
4.3.4	Correspondence with the gauge theory side	56
5	Evaluation of the Wronskians	58
5.1	Products of Wronskians in terms of quasi-momenta	58
5.2	Analytic properties of the Wronskians I: Poles	60
5.3	Analytic properties of the Wronskians II: Zeros	62
5.3.1	WKB approximation and WKB curves	63
5.3.2	Exact WKB curves	64
5.3.3	Determination of the zeros of the Wronskians	70
5.4	Individual Wronskian from the Wiener-Hopf decomposition	72
5.4.1	Separation of the poles	74
5.4.2	Separation of the zeros	75

5.5	Singular part and constant part of the Wronskians	79
6	Complete three-point functions at strong coupling	82
6.1	The S^3 part	82
6.1.1	Contributions from the convolution integrals	83
6.1.2	Contributions from the singular part of the Wronskians	85
6.1.3	Result for the S^3 part	87
6.2	The $EAdS_3$ part	88
6.2.1	Contribution from the action	88
6.2.2	Contribution from the wave function	89
6.2.3	Total contribution from the $EAdS_3$ part	92
6.3	Complete expression for the three-point function	92
7	Examples and comparison with the weak coupling result	93
7.1	Basic set-up	94
7.2	Case of three BPS operators	95
7.3	Limit producing two-point function	99
7.4	Case of one non-BPS and two BPS operators	100
7.5	Frolov-Tseytlin limit and comparison with the weak coupling result	105
7.5.1	Frolov-Tseytlin limit of the three-point function	105
7.5.2	A mechanism for modifying the contours	107
8	Discussions	108
A	Details on the one-cut solutions	110
A.1	Parameters of one-cut solutions in terms of the position of the cut	110
A.2	Pohlmeyer reduction for one-cut solutions	112
A.3	Computation of various integrals	113
B	Pohlmeyer reduction	114
C	Relation between the Pohlmeyer reduction and the sigma model formulation	116
C.1	Reconstruction formula for the Pohlmeyer reduction	116
C.2	Relation between the connections and the eigenvectors	117
D	Details of the WKB expansion	119
D.1	Direct expansion of the solutions to the ALP	119
D.2	Born series expansion of the Wronskians	121

1 Introduction

1.1 Introduction and motivation

After more than fifteen years since the advent of the AdS/CFT correspondence [1–3], we now have a large number of examples of this type of duality in various dimensions. In the majority of these examples, the bulk and the boundary theories share the same (super)conformal symmetry, showing the obvious importance of such a symmetry. On the other hand, the behaviors of the theories in each specific correspondence are actually rather different, especially in different dimensions. This evidently is due to different dynamics and it in turn urges us to understand the common dynamical structure at the root of the duality which is represented in different fashions in the bulk and on the boundary in various examples.

With such a purpose in mind, in this article we shall study the three point functions of certain semiclassical non-BPS states in the strong coupling regime in the context of the duality between the string theory in $AdS_5 \times S^5$ and the $\mathcal{N} = 4$ super Yang-Mills theory in four dimensions. More specifically, we will deal with the string theory in the $EAdS_3 \times S^3$ subspace, where $EAdS_3$ stands for the Euclidean AdS_3 . It should be dual to the so-called $SU(2)$ sector¹ of the super Yang-Mills theory. This should certainly be of great interest in view of the fact that the results for the corresponding quantities at weak coupling have recently become available [4–7]. Detailed comparison of the results in two regimes may allow us to identify the common non-trivial structure beyond kinematics.

As it will be evident, the computation of the three-point functions of non-BPS states in string theory in a curved spacetime is quite non-trivial even at the leading semi-classical level. In the first of such attempts [8], the contribution from the AdS_2 part was evaluated for the string in $AdS_2 \times S^k$, where the string is assumed to be rotating only in S^k . Since the contribution from the sphere part was not computed in [8], the complete answer for the three-point function was not given. In this context, our present work can be regarded as (the extended version of) the completion of the work initiated by [8].

At about the same time, computation of the three-point functions for different type of heavy external states was attempted by the present authors [9]. We took as the external states the so-called Gubser-Klebanov-Polyakov (GKP) strings [10] spinning within AdS_3 with large spins. In this work, the contribution to the three-point function from the action evaluated on the saddle point configuration was computed by a method similar to the one in [8]. However, unlike the case of [8], the GKP string is not point-like on the boundary, and hence the contributions from the non-trivial vertex operators were

¹Actually the global symmetry of this sector is $SO(4) = SU(2) \times SU(2)$, as we will emphasize later.

needed to give the complete answer. Since the precise form of such vertex operators were not known, again the computation had to be left unfinished. This difficulty was later overcome by the development of a new integrability-based method built on the state-operator correspondence and the contribution of the non-trivial wave functions of the external states was obtained [11]. Combined with the contribution from the action evaluated previously, this gave the full answer for the three-point function of the GKP strings in the large spin limit [11].

These works paved the way for the present investigation for more general external states in the product space $EAdS_3 \times S^3$. However, the applications of our general methods developed in [9, 11] to the present case are not quite straightforward. One difficulty is that the external states in the S^3 sector, which are taken to be general one-cut finite gap solutions [12–15] for the purpose of making comparison with the weak coupling result, are much more structured than the large spin limit of the GKP solutions. In particular, this makes the analysis of the analyticity property of the basic quantities on the spectral curve considerably more complex. Another new ingredient concerns the logic of the determination of the internal wave functions for the S^3 sector, which look rather different from those for the AdS part. For the AdS part, the wave functions explicitly depend on the positions on the boundary at which the external string states land and the form of the dependence is well-known from the conformal symmetry, namely the appropriate power of the difference of these positions. For the S^3 part, such landing positions do not exist and one must reconsider how to determine the proper wave functions. We shall develop a unified method with which one can construct the wave function for a string in a general spacetime. Moreover, our method cleanly factorizes the kinematical and the dynamical contributions to the wave functions. This feature is important both conceptually and practically. Also, it should be mentioned that this is the first time where we have to combine the contributions from the two different sectors, S^3 and $EAdS_3$, which nevertheless are interconnected through the Virasoro constraints. We shall see that when these contributions are put together, considerable simplifications occur, showing the intimate interrelation between them, as expected.

The end result of our rather involved computation is a remarkably simple formula for the three-point function, which exhibits intriguing features. First, one recognizes the expressions to be quite analogous to those that appear in the weak coupling result, even before taking any special limits. A priori it is not obvious why the result in the strong coupling limit should resemble the weak coupling answer so closely. This resemblance becomes more conspicuous upon taking the so-called Frolov-Tseytlin limit, where the angular momentum J for the S^3 rotation is quite large so that the ratio $\sqrt{\lambda}/J$, where λ is the 't Hooft coupling, is small. In this limit the integrands of the integrals expressing

the answer become almost identical. However, the integration contours do not quite match. This is not immediately a contradiction since there is no rigorous argument why three-point functions should agree exactly in that limit. Nevertheless, it is of interest to look for a possible mechanism to modify the contours. One important fact to be noted in this regard is that, in addition to the ordinary one-cut solutions we used for our external states, there exist different types of one-cut solutions which can be obtained by taking certain degeneration limits of multi-cut solutions. Since the values of the infinite number of conserved charges do not change in this limiting procedure, these solutions should be considered on equal footing with the corresponding ordinary one-cut solutions. The important difference, however, is that such a “degenerate solution” has one or more additional singularities on the worldsheet. Since the determination of the contours of integration depends crucially on the analytic structure of the saddle point configuration, this phenomenon provides an example of a natural mechanism by which the contour of integration in the formula for the three-point function can be modified. This issue, however, should be studied further in future investigations.

Now as this article has become rather lengthy due to various steps of somewhat involved analyses, it should be helpful to give a brief preview of the basic procedures and exhibit the main result. The next subsection will be devoted to this purpose.

1.2 Preview and the main result

1.2.1 The set-up

The three-point function we wish to compute in the semi-classical approximation has the following structure:

$$G(x_1, x_2, x_3) = e^{-S[X_*]_\epsilon} \prod_{i=1}^3 \mathcal{V}_i[X_*; x_i, Q_i]_\epsilon. \quad (1.1)$$

It consists of the contribution of the action and that of the vertex operators, evaluated on the saddle point configuration denoted by X_* . The subscript ϵ signifies a small cut-off which regulates the divergences contained in S and \mathcal{V}_i . As we shall show, these divergences cancel against each other and the total three-point function is completely finite. The vertex operator $\mathcal{V}_i[X_*; x_i, Q_i]_\epsilon$ is assumed to carry a large charge Q_i of order $O(\sqrt{\lambda})$ and is located at x_i on the boundary of the AdS space.

In the case of a string in $EAdS_3 \times S^3$, the action and the vertex operators are split into the $EAdS_3$ part and the S^3 part. Their contributions are connected solely through the Virasoro constraint $T(z)_{EAdS_3} + T(z)_{S^3} = 0$ (and its anti-holomorphic counterpart). In the semi-classical approximation, an external state is characterized by the asymptotic

behavior of a classical solution, which should be the saddle point configuration for its two-point function. However, conformally invariant vertex operator which creates such a state is practically impossible to construct at present. Moreover, even if one had the vertex operator, it is of no use since the explicit saddle point solution X_* on which to evaluate the vertex operator (and the action) cannot be obtained by existing technology.

Such difficulties, although seemingly insurmountable, can be overcome with the aid of the integrable and analytic structure of the system. For this purpose, it is convenient to formulate the string theory in question as a non-linear sigma model. Since the treatment of the S^3 part and the $EAdS_3$ part are essentially the same in this regard, we shall focus primarily on the S^3 part in this summary. The basic information is then contained in the right-current $j \equiv \mathbb{Y}^{-1}d\mathbb{Y}$ and the left-current $l \equiv d\mathbb{Y}\mathbb{Y}^{-1}$, where \mathbb{Y} is the 2×2 matrix with unit determinant composed of the embedding coordinates Y^I ($I = 1, 2, 3, 4$) of S^3 in the manner

$$\mathbb{Y} = \begin{pmatrix} Z_1 & Z_2 \\ -\bar{Z}_2 & \bar{Z}_1 \end{pmatrix}, \quad Z_1 = Y^1 + iY^2, \quad Z_2 = Y^3 + iY^4. \quad (1.2)$$

\mathbb{Y} transforms under the global symmetry group $SO(4) = SU(2)_L \times SU(2)_R$ as $\mathbb{Y} \rightarrow V_L \mathbb{Y} V_R$, with $V_L \in SU(2)_L$, $V_R \in SU(2)_R$. The equation of motion for Y^I can then be expressed in the Lax form, with the complex spectral parameter x , as

$$\begin{aligned} [\partial + \mathcal{J}_z^r, \bar{\partial} + \mathcal{J}_{\bar{z}}^r] &= 0, \\ \mathcal{J} &= \mathcal{J}_z^r dz + \mathcal{J}_{\bar{z}}^r d\bar{z}, \quad \mathcal{J}_z^r = \frac{j_z}{1-x}, \quad \mathcal{J}_{\bar{z}}^r = \frac{j_{\bar{z}}}{1+x}, \end{aligned} \quad (1.3)$$

which makes the classical integrability of the system manifest. The information of the infinite number of conserved charges is encoded in the monodromy matrix $\Omega(x) = \text{P exp}(-\oint \mathcal{J}(x))$, the eigenvalues of which are given by $\Omega(x) \sim \text{diag}(e^{ip(x)}, e^{-ip(x)})$, where $p(x)$ is the quasi-momentum. One can then define the spectral curve Γ by $\det(y\mathbf{1} - \Omega(x)) = 0$, which describes a two-sheeted Riemann surface in the variable x with a number of cuts with additional singularities. To each such curve corresponds a classical “finite gap solution” [12–15], which can be constructed in terms of the solutions of the so-called (right and left) auxiliary linear problems, to be abbreviated as ALP throughout, given by

$$(i) \quad \left(\partial + \frac{j_z}{1-x} \right) \psi = 0, \quad \left(\bar{\partial} + \frac{j_{\bar{z}}}{1+x} \right) \psi = 0, \quad (1.4)$$

$$(ii) \quad \left(\partial + \frac{x l_z}{1-x} \right) \tilde{\psi} = 0, \quad \left(\bar{\partial} - \frac{x l_{\bar{z}}}{1+x} \right) \tilde{\psi} = 0. \quad (1.5)$$

The solutions ψ and $\tilde{\psi}$ are expressed in terms of the Riemann theta functions and the exponential functions, which depend on the data of the curve such as the location of the branch points and other singularities. We will be interested in the “one-cut solution”,

the curve for which has a single square root branch cut of finite size², since the vertex operators producing such solutions should correspond to the composite operators in the SU(2) sector in $\mathcal{N} = 4$ super Yang-Mills theory.

Now with this setup, let us sketch how one can compute the three point functions with the above one-cut solutions³ as external legs.

1.2.2 Evaluation of the contribution of the action

First consider the evaluation of the action part. As described in [9] for the GKP string and will be detailed for the case of our interest, the action integral can be written in the form $S \sim \int_{\tilde{\Sigma}} \varpi \wedge \eta$, where ϖ and η are, respectively a holomorphic 1-form and a closed 1-form defined on the double cover $\tilde{\Sigma}$ of the worldsheet. By using the Stokes theorem, this can be rewritten as a contour integral $S \sim \int_{\partial\tilde{\Sigma}} \Pi \eta$, where $\partial\tilde{\Sigma}$ is the boundary of $\tilde{\Sigma}$ and the function $\Pi = \int^z \varpi$ is single-valued on $\tilde{\Sigma}$. This expression for the action can be further rewritten, using a generalization of the Riemann bilinear identity developed in [9], into a sum of products of certain contour integrals. The important point is that the contours of these integrals interconnect the vertex insertion points z_1, z_2, z_3 , thereby correlating the behaviors around these points. Therefore, to compute the integral it is natural to study the behavior of the eigenfunctions of the ALP around z_i and more importantly along the paths connecting z_i and z_j .

Although we do not know the exact saddle point solution for the three-point function, we do know the behavior in the vicinity of each z_i since it should be the same as the one-cut solution discussed above. This provides the form of the currents needed to analyze the ALP around z_i . Clearly there are two independent solutions around each z_i and one can compute the local monodromy matrix Ω_i belonging to SL(2,C), which mixes these solutions upon going around z_i . Then one can take the basis of the solutions of ALP at z_i to be the eigenvectors of Ω_i , denoted by i_{\pm} , belonging to the eigenvalues $e^{\pm ip_i(x)}$ of Ω_i . These eigenvectors are normalized⁴ with respect to the SL(2,C) invariant product $\langle \psi, \chi \rangle \equiv \det(\psi, \chi)$, to be referred to as Wronskian throughout this article, as $\langle i_+, i_- \rangle = 1$.

To gain information about the solution of ALP valid in the entire worldsheet, one can make the ‘‘WKB expansion’’ with $\zeta = (1-x)/(1+x)$ as the small parameter corresponding to \hbar . One then finds that the same contour integrals with which the action is expressed appear in the WKB expansion of the Wronskians $\langle i_{\pm}, j_{\pm} \rangle$. Therefore our task is reduced

²As already mentioned in the introduction, this class can contain solutions which are obtained from m -cut solutions by shrinking $m - 1$ of them to infinitesimal size. They may play important roles in obtaining all possible three-point functions of this category.

³When it is not confusing, we use one-cut solution to refer either to the one-cut solution of ALP or the solution of the original equation of motion reconstructed in terms of such solutions.

⁴For the normalization of each eigenvector, see section 2.3.

to their computation.

The crucial information about such Wronskians is contained in the global consistency condition of the monodromy matrices given by

$$\Omega_1 \Omega_2 \Omega_3 = 1. \quad (1.6)$$

Since Ω_i 's cannot in general be diagonalized simultaneously, this serves as a highly non-trivial constraint. In fact this condition allows one to express certain products of two Wronskians in terms of the local quasi-momenta $p_i(x)$'s, an example of which is given by

$$\langle 1_+, 2_+ \rangle \langle 1_-, 2_- \rangle = \frac{\sin \frac{p_1(x) + p_2(x) + p_3(x)}{2} \sin \frac{-p_1(x) - p_2(x) + p_3(x)}{2}}{\sin p_1(x) \sin p_2(x)}. \quad (1.7)$$

It turns out that the knowledge of the Wronskians, such as $\langle 1_+, 2_+ \rangle$, between the eigenfunctions at different insertion points is of utmost importance. All the basic quantities, namely the contour integrals giving the contribution of the action and the wave functions, to be discussed shortly, can be expressed in terms of the Wronskians.

Therefore the crucial task is to separate out, from the relations such as (1.7), the individual Wronskian $\langle i_\pm, j_\pm \rangle$. This can be achieved if we know which of the two factors is responsible for each zero and the pole on the spectral curve, produced by the expression on the right hand side. This information dictates the analyticity property of the individual Wronskian in x and by solving the appropriate Riemann-Hilbert problem we can obtain the Wronskians.

As an example, consider the poles produced by the zeros of $\sin p_1(x)$ on the right hand side of (1.7), namely at $p_1(x_{\text{pole}}) = n\pi$. These are the singular points of the spectral curve where the monodromy matrix $\Omega_1(x_{\text{pole}})$ takes the form of a Jordan block and the bigger of the two eigenvectors 1_\pm diverges. This means that the Wronskian on the left hand side of (1.7) involving such a ‘‘big solution’’ must be responsible for these poles. Now which eigenvector is big and which is small near z_i depends on the value of x . In the case of the ordinary one-cut solution its explicit form tells us that it is dictated by the sign of $\text{Re } q_i(x)$. This means that across the line $\text{Re } q_i(x) = 0$, the analytic property of the eigenfunctions i_\pm changes. We can then extract the regular part of the Wronskian between ‘‘small solutions’’ by using the well-known technique of Wiener-Hopf decomposition, which takes the form of a convolution integral with the contour along the line $\text{Re } q_i(x) = 0$. Due to the two-sheeted nature of the spectral curve, the kernel of the decomposition formula must be appropriately generalized.

Now the remaining analysis, namely that of the zeros of the right hand side of (1.7), is similar in spirit but is much more complicated because it involves the interplay between the three local quasi-momenta $p_1(x), p_2(x), p_3(x)$ and requires a certain knowledge of

the global properties of the solutions of the ALP on the spectral parameter plane. To properly deal with this problem, we will introduce a notion of the “exact WKB curve”. Also, since each $p_i(x)$ is double valued, the convolution kernel will be defined on an eight-sheeted Riemann surface. Moreover it turns out that the contour of integration must be determined not just by $\text{Re } q_i(x) = 0$ for each i but also by certain global “connectivity conditions” expressed in terms of the quantity $N_i \equiv |\text{Re } p_i(x)|$. Despite such technical complexities, we will be able to compute the desired Wronskians in terms of the quasi-momenta $p_i(x)$.

With the procedures described above, one obtains the contribution from the action for the S^3 part. Further, in an analogous manner, the corresponding contribution from the $EAdS_3$ part can be computed.

1.2.3 Evaluation of the contribution of the vertex operators

Let us now turn to the computation of the contribution of the vertex operators. To this end, we extend the powerful method developed in our previous work [11] for the GKP string to more general string. It is based on the state-operator correspondence and the construction of the corresponding wave function in terms of the action-angle variables. If one can construct the action-angle variables (S_i, ϕ_i) , the wave function can be constructed simply as

$$\Psi[\phi] = \exp \left(i \sum_i S_i \phi_i - \mathcal{E}(\{S_i\})\tau \right), \quad (1.8)$$

where $\mathcal{E}(\{S_i\})$ is the worldsheet energy⁵. Although the construction of such variables for a non-linear system is prohibitively hard in general, for integrable systems of the present type there exists a beautiful method [13–15], based on the Sklyanin’s separation of variables [16], which allows us to construct them from the Baker-Akhiezer eigenvector ψ , which is the solution of ALP satisfying the monodromy equation of the form $\Omega(x; \tau, \sigma)\psi(x; \tau, \sigma) = e^{ip(x)}\psi(x; \tau, \sigma)$. More precisely, the dynamical information is encoded in the function $n \cdot \psi(x, \tau)$, where $n = (n_1, n_2)$, to be specified later, is referred to as the “normalization vector”. It is known that for an m -cut solution $n \cdot \psi(x, \tau)$ as a function of x has m zeros at certain positions $x = \{\gamma_1, \gamma_2, \dots, \gamma_m\}$ and the dynamical variables $z(\gamma_i)$ and $p(\gamma_i)$, where $z = \sqrt{\lambda}(x + x^{-1})/(4\pi)$, can be shown to form canonical conjugate pairs. Then by making a suitable canonical transformation, one can construct the action-angle variables (S_i, ϕ_i) , where, in particular, the angle variables are given by

⁵The sum of such energies of course vanishes for the total system due to the Virasoro constraint.

the generalized Abel map

$$\phi_i = 2\pi \sum_{j=1}^m \int_{x_0}^{\gamma_j} \omega_i, \quad i = 1, 2, \dots, m. \quad (1.9)$$

Here, ω_i are suitably normalized holomorphic differentials (with certain singularities depending on the specific problem) and x_0 is an arbitrary base point. In the case of the one-cut solution of our interest, we have one angle variable ϕ_R associated with the right ALP shown in (1.4) and one left angle variable ϕ_L associated with the left ALP described in (1.5). Hereafter we will only refer to the “right sector” for brevity of explanation.

Now as we shall describe in section 2.2, we can write down a simple formula which reconstructs the classical string solution from the Baker-Akhiezer vector⁶ ψ . Therefore, with a choice of the normalization vector n , one can associate the angle variable $\phi_R(n)$ to a classical solution, through the (zeros of the) quantity $n \cdot \psi$.

Let \mathbb{Y} denote the form of the three-point saddle solution near the vertex insertion point z_i . We will call this part of the solution the i th leg. As we have to normalize the three-point function by the two-point function for each leg, what we wish to compute is the angle variable $\phi_R(n)$ associated to \mathbb{Y} *relative to* the one $\phi_R^{\text{ref}}(n)$ associated to the “reference two-point solution” \mathbb{Y}^{ref} which is created by the *same* vertex operator⁷ at z_i .

Now the vertex operators of our interest are those which correspond to the gauge-invariant composite operators in the $SU(2)$ sector of the super Yang-Mills theory. As we discuss in detail in section 4, the basic operators of that category are the charge-diagonal operators which are “highest weight” with respect to the global symmetry group $SU(2)_R \times SU(2)_L \simeq SO(4)$. Focusing just on the $SU(2)_R$ property, one can characterize such an operator by what we call a “polarization spinor”, in this case $n^{\text{diag}} = (1, 0)^t$, which is annihilated by the raising operator of $SU(2)_R$. More general operator of our interest can then be obtained from such a diagonal operator by an $SU(2)_R$ ($\times SU(2)_L$) rotation and is characterized by the polarization spinor n , obtained from n^{diag} by the corresponding $SU(2)_R$ rotation. In this way, each vertex operator is associated with such a spinor n .

What is important is that this “polarization spinor” n can be shown to be identical to the “normalization vector” n which determines the angle variable $\phi_R(n)$ through the quantity $n \cdot \psi$. As was elaborated in our previous work [11], once the normalization vector n is specified, the relative shift $\Delta\phi_R = \phi_R - \phi_R^{\text{ref}}$ of the angle variable for the three-point solution \mathbb{Y} around z_i from that for the two-point reference solution \mathbb{Y}^{ref} can be computed from the knowledge of the transformation matrix $V \in SL(2, \mathbb{C})$ which connects \mathbb{Y} and \mathbb{Y}^{ref}

⁶Precisely speaking, we need the Baker-Akhiezer vectors for both the left and the right ALP, but we ignore such a detail here.

⁷The same vertex operator can produce slightly different semi-classical behavior around it, depending on whether it resides in the two-point function or in the three point function.

in the manner $\mathbb{Y} = \mathbb{Y}^{\text{ref}} V$ in the vicinity of z_i . As it will be shown in section 4, the allowed form of V can be deduced from the property that both \mathbb{Y} and \mathbb{Y}^{ref} are produced from the same vertex operator characterized by the polarization spinor n .

Then, by using the master formula developed in [11], we can express $\Delta\phi_R$ in terms of n , the solutions of the Baker-Akhiezer functions corresponding to \mathbb{Y}^{ref} , and the parameters describing V . Applying this procedure to each leg of the three-point function and by making use of a relation between the normalization vector n and the value of ψ at $x = \infty$, we can express the wave function (for the right sector) in terms of the Wronskians as

$$\Psi_R^{S^3} = \prod_{\{i,j,k\}} \left(\frac{\langle j_-, k_- \rangle}{\langle i_-, j_- \rangle \langle k_-, i_- \rangle} \Big|_{\infty} \frac{\langle n_i, n_j \rangle \langle n_k, n_i \rangle}{\langle n_j, n_k \rangle} \right)^{R_i + R_j - R_k}. \quad (1.10)$$

Here n_i is the polarization spinor associated with the vertex operator \mathcal{V}_i at z_i and R_i is the absolute value of the $SU(2)_R$ charge carried by \mathcal{V}_i . Note that the kinematical part expressed in terms of $\langle n_i, n_j \rangle$ is clearly separated from the dynamical part, which again is composed of the Wronskians of the solutions of the ALP. The wave function for the $EAdS_3$ part can be obtained in a similar fashion. In that case, the Wronskians $\langle n_i, n_j \rangle$ can be expressed in terms of the difference of the landing positions of the three legs on the boundary of $EAdS_3$ and yield the familiar coordinate dependence of the three-point functions.

1.2.4 Final result for the three-point function

We now have all the ingredients for the evaluation of three-point functions. Substituting the explicit expressions of the Wronskians $\langle i_{\pm}, j_{\pm} \rangle$ into the action and the wave function and assembling the contributions from the S^3 part and the $EAdS_3$ part together, we find that remarkable simplifications take place in the sum. The final result for the general one-cut external states is thus found to be

$$\begin{aligned} \langle \mathcal{V}_1 \mathcal{V}_2 \mathcal{V}_3 \rangle &= \frac{1}{N} \frac{C_{123}}{|x_1 - x_2|^{\Delta_1 + \Delta_2 - \Delta_3} |x_2 - x_3|^{\Delta_2 + \Delta_3 - \Delta_1} |x_3 - x_1|^{\Delta_3 + \Delta_1 - \Delta_2}} \\ &\times \langle n_1, n_2 \rangle^{R_1 + R_2 - R_3} \langle n_2, n_3 \rangle^{R_2 + R_3 - R_1} \langle n_3, n_1 \rangle^{R_3 + R_1 - R_2} \\ &\times \langle \tilde{n}_1, \tilde{n}_2 \rangle^{L_1 + L_2 - L_3} \langle \tilde{n}_2, \tilde{n}_3 \rangle^{L_2 + L_3 - L_1} \langle \tilde{n}_3, \tilde{n}_1 \rangle^{L_3 + L_1 - L_2}, \end{aligned} \quad (1.11)$$

where the prefactor $1/N$ comes from the string coupling constant g_s and the logarithm of the structure constant C_{123} is given by

$$\begin{aligned}
\ln C_{123} = & \int_{\mathcal{M}_{-+--}^{uuu}} \frac{z(x)(dp_1 + dp_2 + dp_3)}{2\pi i} \ln \sin\left(\frac{p_1 + p_2 + p_3}{2}\right) + \int_{\mathcal{M}_{+--+}^{uuu}} \frac{z(x)(dp_1 + dp_2 - dp_3)}{2\pi i} \ln \sin\left(\frac{p_1 + p_2 - p_3}{2}\right) \\
& + \int_{\mathcal{M}_{-+-}^{uuu}} \frac{z(x)(dp_1 - dp_2 + dp_3)}{2\pi i} \ln \sin\left(\frac{p_1 - p_2 + p_3}{2}\right) + \int_{\mathcal{M}_{+-}^{uuu}} \frac{z(x)(-dp_1 + dp_2 + dp_3)}{2\pi i} \ln \sin\left(\frac{-p_1 + p_2 + p_3}{2}\right) \\
& - \int_{\mathcal{K}_{-+--}^{uuu}} \frac{z(x)(d\hat{p}_1 + d\hat{p}_2 + d\hat{p}_3)}{2\pi i} \ln \sin\left(\frac{\hat{p}_1 + \hat{p}_2 + \hat{p}_3}{2}\right) - \int_{\mathcal{K}_{+--+}^{uuu}} \frac{z(x)(d\hat{p}_1 + d\hat{p}_2 - d\hat{p}_3)}{2\pi i} \ln \sin\left(\frac{\hat{p}_1 + \hat{p}_2 - \hat{p}_3}{2}\right) \\
& - \int_{\mathcal{K}_{-+-}^{uuu}} \frac{z(x)(d\hat{p}_1 - d\hat{p}_2 + d\hat{p}_3)}{2\pi i} \ln \sin\left(\frac{\hat{p}_1 - \hat{p}_2 + \hat{p}_3}{2}\right) - \int_{\mathcal{K}_{+-}^{uuu}} \frac{z(x)(-d\hat{p}_1 + d\hat{p}_2 + d\hat{p}_3)}{2\pi i} \ln \sin\left(\frac{-\hat{p}_1 + \hat{p}_2 + \hat{p}_3}{2}\right) \\
& - 2 \sum_{j=1}^3 \int_{\Gamma_{j-}^u} \frac{z(x) dp_j}{2\pi i} \ln \sin p_j + 2 \sum_{j=1}^3 \int_{\hat{\Gamma}_{j-}^u} \frac{z(x) d\hat{p}_j}{2\pi i} \ln \sin \hat{p}_j + \text{Contact}. \tag{1.12}
\end{aligned}$$

The notations used in the above expressions are as follows. In the equation (1.11), Δ_i is the conformal dimension of the i -th vertex operator \mathcal{V}_i and n_i and \tilde{n}_i are the polarization spinors for \mathcal{V}_i with respect to $SU(2)_R$ and $SU(2)_L$. In the expression for $\ln C_{123}$, p_i and \hat{p}_i are the quasi-momenta for the i -th leg for the S^3 part and the $EAdS_3$ part respectively. $z(x)$ is the Zhukovsky variable given in (2.36). The symbols $\mathcal{M}_{\pm\pm\pm}^{uuu}$ and Γ_{j-}^u denote the contours of integration for the S^3 part and $\hat{\mathcal{M}}_{\pm\pm\pm}^{uuu}$ and $\hat{\Gamma}_{j-}^u$ are the contours for the $EAdS_3$ contribution. The last term **Contact** stands for some special terms which depend on the detail of the external states. It should be noted that the result above for the three-point function for the operators corresponding to general one-cut solutions is already reminiscent of the expression in the weak coupling regime. In section 7, we demonstrate that our formula gives the correct result for the case of three BPS operators and that it reduces to the two-point function in the limit when the charge of one of the operators becomes negligibly small. Further, we analyze the Frolov-Tseytlin limit for the case of one non-BPS and two BPS operators and find that the integrals giving the three-point coupling take extremely similar forms, except for different contours of integration. For this issue, we point out the existence of a natural mechanism by which the contours can be modified.

Now we briefly indicate the organization of the rest of this article: In section 2, we begin with the description of the string in $EAdS_3 \times S^3$ spacetime and discuss the one-cut solutions we will consider in this work. In section 3, we will study the contribution of the action for the S^3 part to the three-point function and show that the action can be re-expressed in terms of certain contour integrals. In section 4, we describe the evaluation of the wave functions for the S^3 part. Characterizing the vertex operator by a polarization spinor and identifying it with the normalization vector determining the angle variable, we apply the master formula for the shift of the angle variables developed in our previous work to construct the wave functions. Section 5 will be devoted to the explicit evaluation of the Wronskians. The main task is to find the analyticity property of the Wronskian

from the improved WKB analysis of the ALP. Using this information, we can project out the individual Wronskian from the expression of the product of Wronskians in terms of the quasi-momenta $p_i(x)$ by the use of the Wiener-Hopf decomposition. In section 6, all the results obtained up to this point are put together to produce the final result for the three-point functions of the general one-cut external states. In section 7, in addition to some basic checks of our result, we present the analysis of the Frolov-Tseytlin limit and discuss its outcome. Finally, in section 8 we make some important comments on our present work and indicate possible future directions. Several appendices are provided to supply some additional details.

2 String in $EAdS_3 \times S^3$ and classical solutions

We begin by setting up the formalism to deal with the strings in $EAdS_3 \times S^3$ in subsection 2.1 and describe the classical solutions we will use as the external states of the three-point functions in subsection 2.2. We then give a brief account on the basic set-up of the three-point function in subsection 2.3.

2.1 String in $EAdS_3 \times S^3$ spacetime

2.1.1 Preliminaries

In this article, we will exclusively deal with the string propagating in the product space of the Euclidean AdS_3 subspace of AdS_5 (to be denoted by $EAdS_3$) and the sphere S^3 . If we describe the AdS_5 in terms of the embedding coordinates by $X^M \eta_{MN} X^N = -1$, where the superscript M is taken to run as $M = -1, 0, 1, 2, 3, 4$ and the metric is given by $\eta_{MN} = \text{diag}(-1, -1, 1, 1, 1, 1)$, then the $EAdS_3$ subspace is defined by setting $X^0 = X^3 = 0$. Therefore we will parametrize the $EAdS_3 \times S^3$ space in the following way⁸:

$$EAdS_3: \quad X^\mu X_\mu \equiv X^\mu \eta_{\mu\nu} X^\nu = -1, \quad \mu, \nu = -1, 1, 2, 4, \quad (2.1)$$

$$\eta_{\mu\nu} = \text{diag}(-1, 1, 1, 1),$$

$$S^3: \quad Y^I Y_I \equiv Y^I \delta_{IJ} Y^J = 1, \quad I, J = 1, 2, 3, 4. \quad (2.2)$$

The Poincaré coordinates $(x^r, z) = (x^0, x^1, x^2, x^3, z)$ of AdS_5 are defined in the usual way as

$$X^{-1} + X^4 = \frac{1}{z}, \quad X^{-1} - X^4 = z + \frac{x^r x_r}{z}, \quad X^r = \frac{x^r}{z}, \quad (2.3)$$

⁸In order to conform to the standard convention, we have chosen the range of the S^3 embedding coordinates Y^I to be $I = 1, 2, 3, 4$, some of which coincide in name to the range of the $EAdS_3$ coordinates. We believe this will not cause confusion.

where $z = 0$ corresponds to the boundary of AdS_5 . When restricted to the $EAdS_3$ subspace⁹, its boundary is the Euclidean plane parametrized by (x^1, x^2) .

The action of a string in this space is given by

$$S = \frac{\sqrt{\lambda}}{\pi} \int d^2z \left(\partial X^\mu \bar{\partial} X_\mu + \Lambda (X^\mu X_\mu + 1) + \partial Y^I \bar{\partial} Y_I + \tilde{\Lambda} (Y^I Y_I - 1) \right), \quad (2.4)$$

where Λ and $\tilde{\Lambda}$ are Lagrange multiplier fields. Upon eliminating them the equations of motion become

$$\partial \bar{\partial} X^\mu - (\partial X^\nu \bar{\partial} X_\nu) X^\mu = 0, \quad (2.5)$$

$$\partial \bar{\partial} Y^I + (\partial Y^J \bar{\partial} Y_J) Y^I = 0. \quad (2.6)$$

For physical configurations, we must in addition impose the Virasoro constraints, which require that the sum of the stress-energy tensors for the AdS part and the sphere part must vanish. Namely,

$$T_{AdS}(z) + T_S(z) = 0, \quad \bar{T}_{AdS}(\bar{z}) + \bar{T}_S(\bar{z}) = 0, \quad (2.7)$$

$$T_{AdS}(z) = \partial X^\mu \partial X_\mu, \quad T_S(z) = \partial Y^I \partial Y_I, \quad (2.8)$$

$$\bar{T}_{AdS}(\bar{z}) = \bar{\partial} X^\mu \bar{\partial} X_\mu, \quad \bar{T}_S(\bar{z}) = \bar{\partial} Y^I \bar{\partial} Y_I. \quad (2.9)$$

For the AdS part, we shall take the external states to be those without the two-dimensional spins. Then near the vertex insertion point the saddle point solution should approach the two-point solution, which is known to be point-like. The forms of $T_{AdS}(z)$ and $\bar{T}_{AdS}(\bar{z})$ for such a two-point solution are uniquely determined by their transformation properties as a $(2, 0)$ and a $(0, 2)$ tensor respectively and are given in terms of the conformal dimension Δ of the vertex operator as

$$T_{AdS,2pt}(z) = \frac{\kappa^2}{z^2}, \quad \bar{T}_{AdS,2pt}(\bar{z}) = \frac{\kappa^2}{\bar{z}^2}, \quad \kappa = \frac{\Delta}{2\sqrt{\lambda}}. \quad (2.10)$$

Therefore, taking into account the Virasoro condition, near each vertex insertion point z_i we must have

$$T_{AdS}(z) \sim \frac{\kappa_i^2}{(z - z_i)^2}, \quad T_S(z) \sim \frac{-\kappa_i^2}{(z - z_i)^2} \quad \text{as } z \rightarrow z_i, \quad (2.11)$$

and similarly for the anti-holomorphic parts. In the case of three-point functions, the information of such asymptotic behaviors suffices to determine the form of the energy-momentum tensor exactly everywhere. For the $EAdS_3$, the holomorphic part takes the form

$$T(z) = \left(\frac{\kappa_1^2 z_{12} z_{13}}{z - z_1} + \frac{\kappa_2^2 z_{21} z_{23}}{z - z_2} + \frac{\kappa_3^2 z_{31} z_{32}}{z - z_3} \right) \frac{1}{(z - z_1)(z - z_2)(z - z_3)}, \quad (2.12)$$

$$z_{ij} \equiv z_i - z_j. \quad (2.13)$$

⁹If desired, one can also deal with the AdS_3 subspace given by $X^2 = X^3 = 0$, with the Minkowski boundary plane (x^0, x^1) .

Here and hereafter, we shall omit the subscript AdS for the stress tensor for the AdS part and simply write $T(z)$ and $\bar{T}(\bar{z})$ for $T_{AdS}(z)$ and $\bar{T}_{AdS}(\bar{z})$.

We now discuss the methods for constructing the solutions of the equations of motion with the use of the classical integrability of the system. There exist two apparently different formalisms. One is the sigma model formulation [12, 17] and the other is the so-called Pohlmeyer reduction [18, 19]. The former deals with variables which transform covariantly under the global symmetry transformations, whereas the latter employs invariant variables. Because of this feature they have advantages and disadvantages depending on the problem one would like to solve. We shall employ both. It should be remarked however that they are actually connected by a “gauge transformation”, as shown in Appendix C.2.

2.1.2 Sigma model formulation

Consider first the sigma model formulation. We will focus on the S^3 part, as the $EAdS_3$ part can be treated similarly. The embedding coordinates $\{Y_I\}$ are conveniently assembled into a 2×2 matrix with unit determinant given by

$$\mathbb{Y} = \begin{pmatrix} Z_1 & Z_2 \\ -\bar{Z}_2 & \bar{Z}_1 \end{pmatrix}, \quad (2.14)$$

$$Z_1 = Y_1 + iY_2, \quad Z_2 = Y_3 + iY_4, \quad (2.15)$$

which transforms under the global symmetry group $SO(4) = SU(2)_L \times SU(2)_R$ as

$$\mathbb{Y}' = U_L \mathbb{Y} U_R, \quad U_R \in SU(2)_R, \quad U_L \in SU(2)_L. \quad (2.16)$$

The quantities of central importance are the “right” and the “left” currents (or connections) j and l respectively, defined by

$$j \equiv \mathbb{Y}^{-1} d\mathbb{Y}, \quad l \equiv d\mathbb{Y} \mathbb{Y}^{-1}. \quad (2.17)$$

Evidently, j and l are related by $l = \mathbb{Y} j \mathbb{Y}^{-1}$. Under the transformation (2.16) they transform covariantly as $j \rightarrow U_R^{-1} j U_R$ and $l \rightarrow U_L l U_L^{-1}$. Now reflecting the classical integrability of the system these equations can be extended to one parameter family of equations called Lax equations given by

$$[\partial + \mathcal{J}_z^r(x), \bar{\partial} + \mathcal{J}_{\bar{z}}^r(x)] = 0, \quad (2.18)$$

$$\mathcal{J}_z^r(x) \equiv \frac{j_z}{1-x}, \quad \mathcal{J}_{\bar{z}}^r(x) \equiv \frac{j_{\bar{z}}}{1+x},$$

$$[\partial + \mathcal{J}_z^l(x), \bar{\partial} + \mathcal{J}_{\bar{z}}^l(x)] = 0, \quad (2.19)$$

$$\mathcal{J}_z^l(x) \equiv \frac{x l_z}{1-x}, \quad \mathcal{J}_{\bar{z}}^l(x) \equiv -\frac{x l_{\bar{z}}}{1+x},$$

where x is the complex spectral parameter. The two connections $\mathcal{J}^r = \mathcal{J}_z^r dz + \mathcal{J}_{\bar{z}}^r d\bar{z}$ and $\mathcal{J}^l = \mathcal{J}_z^l dz + \mathcal{J}_{\bar{z}}^l d\bar{z}$ are related by the gauge transformation of the form $\mathbb{Y}(d + \mathcal{J}^r)\mathbb{Y}^{-1} = d + \mathcal{J}^l$. It is useful to note that the energy-momentum tensors and hence the Virasoro conditions can be expressed in terms of the currents in a concise way. We have, in the cylinder coordinate,

$$T_S(z) = -\frac{1}{2}\text{Tr}(j_z j_z) = -\kappa^2, \quad \bar{T}_S(\bar{z}) = -\frac{1}{2}\text{Tr}(j_{\bar{z}} j_{\bar{z}}) = -\kappa^2. \quad (2.20)$$

Central to the construction and the analysis of the solutions of the equations of motion are the right and the left auxiliary linear problems, to be abbreviated as ALP, which are coupled linear differential equations for vector functions:

$$\text{right ALP : } (\partial + \mathcal{J}_z^r(x))\psi = 0, \quad (\bar{\partial} + \mathcal{J}_{\bar{z}}^r(x))\psi = 0, \quad (2.21)$$

$$\text{left ALP : } (\partial + \mathcal{J}_z^l(x))\tilde{\psi} = 0, \quad (\bar{\partial} + \mathcal{J}_{\bar{z}}^l(x))\tilde{\psi} = 0. \quad (2.22)$$

Compatibility of the system of ALP implies the original equations of motion. Upon developing ψ and $\tilde{\psi}$ from a point z_0 along a closed spacelike curve, we obtain the right and the left monodromy matrices $\Omega(x)$ and $\tilde{\Omega}(x)$ respectively as

$$\Omega(x; z_0) = \text{P exp} \left(- \oint \mathcal{J}^r \right) = \text{P exp} \left(- \oint \left(\frac{j_z dz}{1-x} + \frac{j_{\bar{z}} d\bar{z}}{1+x} \right) \right), \quad (2.23)$$

$$\tilde{\Omega}(x; z_0) = \text{P exp} \left(- \oint \mathcal{J}^l \right) = \text{P exp} \left(- \oint \left(\frac{x l_z dz}{1-x} - \frac{x l_{\bar{z}} d\bar{z}}{1+x} \right) \right) = \mathbb{Y}\Omega(x; z_0)\mathbb{Y}^{-1}. \quad (2.24)$$

By virtue of the flatness of the connection, expansion of $\Omega(x)$ as a function of x around any point yields an infinite number of conserved charges as coefficients. In particular, expansions around $x = \infty$ and $x = 0$ yield, in the leading behavior, the Noether charges for the global $\text{SU}(2)_R$ and $\text{SU}(2)_L$, respectively, defined by

$$Q_R \equiv \frac{\sqrt{\lambda}}{4\pi} \oint *j = \frac{\sqrt{\lambda}}{4\pi} \int_0^{2\pi} d\sigma j_\tau, \quad (2.25)$$

$$Q_L \equiv \frac{\sqrt{\lambda}}{4\pi} \oint *l = \frac{\sqrt{\lambda}}{4\pi} \int_0^{2\pi} d\sigma l_\tau. \quad (2.26)$$

Indeed, expanding $\Omega(x; z_0)$ around $x = \infty$ and $x = 0$ and using the definitions above, we get

$$\Omega(x; z_0) = 1 - \frac{1}{x} \frac{4\pi}{\sqrt{\lambda}} Q_R + O(x^{-2}), \quad (x \rightarrow \infty), \quad (2.27)$$

$$\mathbb{Y}\Omega(x; z_0)\mathbb{Y}^{-1} = 1 + x \frac{4\pi}{\sqrt{\lambda}} Q_L + O(x^2), \quad (x \rightarrow 0). \quad (2.28)$$

By diagonalizing $\Omega(x; z_0)$, we can obtain a quantity independent of z_0 . Since $\det \Omega(x; z_0) = 1$, its eigenvalues must be of the structure

$$u(x; z_0)\Omega(x; z_0)u(x; z_0)^{-1} = \begin{pmatrix} e^{ip(x)} & 0 \\ 0 & e^{-ip(x)} \end{pmatrix}, \quad (2.29)$$

where $p(x)$ is called the quasi-momentum. Comparing with the diagonalized form of the expressions (2.27) and (2.28), the behaviors of $p(x)$ around $x = \infty$ and $x = 0$ are of the form

$$p(x) - p(\infty) = -\frac{1}{x} \frac{4\pi}{\sqrt{\lambda}} R + O(x^{-2}), \quad (x \rightarrow \infty), \quad (2.30)$$

$$p(x) - p(\infty) = 2\pi m + x \frac{4\pi}{\sqrt{\lambda}} L + O(x^2), \quad (x \rightarrow 0), \quad (2.31)$$

where m is an integer and the right and the left charges R and L are the (positive) eigenvalues of Q_R and Q_L respectively.

For the study of the ALP and construction of the finite gap solutions of our interest, the analytic property of the quasi-momentum is of critical importance. Such a structure is encoded in the spectral curve defined by

$$\Gamma : \quad \Gamma(x, y) = \det(y\mathbf{1} - \Omega(x; z_0)) = 0, \quad (2.32)$$

which is equivalent to $(y - e^{ip(x)})(y - e^{-ip(x)}) = 0$. In the present case, it can be regarded as a two-sheeted Riemann surface with various singularities. From the definition of the monodromy matrix (2.23) and (2.24) and the constraints (2.20), it is clear that $p(x)$ has poles at $x = \pm 1$ with the magnitude of the residue equaling $-2\pi\kappa$. Since $p(x)$ lives on a two-sheeted surface, we specify its branch by defining the signs at these singularities. We shall employ the definition

$$p(x) \sim \frac{-2\pi\kappa}{x-1} + O((x-1)^0), \quad (x \rightarrow 1^+), \quad (2.33)$$

$$p(x) \sim \frac{-2\pi\kappa}{x+1} + O((x+1)^0), \quad (x \rightarrow -1^+). \quad (2.34)$$

where the $+$ superscript on 1^+ signifies that the point is on the first sheet. Similarly, we shall use $-$ superscript for points on the second sheet. We will give a more detailed discussion of the structure of $p(x)$ for the one-cut solutions of our interest in subsection 2.2.

From the structure of the spectral curve and the quasi-momentum $p(x)$ defined upon it, one can extract important information. For this purpose, we first define the a - and b -cycles in the usual way. For the hyperelliptic curve of our interest, an a -cycle is defined as a cycle which goes around the cut on the same sheet. On the other hand, a b -cycle is defined as the one which starts from a point on the first sheet, goes into the second sheet through the cut and eventually comes back to the same point on the first sheet. Clearly, around an a -cycle, we have $\oint_{a_i} dp = 0$. In contrast, the integral along the b -cycle does not vanish in general and gives $\oint_{b_i} dp = 2\pi n_i$, where n_i is an integer called the mode number. Now using the a -type cycles, one can define a set of conserved charges called the *filling*

fractions as

$$S_i \equiv \frac{i}{2\pi} \oint_{a_i} p dz \left(= \oint_{a_i} \frac{z dp}{2\pi i} \right), \quad (2.35)$$

where

$$z \equiv \frac{\sqrt{\lambda}}{4\pi} \left(x + \frac{1}{x} \right) \quad (2.36)$$

is the Zhukovsky variable. In particular, the filling fractions S_∞ and S_0 defined with the contours a_∞ and a_0 , which encircle the point at ∞ and 0 respectively, are of special importance since they are related to the global $SU(2)_R$ and $SU(2)_L$ charges in the following way, as can be checked using (2.30) and (2.31):

$$S_\infty = -R, \quad S_0 = L. \quad (2.37)$$

2.1.3 Pohlmeyer reduction for a string in S^3

The sigma model formulation we have sketched above is convenient for analyzing the property of the system under the global symmetry transformations. Hence it will be used as the basis of the construction of the wave function corresponding to the vertex operators in section 4. On the other hand, for the analysis of the contribution of the action, which is invariant under the global transformation, the formalism of the *Pohlmeyer reduction* will be more convenient.

The essential idea of the Pohlmeyer reduction is to describe the motion of the string in a suitably defined moving frame. This then leads to the Lax equations in terms of the connections which are invariant under the global symmetry transformations. Below we shall only sketch the procedures and then summarize the basic equations we will need later. Further details will be given in Appendix B.

In what follows we shall denote a 4-component field A^I simply as A and use the notations $A \cdot B = A^I B_I$, $A^2 = A^I A_I$. The basic moving frame of 4-component fields, to be called q_i , ($i = 1, 2, 3, 4$), are taken as $q_1 \equiv Y$, $q_2 \equiv a\partial Y + b\bar{\partial}Y$, $q_3 \equiv c\partial Y + d\bar{\partial}Y$ and $q_4 \equiv N$, where N is the unit vector orthogonal to Y , ∂Y and $\bar{\partial}Y$, and the (field-dependent) coefficients a, b, c, d are chosen so that the simple conditions $q_2 \cdot q_3 = -2$, $q_2^2 = q_3^2 = 0$ are satisfied. (Note that since $Y^2 = 1$, we automatically have $q_1^2 = 1$, $q_1 \cdot q_2 = q_1 \cdot q_3 = 0$.) Let us define an $SO(4)$ -invariant field γ by the relation

$$\partial Y \cdot \bar{\partial} Y = \sqrt{T\bar{T}} \cos 2\gamma. \quad (2.38)$$

Then, the coefficients a, b, c, d can be expressed in terms of T, \bar{T} and γ , giving q_2 and q_3

of the form

$$q_2 = -\frac{i}{\sin 2\gamma} \left[\frac{e^{i\gamma}}{\sqrt{T}} \partial Y + \frac{e^{-i\gamma}}{\sqrt{\bar{T}}} \bar{\partial} Y \right], \quad (2.39)$$

$$q_3 = \frac{i}{\sin 2\gamma} \left[\frac{e^{i\gamma}}{\sqrt{\bar{T}}} \bar{\partial} Y + \frac{e^{-i\gamma}}{\sqrt{T}} \partial Y \right]. \quad (2.40)$$

Once the moving frame is prepared, one can compute the derivatives of q_i and express them in terms of q_i again. The result can be assembled into the following equations

$$\partial W + B_z^L W + W B_z^R = 0, \quad \bar{\partial} W + B_{\bar{z}}^L W + W B_{\bar{z}}^R = 0, \quad (2.41)$$

where W is given by

$$W = \frac{1}{2} \begin{pmatrix} q_1 + iq_4 & q_2 \\ q_3 & q_1 - iq_4 \end{pmatrix}, \quad (2.42)$$

and $B_{z,\bar{z}}^{L,R}$ are matrices whose components are expressed in terms of T, \bar{T} and γ . (Explicit forms are given in Appendix B.) From the equations (2.41) one deduces that the left and the right connections B^L and B^R , given in (B.21)–(B.24), are flat, namely

$$[\partial + B_z^L, \bar{\partial} + B_{\bar{z}}^L] = 0, \quad [\partial + B_z^R, \bar{\partial} + B_{\bar{z}}^R] = 0. \quad (2.43)$$

These relations give the equations of motion for the invariant fields in the form

$$\begin{aligned} \partial \bar{\partial} \gamma + \frac{\sqrt{T\bar{T}}}{2} \sin 2\gamma + \frac{2\rho\tilde{\rho}}{\sqrt{T\bar{T}}} \frac{1}{\sin 2\gamma} &= 0, \\ \partial \tilde{\rho} + \frac{2\bar{\partial} \gamma}{\sin 2\gamma} \rho = 0, \quad \bar{\partial} \rho + \frac{2\partial \gamma}{\sin 2\gamma} \tilde{\rho} &= 0, \end{aligned} \quad (2.44)$$

where ρ and $\tilde{\rho}$ are defined by

$$\rho \equiv \frac{1}{2} N \cdot \partial^2 Y, \quad \tilde{\rho} \equiv \frac{1}{2} N \cdot \bar{\partial}^2 Y. \quad (2.45)$$

Just as in the case of the sigma model formulation, the integrability of the system allows one to introduce a spectral parameter ζ , related to x by

$$\zeta = \frac{1-x}{1+x}, \quad (2.46)$$

without spoiling the flatness conditions. The Lax equation so obtained is given by

$$[\partial + B_z(\zeta), \bar{\partial} + B_{\bar{z}}(\zeta)] = 0, \quad (2.47)$$

where

$$\begin{aligned} B_z(\zeta) &\equiv \frac{\Phi_z}{\zeta} + A_z, & B_{\bar{z}}(\zeta) &\equiv \zeta \Phi_{\bar{z}} + A_{\bar{z}}, \\ \Phi_z &\equiv \begin{pmatrix} 0 & -\frac{\sqrt{T}}{2} e^{-i\gamma} \\ -\frac{\sqrt{T}}{2} e^{i\gamma} & 0 \end{pmatrix}, & \Phi_{\bar{z}} &\equiv \begin{pmatrix} 0 & \frac{\sqrt{\bar{T}}}{2} e^{i\gamma} \\ \frac{\sqrt{\bar{T}}}{2} e^{-i\gamma} & 0 \end{pmatrix}, \\ A_z &\equiv \begin{pmatrix} -\frac{i\partial\gamma}{2} & \frac{\rho e^{i\gamma}}{\sqrt{T} \sin 2\gamma} \\ \frac{\rho e^{-i\gamma}}{\sqrt{T} \sin 2\gamma} & \frac{i\bar{\partial}\gamma}{2} \end{pmatrix}, & A_{\bar{z}} &\equiv \begin{pmatrix} \frac{i\bar{\partial}\gamma}{2} & \frac{\tilde{\rho} e^{-i\gamma}}{\sqrt{\bar{T}} \sin 2\gamma} \\ \frac{\tilde{\rho} e^{i\gamma}}{\sqrt{\bar{T}} \sin 2\gamma} & -\frac{i\partial\gamma}{2} \end{pmatrix}. \end{aligned} \quad (2.48)$$

One can consider the auxiliary linear problem also for the Pohlmeyer connections (2.47),

$$(\partial + B_z(\zeta))\hat{\psi} = 0, \quad (\bar{\partial} + B_{\bar{z}}(\zeta))\hat{\psi} = 0, \quad (2.49)$$

where $\hat{\psi}$ denotes the solution in this formulation. As shown in Appendix C.2, the Pohlmeyer connections (2.47) are actually related to the connections in the sigma model formulation, (2.21) and (2.22), by gauge transformations. Correspondingly, the solutions to the ALP are also related by gauge transformations as

$$\psi = \mathcal{G}^{-1}\hat{\psi}, \quad \tilde{\psi} = \tilde{\mathcal{G}}^{-1}\hat{\psi}, \quad (2.50)$$

where ψ and $\tilde{\psi}$ are the solutions to the right and the left ALP respectively and \mathcal{G} and $\tilde{\mathcal{G}}$ are the gauge transformations, the explicit form of which are given in Appendix C.2. Here and hereafter, we shall often refer to the use of the Pohlmeyer formulation as choosing the *Pohlmeyer gauge*.

2.2 One-cut finite gap solutions in S^3

We now describe a particular class of solutions to the equations of motion and the Virasoro constraints, which can be constructed by the so-called finite gap integration method [13–15]. These solutions describe the local behaviors of the saddle point solution for the three-point function in the vicinity of the vertex insertion point. The class of our interest is characterized by the associated spectral curve having one square-root branch cut of finite size and will be referred to as a *one-cut solution*. We will first consider the “basic” one-cut solutions, which are customarily referred to as genus 0 solutions, and study their properties in detail. Then, we describe another class of one-cut solutions which are obtained from multi-cut solutions by certain degeneration procedure. We show that they contain additional singularities on the worldsheet, which may play an important role when we compare the three point functions at strong and weak couplings in section 7.

2.2.1 Basic one-cut solution and “reconstruction” formula

A powerful method for constructing a large class of classical solutions in the sigma model formulation is the so-called finite gap integration method. (For a comprehensive review, see [15].) The method consists of two steps. As the first step, the solutions to the left and the right ALP, called the Baker-Akhiezer functions, are constructed by treating the problems as Riemann-Hilbert problems on a finite genus Riemann surface. Namely, by proving that the function satisfying all the required analytic properties is unique, one

constructs such a function in terms of the Riemann theta functions and the exponential functions. Then, as the second step, one develops the “reconstruction” formula¹⁰, which constructs the solutions to the original equations of motion from the knowledge of the Baker-Akhiezer functions. In this subsection, we will describe the simplest class of solutions corresponding to the case of genus zero Riemann surface, or a two-sheeted surface with one square-root branch cut. Such solutions will be referred to as the basic one-cut solutions.

Consider first the right ALP given in (1.4) and let $\psi_{\pm}(x, z, \bar{z})$ be the Baker-Akhiezer vector which are at the same time the eigenvectors of the monodromy matrix $\Omega(x)$ corresponding to the eigenvalues $e^{\pm ip(x)}$ respectively. According to the general theory of finite gap integration, ψ_{\pm} corresponding to the one-cut solution are given by simple exponential functions as

$$\psi_{+}(x; \tau, \sigma) = \begin{pmatrix} c_1^{+} \exp\left(\frac{i\sigma}{2\pi} \int_{\infty^{+}}^x dp + \frac{\tau}{2\pi} \int_{\infty^{+}}^x dq\right) \\ c_2^{+} \exp\left(\frac{i\sigma}{2\pi} \int_{\infty^{-}}^x dp + \frac{\tau}{2\pi} \int_{\infty^{-}}^x dq\right) \end{pmatrix}, \quad (2.51)$$

$$\psi_{-}(x; \tau, \sigma) = \psi_{+}(\hat{\sigma}x; \tau, \sigma). \quad (2.52)$$

where c_i^{+} are constants, $\hat{\sigma}x$ denotes the point x on the opposite sheet, and $\infty^{+}(\infty^{-})$ is the point at infinity on the first (resp. second) sheet. The quantity dp is the differential of the quasi-momentum $p(x)$, while dq is the differential of the quasi-energy $q(x)$. Just like $p(x)$, the quasi-energy $q(x)$ is defined by the pole behavior at $x = \pm 1^{+}$ of the form

$$q(x) \sim \frac{-2\pi\kappa}{x-1} + O((x-1)^0), \quad (x \rightarrow 1^{+}), \quad (2.53)$$

$$q(x) \sim \frac{+2\pi\kappa}{x+1} + O((x+1)^0), \quad (x \rightarrow -1^{+}). \quad (2.54)$$

The structure and the signs of the residue at $x = \pm 1$ for $q(x)$ are determined so that the holomorphicity of the solution (2.51) at $x \simeq \pm 1$ is as dictated by the ALP. For example at $x = 1$ the holomorphic part of the ALP is dominating and hence the Baker-Akhiezer vector should be holomorphic. This is in fact realized since $p(x) = q(x)$ near $x = 1$ and hence the exponent of ψ_{\pm} is a function of the combination $z = \tau + i\sigma$. In the same way, at $x = -1$ the exponent of ψ_{\pm} becomes anti-holomorphic as desired.

Now for the left ALP, the Baker-Akhiezer eigenvectors, denoted by $\tilde{\psi}_{\pm}(x, z, \bar{z})$, are given by

$$\tilde{\psi}_{+}(x; \tau, \sigma) = \begin{pmatrix} c_1^{-} \exp\left(\frac{i\sigma}{2\pi} \int_{0^{+}}^x dp + \frac{\tau}{2\pi} \int_{0^{+}}^x dq\right) \\ c_2^{-} \exp\left(\frac{i\sigma}{2\pi} \int_{0^{-}}^x dp + \frac{\tau}{2\pi} \int_{0^{-}}^x dq\right) \end{pmatrix}, \quad (2.55)$$

$$\tilde{\psi}_{-}(x; \tau, \sigma) = \tilde{\psi}_{+}(\hat{\sigma}x; \tau, \sigma), \quad (2.56)$$

¹⁰Although it is usually referred to as the “reconstruction” formula, in practice it is used as a solution-generating formula. This is because the Baker-Akhiezer functions are constructed not by solving ALP with specific known connections but by more generic methods.

where the notations are similar and should be self-explanatory.

We will be interested in the case where the branch cut runs between u and its complex conjugate \bar{u} on the spectral curve. Such a cut is described by a factor of the form

$$y(x) \equiv \sqrt{(x-u)(x-\bar{u})}. \quad (2.57)$$

We define the branch of $y(x)$ to be such that the sign of $y(x)$ is $+1$ at $x = 1^+$. Then $p(x)$ and $q(x)$ satisfying the prescribed analyticity properties are fixed to be

$$p(x) = -2\pi\kappa y(x) \left(\frac{1}{|1-u|} \frac{1}{x-1} + \epsilon \frac{1}{|1+u|} \frac{1}{x+1} \right), \quad (2.58)$$

$$q(x) = -2\pi\kappa y(x) \left(\frac{1}{|1-u|} \frac{1}{x-1} - \epsilon \frac{1}{|1+u|} \frac{1}{x+1} \right), \quad (2.59)$$

$$\epsilon = \begin{cases} +1 & \text{for } |\operatorname{Re} u| > 1 \\ -1 & \text{for } |\operatorname{Re} u| < 1 \end{cases}. \quad (2.60)$$

Here we fixed $p(x)$ and $q(x)$ such that they vanish at the branch points although the analyticity properties only determine the differential dp and dq . This choice is suitable for the purpose of this paper since the solutions to the ALP in the Pohlmeyer gauge. The forms of $p(x)$ and $q(x)$ depend on whether the cut is placed to the right or to the left of $x = 1$. Substituting these forms into the formulas for ψ_{\pm} and $\tilde{\psi}_{\pm}$ we get the one-cut solutions for the ALP.

Let us now describe the second step, the (re)construction of the solutions of the equations of motion from the Baker-Akhiezer vectors. Although this has been discussed in the literature [13–15], we present below a more transparent formula. Let us form a 2×2 matrix Ψ in terms of the two independent Baker-Akhiezer column vectors ψ_{\pm} satisfying the right ALP as $\Psi = (\psi_+ \psi_-)$ and consider the quantity

$$\tilde{\Psi} \equiv \mathbb{Y}\Psi. \quad (2.61)$$

Then, by using the definitions $l_z = \partial\mathbb{Y}\mathbb{Y}^{-1}$ and $j_z = \mathbb{Y}^{-1}\partial\mathbb{Y}$, we can easily show that

$$\left(\partial + \frac{x l_z}{1-x} \right) \tilde{\Psi} = \mathbb{Y} \left(\partial + \frac{j_z}{1-x} \right) \Psi = 0, \quad (2.62)$$

$$\left(\bar{\partial} - \frac{x l_{\bar{z}}}{1+x} \right) \tilde{\Psi} = \mathbb{Y} \left(\partial + \frac{j_{\bar{z}}}{1+x} \right) \Psi = 0. \quad (2.63)$$

If we express $\tilde{\Psi}$ in terms of two column vectors $\tilde{\psi}_{\pm}$ as $\tilde{\Psi} = (\tilde{\psi}_+ \tilde{\psi}_-)$, the above equations show that $\tilde{\psi}_{\pm}$ are actually two independent solutions to the left ALP. This means that there exist solutions ψ_{\pm} and $\tilde{\psi}_{\pm}$ to the right and the left ALP respectively so that \mathbb{Y} can be expressed as

$$\mathbb{Y} = \tilde{\Psi}\Psi^{-1}. \quad (2.64)$$

This general relation by itself, however, is not useful since even if we provide a solution Ψ explicitly, finding $\tilde{\Psi}$ which satisfies (2.64) tantamounts to finding \mathbb{Y} itself. Now the formula (2.64) turns into a genuine reconstruction formula when we consider the special values of the spectral parameter x . If we set $x = 0$, it is evident from the form of ALP redisplayed above in (2.62) and (2.63) that the left ALP equations for $\tilde{\Psi}$ reduce to $\partial\tilde{\Psi} = \bar{\partial}\tilde{\Psi} = 0$, and hence $\tilde{\Psi}(x = 0)$ becomes a constant matrix. Therefore the solution \mathbb{Y} is reconstructed from the right ALP solution Ψ as $\mathbb{Y}(z, \bar{z}) = \tilde{\Psi}(x = 0)\Psi^{-1}(z, \bar{z}; x = 0)$, where the constant matrix $\tilde{\Psi}(x = 0)$ represents the freedom of making a global transformation from left. Similarly, by setting $x = \infty$, we can make the right ALP equations trivial, namely $\partial\Psi = \bar{\partial}\Psi = 0$. Then $\Psi(x = \infty)$ becomes a constant matrix and \mathbb{Y} can be reconstructed from the left ALP solution $\tilde{\Psi}$ as $\mathbb{Y}(z, \bar{z}) = \tilde{\Psi}(z, \bar{z}; x = \infty)\Psi^{-1}(x = \infty)$. Summarizing, we have two types of simple reconstruction formulas

$$\mathbb{Y}(z, \bar{z}) = \tilde{\Psi}(0)\Psi^{-1}(z, \bar{z}; 0), \quad (2.65)$$

$$\mathbb{Y}(z, \bar{z}) = \tilde{\Psi}(z, \bar{z}; \infty)\Psi^{-1}(\infty). \quad (2.66)$$

By using the reconstruction formula given above, one can write down the general basic one-cut solution explicitly. It can be written in the form [12, 15]

$$\mathbb{Y} = \begin{pmatrix} \cos \frac{\theta_0}{2} e^{\nu_1\tau + im_1\sigma} & \sin \frac{\theta_0}{2} e^{\nu_2\tau + im_2\sigma} \\ -\sin \frac{\theta_0}{2} e^{-\nu_2\tau - im_2\sigma} & \cos \frac{\theta_0}{2} e^{-\nu_1\tau - im_1\sigma} \end{pmatrix}, \quad (2.67)$$

where the parameters ν_i, m_i and θ_0 must satisfy the following conditions expressing the equations of motion and the Virasoro conditions:

$$\nu_1^2 - m_1^2 = \nu_2^2 - m_2^2, \quad (2.68)$$

$$4\kappa^2 = (\nu_1^2 + m_1^2) \cos^2 \frac{\theta_0}{2} + (\nu_2^2 + m_2^2) \sin^2 \frac{\theta_0}{2}, \quad (2.69)$$

$$\nu_1 m_1 \cos^2 \frac{\theta_0}{2} + \nu_2 m_2 \sin^2 \frac{\theta_0}{2} = 0. \quad (2.70)$$

Applying the reconstruction formula (2.65) with the constant matrix $\tilde{\Psi}(0)$ taken to be the identity matrix and using the form of ψ_+ given in (2.51), we easily find that the parameters m_i and ν_i can be expressed in terms of $p(x)$ and $q(x)$ as

$$m_1 = \frac{1}{2\pi} \int_{0^+}^{\infty^+} dp, \quad \nu_1 = \frac{1}{2\pi} \int_{0^+}^{\infty^+} dq, \quad (2.71)$$

$$m_2 = \frac{1}{2\pi} \int_{0^+}^{\infty^-} dp, \quad \nu_2 = \frac{1}{2\pi} \int_{0^+}^{\infty^-} dq. \quad (2.72)$$

The right and the left Noether charges R and L can be computed directly from the solution

(2.67) and are given in terms of the parameters ν_i , m_i and θ_0 in a universal manner as

$$\frac{R}{\sqrt{\lambda}} = \frac{1}{2} \left(-\nu_1 \cos^2 \frac{\theta_0}{2} + \nu_2 \sin^2 \frac{\theta_0}{2} \right), \quad (2.73)$$

$$\frac{L}{\sqrt{\lambda}} = \frac{1}{2} \left(-\nu_1 \cos^2 \frac{\theta_0}{2} - \nu_2 \sin^2 \frac{\theta_0}{2} \right). \quad (2.74)$$

Explicit expressions of R and L in terms of the position of the cut are given in Appendix A.1. As a result, we find that the charges R and L are positive irrespective of the position of the cut. This means that they should be regarded not as the charges themselves but as their *absolute magnitudes*. On the other hand, the relative magnitude of R and L depends on the position of the cut as

$$R < L \quad \text{for} \quad |\operatorname{Re} u| > 1, \quad (2.75)$$

$$R > L \quad \text{for} \quad |\operatorname{Re} u| < 1. \quad (2.76)$$

In section 4.3.4, we will see that the difference in the relative magnitude corresponds to the difference of the class of vertex operators for which the solution is the saddle point of the two-point function.

2.2.2 One-cut solutions from multi-cut solutions

We now discuss a more general type of “one-cut” solutions, namely the ones with additional cuts of infinitesimal size besides a cut of finite size. As we shall discuss in section 7.5.2, this type of solutions may play an important role in the comparison of the three-point functions at strong and weak couplings. Besides such specific reason, as these infinitesimal cuts do not contribute to any of the (infinite number of) conserved charges, they should, on general grounds, be considered on an equal footing with the corresponding solutions carrying the same charges. As a matter of fact, it is much more natural to consider solutions with infinite number of infinitesimal cuts, as they correspond to the infinite number of angle variables which must exist for a string theory even when their conjugate action variables have vanishing values¹¹. Now adding an infinitesimal cut to the genus g Riemann surface is equivalent to shrinking a cut in the genus $g + 1$ surface¹². As we shall see, depending on the choice of the parameters we either get back an ordinary genus g finite gap solution or we obtain a new solution with additional singularities.

In contrast to the one-cut solution corresponding to genus zero we have been considering, for a genus g finite gap solution with $g \geq 1$ the components of the Baker-Akhiezer

¹¹As already emphasized in [11], in order to construct a three-point solution in the framework of the finite gap method, which is tailored for construction of two-point solutions, inclusion of infinite number of small infinitesimal cuts is necessary as one has to produce an additional singularity corresponding to the third vertex operator.

¹²A similar discussion of this process can be found in [20].

vector are given by the following expressions containing ratios of Riemann theta functions $\Theta(z)$ in addition to the exponential part:

$$\psi_1 = h_+(x) \frac{\Theta(\mathcal{A}(x) + k\sigma - i\omega\tau - \zeta_{\gamma_-(0)})\Theta(\mathcal{A}(\infty^+) - \zeta_{\gamma_-(0)})}{\Theta(\mathcal{A}(x) - \zeta_{\gamma_-(0)})\Theta(\mathcal{A}(\infty^+) + k\sigma - i\omega\tau - \zeta_{\gamma_-(0)})} \exp\left(\frac{i\sigma}{2\pi} \int_{\infty^+}^x dp + \frac{\tau}{2\pi} \int_{\infty^+}^x dq\right), \quad (2.77)$$

$$\psi_2 = h_-(x) \frac{\Theta(\mathcal{A}(x) + k\sigma - i\omega\tau - \zeta_{\gamma_+(0)})\Theta(\mathcal{A}(\infty^-) - \zeta_{\gamma_+(0)})}{\Theta(\mathcal{A}(x) - \zeta_{\gamma_+(0)})\Theta(\mathcal{A}(\infty^-) + k\sigma - i\omega\tau - \zeta_{\gamma_+(0)})} \exp\left(\frac{i\sigma}{2\pi} \int_{\infty^-}^x dp + \frac{\tau}{2\pi} \int_{\infty^-}^x dq\right). \quad (2.78)$$

As it is not our purpose here to review the details of the finite gap construction, below we will only explain the minimum of the ingredients and refer the reader to a review article such as [15]. Also, for simplicity and clarity, we will focus on the case of the degeneration from $g = 1$ to $g = 0$. This suffices to explain the essence of the construction and the generalization to the case of higher genus is straightforward.

For a $g = 1$ two-cut solution, the Riemann theta function $\Theta(z)$ reduces to the elliptic theta function $\theta(z)$ defined by

$$\theta(z) \equiv \sum_{m \in \mathbb{Z}} \exp(imz + \pi i \Pi m^2), \quad (2.79)$$

where Π is the period given by the integral of the holomorphic differential w over the b -cycle of the torus

$$\Pi = \oint_b w. \quad (2.80)$$

As usual, w is normalized by the integral over the a -cycle as $\oint_a w = 1$. $\mathcal{A}(x)$ appearing in the argument of the Θ -functions is the Abel map defined by

$$\mathcal{A}(x) = 2\pi \int_{\infty^+}^x w. \quad (2.81)$$

$h_{\pm}(x)$ are normalization constants and k and ω are the “momentum” and the “energy” defined by the integrals

$$k \equiv \frac{1}{2\pi} \oint_b dp, \quad \omega \equiv \frac{1}{2\pi} \oint_b dq. \quad (2.82)$$

A quantity of importance is the constant $\zeta_{\gamma_{\pm}(0)}$ defined by

$$\zeta_{\gamma_{\pm}(0)} \equiv \mathcal{A}(\gamma_{\pm}(0)) + \mathcal{K}, \quad (2.83)$$

In this formula, \mathcal{K} is the “vector of Riemann constants”, which for a torus is simply a number proportional to the period Π as¹³

$$\mathcal{K} = \pi\Pi. \quad (2.84)$$

¹³For its definition for a general genus g surface, see for example [21].

Finally $\gamma_{\pm}(0)$ are certain points¹⁴ on the Riemann surface, which determine the initial conditions for the solution.

Let us now study what happens when we pinch the a -cycle. In order to keep the normalization condition $\oint_a w = 1$ intact, w must behave near the position of the infinitesimal cut x_c as

$$w \sim \begin{cases} \frac{1}{2\pi i} \frac{1}{x-x_c} & \text{for } x \text{ on the first sheet} \\ -\frac{1}{2\pi i} \frac{1}{x-x_c} & \text{for } x \text{ on the second sheet} \end{cases} . \quad (2.85)$$

This means that the imaginary part of the period Π defined by the integral over the b -cycle approaches positive infinity in the manner

$$\Pi = \oint_b w \sim \frac{1}{2\pi i} \int_{x_c-\epsilon}^{x_c+\epsilon} \frac{dx}{x-x_c} \sim -\frac{i}{\pi} \ln \epsilon \rightarrow +i\infty . \quad (2.86)$$

Now writing the θ -function as

$$\theta(z) = \sum_{m \in \mathbb{Z}} \exp(imz + \pi i(\operatorname{Re} \Pi)m^2) \cdot \exp(-\pi \operatorname{Im} \Pi m^2) , \quad (2.87)$$

we see that the last factor vanishes as $\operatorname{Im} \Pi \rightarrow \infty$, except for $m = 0$. Therefore in this limit we get $\theta(z) \rightarrow 1$ and one gets the usual genus 0 solution with only the exponential part.

Now if we identify $z = k\sigma - i\omega\tau$ in the formulas for ψ_i given in (2.77) and (2.78), the arguments of the θ -functions containing z are actually of the form $z - a$, with a constant shift a given by $a = \zeta_{\gamma_{\pm}(0)} + \dots$. What is important is that $\zeta_{\gamma_{\pm}(0)}$ diverges as we pinch the a -cycle. First, obviously $\operatorname{Im} \mathcal{K}$ diverges as $\pi \operatorname{Im} \Pi$. Second, if $\gamma_{\pm}(0)$ is at the position of the shrunk cut x_c , $\operatorname{Im} \mathcal{A}(\gamma_{\pm}(0))$ diverges just like $\pi \operatorname{Im} \Pi$:

$$\mathcal{A}(\gamma_{\pm}(0)) = 2\pi \int_{\infty+}^{x_c+\epsilon} dw \sim 2\pi \frac{1}{2\pi i} \ln \epsilon \sim i\pi \operatorname{Im} \Pi \rightarrow i\infty . \quad (2.88)$$

Since $\mathcal{A}(\gamma_{\pm}(0))$ is finite otherwise, we must distinguish two cases: case (a) $\operatorname{Im} \zeta_{\gamma_{\pm}(0)} \sim 2\pi \operatorname{Im} \Pi$ for $\gamma_{\pm}(0) = x_c$ and case (b) $\operatorname{Im} \zeta_{\gamma_{\pm}(0)} \sim \pi \operatorname{Im} \Pi$ for $\gamma_{\pm}(0) \neq x_c$. Therefore let us write $a = l \operatorname{Im} \pi \Pi + c$, where $l = 2$ or $l = 1$ and c is a finite constant. Then the θ -function with this shift can be written as

$$\theta(z - a) = \sum_{m \in \mathbb{Z}} \exp(im(z - \pi \operatorname{Re} \Pi - c) + \pi i(\operatorname{Re} \Pi)m^2) \cdot \exp(-\pi \operatorname{Im} \Pi(m^2 - lm)) . \quad (2.89)$$

First consider the case (a). It is easy to see that terms with negative m all vanish in the limit $\operatorname{Im} \Pi \rightarrow \infty$. On the other hand, the terms with $m = 0$ and $m = 2$ are finite

¹⁴Precisely speaking, $\gamma_{\pm}(0)$ are certain divisors $\gamma_{\pm}(t)$ depending on the infinite set of higher times $t = (t_0, t_1, t_2, \dots)$ evaluated at $t = 0$. For a detailed definition, see [15].

and those with $m \geq 3$ vanish in the degeneration limit while the single term with $m = 1$ diverges. In other words,

$$\theta(z - a) \rightarrow \hat{C}e^{iz}, \quad \hat{C} \rightarrow \infty. \quad (2.90)$$

As the θ -functions occur in pairs in the numerator and the denominator in ψ_i , their ratio goes to a z -independent finite constant in the degeneration limit and we get back the usual $g = 0$ one-cut solution. In fact, by repeating this type of process, one can produce a finite gap solution from an infinite gap solution, which must be the generic situation for theories with infinite degrees of freedom, such as string theory.

Next consider the case (b). For $l = 1$, two terms in the series survive in the limit $\text{Im } \Pi \rightarrow \infty$, namely $m = 0$ and $m = 1$. Therefore we obtain a non-trivial function of the form

$$\theta(z - a) \rightarrow 1 + Ce^{iz} = 1 + Ce^{ik\sigma + \omega\tau}, \quad (2.91)$$

where C is a constant. In particular, this function can vanish at certain points, the number of which depend on the magnitude of k . Such a θ -function in the denominator of the expressions for ψ_i gives rise to additional simple poles on the worldsheet. In distinction to the singularity due to a vertex operator, these singularities do not carry any charges (including infinitely many higher charges) because the solution is obtained without changing the form of $p(x)$.

Although we will not explicitly make use of the degenerate multi-cut solutions discussed above in the bulk of our investigation, they will be recognized in section 7.5.2 as providing an example of a concrete mechanism by which extra singularities can be naturally produced. Existence of such singularities can modify the contours of the integrals that express the three-point coupling and may play an important role in the interpretation of our final result.

2.3 Some properties of the eigenvectors of the monodromy matrix

As described in the preceding subsections, the solutions of the ALP play the central role in the construction of the two-point solutions to the equations of motion. Now for the construction of the three-point functions, to be discussed starting from the next section, what will be of vital importance are the special linear combinations of the solutions of ALP, namely the eigenvectors of the local monodromy matrix Ω_i , defined around each vertex insertion point z_i . We will denote such eigenvectors and eigenvalues as i_{\pm} and $e^{\pm ip_i(x)}$, which satisfy the relations

$$\Omega_i i_{\pm} = e^{\pm p_i(x)} i_{\pm}. \quad (2.92)$$

In what follows, we will describe some important properties of i_{\pm} and related states.

Of crucial importance in the computation of three-point functions will be the $SL(2, \mathbb{C})$ invariant product for i_{\pm} and j_{\pm} given by

$$\langle i_{\pm}, j_{\pm} \rangle \equiv \det(i_{\pm}, j_{\pm}). \quad (2.93)$$

In the rest of the paper, we shall refer to this skew-product as *Wronskian*. Since the Wronskians are invariant under gauge transformations, we can use the results in various gauges interchangeably. For example, from the relation (2.50) between the eigenvectors in the sigma model formulation and the Pohlmeyer formulation, we have the equalities

$$\langle i_{\pm}, j_{\pm} \rangle = \langle \tilde{i}_{\pm}, \tilde{j}_{\pm} \rangle = \langle \hat{i}_{\pm}, \hat{j}_{\pm} \rangle. \quad (2.94)$$

For later convenience, let us fix the normalization of the eigenvectors i_{\pm} . We will first impose the usual condition

$$\langle i_{+}, i_{-} \rangle = 1. \quad (2.95)$$

This, however, does not fully fix the normalization of the individual eigenfunctions, as we can rescale i_{\pm} as $i_{+} \rightarrow ai_{+}$ and $i_{-} \rightarrow a^{-1}i_{-}$, without violating the condition (2.95). To determine the normalization completely, we will make use of the asymptotic behavior of i_{\pm} around the puncture z_i . For this purpose, it is convenient to employ the Pohlmeyer gauge, as it is invariant under the global symmetry transformation. Now although the explicit form of the solution for the three-point function is not known, it can be approximated by the solution for the two-point function in the vicinity of the vertex operators. Therefore, we can determine the normalization of \hat{i}_{\pm} by demanding that they coincide with the corresponding two-point functions at the insertion point of the vertex operator:

$$\hat{i}_{\pm}(x; \tau^{(i)}, \sigma^{(i)}) \longrightarrow \hat{i}_{\pm}^{2\text{pt}}(x; \tau = \tau^{(i)}, \sigma = \sigma^{(i)}). \quad (2.96)$$

In this formula, $(\tau^{(i)}, \sigma^{(i)})$ are the local cylinder coordinates around z_i , defined by

$$\tau^{(i)} + i\sigma^{(i)} = \ln \left(\frac{z - z_i}{\epsilon_i} \right). \quad (2.97)$$

Here we have chosen the origin of $\tau^{(i)}$ to be such that $\tau^{(i)} = 0$ on the small circle $|z - z_i| = \epsilon_i$, which will serve to separate the contributions from the action and the wave function in subsequent sections. Using the results of Appendix A, the eigenvectors for the two-point function $\hat{i}_{\pm}^{2\text{pt}}$ can be computed as

$$\hat{i}_{+}^{2\text{pt}}(x; \tau, \sigma) = \begin{pmatrix} \frac{e^{\pi i/8}}{\sqrt{2}} \left(\frac{x - \bar{u}_i}{x - u_i} \right)^{1/4} \left(\frac{\bar{u}_i^2 - 1}{u_i^2 - 1} \right)^{1/8} \\ \frac{e^{\pi i/8}}{\sqrt{2}} \left(\frac{x - u_i}{x - \bar{u}_i} \right)^{1/4} \left(\frac{u_i^2 - 1}{\bar{u}_i^2 - 1} \right)^{1/8} \end{pmatrix} \exp \left(\frac{q_i(x)\tau + ip_i(x)\sigma}{2\pi} \right), \quad (2.98)$$

$$\hat{i}_{-}^{2\text{pt}}(x; \tau, \sigma) = \begin{pmatrix} \frac{e^{-\pi i/8}}{\sqrt{2}} \left(\frac{x - \bar{u}_i}{x - u_i} \right)^{1/4} \left(\frac{\bar{u}_i^2 - 1}{u_i^2 - 1} \right)^{1/8} \\ -\frac{e^{-\pi i/8}}{\sqrt{2}} \left(\frac{x - u_i}{x - \bar{u}_i} \right)^{1/4} \left(\frac{u_i^2 - 1}{\bar{u}_i^2 - 1} \right)^{1/8} \end{pmatrix} \exp \left(-\frac{(q_i(x)\tau + ip_i(x)\sigma)}{2\pi} \right), \quad (2.99)$$

where u_i and \bar{u}_i are the positions of the branch points of the quasi-momentum $p_i(x)$ for the i -th puncture. The conditions (2.96), (2.98) and (2.99) determine the normalization of i_{\pm} completely. The important property of the eigenvectors so normalized is that they transform in the following way when they cross the branch cut¹⁵:

$$\hat{i}_+(x)\Big|_{\text{on 2nd sheet}} = \hat{i}_-(x)\Big|_{\text{on 1st sheet}}, \quad \hat{i}_-(x)\Big|_{\text{on 2nd sheet}} = -\hat{i}_+(x)\Big|_{\text{on 1st sheet}}. \quad (2.100)$$

This relation will be used in section 5.5 to determine the normalization of certain Wronskians.

3 Structures of the action for the S^3 part

Let us now start our study of the three-point functions. In what follows, we will denote their structure as

$$\langle \mathcal{V}_1 \mathcal{V}_2 \mathcal{V}_3 \rangle = \exp(F_{S^3} + F_{EAdS_3}), \quad (3.1)$$

where

$$F_{S^3} = \mathcal{F}_{\text{action}} + \mathcal{F}_{\text{vertex}}, \quad (3.2)$$

$$F_{EAdS_3} = \hat{\mathcal{F}}_{\text{action}} + \hat{\mathcal{F}}_{\text{vertex}}. \quad (3.3)$$

In this section, we focus on the contribution of the action for the S^3 part, namely $\mathcal{F}_{\text{action}}$. First, in subsection 3.1, we rewrite the action as a boundary contour integral using the Stokes theorem and then apply the generalized Riemann bilinear identity derived in [9] to bring it to a more convenient form. Next we turn in subsection 3.2 to the analysis of the WKB expansion of the auxiliary linear problem. We then find that the same contour integrals we used to rewrite the action appear also in the WKB expansion of the Wronskians of the solutions to the ALP. Using this relation, we re-express the action in terms of the Wronskians in subsection 3.3. The resultant expression will be used for the explicit evaluation of the contribution of the action in section 6.

3.1 Contour integral representation of the action

For the three-point function of our interest, the (regularized) action for the S^3 part of the string is given by

$$S_{S^3} = \frac{\sqrt{\lambda}}{\pi} \int_{\Sigma \setminus \{\epsilon_i\}} d^2z \partial Y_I \bar{\partial} Y_I, \quad (3.4)$$

¹⁵Note that the extra minus sign is necessary in the second equation of (2.100) in order to retain the condition (2.95).

where the symbol $\Sigma \setminus \{\epsilon_i\}$ denotes the worldsheet for the three-point function, which is a two-sphere with a small disk of radius ϵ_i cut out at each vertex operator insertion point z_i . Such a point will often be referred to as a puncture also. In [8] and [22], such worldsheet cut-offs are related to the spacetime cut-off in AdS in order to obtain the spacetime dependence of the correlation functions without introducing the vertex operators. In contrast, as we shall separately take into account the contribution of the vertex operators, ϵ_i 's can be taken to be arbitrary in our approach, as long as they are sufficiently small and the same for the S^3 part and the $EAdS_3$ part.

As the action is invariant under the global symmetry transformations, it is natural to express (3.4) in terms of the quantities used in the Pohlmeyer reduction. From (2.38), we can indeed write

$$S_{S^3} = \frac{\sqrt{\lambda}}{\pi} \int_{\Sigma \setminus \{\epsilon_i\}} d^2z \sqrt{T\bar{T}} \cos 2\gamma. \quad (3.5)$$

We further rewrite (3.5) by introducing the following one-forms:

$$\varpi \equiv \sqrt{T} dz, \quad (3.6)$$

$$\eta \equiv -\sqrt{\bar{T}} \cos 2\gamma d\bar{z} + \frac{2}{\sqrt{T}} \left(-(\partial\gamma)^2 + \frac{\rho^2}{T} \right) dz. \quad (3.7)$$

The second term on the right hand side of (3.7) is added to make η closed, as one can verify using the relation (2.44). With these one-forms, we can re-express the action (3.5) as a wedge product of the form

$$S_{S^3} = \frac{i\sqrt{\lambda}}{2\pi} \int_{\Sigma \setminus \{\epsilon_i\}} \varpi \wedge \eta, \quad (3.8)$$

where an extra prefactor $i/2$ comes from the definition of the volume form, $dz \wedge d\bar{z} = -2i d^2z$. Then denoting the integral of $\varpi(z)$ as

$$\Pi(z) = \int_{z_0}^z \varpi(z') dz', \quad (3.9)$$

the action can be rewritten, using the Stokes theorem, as a contour integral along a boundary $\partial\tilde{\Sigma}$ of a certain region $\tilde{\Sigma}$ (see figure 3.1):

$$S_{S^3} = \frac{i\sqrt{\lambda}}{4\pi} \int_{\tilde{\Sigma}} \varpi \wedge \eta = \frac{i\sqrt{\lambda}}{4\pi} \int_{\tilde{\Sigma}} d(\Pi\eta) = \frac{i\sqrt{\lambda}}{4\pi} \int_{\partial\tilde{\Sigma}} \Pi\eta. \quad (3.10)$$

To determine the proper region of integration $\tilde{\Sigma}$, we need to know the analytic structure of $\Pi(z)$, which in turn is dictated by that of $T(z)$. As already explained in section 2, in

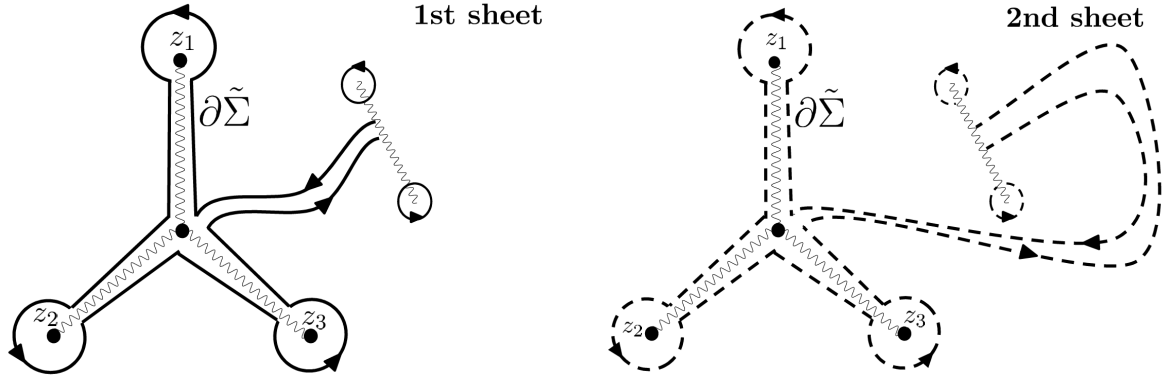


Figure 3.1: The contour $\partial\tilde{\Sigma}$ which forms the boundary of the double cover of the worldsheet $\tilde{\Sigma}$, depicted as the union of the first and the second sheet. There are three logarithmic branch cuts attached to the puncture in the middle, in addition to one square-root branch cut, shown as a wavy segment, through which the two sheets are connected.

the case of three-point functions the information of the asymptotic behavior of $T(z)$ at each puncture z_i is sufficiently restrictive to determine $T(z)$ exactly to be of the form

$$T(z) = \left(\frac{\kappa_1^2 z_{12} z_{13}}{z - z_1} + \frac{\kappa_2^2 z_{21} z_{23}}{z - z_2} + \frac{\kappa_3^2 z_{31} z_{32}}{z - z_3} \right) \frac{1}{(z - z_1)(z - z_2)(z - z_3)}, \quad (3.11)$$

$$z_{ij} \equiv z_i - z_j.$$

From this, one can show that $\Pi(z)$ has three logarithmic branch cuts running from the punctures z_i , and one square-root branch cut connecting two zeros of $T(z)$, to be denoted by t_1 and t_2 . Therefore, we should take $\tilde{\Sigma}$ to be the double cover ($y^2 = T(z)$) of the worldsheet Σ with an appropriate boundary $\partial\tilde{\Sigma}$, so that $\Pi(z)$ is single-valued on the whole integration region. In what follows, we will consider the case where the branch cut is located between z_1 and z_3 as depicted in figure 3.2. In such a case, the branch of the square-root of $T(z)$ can be chosen so that it behaves near the punctures on the first sheet as

$$\begin{aligned} \sqrt{T(z)} &\sim \frac{\kappa_i}{z - z_i} && \text{as } z \rightarrow z_i \quad (i = 1, 3), \\ &\sim \frac{-\kappa_2}{z - z_2} && \text{as } z \rightarrow z_2. \end{aligned} \quad (3.12)$$

Although the discussion to follow is tailored for this particular case, the final result for the three-point function, to be obtained in section 6, will turn out to be completely symmetric under the permutation of the punctures.

At this point, we shall apply the generalized Riemann bilinear identity, derived in [9], to the integral (3.10). As the derivation is lengthy, we refer the reader to [9] for details

and just present the result¹⁶. It can be written as

$$\int_{\tilde{\Sigma}} \varpi \wedge \eta = \text{Local} + \text{Double} + \text{Global} + \text{Extra}, \quad (3.13)$$

where the definition of each term will be given successively below¹⁷. The first term, **Local**, denotes the contribution from the product of contour integrals, each of which is just around the puncture and hence called “local”. It is of the form

$$\text{Local} = \sum_i \oint_{\mathcal{C}_i} \varpi \oint_{\mathcal{C}_i} \eta + \sum_{i < j} \left(\oint_{\mathcal{C}_i} \varpi \oint_{\mathcal{C}_j} \eta - (\varpi \leftrightarrow \eta) \right), \quad (3.14)$$

where \mathcal{C}_i is a contour encircling the puncture z_i counterclockwise. Here and hereafter, the symbol $(\varpi \leftrightarrow \eta)$ stands for the contribution obtained by exchanging ϖ and η in the preceding term. The second term, **Double**, denotes the double integrals around the punctures given by

$$\text{Double} = -2 \sum_i \oint_{\mathcal{C}_i} \eta \int_{z_i^*}^z \varpi. \quad (3.15)$$

The third term, **Global**, denotes the contribution from the product of contour integrals, one of which is along a contour connecting two different punctures. It is given by

$$\text{Global} = \left(\oint_{\mathcal{C}_1 + \mathcal{C}_2 - \mathcal{C}_3} \varpi \int_{\ell_{21}} \eta + \oint_{\mathcal{C}_2 + \mathcal{C}_3 - \mathcal{C}_1} \varpi \int_{\ell_{23}} \eta + \oint_{\mathcal{C}_3 + \mathcal{C}_1 - \mathcal{C}_2} \varpi \int_{\ell_{31}} \eta \right) - (\varpi \leftrightarrow \eta). \quad (3.16)$$

More precisely, ℓ_{ij} denotes the contour connecting z_i^* and z_j^* , where z_i^* is the point near the puncture z_i satisfying $z_i^* - z_i = \epsilon_i$. The barred indices indicate the points on the second sheet of the double cover $y^2 = T(z)$. For instance, $\mathcal{C}_{\bar{i}}$ is a contour encircling the point $z_{\bar{i}}$, which is on the second sheet right below z_i . Finally, the term **Extra** denotes additional terms which come from the integrals around the zeros of \sqrt{T} , to be denoted by t_k , at which η becomes singular, and is given by

$$\text{Extra} = \sum_k \oint_{\mathcal{D}_k} \Pi \eta. \quad (3.17)$$

Here \mathcal{D}_k is the contour which encircles t_k twice as depicted in figure 3.2.

Among these four terms, **Local** and **Double** are expressed solely in terms of the integrals around the punctures and are easy to compute. The explicit results, computed in

¹⁶By decomposing the contours ℓ_{ij} 's in (3.13) into d and ℓ_i 's defined in [9], we arrive at the formula derived in [9].

¹⁷In [8] and [22], the ordinary Riemann bilinear identity was applied to derive an expression similar to (3.13) but without the terms **Local** and **Double**. In their cases, **Local** and **Double** vanish and the use of the ordinary Riemann bilinear identity is justified. On the other hand, these two terms do not vanish in our case and we must use the generalized Riemann bilinear identity.

Appendix A.3 are¹⁸

$$\oint_{\mathcal{C}_i} \varpi = 2\pi i \kappa_i, \quad \oint_{\mathcal{C}_i} \eta = 2\pi i \kappa_i \Lambda_i, \quad (3.18)$$

$$\oint_{\mathcal{C}_i} \eta \int_{z_i^*}^z \varpi = -2\pi \kappa_i^2 \Lambda_i, \quad \text{for } i = 1, \bar{2}, 3. \quad (3.19)$$

Here Λ_i 's are given in terms of γ_i and ρ_i , defined in (A.21) and (A.22) respectively, as

$$\Lambda_i = \cos 2\gamma_i + \frac{2\rho_i^2}{\kappa_i^4}. \quad (3.20)$$

It is important to note that **Local** and **Double** are real since κ_i and g_i are all real. Therefore they contribute exclusively to the imaginary part of the action (3.10) and hence only yield an overall phase of the three-point functions. We shall neglect such quantities in this paper.

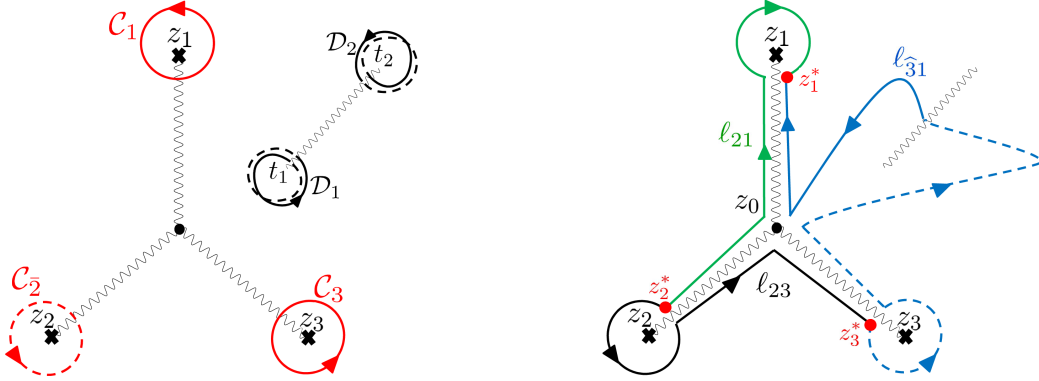


Figure 3.2: Definitions of the contours used to rewrite the action: The contours which enclose the punctures (\mathcal{C}_i) are shown in the left figure and the ones which connect two punctures (l_{ij}) are shown in the right figure. In both figures, the portions of the contours on the second sheet are drawn as dashed lines. Also depicted in the right figure are the starting points and the end points of the contours, z_i^* 's.

Among the remaining two types of terms, **Extra** can be explicitly evaluated as follows. Since the worldsheet is assumed to be smooth except at the punctures, the quantity $\sqrt{T\bar{T}} \cos 2\gamma$, which is the integrand of the action integral given in (3.5), should not vanish even at the zeros of $T(z)$. This in turn implies that γ is logarithmically divergent at such points in the manner

$$\gamma \sim \pm \frac{i}{2} \ln |z - t_k| \quad \text{as } z \rightarrow t_k. \quad (3.21)$$

¹⁸The one-forms ϖ and η flip the sign under the exchange of two sheets. Therefore (3.18) is odd whereas (3.19) is even under such sheet-exchange. In (3.19), κ_i for $i = \bar{2}$ is set to be equal to κ_2 .

Then, by approximating $T(z)$ as $T(z) \sim c(z - t_k)$ around t_k , we can write down the leading singular behavior of η around t_k as

$$\eta \sim -\frac{2}{\sqrt{T}}(\partial\gamma)^2 d\bar{z} \sim \frac{d\bar{z}}{8\sqrt{c}(z - t_k)^{5/2}}. \quad (3.22)$$

Thus the integral along \mathcal{D}_k can be computed as

$$\oint_{\mathcal{D}_k} \Pi\eta = \oint_{\mathcal{D}_k} \frac{2\sqrt{c}(z - t_k)^{3/2}}{3} \frac{d\bar{z}}{8\sqrt{c}(z - t_k)^{5/2}} = -\frac{\pi i}{6}. \quad (3.23)$$

Since there exist two zeros, **Extra** is twice this integral and hence is given by

$$\text{Extra} = -\frac{\pi i}{3}. \quad (3.24)$$

For later convenience, we shall derive another expression for the action using a different set of one-forms given by

$$\bar{\varpi} = \sqrt{T}d\bar{z}, \quad (3.25)$$

$$\tilde{\eta} = -\sqrt{T} \cos 2\gamma dz + \frac{2}{\sqrt{T}} \left(-(\bar{\partial}\gamma)^2 + \frac{\rho^2}{T} \right) d\bar{z}, \quad (3.26)$$

and then consider the average of the two expressions. Using the forms above, the action can be written as

$$S_{S^3} = -\frac{i\sqrt{\lambda}}{4\pi} \int_{\hat{\Sigma}} \bar{\varpi} \wedge \tilde{\eta}. \quad (3.27)$$

As compared to (3.10), the expression (3.27) has an extra minus sign, which is due to the property $dz \wedge d\bar{z} = -d\bar{z} \wedge dz$. Applying the generalized Riemann bilinear identity to (3.27), we get

$$-\int_{\hat{\Sigma}} \bar{\varpi} \wedge \tilde{\eta} = -(\overline{\text{Local}} + \overline{\text{Double}} + \overline{\text{Global}} + \overline{\text{Extra}}), \quad (3.28)$$

where $\overline{\text{Local}}$, $\overline{\text{Double}}$ and $\overline{\text{Global}}$ are given respectively by (3.14), (3.15) and (3.16) with ϖ and η replaced by $\bar{\varpi}$ and $\tilde{\eta}$. The integrals of $\bar{\varpi}$ and $\tilde{\eta}$ around the punctures are given by¹⁹

$$\oint_{\mathcal{C}_i} \bar{\varpi} = -2\pi i \kappa_i, \quad \oint_{\mathcal{C}_i} \tilde{\eta} = -2\pi i \kappa_i \bar{\Lambda}_i, \quad (3.29)$$

$$\oint_{\mathcal{C}_i} \tilde{\eta} \int_{z_i^*}^z \bar{\varpi} = -2\pi \kappa_i^2 \bar{\Lambda}_i, \quad \text{for } i = 1, \hat{2}, 3 \quad (3.30)$$

where $\bar{\Lambda}_i$'s are given in terms of γ_i and $\tilde{\rho}_i$, defined in Appendix A.2, as

$$\bar{\Lambda}_i = \cos 2\gamma_i + \frac{2\tilde{\rho}_i^2}{\kappa_i^4}. \quad (3.31)$$

¹⁹(3.29) is odd and (3.30) is even under the exchange of the first and the second sheets, as in the case of the integrals of ϖ and η given in (3.18) and (3.19).

Again $\overline{\text{Local}}$ and $\overline{\text{Double}}$ are real and they contribute only to the overall phase. On the other hand, $\overline{\text{Extra}}$ can be evaluated just like Extra and yields $+\pi i/3$. Thus, by averaging over the two expressions (3.13) and (3.28) and neglecting terms which contribute exclusively to the overall phase, we arrive at the following more symmetric expression:

$$\frac{1}{2} \left(\int_{\tilde{\Sigma}} \varpi \wedge \eta - \int_{\tilde{\Sigma}} \bar{\varpi} \wedge \tilde{\eta} \right) = -\frac{\pi i}{3} + \frac{1}{2} (\text{Global} - \overline{\text{Global}}) . \quad (3.32)$$

The quantity (3.32) consists of various integrals along the contours \mathcal{C}_i and ℓ_{ij} . Among them, the ones along \mathcal{C}_i can be easily computed using (3.18) and (3.29). The integral of ϖ along ℓ_{ij} can also be computed in principle as we know the explicit form of ϖ . Thus the major nontrivial task is the evaluation of $\int_{\ell_{ij}} \eta$ and $\int_{\ell_{ij}} \tilde{\eta}$. In the rest of this section, we will see how these integrals are related to the Wronskians of the form $\langle i_{\pm}, j_{\pm} \rangle$, where i_{\pm} are the Baker-Akhiezer eigenvectors at z_i of the ALP, corresponding to the eigenvalues $e^{\pm ip_i(x)}$.

3.2 WKB expansions of the auxiliary linear problem

We now perform the WKB expansion of the auxiliary linear problem and observe that the contour integrals of our interest, $\int_{\ell_{ij}} \eta$ and $\int_{\ell_{ij}} \tilde{\eta}$, appear in the expansion of the Wronskians between the eigenvectors of the monodromy matrices.

Let us first consider the WKB expansion of the solutions to the ALP. For this purpose, it is convenient to use the ALP of the Pöhlmeier reduction (2.49). The use of (2.49) has two main virtues. First, as Φ 's are given explicitly in terms of $T(z)$ and $\bar{T}(\bar{z})$, it is easier to perform the expansion around $\zeta = 0$ or around $\zeta = \infty$. Second, since the connection (2.47) is expressed solely in terms of the quantities invariant under the global symmetry transformation, we can directly explore the dynamical aspect of the problem setting aside all the kinematical information.

We shall first perform the expansion around $\zeta = 0$. To facilitate this task, it is convenient to perform a further gauge transformation and convert (2.49) to the “diagonal gauge”, where the ALP take the form

$$\left(\partial + \frac{1}{\zeta} \Phi_z^d + A_z^d \right) \hat{\psi}^d = 0, \quad (\bar{\partial} + \zeta \Phi_{\bar{z}}^d + A_{\bar{z}}^d) \hat{\psi}^d = 0. \quad (3.33)$$

In the above, $\hat{\psi}^d$ in the diagonal gauge is defined by

$$\hat{\psi}^d \equiv \frac{1}{\sqrt{2}} \begin{pmatrix} e^{i\gamma/2} & -e^{-i\gamma/2} \\ e^{i\gamma/2} & e^{-i\gamma/2} \end{pmatrix} \hat{\psi}, \quad (3.34)$$

and $\Phi^{d'}$'s and $A^{d'}$'s are given by

$$\begin{aligned}\Phi_z^d &= \frac{\sqrt{T}}{2} \begin{pmatrix} 1 & 0 \\ 0 & -1 \end{pmatrix}, & \Phi_{\bar{z}}^d &= \frac{\sqrt{T}}{2} \begin{pmatrix} -\cos 2\gamma & i \sin 2\gamma \\ -i \sin 2\gamma & \cos 2\gamma \end{pmatrix}, \\ A_z^d &= \begin{pmatrix} -\frac{\rho}{\sqrt{T}} \cot 2\gamma & \frac{i\rho}{\sqrt{T}} - i\partial\gamma \\ -\frac{i\rho}{\sqrt{T}} - i\partial\gamma & \frac{\rho}{\sqrt{T}} \cot 2\gamma \end{pmatrix}, & A_{\bar{z}}^d &= \frac{-\tilde{\rho}}{\sqrt{T} \sin 2\gamma} \begin{pmatrix} 1 & 0 \\ 0 & -1 \end{pmatrix}.\end{aligned}\quad (3.35)$$

Note that the leading terms in the ALP equations as $\zeta \rightarrow 0$, namely Φ_z^d for the first equation and $A_{\bar{z}}^d$ for the second, have been diagonalized. Because of this feature, the leading exponential behavior of the two linearly independent solutions around $\zeta \sim 0$ can be readily determined as

$$\hat{\psi}_1^d \sim \begin{pmatrix} 0 \\ 1 \end{pmatrix} \exp \left[\frac{1}{2\zeta} \int_{z_0}^z \varpi \right], \quad \hat{\psi}_2^d \sim \begin{pmatrix} 1 \\ 0 \end{pmatrix} \exp \left[\frac{-1}{2\zeta} \int_{z_0}^z \varpi \right], \quad (3.36)$$

By performing the WKB expansion around $\zeta \sim 0$ systematically, one can also determine the subleading terms of (3.36) in ζ , as shown in Appendix D.1.

The quantities of prime interest in the subsequent discussions are the Wronskians of the eigenvectors of the monodromy matrices. To perform the WKB expansion of such Wronskians, we need to have a good control over the asymptotics of the Wronskians $\langle i_{\pm}, j_{\pm} \rangle$ around $\zeta = 0$. For this purpose, both of the eigenvectors in the Wronskian need to be small solutions since big solutions can contain a multiple of small solutions and hence are ambiguous [23–26]. When ζ is sufficiently close to zero, one can show that the plus solutions i_+ are the small solutions if $\text{Re } \zeta$ is positive whereas it is the minus solutions i_- which are small if $\text{Re } \zeta$ is negative. Thus, the Wronskians that can be expanded consistently around $\zeta = 0$ are $\langle i_+, j_+ \rangle$'s for $\text{Re } \zeta > 0$ and $\langle i_-, j_- \rangle$'s for $\text{Re } \zeta < 0$. The detailed form of the expansion can be determined by employing the Born series expansion explained in Appendix D.2 and the results are given in the following simple form:

For $\text{Re } \zeta > 0$,

$$\langle 2_+, 1_+ \rangle = \exp(-S_{2 \rightarrow 1}), \quad \langle 2_+, 3_+ \rangle = \exp(-S_{2 \rightarrow 3}), \quad \langle 3_+, 1_+ \rangle = \exp(-S_{3 \rightarrow 1}), \quad (3.37)$$

For $\text{Re } \zeta < 0$,

$$\langle 2_-, 1_- \rangle = \exp(S_{2 \rightarrow 1}), \quad \langle 2_-, 3_- \rangle = \exp(S_{2 \rightarrow 3}), \quad \langle 1_-, 3_- \rangle = \exp(S_{3 \rightarrow 1}). \quad (3.38)$$

In these expressions, $S_{i \rightarrow j}$ stands for the quantity

$$S_{i \rightarrow j} = \frac{1}{2\zeta} \int_{\ell_{ij}} \varpi + \int_{\ell_{ij}} \alpha + \frac{\zeta}{2} \int_{\ell_{ij}} \eta + \dots, \quad (3.39)$$

where the one-form α is given in (D.41) in Appendix D.2. A remarkable feature of (3.39) is that the integral of our interest $\int_{\ell_{ij}} \eta$ makes its appearance in the exponent $S_{i \rightarrow j}$.

Now to make use of the averaging procedure described in the previous subsection, we need the other type of integrals $\int_{\ell_{ij}} \tilde{\eta}$ which appear in $\overline{\text{Global}}$. To obtain them, we need to expand the Wronskians this time around $\zeta = \infty$. Since the discussion is similar to the expansion around $\zeta = 0$, we will not elaborate on the details and simply give the results:

For $\text{Re } \zeta > 0$,

$$\langle 2_+, 1_+ \rangle = \exp\left(-\tilde{S}_{2 \rightarrow 1}\right), \quad \langle 2_+, 3_+ \rangle = \exp\left(-\tilde{S}_{2 \rightarrow 3}\right), \quad \langle 3_+, 1_+ \rangle = \exp\left(-\tilde{S}_{3 \rightarrow 1}\right), \quad (3.40)$$

For $\text{Re } \zeta < 0$,

$$\langle 2_-, 1_- \rangle = \exp\left(\tilde{S}_{2 \rightarrow 1}\right), \quad \langle 2_-, 3_- \rangle = \exp\left(\tilde{S}_{2 \rightarrow 3}\right), \quad \langle 1_-, 3_- \rangle = \exp\left(\tilde{S}_{3 \rightarrow 1}\right), \quad (3.41)$$

Here $\tilde{S}_{i \rightarrow j}$ is defined by

$$\tilde{S}_{i \rightarrow j} = \frac{\zeta}{2} \int_{\ell_{ij}} \bar{\varpi} + \int_{\ell_{ij}} \tilde{\alpha} + \frac{1}{2\zeta} \int_{\ell_{ij}} \tilde{\eta} + \dots, \quad (3.42)$$

where $\tilde{\alpha}$ is a one-form given in (D.42) in Appendix D.2. Making use of these two types of expansions, we will be able to rewrite the action in terms of the Wronskians, as described in the next subsection.

3.3 The action in terms of the Wronskians

We are now ready to derive an explicit expression of the action in terms of the Wronskians. As shown in the previous subsection, the integrals we used to rewrite the action, namely $\oint_{\ell_{ij}} \eta$ and $\oint_{\ell_{ij}} \tilde{\eta}$, can be extracted from the Wronskians. For instance, consider the integral $\oint_{\ell_{21}} \eta$, which appears in $\langle 2_-, 1_- \rangle$. Differentiating $\ln\langle 2_-, 1_- \rangle$ with respect to ζ using (3.38) and (3.39), we get

$$\partial_\zeta \ln\langle 2_-, 1_- \rangle = -\frac{1}{\zeta^2} \int_{\ell_{21}} \bar{\varpi} + \frac{1}{2} \int_{\ell_{21}} \eta + O(\zeta). \quad (3.43)$$

Therefore we can get the integral $\oint_{\ell_{21}} \eta$ by subtracting the first divergent term and then taking the limit $\zeta \rightarrow 0$. Similarly $\oint_{\ell_{21}} \tilde{\eta}$ can be obtained from $\langle 2_-, 1_- \rangle$ in the $\zeta \rightarrow \infty$ limit. Such procedures can be compactly implemented if we use the variable x instead of ζ , which are related as in (2.46). Then, we can write

$$\oint_{\ell_{21}} \eta = -4 : \partial_x \ln\langle 2_-, 1_- \rangle :_+, \quad \oint_{\ell_{21}} \tilde{\eta} = -4 : \partial_x \ln\langle 2_-, 1_- \rangle :_-, \quad (3.44)$$

where the ‘‘normal ordering’’ symbol $:A(x):_\pm$ is defined by

$$:A(x):_\pm \equiv \lim_{x \rightarrow \pm 1} [A(x) - (\text{double pole at } x = \pm 1)]. \quad (3.45)$$

This precisely subtracts the divergent term mentioned above. Substituting such expressions to the definitions of **Global** and $\overline{\text{Global}}$, we can express them in terms of the Wronskians. Then, using (3.32), we arrive at the following expression for the contribution from the S^3 part of the action $\mathcal{F}_{\text{action}}$:

$$\mathcal{F}_{\text{action}} = -S_{S^3} = \frac{\sqrt{\lambda}}{6} + \mathcal{A}_{\varpi} + \mathcal{A}_{\eta}. \quad (3.46)$$

The first term in (3.46) expresses the contributions of **Extra** and $\overline{\text{Extra}}$. The second term \mathcal{A}_{ϖ} denotes the contribution of $\int_{\ell_{ij}} \varpi$ and $\int_{\ell_{ij}} \bar{\varpi}$ in **Global** and $\overline{\text{Global}}$ and is given by

$$\begin{aligned} \mathcal{A}_{\varpi} = & \frac{\sqrt{\lambda}}{4} \left((\kappa_1 \Lambda_1 + \kappa_2 \Lambda_2 - \kappa_3 \Lambda_3) \int_{\ell_{21}} \varpi + (\kappa_1 \Lambda_1 - \kappa_2 \Lambda_2 + \kappa_3 \Lambda_3) \int_{\ell_{31}} \varpi \right. \\ & \left. + (-\kappa_1 \Lambda_1 + \kappa_2 \Lambda_2 + \kappa_3 \Lambda_3) \int_{\ell_{23}} \varpi \right) + (\Lambda_i \rightarrow \bar{\Lambda}_i, \varpi \rightarrow \bar{\varpi}), \end{aligned} \quad (3.47)$$

where Λ_i and $\bar{\Lambda}_i$ are as given in (3.20) and (3.31) and $(\Lambda_i \rightarrow \bar{\Lambda}_i, \varpi \rightarrow \bar{\varpi})$ in the last line denotes the terms obtained by replacing Λ_i and ϖ in the second line with $\bar{\Lambda}_i$ and $\bar{\varpi}$ respectively. The third term \mathcal{A}_{η} is the contribution of $\int_{\ell_{ij}} \eta$ and $\int_{\ell_{ij}} \tilde{\eta}$, which is expressed in terms of the Wronskians in the following way:

$$\begin{aligned} \mathcal{A}_{\eta} = & \sqrt{\lambda} \left[(\kappa_1 + \kappa_2 - \kappa_3) (\cdot \partial_x \ln \langle 2_-, 1_- \rangle \cdot_+ - \cdot \partial_x \ln \langle 2_+, 1_+ \rangle \cdot_-) \right. \\ & + (\kappa_1 - \kappa_2 + \kappa_3) (\cdot \partial_x \ln \langle 3_-, 1_- \rangle \cdot_+ - \cdot \partial_x \ln \langle 3_+, 1_+ \rangle \cdot_-) \\ & \left. + (-\kappa_1 + \kappa_2 + \kappa_3) (\cdot \partial_x \ln \langle 2_-, 3_- \rangle \cdot_+ - \cdot \partial_x \ln \langle 2_-, 3_- \rangle \cdot_-) \right]. \end{aligned} \quad (3.48)$$

The general formula (3.46) will later be used in section 6 to compute the three-point functions.

4 Structure of the contribution from the vertex operators

Having found the structure of the contribution of the action part, we shall now study that of the vertex operators.

4.1 Basic idea and framework

Before plunging into the details of the analysis, let us describe in this subsection the basic idea and the framework, which includes a brief review of the methods developed in our previous work [11].

As explained in detail in [9], the precise form of the conformally invariant vertex operator corresponding to a string solution in a curved spacetime, such as AdS_3 discussed there or $EAdS_3 \times S^3$ of our interest in this paper, is in general not known. In particular, for a non-BPS solution with non-trivial σ dependence the corresponding vertex operator would contain infinite number of derivatives and is hard to construct. To overcome this difficulty, we have developed in [11] a powerful method of computing the contribution of the vertex operators by using the state-operator correspondence and the construction of the corresponding wave function in terms of the action-angle variables. Although it was applied in [11] to the case of the GKP string in AdS_3 , the basic idea of the method is applicable to more general situations, including the present one, albeit with appropriate modifications and refinements.

Let us briefly review the essential ingredients of the method. (For details, see section 3 of [11].) The state-operator correspondence, in the semi-classical approximation, is expressed by the following equation:

$$\mathcal{V}[q_*(z=0)]e^{-S_{q_*}(\tau<0)} = \Psi[q_*]|_{\tau=0}. \quad (4.1)$$

Here q_* signifies the saddle point configuration, $\mathcal{V}[q_*(z=0)]$ is the value of the vertex operator inserted at the origin of the worldsheet $z = e^{\tau+i\sigma} = 0$, corresponding to the cylinder time $\tau = -\infty$, the factor $\exp[-S_{q_*}(\tau < 0)]$ is the amplitude to develop into the state on a unit circle and the $\Psi[q_*]|_{\tau=0}$ is the semi-classical wave function describing the state on that circle. In particular, if we can construct the action-angle variables (S_i, ϕ_i) of the system and use $\{\phi_i\}$ as q , then the wave function evaluated at the cylinder time τ can be expressed simply as

$$\Psi[\phi] = \exp\left(i \sum_i S_i \phi_i - \mathcal{E}(\{S_i\})\tau\right), \quad (4.2)$$

where the action variables S_i and the worldsheet energy $\mathcal{E}(\{S_i\})$ are constant.

In the case of the classical string in $R \times S^3$, the method for the construction of the action-angle variables was developed in [13–15], employing the so-called Sklyanin’s separation of variables [16]. This method was adapted to the case of the GKP string in AdS_3 in [11] and, as we shall see, can be applied to the present case of the string in $EAdS_3 \times S^3$ with appropriate modifications. In this method, the essential dynamical information is contained in the two-component Baker-Akhiezer vectors ψ_{\pm} , which satisfy the ALP for the right sector and are the eigenvectors of the monodromy matrix Ω

$$\Omega(x; \tau, \sigma)\psi_{\pm}(x; \tau, \sigma) = e^{\pm ip(x)}\psi_{\pm}(x; \tau, \sigma). \quad (4.3)$$

More precisely, the dynamical information is encoded in the normalized Baker-Akhiezer vector $h(x; \tau)$, defined to be proportional to $\psi(x; \tau, \sigma = 0)$ (conventionally taken to be

ψ_+) and satisfying the normalization condition

$$n \cdot h = n_1 h_1 + n_2 h_2 = 1, \quad h = \frac{1}{n \cdot \psi} \psi, \quad (4.4)$$

where n is called the *normalization vector*. For a finite gap solution associated to a genus g algebraic curve, $h(x; \tau)$ as a function of x is known to have $g + 1$ poles at the positions $x = \{\gamma_1, \gamma_2, \dots, \gamma_{g+1}\}$ and the dynamical variables $z(\gamma_i)$ and $p(\gamma_i)$, where z is the Zhukovsky variable defined in (2.36), can be shown to form canonical conjugate pairs. Then by making a suitable canonical transformation, one can go to the action-angle pairs (S_i, ϕ_i) , where, in particular, the angle variable is given by the generalized Abel map

$$\phi_i = 2\pi \sum_j \int_{x_0}^{\gamma_j} \omega_i. \quad (4.5)$$

Here, ω_i are suitably normalized holomorphic differentials (with certain singularities depending on the specific problem) and x_0 is an arbitrary base point. Now since one can reconstruct the classical string solution from the Baker-Akhiezer vector ψ (and $\tilde{\psi}$, which is the solution of the left ALP) as shown in (2.65) and (2.66), with a choice of the normalization vector n one can associate a set of angle variables ϕ_i to a classical solution. In fact, the angle variables can be thought to be determined by the quantity $n \cdot \psi$, since the poles of the normalized vector h occur at the zeros of $n \cdot \psi$, as is clear from (4.4). As we are actually dealing with a quantum system using semi-classical approximation, a classical solution should be thought of as being produced by a quantum vertex operator carrying a large charge. Further, since in our framework the vertex operator is replaced by the corresponding wave function, the angle variables defined through a classical solution should be used to describe the wave function of the corresponding semiclassical state.

Now the serious problem is that we do not know the exact saddle point solution for the three-point function. The only information we know is that in the vicinity of each vertex insertion point z_i , the exact three-point solution, to be represented by a 2×2 matrix \mathbb{Y} given by

$$\mathbb{Y} = \begin{pmatrix} Z_1 & Z_2 \\ -\bar{Z}_2 & \bar{Z}_1 \end{pmatrix}, \quad Z_1 = Y_1 + iY_2, \quad Z_2 = Y_3 + iY_4, \quad (4.6)$$

which must be almost identical to the two-point solution produced by the same vertex operator. Let us denote such a solution by \mathbb{Y}^{ref} and call it a reference solution. As we have to normalize the three-point function precisely by such a two-point function for each leg, what is important is the difference between \mathbb{Y} and \mathbb{Y}^{ref} . Note that even if they are produced by the same vertex operator, they are different because \mathbb{Y} is influenced by the presence of other vertex operators in the three-point function.

Here and in what follows, the global isometry group $G = \text{SU}(2)_L \times \text{SU}(2)_R$ and its complexification $G^c = \text{SL}(2, \mathbb{C})_L \times \text{SL}(2, \mathbb{C})_R$ play the central roles. Being the symmetry

groups of the equations of motion (and the Virasoro conditions), two solutions of the equations of motion are connected by the action of G and/or G^c . The difference between their actions are that (when expressed in terms of the Minkowski worldsheet variables) while G connects a real solution to a real solution, G^c transforms a real solution to a complex solution. Since the three-point interaction is inherently a tunneling process, the saddle point solution for such a process must be complex. Therefore near z_i the two solutions \mathbb{Y} and \mathbb{Y}^{ref} must be connected by an element of G^c in the manner

$$\mathbb{Y} = \tilde{V}\mathbb{Y}^{\text{ref}}V, \quad \tilde{V} \in \text{SL}(2, \mathbb{C})_L, V \in \text{SL}(2, \mathbb{C})_R \quad (4.7)$$

This means that the angle variables associated to \mathbb{Y} , as defined relative to the ones associated to \mathbb{Y}^{ref} , should be computable from the knowledge of the transformation matrices \tilde{V} and V . This connection was made completely explicit in [11] and the master formulas giving such shifts of the angle variables were obtained. Corresponding to the solutions $\psi(x)$ and $\tilde{\psi}(x)$ of the the right and the left ALP respectively, there are right angle variable ϕ_R and the left angle variable ϕ_L . Their shifts are given by²⁰

$$\Delta\phi_R = -i \ln \left(\frac{(n \cdot \psi_+(\infty))(n \cdot \psi_-^{\text{ref}}(\infty))}{(n \cdot \psi_+^{\text{ref}}(\infty))(n \cdot \psi_-(\infty))} \right), \quad (4.8)$$

$$\Delta\phi_L = -i \ln \left(\frac{(\tilde{n} \cdot \tilde{\psi}_+(0))(\tilde{n} \cdot \tilde{\psi}_-^{\text{ref}}(0))}{(\tilde{n} \cdot \tilde{\psi}_+^{\text{ref}}(0))(\tilde{n} \cdot \tilde{\psi}_-(0))} \right) \quad (4.9)$$

where n and \tilde{n} are the normalization vectors for the right and the left sector and $\psi_{\pm}(x)$ and $\psi_{\pm}^{\text{ref}}(x)$ are the Baker-Akhiezer eigenvectors corresponding to the solutions \mathbb{Y} and \mathbb{Y}^{ref} respectively and are related by

$$\psi_{\pm} = V^{-1}\psi_{\pm}^{\text{ref}}, \quad \tilde{\psi}_{\pm} = \tilde{V}\tilde{\psi}_{\pm}^{\text{ref}}. \quad (4.10)$$

How V and \tilde{V} can be obtained will be described in detail in subsection 4.3.

The remaining problem is to fix the normalization vectors n and \tilde{n} , relevant for the left and the right sectors. In the case of the string which is entirely in AdS_3 [11], we fixed them by the following argument. Consider for simplicity the wave function corresponding to a conformal primary operator of the gauge theory sitting at the origin of the boundary of AdS_5 . Such an operator is characterized by the invariance under the special conformal transformation. Therefore the corresponding wave function and the angle variables comprising it should also be invariant. Explicitly it requires that $n \cdot \psi$ and $\tilde{n} \cdot \tilde{\psi}$ must be preserved under the special conformal transformation and this determined n and \tilde{n} .

²⁰These equations are obtained from the fundamental formula (3.74) of [11] by substituting the definition of the function $f(x)$ given in (3.62) of the same reference and noting the expression of the function $h(x)$ shown in (4.4) of this paper.

The essence of the argument we shall employ for the case of a string in $EAdS_3 \times S^3$ studied in the present work is the same. However because the structures of the gauge theory operators and the corresponding string solutions are more complicated, we need to generalize and refine the argument. As a result of this improvement, not only has the determination of the normalization vectors become more systematic but also their physical meaning has been identified more clearly. Moreover, the entire procedure of the constructions of the wave functions for the S^3 part and the $EAdS_3$ part has become completely parallel and transparent. Below we shall begin the analysis first from the gauge theory side.

4.2 Characterization of the gauge theory operators by symmetry properties

As sketched above, in order to construct the wave functions expressing the effect of the insertion of the vertex operators, we must study how to characterize the global symmetry properties of the vertex operators and the classical configurations that they produce in their vicinity.

For this purpose, it is convenient to first look at the symmetry properties of the corresponding gauge theory operators. The three composite operators $\mathcal{O}_1(x_1), \mathcal{O}_2(x_2), \mathcal{O}_3(x_3)$ making up the three-point functions in the so-called ‘‘SU(2) sector’’ are composed of the complex scalar fields $Z \equiv \Phi_1 + i\Phi_2$, $X \equiv \Phi_3 + i\Phi_4$ and their complex conjugates \bar{Z} and \bar{X} , where Φ_I ($I = 1, 2, 3, 4$) are four of the six real hermitian fields in the adjoint representation of the gauge group. Under the global symmetry group $SO(4) = SU(2)_R \times SU(2)_L$, these fields transform in the doublet representations of $SU(2)_R$ and $SU(2)_L$ with the right and the left charges \mathcal{R} and \mathcal{L} given in Table 1:

Table 1. The $SU(2)_R$ and $SU(2)_L$ charges for the basic scalar fields.

	\mathcal{R}	\mathcal{L}
Z	+1/2	+1/2
\bar{Z}	-1/2	-1/2
X	-1/2	+1/2
\bar{X}	+1/2	-1/2

Table 2. Roles of the scalar fields for the operators \mathcal{O}_i .

	vacuum	excitation
\mathcal{O}_1	Z	X
\mathcal{O}_2	\bar{Z}	\bar{X}
\mathcal{O}_3	Z	\bar{X}

These transformation properties are succinctly represented by the 2×2 matrix

$$\Phi = \begin{pmatrix} Z & X \\ -\bar{X} & \bar{Z} \end{pmatrix}, \quad (4.11)$$

which gets transformed as $U_L \Phi U_R$, where $U_L \in SU(2)_L, U_R \in SU(2)_R$. In spite of this $SO(4)$ symmetry, in the existing literature [27] the operators \mathcal{O}_i are taken to be com-

posed of a special pair of fields²¹ indicated in Table 2. For example, \mathcal{O}_1 is of the form $\text{tr}(ZZ \cdots XZZX \cdots Z)$. In the spin-chain interpretation, Z and X represent the up and the down spin respectively so that \mathcal{O}_1 is a state built upon the all-spin-up vacuum state $\text{tr} Z^l$ on l sites by flipping some of the up-spins into the down-spins which represent excitations. Therefore at each site there is an $\text{SU}(2)$ group acting on a spin, and according to Table 1 it is identified with $\text{SU}(2)_R$ for this case. For the entire operator \mathcal{O}_1 , what is relevant is the total $\text{SU}(2)_R$, the generator of which will be denoted by S_R^i .

Let us now characterize the spin-chain states corresponding to the operators of the type \mathcal{O}_1 from the point of view of this total $\text{SU}(2)_R$. First, since the constituents Z and X carry definite spin quantum numbers, every state of type \mathcal{O}_1 carries a definite right and left global charges. Second, every such state is actually a highest weight state annihilated by the operator $S_R^+ = S_R^1 + iS_R^2$. For the vacuum state $|Z^l\rangle = |\uparrow^l\rangle$ it is obvious. As for the excited states, they can be written as the Bethe states $\prod_{i=1} B(u_i)|\uparrow^l\rangle$, where $B(u_i)$ is the familiar magnon creation operator carrying the spectral parameter u_i . It is well-known [28] that such a state is a highest weight state of the total $\text{SU}(2)_R$ and hence annihilated by the same S_R^+ , provided that the Bethe state is “on-shell”, namely that the spectral parameters satisfy the Bethe ansatz equations. Therefore we have found that kinematically all the operators of type \mathcal{O}_1 can be characterized as the highest weight state of the total $\text{SU}(2)_R$.

Now in order to deal with other operators built upon a “vacuum state” different from $\text{tr} Z^l$, let us introduce the general linear combinations of Φ_I as $\vec{P} \cdot \vec{\Phi} = \sum_{I=1}^4 P_I \Phi_I$. To discuss the transformation property under $\text{SU}(2)_R \times \text{SU}(2)_L$, it is more convenient to deal with the matrix

$$\mathbb{P} \equiv \begin{pmatrix} P_1 + iP_2 & P_3 + iP_4 \\ -(P_3 - iP_4) & P_1 - iP_2 \end{pmatrix} = P_I \Sigma_I, \quad (4.12)$$

$$\Sigma_I \equiv (1, i\sigma_3, i\sigma_2, i\sigma_1). \quad (4.13)$$

Then, we have the representation

$$\vec{P} \cdot \vec{\Phi} = \frac{1}{2} \text{tr} (\sigma_2 \mathbb{P}^t \sigma_2 \Phi). \quad (4.14)$$

In this notation, \mathbb{P} corresponding to Z, \bar{Z}, X, \bar{X} take the form $\mathbb{P}_Z = 1 - \sigma_3, \mathbb{P}_{\bar{Z}} = 1 + \sigma_3, \mathbb{P}_X = -(\sigma_1 - i\sigma_2), \mathbb{P}_{\bar{X}} = \sigma_1 + i\sigma_2$.

As we argued above, all the on-shell states built upon a common vacuum are annihilated by the same S_R^+ . In other words as long as the global transformation property is concerned, the vacuum state can be considered as the representative of all the states built

²¹The reason for this choice is that it is the simplest one that can produce non-extremal three-point functions.

upon it. Further, since the local spin state is identical at each site for the vacuum state we can characterize the vacuum by the form of the “annihilation operator” s_R^+ acting on a single spin state. As it will be slightly more convenient, instead of the annihilation operator, we will use the “raising operator” $K = \exp(\alpha s_R^+)$, where α is any constant. The vacuum is then characterized by the form of K that leaves its building block *invariant*.

Let us explain this idea concretely for the operator Z , which is the building block for the simplest vacuum state $\text{tr} Z^l$. In the general notation (4.14), we can express Z as $Z = \frac{1}{2} \text{tr} (\sigma_2 \mathbb{P}_Z^t \sigma_2 \Phi)$ with $\mathbb{P}_Z = 1 - \sigma_3$. Now let us look for the raising operators K_Z and \tilde{K}_Z for $\text{SU}(2)_R$ and $\text{SU}(2)_L$ respectively, which leave Z invariant. Since Φ transforms into $\tilde{K}_Z \Phi K_Z$, the invariance condition reads

$$\frac{1}{2} \text{tr} (\sigma_2 \mathbb{P}_Z^t \sigma_2 \tilde{K}_Z \Phi K_Z) = \frac{1}{2} \text{tr} (\sigma_2 \mathbb{P}_Z^t \sigma_2 \Phi). \quad (4.15)$$

This is equivalent to the condition

$$\mathbb{P}_Z = \tilde{K}_Z^{-1} \mathbb{P}_Z K_Z^{-1}. \quad (4.16)$$

It is easy to find the solutions²², which read

$$K_Z = \begin{pmatrix} 1 & \beta \\ 0 & 1 \end{pmatrix} = e^{\frac{1}{2} \beta \sigma_+}, \quad \tilde{K}_Z = \begin{pmatrix} 1 & 0 \\ \tilde{\beta} & 1 \end{pmatrix} = e^{\frac{1}{2} \tilde{\beta} \sigma_-}, \quad (4.17)$$

where β and $\tilde{\beta}$ are arbitrary constants.

Next we consider a general case where the vacuum state is given by $\text{tr} (\vec{P} \cdot \vec{\Phi})^l$, with arbitrary \vec{P} . Since, in general, $\vec{P} \cdot \vec{\Phi}$ does not carry a definite set of left and right charges defined as in Table 1, this state and the ones built upon it by some spin-chain type excitations are not charge eigenstates. Nevertheless, we can characterize this family of states again by the raising operators K and \tilde{K} which leave $\vec{P} \cdot \vec{\Phi}$ invariant. Just as in (4.16), this condition is expressed as

$$\mathbb{P} = \tilde{K}^{-1} \mathbb{P} K^{-1}. \quad (4.18)$$

where \mathbb{P} corresponds to \vec{P} . Since $\vec{P} \cdot \vec{\Phi}$ can be obtained from Z by an $\text{SU}(2)_L \times \text{SU}(2)_R$ transformation, \mathbb{P} can be obtained from \mathbb{P}_Z by a corresponding transformation of the form

$$\mathbb{P} = U_L \mathbb{P}_Z U_R. \quad (4.19)$$

Then combined with (4.18) we readily obtain the relation $\mathbb{P}_Z = (U_L^{-1} \tilde{K}^{-1} U_L) \mathbb{P}_Z (U_R K^{-1} U_R^{-1})$. Comparing this with (4.16) we can express the raising operators K and \tilde{K} in terms of the ones for the operator Z given in (4.17) in the form

$$K = U_R^{-1} K_Z U_R, \quad \tilde{K} = U_L \tilde{K}_Z U_L^{-1}. \quad (4.20)$$

²²The most general solutions are of the form $\begin{pmatrix} \alpha & \beta \\ 0 & \alpha^{-1} \end{pmatrix}$ and $\begin{pmatrix} \alpha^{-1} & 0 \\ \tilde{\beta} & \alpha \end{pmatrix}$. However since we are interested in the raising type operators, it is sufficient to consider the operators of the form (4.17).

Now these raising operators can in turn be characterized by the two-component vectors n and \tilde{n} , which are left invariant under the following action of K and \tilde{K} respectively²³ :

$$K^t n = n, \quad \tilde{K}^t \tilde{n} = \tilde{n}. \quad (4.21)$$

Since the overall factor for these vectors are inessential, we can normalize them to have unit length as $n^\dagger n = \tilde{n}^\dagger \tilde{n} = 1$. We shall refer to them as *polarization spinors*, as they characterize, so to speak, the “direction of polarization” of the highest weight operator $\vec{P} \cdot \vec{\Phi}$. It should be noted that from the knowledge of n and \tilde{n} , one can reconstruct \mathbb{P} which is invariant under the raising operators, as in (4.18). In fact, if we set

$$\mathbb{P} = -2i\sigma_2 \tilde{n} n^t, \quad (4.22)$$

one can easily check that this \mathbb{P} satisfies (4.18), with the use of the defining equations (4.21) and a simple formula $\sigma_2 U^{-1} \sigma_2 = U^t$ valid for any invertible 2×2 matrix U satisfying $\det U = 1$.

Let us illustrate these concepts by computing the polarization spinors for the operators Z and \bar{Z} respectively. For the operator Z we already computed the right and the left raising operators in (4.17). Then it is easy to see that the corresponding polarization spinors n_Z and \tilde{n}_Z satisfying $K_Z^t n_Z = n_Z$ and $\tilde{K}_Z^t \tilde{n}_Z = \tilde{n}_Z$ are given by

$$n_Z = \begin{pmatrix} 0 \\ 1 \end{pmatrix}, \quad \tilde{n}_Z = \begin{pmatrix} 1 \\ 0 \end{pmatrix}. \quad (4.23)$$

As a check, from the formula (4.22), we immediately get $\mathbb{P}_Z = \begin{pmatrix} 0 & 0 \\ 0 & 2 \end{pmatrix}$, which is the desired form. As for the operator \bar{Z} , repeating the similar analysis, the raising operators leaving $\mathbb{P}_{\bar{Z}} = 1 + \sigma_3$ invariant can be readily obtained to be

$$K_{\bar{Z}} = \begin{pmatrix} 1 & 0 \\ \alpha & 1 \end{pmatrix}, \quad \tilde{K}_{\bar{Z}} = \begin{pmatrix} 1 & \tilde{\alpha} \\ 0 & 1 \end{pmatrix}, \quad (4.24)$$

with α and $\tilde{\alpha}$ being arbitrary constants. The corresponding polarization spinors can be taken to be

$$n_{\bar{Z}} = \begin{pmatrix} 1 \\ 0 \end{pmatrix}, \quad \tilde{n}_{\bar{Z}} = \begin{pmatrix} 0 \\ 1 \end{pmatrix}. \quad (4.25)$$

Finally consider the normalization spinors for a general operator $\vec{P} \cdot \vec{\Phi}$ which is related to $Z = \vec{P}_Z \cdot \vec{\Phi}$ through the relation of the form (4.19). Since the raising operators for such an operator are obtained from those for Z in the manner (4.20), the polarization vectors n and \tilde{n} are expressed in terms of n_Z and \tilde{n}_Z as

$$n = U_R^t n_Z, \quad \tilde{n} = (U_L^t)^{-1} \tilde{n}_Z. \quad (4.26)$$

²³Intentionally we are using the same letters n and \tilde{n} for the vectors introduced here as those used previously for the normalization vectors. This is because they will be shown to be identical.

As an application of this formula, let us re-derive $n_{\bar{Z}}$ and $\tilde{n}_{\bar{Z}}$ from this perspective. Since $\mathbb{P}_{\bar{Z}} = 1 + \sigma_3$ and $\mathbb{P}_Z = 1 - \sigma_3$, it is easy to see that they are related by an $SU(2)_L \times SU(2)_R$ transformation of the form

$$\mathbb{P}_{\bar{Z}} = U_L \mathbb{P}_Z U_R, \quad U_L = i\sigma_2, \quad U_R = -i\sigma_2. \quad (4.27)$$

In fact this transformation realizes the mapping $(Z, X) \rightarrow (\bar{Z}, -\bar{X})$. Substituting the forms of U_L and U_R into the above formula (4.26), we obtain $U_R^t n_Z = (1, 0)^t$ and $(U_L^t)^{-1} \tilde{n}_Z = -(0, 1)^t \propto (0, 1)^t$, which agree with (4.25).

Summarizing, we can say that, as far as the global symmetry properties are concerned, the operators of type \mathcal{O}_1 and \mathcal{O}_3 are characterized by the polarization spinors n_Z and \tilde{n}_Z , while the operators of type \mathcal{O}_2 are associated with $n_{\bar{Z}}$ and $\tilde{n}_{\bar{Z}}$. For more general operators built upon the vacuum $\text{tr}(\vec{P} \cdot \vec{\Phi})^l$, the corresponding polarization spinors are obtained from n_Z and \tilde{n}_Z by appropriate transformations which connect \mathbb{P} with \mathbb{P}_Z as shown in (4.26).

The importance of the above analysis is that, as we shall describe below, precisely the same characterization scheme must be valid for the vertex operators in string theory which correspond to the gauge theory composite operators like \mathcal{O}_i . Moreover, it will be shown that the polarization spinors introduced purely from the group theoretic point of view above will be identified with the “normalization vectors” that appeared in (4.4), which play pivotal roles in the construction of the angle variables and hence the construction of the wave functions describing the contribution of the vertex operators.

4.3 Wave functions for the S^3 part

4.3.1 Symmetry structure of the vertex operators and the classical solutions

We now begin the explicit construction of the wave functions contributing to the three-point functions in string theory. As emphasized in the introduction, an essential ingredient for the success of the computation of the three-point functions is the separation of the kinematical and the dynamical factors. Although the dynamics is quite different between the gauge theory and the corresponding string theory, the kinematical symmetry properties correspond quite directly between the gauge theory operators and the vertex operators of string theory. Therefore in this subsection we will describe how we can implement the scheme of the symmetry characterization of the operators developed in the preceding subsection for the gauge theory operators to the vertex operators and the classical solutions produced by them. Since the analysis concerning the each factor of the symmetry group $SU(2)_R \times SU(2)_L$ is completely similar and can be performed independently, after some general discussions we will almost exclusively focus on the $SU(2)_R$ part of the symmetry transformations and various corresponding quantities for clarity of presentations.

In the saddle point approximation scheme we are employing, we cannot directly deal with the vertex operator: What we can deal with are the classical solutions produced by the vertex operators carrying large charges. Therefore we need to extract the information of the quantum vertex operators indirectly through such classical solutions.

For definiteness, we first focus on a solution with diagonal $SU(2)_R \times SU(2)_L$ charges describing a two-point function of an operator built on the $\text{tr}(Z^l)$ -vacuum (\mathcal{O}_1 and \mathcal{O}_3 in section 4.2) and its conjugate²⁴. In what follows, we shall denote such a solution by \mathbb{Y}^{diag} . Then we can associate a pair of polarization spinors n_Z and \tilde{n}_Z and the raising operators (4.17) to the vertex operator that produces the solution. For convenience, we display them again with appropriate renaming:

$$n^{\text{diag}} = \begin{pmatrix} 0 \\ 1 \end{pmatrix}, \quad \tilde{n}^{\text{diag}} = \begin{pmatrix} 1 \\ 0 \end{pmatrix}, \quad (4.28)$$

$$K^{\text{diag}}(\beta) = \begin{pmatrix} 1 & \beta \\ 0 & 1 \end{pmatrix}, \quad \tilde{K}^{\text{diag}}(\tilde{\beta}) = \begin{pmatrix} 1 & 0 \\ \tilde{\beta} & 1 \end{pmatrix}. \quad (4.29)$$

All the solutions describing a two-point function of mutually conjugate operators, $\langle \mathcal{O}\bar{\mathcal{O}} \rangle$, can be obtained from this basic solution \mathbb{Y}^{diag} by an $SU(2)_R \times SU(2)_L$ transformation. Since a normalized three-point function in the gauge theory can be obtained by dividing an unnormalized one by $\langle \mathcal{O}\bar{\mathcal{O}} \rangle$ -type two-point functions as

$$\frac{\langle \mathcal{O}_i \mathcal{O}_j \mathcal{O}_k \rangle}{\sqrt{\langle \mathcal{O}_i \bar{\mathcal{O}}_i \rangle \langle \mathcal{O}_j \bar{\mathcal{O}}_j \rangle \langle \mathcal{O}_k \bar{\mathcal{O}}_k \rangle}}, \quad (4.30)$$

the aforementioned solutions, to be denoted by \mathbb{Y}^{ref} , can be used as *reference solutions* to determine the normalization of the wave function. An important feature of such solutions is that they are real-valued when expressed in terms of the Minkowski worldsheet variables. This qualification will be extremely important since the equation of motion is actually invariant under a larger group $SL(2, \mathbb{C})_R \times SL(2, \mathbb{C})_L$ and its action can produce “complex” solutions which signify tunneling. Such a tunneling process is necessary for the three-point interactions to take place, as we shall see.

From now on till the end of this subsection, we shall suppress all the left transformations and display only the right transformations. The results for the left transformations will be summarized in subsection 4.3.3.

Now consider a three-point function produced by vertex operators, corresponding to the gauge theory operators, inserted at z_i on the worldsheet. We will take the operators to be those obtained by $SO(4)$ rotations of the operators built on the $\text{tr}(Z^l)$ -vacuum. This suffices for the present purpose since such three-point functions include²⁵ the ones

²⁴What is meant by “conjugation” is the usual complex conjugation of the fields, $Z \rightarrow \bar{Z}$ and $X \rightarrow \bar{X}$.

²⁵Note that \mathcal{O}_1 and \mathcal{O}_3 in section 4.2 are built on the $\text{tr}(Z^l)$ -vacuum while \mathcal{O}_2 can be obtained from the operator built on $\text{tr}(Z^l)$ by an $SO(4)$ rotation (4.27), which effects $(Z, X) \rightarrow (\bar{Z}, -\bar{X})$.

discussed in section 4.2.

Although the saddle point solution for such a three-point function is so far not available explicitly, let us denote the solution in the vicinity of z_i by \mathbb{Y} . Asymptotically as $z \rightarrow z_i$ such a configuration must be well-approximated by a two-point reference solution \mathbb{Y}^{ref} , which is produced by the *same* vertex operator. Even if they are produced by the same vertex operator, \mathbb{Y} and \mathbb{Y}^{ref} are different since \mathbb{Y} is influenced non-trivially and dynamically by the other two vertex operators present. We write the transformation between them at $z \simeq z_i$ as²⁶

$$\mathbb{Y}(z \simeq z_i) = \mathbb{Y}^{\text{ref}} V \quad (z \rightarrow z_i), \quad V \in \text{SL}(2, \mathbb{C})_R. \quad (4.31)$$

This relative difference is the quantity of interest since we need to normalize the three-point function by the two-point functions. In general V belongs to $\text{SL}(2, \mathbb{C})_R \supset \text{SU}(2)_R$, since the three-point interaction is necessarily a tunneling process. In contrast the reference solution \mathbb{Y}^{ref} can be obtained from \mathbb{Y}^{diag} by a transformation belonging to $\text{SU}(2)_R$ in the form

$$\mathbb{Y}^{\text{ref}} = \mathbb{Y}^{\text{diag}} U^{\text{ref}}, \quad U^{\text{ref}} \in \text{SU}(2)_R. \quad (4.32)$$

The relation between \mathbb{Y} , \mathbb{Y}^{ref} and \mathbb{Y}^{diag} is sketched in figure 4.1.

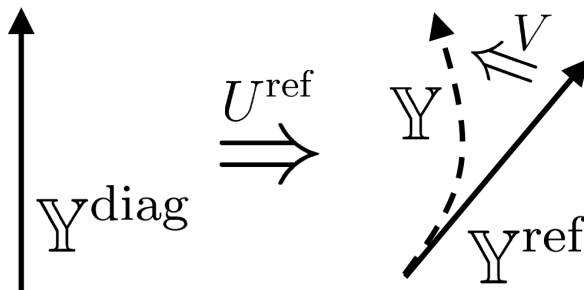


Figure 4.1: A schematic picture which explains the relation between the local three-point solution \mathbb{Y} and the two-point solutions \mathbb{Y}^{diag} and \mathbb{Y}^{ref} . \mathbb{Y}^{ref} is obtained from \mathbb{Y}^{diag} by a *real* global transformation U^{ref} , while \mathbb{Y} and \mathbb{Y}^{ref} , which are produced by the same vertex operator, are related through a *complexified* global transformation V .

Now just as we did already for the solution \mathbb{Y}^{diag} , we can associate to the solution \mathbb{Y}^{ref} the polarization spinor n^{ref} and the raising transformation K^{ref} which leaves it invariant. Then from the general formula (4.26) and (4.20) we can express them in terms of the

²⁶Note that \mathbb{Y}^{ref} is the solution for the two-point function, expressed globally in terms of the cylinder coordinate. Thus we need to express \mathbb{Y} in terms of the local coordinate $(\tau^{(i)}, \sigma^{(i)})$ given in (2.97) to compare two solutions.

quantities associated to the diagonal solution as

$$n^{\text{ref}} = (U^{\text{ref}})^t n^{\text{diag}}, \quad (4.33)$$

$$K^{\text{ref}}(\beta) = (U^{\text{ref}})^{-1} K^{\text{diag}}(\beta) U^{\text{ref}}. \quad (4.34)$$

By the same token we can associate the polarization spinor n and the raising transformation K to the local solution \mathbb{Y} . However since \mathbb{Y} is produced by the same vertex operator as \mathbb{Y}^{ref} , we must have $n = n^{\text{ref}}$. As for K , just as in (4.34), under the transformation V which produces \mathbb{Y} from \mathbb{Y}^{ref} , the raising operator $K^{\text{ref}}(\beta)$ transforms into $K(\beta)$ in the manner $K(\beta) = V^{-1} K^{\text{ref}}(\beta) V$. Since this operator must leave n and hence n^{ref} invariant, we must have

$$V^{-1} K^{\text{ref}}(\beta) V = K^{\text{ref}}(\beta') \quad (4.35)$$

for some β' . Substituting the relation (4.34), we get

$$\begin{aligned} (V')^{-1} K^{\text{diag}}(\beta) V' &= K^{\text{diag}}(\beta'), \\ V' &\equiv U^{\text{ref}} V (U^{\text{ref}})^{-1}. \end{aligned} \quad (4.36)$$

This means that the operator V' transforms a raising operator into a raising operator for the diagonal solution. It is not difficult to show that the general form of such an operator is $\begin{pmatrix} a & b \\ 0 & a^{-1} \end{pmatrix}$. Note that this contains a scale transformation which is in $\text{SL}(2, \mathbb{C})_R$ but not in $\text{SU}(2)_R$. From this result we can solve for V and its inverse and obtain the following useful representations

$$V = (U^{\text{ref}})^{-1} \begin{pmatrix} a & b \\ 0 & a^{-1} \end{pmatrix} U^{\text{ref}}, \quad (4.37)$$

$$V^{-1} = (U^{\text{ref}})^{-1} \begin{pmatrix} a^{-1} & -b \\ 0 & a \end{pmatrix} U^{\text{ref}}. \quad (4.38)$$

At this stage we need not know the actual values of a and b in these formulas. b will turn out to be irrelevant and a will be expressed in terms of certain Wronskians.

4.3.2 Construction of the wave function for the right sector

We are now ready for the construction of the wave function for the right sector using the formula for the shift of the angle variable ϕ_R given in (4.8).

First we need to fix the normalization vector n appearing in that formula. As we shall show, the answer is that it coincides precisely with the polarization spinor n introduced from the group theoretical point of view in (4.21) in subsection 4.2. Recall that in the formalism developed in [13–15], the zeros of $n \cdot \psi(x)$, where ψ is the Baker-Akhiezer vector and n is the normalization vector, determines the angle variables. When one

makes a global $\text{SL}(2, \mathbb{C})_R$ transformation V_R on the string solution \mathbb{Y} like $\mathbb{Y} \rightarrow \mathbb{Y}V_R$, the Baker-Akhiezer vector transforms like $\psi \rightarrow V_R^{-1}\psi$. In particular, take V_R to be the raising operator K under which the vertex operator producing the solution \mathbb{Y} is invariant. Then the wave function corresponding to the vertex operator and hence the angle variables comprising it must also be invariant. This means that the zeros of $n \cdot (K^{-1}\psi) = (K^t n) \cdot \psi$ must coincide with the zeros of $n \cdot \psi$ and hence we must have $K^t n \propto n$. However since K is similar to K^{diag} , it is clear that the constant of proportionality can only be unity and n must satisfy $K^t n = n$. This, however, is nothing but the definition of the polarization spinor given in (4.21). In other words, the proper choice of the normalization vector for constructing the wave function is precisely the polarization spinor associated to the vertex operator to which the wave function corresponds.

Having found the proper choice of the normalization vector in the formula (4.8) for the shift of the angle variable ϕ_R , what remains to be understood is how to evaluate the inner products $n \cdot \psi_{\pm}(\infty)$ and $n \cdot \psi_{\pm}^{\text{ref}}(\infty)$. Corresponding to the relation (4.31), in the vicinity of z_i , ψ_{\pm} and ψ_{\pm}^{ref} are related by the constant transformation V as $\psi_{\pm}(z \simeq z_i) = V^{-1}\psi_{\pm}^{\text{ref}}(z \simeq z_i)$. Now recall the form of the ALP for the right sector given in (1.4). We see that for $x = \infty$ the coefficients of the connections j_z and $j_{\bar{z}}$ vanish and hence the solutions $\psi_{\pm}(x = \infty)$ and $\psi_{\pm}^{\text{ref}}(x = \infty)$ themselves become constant. Combining these pieces of information, we obtain the relation

$$\psi_{\pm}(\infty) = V^{-1}\psi_{\pm}^{\text{ref}}(\infty). \quad (4.39)$$

The right hand side can be evaluated using the representation (4.38) as

$$\psi_{\pm}(\infty) = (U^{\text{ref}})^{-1} \begin{pmatrix} a^{-1} & -b \\ 0 & a \end{pmatrix} U^{\text{ref}}\psi_{\pm}^{\text{ref}}(\infty) = (U^{\text{ref}})^{-1} \begin{pmatrix} a^{-1} & -b \\ 0 & a \end{pmatrix} \psi_{\pm}^{\text{diag}}(\infty), \quad (4.40)$$

where $\psi_{\pm}^{\text{diag}}(x)$ is the Baker-Akhiezer vector for \mathbb{Y}^{diag} , which is related to $\psi_{\pm}^{\text{ref}}(x)$ by

$$\psi_{\pm}^{\text{ref}}(x) = (U^{\text{ref}})^{-1} \psi_{\pm}^{\text{diag}}(x). \quad (4.41)$$

We now need to know $\psi_{\pm}^{\text{diag}}(\infty)$, which are the eigenstates of the monodromy matrix near $x = \infty$ corresponding to the eigenvalues $e^{\pm ip(x)}$. For a charge-diagonal solution \mathbb{Y}^{diag} , the monodromy matrix near $x = \infty$ is diagonal and hence is either of the form (a) $\text{diag}(e^{ip(x)}, e^{-ip(x)})$ or (b) $\text{diag}(e^{-ip(x)}, e^{ip(x)})$, depending on the solution. For the case (a) the eigenvectors are $\psi_{+}^{\text{diag}}(\infty) = (1, 0)^t$, $\psi_{-}^{\text{diag}}(\infty) = (0, 1)^t$, while for the case (b) their forms are swapped. Since \mathbb{Y}^{diag} is produced by the vertex operator with the definite polarization spinor specified in (4.28), there should be a definite answer. To determine the proper choice of (a) or (b), we need to construct the wave function for each choice and see if it has the same transformation property as the corresponding operator in the

gauge theory. As it will be checked later in this subsection, it turned out that the case (b) is the correct choice. Therefore we will take

$$\psi_+^{\text{diag}}(\infty) = \begin{pmatrix} 0 \\ 1 \end{pmatrix}, \quad \psi_-^{\text{diag}}(\infty) = \begin{pmatrix} 1 \\ 0 \end{pmatrix}. \quad (4.42)$$

Substituting them into (4.40), we obtain the important relations

$$\psi_+(\infty) = (U^{\text{ref}})^{-1} \left(a\psi_+^{\text{diag}}(\infty) - b\psi_-^{\text{diag}}(\infty) \right) = a\psi_+^{\text{ref}}(\infty) - b\psi_-^{\text{ref}}(\infty), \quad (4.43)$$

$$\psi_-(\infty) = (U^{\text{ref}})^{-1} a^{-1} \psi_-^{\text{diag}}(\infty) = a^{-1} \psi_-^{\text{ref}}(\infty). \quad (4.44)$$

As for the polarization spinor, observe that by inspection the following relation holds:

$$n^{\text{diag}} = (-i\sigma_2)\psi_-^{\text{diag}}(\infty). \quad (4.45)$$

This relation is actually universal in the following sense. Let us act $(U^{\text{ref}})^t$ from left. Then the relation becomes

$$\begin{aligned} ((U^{\text{ref}})^t n^{\text{diag}}) n^{\text{ref}} &= (U^{\text{ref}})^t (-i\sigma_2) \psi_-^{\text{diag}}(\infty) \\ &= (-i\sigma_2) (U^{\text{ref}})^{-1} \psi_-^{\text{diag}}(\infty) \\ &= -i\sigma_2 \psi_-^{\text{ref}}(\infty), \end{aligned} \quad (4.46)$$

where we used the identity $\sigma_2 (U^{\text{ref}})^t \sigma_2 = (U^{\text{ref}})^{-1}$. Thus, exactly the same form of relation holds for the reference solution and in fact for any solution related by an $SU(2)_R$ transformation. Together with the formula (4.44) we get the relation

$$n = -ia\sigma_2 \psi_-(\infty), \quad (4.47)$$

which will be extremely important.

Let us now recall the formula (4.8) for the shift of the angle variable ϕ_R . Displaying it again for convenience, it is of the form

$$\Delta\phi_R = -i \ln \left(\frac{(n \cdot \psi_+(\infty))(n \cdot \psi_-^{\text{ref}}(\infty))}{(n \cdot \psi_+^{\text{ref}}(\infty))(n \cdot \psi_-(\infty))} \right). \quad (4.48)$$

From (4.43) and (4.46), we can write $n \cdot \psi_+(\infty) = an \cdot \psi_+^{\text{ref}}(\infty)$. As for $n \cdot \psi_-(\infty)$, use of (4.44) gives $n \cdot \psi_-(\infty) = a^{-1}n \cdot \psi_-^{\text{ref}}(\infty)$. Now due to the relation (4.46), the quantity $n \cdot \psi_-(\infty) = n^{\text{ref}} \cdot \psi_-(\infty)$, which appears both in the numerator and the denominator of the formula (4.48), vanishes. Therefore we must first regularize n slightly to make the quantity $n \cdot \psi_-(\infty)$ finite, cancel them in the formula and then remove the regularization. As for the same quantity appearing in $n \cdot \psi_+(\infty)$, we can safely set it to zero from the beginning since $n \cdot \psi_+^{\text{ref}}(\infty)$ is non-vanishing. In this way we find that $n \cdot \psi_{\pm}^{\text{ref}}(\infty)$'s all cancel out and we are left with an extremely simple formula for $\Delta\phi_R$ given by

$$\Delta\phi_R = -i \ln a^2. \quad (4.49)$$

Note that the shift depends only on the quantity a , which parametrizes the scale transformation not belonging to $SU(2)_R$, showing the tunneling nature of the effect.

Let us now write the formula (4.47) for the operator at z_i with a subscript i as $n_i = -ia_i\sigma_2i_-(\infty)$. Then, from the definition of the Wronskian we obtain $\langle n_i, n_j \rangle = a_i a_j \langle i_-, j_- \rangle \Big|_\infty$. Writing out all the relations of this form and forming appropriate ratios, we can easily extract out each a_i^2 . The result can be written in a universal form as

$$a_i^2 = \frac{\langle j_-, k_- \rangle}{\langle i_-, j_- \rangle \langle k_-, i_- \rangle} \Big|_\infty \frac{\langle n_i, n_j \rangle \langle n_k, n_i \rangle}{\langle n_j, n_k \rangle}. \quad (4.50)$$

Then substituting this expression into the formula (4.49) we obtain the shift of the angle variable ϕ_R at the position z_i as

$$e^{i\Delta\phi_{R,i}} = \frac{\langle j_-, k_- \rangle}{\langle i_-, j_- \rangle \langle k_-, i_- \rangle} \Big|_\infty \frac{\langle n_i, n_j \rangle \langle n_k, n_i \rangle}{\langle n_j, n_k \rangle}. \quad (4.51)$$

This formula is remarkable in that it cleanly separates the kinematical part composed of $\langle n_i, n_j \rangle$ and the dynamical part described by $\langle i_-, j_- \rangle \Big|_\infty$.

As the last step of the construction of the wave function, we need to pay attention to the convention of [15] that we are adopting. In that work, the Poisson bracket is defined to be $\{p, q\} = 1$ for the usual momentum p and the coordinate q . In this convention the Poisson bracket of the action angle variables was worked out to be given by $\{\phi, S\} = 1$. In other words the action variable S corresponds to q and the angle variable ϕ corresponds to p . Therefore upon quantization in the angle variable representation, we must set $S = i\partial/\partial\phi$. This means that the wave function that carries charge S is given by $e^{-iS\phi}$, not by $e^{iS\phi}$.

Recalling the relation (2.37) between the action variable S_∞ and the right charge R , namely $S_\infty = -R$, and employing the formula (4.51), the contribution to the wave function from the right sector is obtained as

$$\Psi_R^{S_3} = \exp\left(-i \sum_{i=1}^3 (-R_i) \Delta\phi_{R,i}\right) = \prod_{\{i,j,k\}} \left(\frac{\langle n_i, n_j \rangle}{\langle i_-, j_- \rangle \Big|_\infty} \right)^{R_i + R_j - R_k}, \quad (4.52)$$

where $\{i, j, k\}$ denotes the cyclic permutations of $\{1, 2, 3\}$.

At this stage, let us confirm that the wave function so constructed indeed carries the correct charge. To see this, it suffices to consider the $U(1)$ transformation which corresponds to the diagonal right-charge rotations. Let us examine the case of the charge-diagonal operator built upon the Z -type vacuum, such as \mathcal{O}_1 or \mathcal{O}_3 in section 4.2. In such a case the reference state is the charge-diagonal state itself, hence $U^{\text{ref}} = 1$. Then if we set $a = e^{i\theta/2}, b = 0$ in the formula (4.37), the $SU(2)_R$ transformation matrix V becomes $\text{diag}(e^{i\theta/2}, e^{-i\theta/2})$, which is a $U(1)$ transformation under which Z and \bar{Z} , carrying the

right charge $1/2$ and $-1/2$ respectively, transform as $Z \rightarrow e^{i\theta/2}Z$ and $\bar{Z} \rightarrow e^{-i\theta/2}$. Now according to (4.49), under such a transformation the wave function acquires the phase $e^{-i(-R)\ln a^2} = e^{iR\theta}$. This shows that the wave function has the same (positive) charge R as the operator of the form $\text{tr}(Z^{2R})$. This proves that the choice of $\psi_{\pm}^{\text{diag}}(\infty)$ we made in (4.42) is the correct one. If we had made the other choice, the wave function would have acquired the phase $e^{-iR\theta}$, which contradicts the fact that the corresponding operator in the gauge theory is built on the $\text{tr}(Z^l)$ -vacuum. Similar argument can be made for the left sector and again one can check that the wave function (4.52) carries the correct charges.

4.3.3 Contribution of the left sector and complete wave function for the S^3 part

We now briefly describe the analysis for the left sector, to complete the construction of the wave function for the S^3 part.

The procedure is exactly the same as for the right sector but there are a couple of notable differences. First, the transformation matrices act from the left and consequently in various formulas the matrices are replaced by their inverses. In particular, the formulas corresponding to (4.37) and (4.39) for the transformation \tilde{V} that connects three-point solution and the reference solution in the manner $\mathbb{Y} = \tilde{V}\mathbb{Y}^{\text{ref}}$ take the form

$$\tilde{V} = \tilde{U}^{\text{ref}} \begin{pmatrix} a & 0 \\ b & a^{-1} \end{pmatrix} (\tilde{U}^{\text{ref}})^{-1}, \quad (4.53)$$

$$\tilde{\psi}_{\pm}(0) = \tilde{V}\tilde{\psi}_{\pm}^{\text{ref}}(0), \quad (4.54)$$

where $\tilde{U}^{\text{ref}} \in \text{SU}(2)_L$ is the matrix effecting the connection $\mathbb{Y}^{\text{ref}} = \tilde{U}^{\text{ref}}\mathbb{Y}^{\text{diag}}$. Second, the raising matrix for the diagonal solution is now lower triangular, namely

$$\tilde{K}^{\text{diag}}(\beta) = \begin{pmatrix} 1 & 0 \\ \beta & 1 \end{pmatrix}. \quad (4.55)$$

Thirdly, the polarization spinor for Z is $\tilde{n}^{\text{diag}} = (1, 0)^t$, as discussed in (4.25). Lastly, because of the form of the ALP for the left sector, the Baker-Akhiezer vector becomes coordinate-independent at $x = 0$ instead of at $x = \infty$.

Let us now list the basic results for the left sector, omitting the intermediate details. Just as for the right sector, the formulas below are valid for any type of operator.

$$\psi_+^{\text{diag}} = \begin{pmatrix} 0 \\ 1 \end{pmatrix}, \quad \psi_-^{\text{diag}} = \begin{pmatrix} 1 \\ 0 \end{pmatrix}, \quad (4.56)$$

$$\tilde{\psi}_+(0) = a^{-1}\tilde{\psi}_+^{\text{ref}}(0) + b\tilde{\psi}_-^{\text{ref}}(0), \quad \tilde{\psi}_-(0) = a\tilde{\psi}_-^{\text{ref}}(0), \quad (4.57)$$

$$\tilde{n} = ai\sigma_2\tilde{\psi}_+(0), \quad \Delta\phi_L = -i\ln a^{-2}. \quad (4.58)$$

Using these formulas, we obtain the contribution to the wave function from the left sector as

$$\Psi_L^{S^3} = \exp\left(-i \sum_{i=1}^3 L_i \Delta \phi_{L,i}\right) = \prod_{\{i,j,k\}} \left(\frac{\langle \tilde{n}_i, \tilde{n}_j \rangle}{\langle i_+, j_+ \rangle|_0} \right)^{L_i + L_j - L_k}, \quad (4.59)$$

where we used the gauge invariance of the Wronskians and replaced $\langle \tilde{i}_+, \tilde{j}_+ \rangle$ with $\langle i_+, j_+ \rangle$. Together with $\Psi_R^{S^3}$ obtained in (4.52) we now have the complete wave function for the S^3 part. It is of the structure

$$\begin{aligned} e^{\mathcal{F}_{\text{vertex}}} &= \Psi_L^{S^3} \Psi_R^{S^3} e^{\mathcal{V}_{\text{energy}}}, \\ \mathcal{F}_{\text{vertex}} &= \mathcal{V}_{\text{kin}} + \mathcal{V}_{\text{dyn}} + \mathcal{V}_{\text{energy}}. \end{aligned} \quad (4.60)$$

Let us explain each term (4.60) in order. The first term \mathcal{V}_{kin} stands for the kinematical part composed of the Wronskians $\langle n_i, n_j \rangle$ and $\langle \tilde{n}_i, \tilde{n}_j \rangle$,

$$\begin{aligned} \mathcal{V}_{\text{kin}} &= \\ &(R_1 + R_2 - R_3) \ln \langle n_1, n_2 \rangle + (R_2 + R_3 - R_1) \ln \langle n_2, n_3 \rangle + (R_3 + R_1 - R_2) \ln \langle n_3, n_1 \rangle \\ &+ (L_1 + L_2 - L_3) \ln \langle \tilde{n}_1, \tilde{n}_2 \rangle + (L_2 + L_3 - L_1) \ln \langle \tilde{n}_2, \tilde{n}_3 \rangle + (L_3 + L_1 - L_2) \ln \langle \tilde{n}_3, \tilde{n}_1 \rangle. \end{aligned} \quad (4.61)$$

The second term \mathcal{V}_{dyn} refers to the dynamical part consisting of the Wronskians $\langle i_-, j_- \rangle|_\infty$ and $\langle \tilde{i}_+, \tilde{j}_+ \rangle|_0$,

$$\begin{aligned} \mathcal{V}_{\text{dyn}} &= \\ &-(R_1 + R_2 - R_3) \ln \langle 1_-, 2_- \rangle|_\infty - (R_2 + R_3 - R_1) \ln \langle 2_-, 3_- \rangle|_\infty - (R_3 + R_1 - R_2) \ln \langle 3_-, 1_- \rangle|_\infty \\ &-(L_1 + L_2 - L_3) \ln \langle 1_+, 2_+ \rangle|_0 - (L_2 + L_3 - L_1) \ln \langle 2_+, 3_+ \rangle|_0 - (L_3 + L_1 - L_2) \ln \langle 3_+, 1_+ \rangle|_0. \end{aligned} \quad (4.62)$$

The last term $\mathcal{V}_{\text{energy}}$ denotes the contribution involving the worldsheet energy shown in the last term of (4.2). Such a term is necessary for the following reason. As explained below (2.97) and at the beginning of section 3.1, we evaluate our wave function on the circle defined by $\tau^{(i)} = 0$, corresponding to $\ln |z - z_i| = \ln \epsilon_i$. On the other hand, the wave function introduced through the state operator mapping in (4.1) is defined on the unit circle described by $\ln |z - z_i| = 0$. The term $\mathcal{V}_{\text{energy}}$ is needed to fill this gap. As the energy of the each external state is given²⁷ by $2\sqrt{\lambda} \kappa_i^2$, $\mathcal{V}_{\text{energy}}$ can be evaluated explicitly as

$$\mathcal{V}_{\text{energy}} = 2\sqrt{\lambda} \sum_{i=1}^3 \kappa_i^2 \ln \epsilon_i. \quad (4.63)$$

²⁷The energy can be computed from the behavior of the stress-energy tensor around the puncture (2.11).

Before ending this subsection, let us make two comments. First, it is not guaranteed at this stage that the wave function thus constructed produces a correctly normalized two-point function. In addition, as discussed in [11], there may be additional contributions which come from the canonical change of variables, $\{\mathbb{Y}, \partial_\tau \mathbb{Y}\} \rightarrow \{\phi_i, S_i\}$. However, in section 7.3, it will be checked that our result for the three-point function reproduces the normalized two-point function in an appropriate limit. Therefore we can a posteriori confirm that the wave function is properly normalized and the additional contributions are absent. Second, one recognizes that the power of $\langle n_i, n_j \rangle$, namely $R_i + R_j - R_k$, is the familiar combination, made out of conformal weights and spins, for the coordinate differences in the three-point functions of a conformal field theory, *except for the overall sign*. In the next subsection, we will elaborate on this structure of the power from the point of view of the dual gauge theory. Also in section 6.2, where we construct the wave function for the $EAdS_3$ part, the above difference in the overall sign will be explained.

Summarizing, the product of (4.52) and (4.59) gives the general form of the wave functions for the three-point function. It is expressed in terms of the two types of Wronskians. One type is the Wronskians between the solutions of the ALP around vertex insertion points. They will be evaluated in section 5. The others are the Wronskians between the polarization spinors associated with the vertex operators, which are of purely kinematical nature and hence should be common to the string and the gauge theory sides.

4.3.4 Correspondence with the gauge theory side

We shall now examine our formula for the wave function from the point of view of correspondence with the gauge theory side.

First consider the question of how to distinguish the different types of gauge theory operators \mathcal{O}_i from their corresponding wave functions in string theory. The wave function constructed above is expressed in terms of the polarization spinors, which depend only on the type of the vacuum on which the corresponding gauge theory operator is built, the eigenvectors of the ALP in the vicinity of the insertion point z_i , and the charges carried by the vertex operators. A natural question is how we can distinguish the type of vertex operators involved from these data. Operators of \mathcal{O}_1 and \mathcal{O}_2 in section 4.2 can be distinguished by the structure of their polarization spinors because the vacuum on which they are built are different. On the other hand, operators of \mathcal{O}_1 and \mathcal{O}_3 , which are built on the same type of the vacuum, are characterized by the same polarization spinors and hence it appears that one cannot distinguish them from the formula for the wave function. Since these operators differ only in the types of excitations, X or \bar{X} , the question is how this is reflected. The answer is in the relation between the absolute magnitude of the

charges \mathcal{R} and \mathcal{L} , which are given by R and L respectively. Because the charges carried by the operator X are $(\mathcal{R}, \mathcal{L}) = (-1/2, 1/2)$, the magnitude of the total charges of the type \mathcal{O}_1 operator built upon Z -vacuum with X as excitations must satisfy the inequality $R < L$. Similarly, the magnitudes of the total charges for the operator of type \mathcal{O}_2 also obey $R < L$. On the other hand, for the operator of type \mathcal{O}_3 , we have $R > L$.

Such distinction is reflected not only on the charges but also on the dynamical property of the eigenstates i_{\pm} appearing in the wave function formula. As discussed in (2.75) and (2.76), the relative magnitude of R and L for a one-cut solution is determined by the position of the cut in the quasi-momentum $p(x)$: When the real part of the position of the branch cut is in the interval $[-1, 1]$ in the spectral parameter space such a solution has $R > L$ and hence corresponds to the operator of type \mathcal{O}_3 . Contrarily the operator of type \mathcal{O}_1 having $R < L$ corresponds to a solution with the cut outside the above interval. Conceptually this is quite intriguing. From the spin-chain perspective, \mathcal{O}_1 and \mathcal{O}_3 form distinct types of spin chains, which cannot be transformed into each other by an $SU(2)_R \times SU(2)_L$ transformation. On the other hand, in string theory the solutions corresponding to these distinct spin chains are described in a more unified way. It would be interesting to realize such a unified treatment on the gauge theory side as well.

Let us next examine the role and the meaning of the kinematical factor \mathcal{V}_{kin} from the point of view of the dual gauge theory. In this regard, note that the quantity $\langle n_i, n_j \rangle$, being a skew product, vanishes when n_i and n_j coincide. This in fact happens for the case of the operators \mathcal{O}_1 and \mathcal{O}_3 discussed in section 4.2, which are built upon the same Z -vacuum and hence carry the same polarization spinors. There are three possibilities. If the power $R_i + R_j - R_k$ is positive, then the wave function and hence the three-point function vanishes. This would express a selection rule. On the other hand, if it is negative, the three-point function diverges. For an internal symmetry such as $SU(2)_R$ this should not occur. The last possibility is that the power is exactly zero. In this case, we should regularize $\langle n_i, n_j \rangle$ slightly away from zero and then apply the vanishing power to get the result, which is unity.

Let us see which of these cases is actually realized for the set of operators $\mathcal{O}_1, \mathcal{O}_2$ and \mathcal{O}_3 in section 4.2. Let l_i be the total length of the operator \mathcal{O}_i and M_i be the number of excitations. The number of “vacuum fields” is then given by $l_i - M_i$. There are two obvious conservation laws for these numbers if all the fields and anti-fields of the set $\{\mathcal{O}_i\}$ are fully contracted to form propagators. One is the conservation concerning excitations, *i.e.*, the total number of X ’s should equal the total number of \bar{X} ’s. The other is the conservation concerning the vacuum fields, *i.e.* the total number of Z ’s should equal the total number of \bar{Z} ’s. From the structure of \mathcal{O}_i ’s it is easy to find that these two conservation laws are

expressed as

$$\begin{aligned} (i) \quad M_1 &= M_2 + M_3, \\ (ii) \quad l_1 + l_3 - l_2 &= 2M_3. \end{aligned} \tag{4.64}$$

Now consider the right and the left charges carried by \mathcal{O}_i . From Table 1, and the compositions of \mathcal{O}_i , we get, for example, $R_1 = \frac{1}{2}l_1 - M_1$, $L_1 = \frac{1}{2}l_1$, etc.. Then, computing the powers of interest we get

$$R_1 + R_3 - R_2 = M_3 + M_2 - M_1 = 0, \tag{4.65}$$

$$L_1 + L_3 - L_2 = \frac{1}{2}(l_1 + l_3 - l_2) - M_3 = 0. \tag{4.66}$$

Therefore precisely due to the conservation laws, (i) and (ii) above, of the number of contracting fields, the powers that occur for the vanishing Wronskians $\langle n_1, n_3 \rangle$ and $\langle \tilde{n}_1, \tilde{n}_3 \rangle$ are zero. Hence, in the computation of the three-point function of \mathcal{O}_i 's such factors simply produce unity.

Up to this point we have obtained the general formulas for the contribution of the action part and the wave function part, both of which are expressed in terms of the Wronskians of the form $\langle i_{\pm}, j_{\pm} \rangle$. In the next section we will evaluate these quantities to substantiate the general formulas.

5 Evaluation of the Wronskians

In the previous two sections, we have shown that both the contribution of the action and that of the vertex operators are expressible in terms of the Wronskians $\langle i_{\pm}, j_{\pm} \rangle$ between the eigenvectors of the monodromy matrices. The goal of this section is to evaluate those Wronskians. First, in section 5.1, we show that certain products of Wronskians are expressed in terms of the quasi-momenta. Next, in sections 5.2 and 5.3, we determine the analytic properties (*i.e.* poles and zeros) of each Wronskian as a function of the spectral parameter x . With such a knowledge, we apply, in section 5.4, a generalized version of the Wiener-Hopf decomposition formula to the products of the Wronskians and determine the individual factor. Finally, in section 5.5, we compute the singular part and the constant part of the Wronskian, which cannot be determined by the Wiener-Hopf method.

5.1 Products of Wronskians in terms of quasi-momenta

To obtain the information of the Wronskian $\langle i_{\pm}, j_{\pm} \rangle$ between the eigenvectors of the ALP at different points, we need some condition which governs the global property of such Wronskians. As we shall see, such a condition is provided by the global consistency

condition for the product of the local monodromy matrices Ω_i associated with the vertex insertion points z_i . Since the total monodromy must be trivial upon going around the entire worldsheet, we must have

$$\Omega_1 \Omega_2 \Omega_3 = 1. \quad (5.1)$$

Although this appears to be a rather weak condition, it is sufficiently powerful to determine the forms of certain products of the Wronskians in terms of the quasi-momenta $p_i(x)$, as discussed in [8, 9]. Let us quickly reproduce those expressions. Take the basis in which Ω_1 is diagonal, namely

$$\Omega_1 = \begin{pmatrix} e^{ip_1} & 0 \\ 0 & e^{-ip_1} \end{pmatrix}. \quad (5.2)$$

Since the set of eigenvectors j_{\pm} at z_j form a complete basis, one can expand the eigenvectors i_{\pm} at z_i in terms of them in the following way:

$$i_{\pm} = \langle i_{\pm}, j_- \rangle j_+ - \langle i_{\pm}, j_+ \rangle j_-. \quad (5.3)$$

Making use of this formula, Ω_2 can be expressed in the Ω_1 -diagonal basis as

$$\Omega_2 = M_{12} \begin{pmatrix} e^{ip_2} & 0 \\ 0 & e^{-ip_2} \end{pmatrix} M_{21}, \quad (5.4)$$

where the matrix M_{ij} , effecting the change of basis, is given by

$$M_{ij} = \begin{pmatrix} -\langle i_-, j_+ \rangle & -\langle i_-, j_- \rangle \\ \langle i_+, j_+ \rangle & \langle i_+, j_- \rangle \end{pmatrix}. \quad (5.5)$$

Now owing to the constraint (5.1), Ω_1 and Ω_2 must satisfy the following relation:

$$\text{tr} (\Omega_1 \Omega_2) = \text{tr} \Omega_3^{-1} = 2 \cos p_3. \quad (5.6)$$

Substituting the equations (5.2) and (5.4) into (5.6), we obtain an equation for $\langle 1_{\pm}, 2_{\pm} \rangle$ of the form

$$\cos(p_1 - p_2) \langle 1_+, 2_+ \rangle \langle 1_-, 2_- \rangle - \cos(p_1 + p_2) \langle 1_+, 2_- \rangle \langle 1_-, 2_+ \rangle = \cos p_3. \quad (5.7)$$

This equation, together with the Schouten identity²⁸ for 1_{\pm} and 2_{\pm} given by

$$\langle 1_+, 2_+ \rangle \langle 1_-, 2_- \rangle - \langle 1_+, 2_- \rangle \langle 1_-, 2_+ \rangle = \langle 1_+, 1_- \rangle \langle 2_+, 2_- \rangle = 1, \quad (5.8)$$

²⁸The general form of the Schouten identity is given by $\langle i, j \rangle \langle k, l \rangle + \langle i, k \rangle \langle j, l \rangle + \langle i, l \rangle \langle j, k \rangle = 0$. It can be proven directly from the definition of the Wronskians.

completely determines the products of Wronskians, $\langle 1_+, 2_+ \rangle \langle 1_-, 2_- \rangle$ and $\langle 1_+, 2_- \rangle \langle 1_-, 2_+ \rangle$. In a similar manner, products of certain other Wronskians can also be obtained, which are summarized as the following set of equations²⁹:

$$\langle 1_+, 2_+ \rangle \langle 1_-, 2_- \rangle = \frac{\sin \frac{p_1+p_2+p_3}{2} \sin \frac{p_1+p_2-p_3}{2}}{\sin p_1 \sin p_2}, \quad (5.9)$$

$$\langle 2_+, 3_+ \rangle \langle 2_-, 3_- \rangle = \frac{\sin \frac{p_1+p_2+p_3}{2} \sin \frac{-p_1+p_2+p_3}{2}}{\sin p_2 \sin p_3}, \quad (5.10)$$

$$\langle 3_+, 1_+ \rangle \langle 3_-, 1_- \rangle = \frac{\sin \frac{p_1+p_2+p_3}{2} \sin \frac{p_1-p_2+p_3}{2}}{\sin p_3 \sin p_1}, \quad (5.11)$$

$$\langle 1_+, 2_- \rangle \langle 1_-, 2_+ \rangle = \frac{\sin \frac{p_1-p_2+p_3}{2} \sin \frac{p_1-p_2-p_3}{2}}{\sin p_1 \sin p_2}, \quad (5.12)$$

$$\langle 2_+, 3_- \rangle \langle 2_-, 3_+ \rangle = \frac{\sin \frac{p_1+p_2-p_3}{2} \sin \frac{-p_1+p_2-p_3}{2}}{\sin p_2 \sin p_3}, \quad (5.13)$$

$$\langle 3_+, 1_- \rangle \langle 3_-, 1_+ \rangle = \frac{\sin \frac{-p_1+p_2+p_3}{2} \sin \frac{-p_1-p_2+p_3}{2}}{\sin p_3 \sin p_1}. \quad (5.14)$$

What we need for the computation of the three-point functions, however, are the individual Wronskians and not just the products given in (5.9)–(5.14). Such a knowledge will be extracted based on the analytic properties of the Wronskians regarded as functions of the complex spectral parameter x . We will analyze such properties in the next two subsections.

5.2 Analytic properties of the Wronskians I: Poles

An individual Wronskian, viewed as a function of x , is almost uniquely determined³⁰ by its analytic properties, namely the positions of the poles and the zeros. From the expressions exhibited in (5.9)–(5.14), we know that the products of Wronskians have poles at $\sin p_i = 0$ and zeros at $\sin((\pm p_1 \pm p_2 \pm p_3)/2) = 0$. Therefore the question is which factor of the product is responsible for such a pole and/or a zero. In this subsection, we will describe how to analyze the structure of the poles.

To illustrate the basic idea, we will consider the Wronskians $\langle 1_+, 2_+ \rangle$ and $\langle 1_-, 2_- \rangle$ as examples, for which the product is given by

$$\langle 1_+, 2_+ \rangle \langle 1_-, 2_- \rangle = \frac{\sin \frac{p_1+p_2+p_3}{2} \sin \frac{p_1+p_2-p_3}{2}}{\sin p_1 \sin p_2}.$$

²⁹Note that the equations (5.9)–(5.14) appear slightly different in form from those derived in [9]. This is because 2_+ in this paper corresponds to 2_- in [9] and 2_- in this paper corresponds to -2_+ in [9].

³⁰As we will discuss later, the Wronskian also contains essential singularities at $x = \pm 1$. In addition, an overall proportionality constant cannot be determined by the positions of zeros and poles. These ambiguities will be fixed in section 5.5.

Let us focus on the pole associated with $\sin p_1 = 0$ and denote the position of the pole by x_{pole} . There are two types of points at which $\sin p_1$ vanishes, the branch points and the ‘‘singular points’’. First consider the case where x_{pole} is a singular point, at which the two eigenvalues of the monodromy matrix Ω_1 degenerate to either $+1$ or -1 . This, however, does not mean that Ω_1 is proportional to the unit matrix for the following reason: If $\Omega_1 \propto 1$, the monodromy condition $\Omega_1\Omega_2\Omega_3 = 1$ forces p_2 to be equal to $+p_3$ or $-p_3$ modulo π . However, since p_1 , p_2 and p_3 can be chosen completely independently, there is no reason for such special relation to hold. Thus, the only remaining possibility is that the monodromy matrix Ω_1 takes the form of a Jordan-block at $x = x_{\text{pole}}$, namely,

$$\Omega_1(x_{\text{pole}}) \sim \pm \begin{pmatrix} 1 & c \\ 0 & 1 \end{pmatrix}. \quad (5.15)$$

In this case, the eigenvectors 1_+ and 1_- degenerate at $x = x_{\text{pole}}$ and we have one eigenvector. To see what happens at $x = x_{\text{pole}}$ more explicitly, let us study the asymptotic behavior of 1_{\pm} near z_1 . In the vicinity of each puncture, the saddle point solution for the three-point function can be well-approximated by an appropriate solution for a two-point function. Consequently, the eigenvectors for the three-point function 1_{\pm} can also be approximated near z_1 by the eigenvectors for the two-point function $1_{\pm}^{2\text{pt}}$. As shown in (2.96), this structure can be seen most transparently in the Pohlmeyer gauge. Working out the subleading corrections, we obtain the following expansion for the eigenfunctions $\hat{1}_{\pm}$:

$$\hat{1}_+ = \hat{1}_+^{2\text{pt}} \left(1 + c_1(\sigma^{(1)}, x)e^{a_1\tau^{(1)}} + c_2(\sigma^{(1)}, x)e^{a_2\tau^{(1)}} + \dots \right), \quad (5.16)$$

$$\hat{1}_- = \hat{1}_-^{2\text{pt}} \left(1 + \tilde{c}_1(\sigma^{(1)}, x)e^{\tilde{a}_1\tau^{(1)}} + \tilde{c}_2(\sigma^{(1)}, x)e^{\tilde{a}_2\tau^{(1)}} + \dots \right). \quad (5.17)$$

Here $\tau^{(1)}$ and $\sigma^{(1)}$ are the local coordinates near z_1 given in (2.97) and c_k and \tilde{c}_k are 2×2 matrices dependent only on $\sigma^{(1)}$ and x . The constants a_k in the exponents are such that successive terms are becoming smaller by exponential factors as $\tau \rightarrow -\infty$. An important observation is that since $\hat{1}_{\pm}^{2\text{pt}}$ are eigenfunctions corresponding to a two-point function, they are insensitive to the global monodromy constraint (5.1) on the three-point function and hence non-degenerate at $x = x_{\text{pole}}$. An apparent puzzle now is how exponentially small corrections can produce the degeneracy of $\hat{1}_{\pm}$.

The answer is the following. Since one of the solutions $\hat{1}_{\pm}^{2\text{pt}}$ is exponentially increasing (*i.e.* big) and the other is decreasing (*i.e.* small) as $\tau \rightarrow -\infty$, let us consider the case where $\hat{1}_+^{2\text{pt}}$ is big and $\hat{1}_-^{2\text{pt}}$ is small. Now for $\hat{1}_{\pm}$ to become degenerate at $x = x_{\text{pole}}$, logically there are three possibilities

$$(a) \quad \hat{1}_+ = \alpha \hat{1}_-, \quad \alpha = \text{finite}, \quad (5.18)$$

$$(b) \quad \hat{1}_+ = \beta \hat{1}_-, \quad \beta \rightarrow \infty, \quad (5.19)$$

$$(c) \quad \hat{1}_- = \beta \hat{1}_+, \quad \beta \rightarrow \infty. \quad (5.20)$$

First, since $\hat{1}_+^{2\text{pt}}$ is much larger than $\hat{1}_-^{2\text{pt}}$ by assumption, the case (a) cannot occur. Now consider the case where x is slightly different from x_{pole} . Then β is large but finite and the relations (b) or (c) must be realized approximately. But it is obvious that (b) is the only consistent relation since exponentially small solution can appear in the big solution but not the other way around. Therefore we must have the situation

$$\hat{1}_+ = \hat{1}_+^{2\text{pt}} + \cdots + \beta \hat{1}_- + \cdots, \quad (5.21)$$

As $x \rightarrow x_{\text{pole}}$, β diverges and (5.21) goes over to the relation (b). The situation is the same if $\hat{1}_-$ is the big solution: Always the big solution diverges at the degeneration point, while the small solution remains finite³¹.

Similar argument can be applied to the other Wronskians, making use of the general asymptotic behavior of the eigenvectors in the Pohlmeier gauge, which is of the form

$$\hat{i}_\pm \sim e^{\pm q(x)\tau^{(i)}} \quad (z \sim z_i). \quad (5.22)$$

It is clear from this expression that which one of the \hat{i}_\pm diverges as $z \rightarrow z_i$ is governed by the sign of the real part of the quasi-energy $q(x)$. Since the divergence of the eigenfunction produces a pole on the Wronskian containing it, we can determine which Wronskian of the product is responsible for the pole with the following general rule: At $\sin p_i = 0$, the Wronskians behave as

$$\text{Re } q(x) > 0 \Rightarrow \langle i_+, * \rangle = \text{finite}, \quad \langle i_-, * \rangle = \infty, \quad (5.23)$$

$$\text{Re } q(x) < 0 \Rightarrow \langle i_+, * \rangle = \infty, \quad \langle i_-, * \rangle = \text{finite}. \quad (5.24)$$

Hence, for $\text{Re } q(x) > 0$ the pole occurs in $\langle i_-, * \rangle$, while for $\text{Re } q(x) < 0$ it occurs in $\langle i_+, * \rangle$.

5.3 Analytic properties of the Wronskians II: Zeros

Having determined the pole structure, let us next discuss the zeros of the Wronskians. The determination of the zeros is substantially more difficult since, in contrast to the poles which are local phenomena, the zeros are determined by the global properties on the Riemann surface. As shown in previous works [24–26], the notion of the WKB curve [23] is one of the main tools to explore such global properties. However, as its name indicates, the WKB curve is useful only when the leading term in the WKB expansion is sufficiently accurate. For this reason, it is not powerful enough to fully determine the zeros of the Wronskians in the whole region of the spectral parameter space. In this subsection we shall introduce an appropriate generalization of the WKB curve, to be called the *exact WKB curve*, to overcome this difficulty.

³¹ Remark: This does not mean of course that there is only one solution at the degeneration point. There must exist another independent solution of new structure, namely the structure which is different from $\hat{1}_\pm$. However, as long as we stick to this basis, what we see is that one of the solutions diverges and disappears.

5.3.1 WKB approximation and WKB curves

In order to motivate the generalized version, we shall first briefly review the ordinary WKB curves defined in [23].

When the expansion parameter ζ is sufficiently small, the leading term of the WKB expansion for the solutions to ALP (3.33) around z_i is given by

$$\hat{\psi} \sim \exp\left(\pm \frac{1}{\zeta} \int_{z_i^*}^z \sqrt{T} dz\right). \quad (5.25)$$

Of the two independent solutions given above, one is the *small solution*, which decreases exponentially as it approaches z_i and the other is the *big solution*, which increases exponentially in the same limit. In order to make the variation of the magnitude of the solution more precise, one defines the WKB curves as the curves along which the phase of the leading term (5.25) in the WKB expansion is constant. More explicitly, they are characterized by the equation

$$\text{Im}\left(\frac{\sqrt{T}}{\zeta} dz\right) = 0. \quad (5.26)$$

By analyzing the structure of (5.26), one finds the following three characteristic properties of the WKB curves. (i) At generic points on the worldsheet, the WKB curves are non-intersecting. (ii) At a puncture, the WKB curves radiate in all directions from the puncture. (iii) At a zero of $T(z)$, there are three special WKB curves which radiate from the zero and separate three different regions of the WKB curves. For details, see figure 5.1.

Along the WKB curve, the magnitude of the leading term in the WKB expansion (5.25) increases or decreases monotonically, until they reach a zero or a pole of $T(z)$. Thus, if two punctures z_i and z_j are connected by a WKB curve and the spectral parameter ζ is sufficiently small, the small solution s_i defined around z_i will grow exponentially as it approaches the other puncture z_j . In other words, the small solution s_i behaves like the big solution around z_j . Therefore s_i will be linearly independent of s_j and hence the Wronskian between these two small solutions $\langle s_i, s_j \rangle$ must be non-vanishing.

With this logic, we conclude that the Wronskians $\langle i_{\pm}, j_{\pm} \rangle$ are non-vanishing if the following three conditions are satisfied: (a) Two punctures z_i and z_j are connected by a WKB curve. (b) Two eigenvectors i_{\pm} and j_{\pm} are both small solutions. (c) The leading WKB solutions (5.25) are sufficiently accurate.

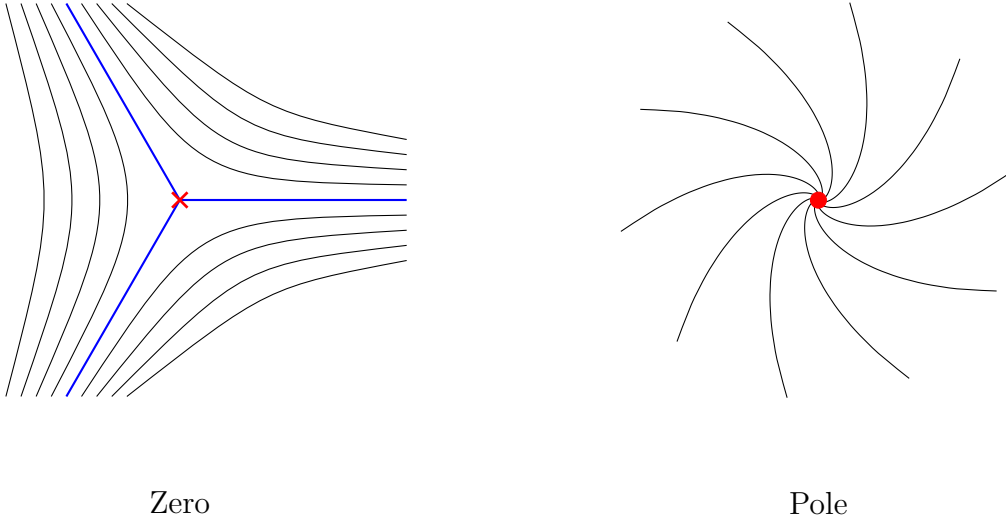


Figure 5.1: Sketch of WKB curves near a zero (a red cross in the left figure) and a pole (a red circle in the right figure). There are exactly three WKB curves that emanate from a zero. In contrast, there are infinitely many WKB curves radiating from a pole in all directions.

5.3.2 Exact WKB curves

Evidently, the analysis above is valid only in a restricted region of the spectral parameter plane where the approximation by the leading term of the WKB expansion is reliable. Actually, even if we improve the approximation by going to the next order approximation, we still cannot cover the entire spectral parameter plane because such an expansion is only an asymptotic series. It is indeed possible that as we change x the small and the big solutions interchange their roles. Such a phenomenon is clearly non-perturbative and cannot be captured by the usual expansion. So to understand the structure of the zeros on the whole spectral parameter plane, it is necessary to generalize the notion of WKB curves in a non-perturbative fashion.

In order to seek such an improvement, we need to look closely at the general structure of the conventional WKB expansion. Let us denote the components of the solution $\hat{\psi}^d$ to the ALP in the diagonal gauge (3.33) as

$$\hat{\psi}^d = \begin{pmatrix} \psi^{(1)} \\ \psi^{(2)} \end{pmatrix}. \quad (5.27)$$

By substituting (5.27) into the ALP (3.33), we obtain the equations for the components $\psi^{(1)}$ and $\psi^{(2)}$. Then, upon eliminating $\psi^{(2)}$ in favor of $\psi^{(1)}$, we get a second-order differential equation for $\psi^{(1)}$. To solve this equation, we expand $\psi^{(1)}$ in powers of ζ in the form

$$\psi^{(1)} = \sqrt{\frac{\rho}{T} - \frac{\partial\gamma}{\sqrt{T}}} \exp \left[\int_{z_0}^z \left(\frac{W_{-1}}{\zeta} + W_0 + \zeta W_1 + \dots \right) \right]. \quad (5.28)$$

One can then determine the one-forms W_n order by order recursively. This procedure is described in Appendix D.1. As a result of such a computation, we find that the WKB expansions for two linearly independent solutions to the ALP can be expressed in the following form:

$$\begin{pmatrix} f_{\pm}^{(1)} \\ f_{\pm}^{(2)} \end{pmatrix} \exp\left(\pm \int_{z_0}^z W_{\text{WKB}}(z, \bar{z}; \zeta)\right). \quad (5.29)$$

Here $W_{\text{WKB}} \equiv W_{\text{WKB}}^z dz + W_{\text{WKB}}^{\bar{z}} d\bar{z}$ is the one-form defined as a power series in ζ , with the leading term given by $\sqrt{T}dz/(2\zeta)$. On the other hand, the functions $f_{\pm}^{(1)}$ and $f_{\pm}^{(2)}$ are defined in terms of W_{WKB}^z by

$$f_{\pm}^{(1)} \equiv k_{\text{WKB}} = \sqrt{\frac{\rho - \sqrt{T}\partial\gamma}{T W_{\text{WKB}}^z}}, \quad (5.30)$$

$$f_{\pm}^{(2)} \equiv \frac{-i}{\sqrt{W_{\text{WKB}}^z}} \left[\pm W_{\text{WKB}}^z + \left(\frac{\sqrt{T}}{2\zeta} - \frac{\rho \cos 2\gamma}{\sqrt{T}} + \frac{\partial \ln k_{\text{WKB}}}{2} \right) \right]. \quad (5.31)$$

With this structure in mind, we now introduce an improved notion of the WKB curve, to be called the ‘‘exact WKB curve’’, by writing the exact solutions to the ALP in the form

$$\hat{\psi}^d = \begin{pmatrix} f_{\text{ex}}^{(1)} \\ f_{\text{ex}}^{(2)} \end{pmatrix} \exp\left(\int_{z_0}^z W_{\text{ex}}(z, \bar{z}; \zeta)\right), \quad (5.32)$$

where $f_{\text{ex}}^{(1)}$ and $f_{\text{ex}}^{(2)}$ are given by

$$f_{\text{ex}}^{(1)} = \sqrt{\frac{\rho - \sqrt{T}\partial\gamma}{T W_{\text{ex}}^z}}, \quad f_{\text{ex}}^{(2)} = \frac{-i}{\sqrt{W_{\text{ex}}^z}} \left[W_{\text{ex}}^z + \left(\frac{\sqrt{T}}{2\zeta} - \frac{\rho \cos 2\gamma}{\sqrt{T}} + \frac{\partial \ln f_{\text{ex}}^{(1)}}{2} \right) \right]. \quad (5.33)$$

Note that the expression (5.32) is identical in form to (5.29) with the plus sign chosen. However, there is an essential difference. While W_{WKB} is given by the asymptotic series in powers of ζ and is hence ambiguous non-perturbatively, W_{ex} on the other hand is unambiguous as it is defined directly by the exact solution $\hat{\psi}$. Of course, if we expand W_{ex} perturbatively in powers of ζ , the series will coincide with W_{WKB} . In this sense, W_{ex} can be regarded as the non-perturbative completion of W_{WKB} . Now one of the virtues of the expression (5.32) is that we can easily construct another solution satisfying $\langle \hat{\psi}^d, \hat{\psi}'^d \rangle = 1$ by choosing the opposite the signs as

$$\hat{\psi}'^d = \begin{pmatrix} f'_{\text{ex}}{}^{(1)} \\ f'_{\text{ex}}{}^{(2)} \end{pmatrix} \exp\left(-\int_{z_0}^z W_{\text{ex}}(z, \bar{z}; \zeta)\right), \quad (5.34)$$

where $f'_{\text{ex}}{}^{(1)}$ and $f'_{\text{ex}}{}^{(2)}$ are given by

$$f'_{\text{ex}}{}^{(1)} = \sqrt{\frac{\rho - \sqrt{T}\partial\gamma}{T W_{\text{ex}}^z}}, \quad f'_{\text{ex}}{}^{(2)} = \frac{-i}{\sqrt{W_{\text{ex}}^z}} \left[-W_{\text{ex}}^z + \left(\frac{\sqrt{T}}{2\zeta} - \frac{\rho \cos 2\gamma}{\sqrt{T}} + \frac{\partial \ln f'_{\text{ex}}{}^{(1)}}{2} \right) \right]. \quad (5.35)$$

Using the definition (5.32), let us now discuss the generalization of the WKB curves. The quantity $\sqrt{T}dz/\zeta$ used to define the original WKB curves is proportional to the leading term in the expansion of W_{WKB} . Therefore the most natural generalization of the WKB curves would be to use W_{ex} , which is a non-perturbative completion of W_{WKB} , to define them as

$$\text{Im} (W_{\text{ex}}(z; \zeta)) = 0. \quad (5.36)$$

Unfortunately, there is a problem with this definition. Since there are many exact solutions to the ALP, a different choice of the solution $\hat{\psi}^d$ leads to a different W_{ex} and thus to different curves. We can avoid this problem by defining the curves in terms of the small solution s_i (for a general value of ζ) near each puncture z_i . We shall call them the *exact WKB curves* and denote them by $\text{EWKB}_{(i)}$.

The precise definition is given as follows: The exact WKB curves associated to the puncture z_i are defined as the curves satisfying the equation

$$\text{Im} (W_{\text{ex}}^{(i)}(z; \zeta)) = 0, \quad (5.37)$$

where $W_{\text{ex}}^{(i)}$ is the exponential factor for the solution s_i , which is the smaller of the two eigenvectors i_+ and i_- . Explicitly, it is defined through the expression

$$s_i \propto \begin{pmatrix} f_{\text{ex}}^{(1)} \\ f_{\text{ex}}^{(2)} \end{pmatrix} \exp \left(\int_{z_0}^z W_{\text{ex}}^{(i)}(z, \bar{z}; \zeta) \right). \quad (5.38)$$

Let us now make several comments. First, it is easy to see that this definition of the exact WKB curves reduces to that of the ordinary WKB curves when ζ is sufficiently small. Second, as in (5.34), with a flip of sign in the exponent, we can obtain another solution

$$b_i \equiv \begin{pmatrix} f_{\text{ex}}^{\prime(1)} \\ f_{\text{ex}}^{\prime(2)} \end{pmatrix} \exp \left(- \int_{z_0}^z W_{\text{ex}}^{(i)}(z, \bar{z}; \zeta) \right), \quad (5.39)$$

which is big near the puncture z_i and satisfies $\langle s_i, b_i \rangle = 1$. Such a solution b_i , however, is not guaranteed to be an eigenvector since the eigenvector distinct from s_i is in general given by a linear combination of the form $b_i + cs_i$.

Now the definition of $\text{EWKB}_{(i)}$ given above refers to a specific puncture from which the curves emanate. In order for the notion of the exact WKB curve to be valid for the entire worldsheet, we must guarantee that the definitions of $\text{EWKB}_{(i)}$'s for $i = 1, 2, 3$ are consistent in the region where they overlap. To check this, let us consider the behavior of the small solution s_i as we follow an $\text{EWKB}_{(i)}$. Along such a curve the phase of the

exponential factor of s_i stays constant, while its magnitude increases monotonically³², until it reaches some endpoint. Consider the case in which this endpoint is the puncture at z_j . In such a case, we know that s_i grows exponentially as it approaches z_j and in fact behaves like a big solution b_j , up to an admixture of the exponentially small solution s_j . Thus, with sufficient accuracy, s_i can be expressed in the small neighborhood of z_j as

$$s_i \propto b_j = \begin{pmatrix} f_{\text{ex}}^{\prime(1)} \\ f_{\text{ex}}^{\prime(2)} \end{pmatrix} \exp \left(- \int_{z_0}^z W_{\text{ex}}^{(j)}(z, \bar{z}; \zeta) \right). \quad (5.40)$$

But since the exponent of the small solution s_j , which is used to define $\text{EWKB}_{(j)}$, is the same as that of b_j except for the sign, we see that by definition the curve we have been following becomes an $\text{EWKB}_{(j)}$ curve in the vicinity of z_j , when z_i and z_j are connected by such a curve. Therefore the definitions of $\text{EWKB}_{(i)}$ and $\text{EWKB}_{(j)}$ are indeed globally consistent.

Let us now make use of the exact WKB curves to determine the analytic properties of the Wronskians. First, by following exactly the same logic as in the case of the ordinary WKB curves, we can immediately conclude that the Wronskian involving two small solutions s_i and s_j must be nonzero if two punctures z_i and z_j are connected by some exact WKB curves. Although this is an extremely useful information, the problem seems to be that, unlike the ordinary WKB curves, we do not know the configurations of the EWKB curves since the exact solutions to the ALP are not available.

Nevertheless, we shall show below that by making use of a characteristic quantity defined locally around each puncture for the EWKB curves, it is possible to fully classify the topology (connectivity) of the curves on the entire worldsheet. The quantity in question is the ‘‘number density’’ of the EWKB curves emanating from a puncture at z_i . To motivate its definition, consider two such curves which emanate from z_i and end at z_j and let the constant phase of $W_{\text{ex}}^{(i)}$ along the two curves be ϕ_1 and ϕ_2 . Evidently the magnitude of the difference $|\phi_1 - \phi_2|$ is the same around z_i and around z_j , that is, it is conserved. If there is no singularity in the region between these lines, we can draw in more EWKB curves connecting z_i and z_j . Because of the property of the constancy of the phase difference noted above, it is quite natural to draw the curves in such a way that the difference of the phases of the adjacent curves is some fixed unit angle. Going around z_i and counting the number of such lines, we can define the number (density) of the $\text{EWKB}_{(i)}$ curves as³³

$$N_i \equiv \frac{1}{2\pi} \oint_{\mathcal{C}_i} |\text{Im } W_{\text{ex}}^{(i)}|, \quad (5.41)$$

³²Strictly speaking the small eigenvector (5.38) also contains a prefactor in front of the exponential. This prefactor, however, does not play a significant role in our discussion since it drops out if we consider the ratio of two solutions s_i/b_i . It is in fact sufficient to know the ratio in order to identify the small solution and the big solution.

³³In (5.41), we have chosen a convenient normalization of N_i .

where \mathcal{C}_i is an infinitesimal circle around z_i . Although N_i is not an integer in general, we will call it “a number of lines”. Actually we can express N_i in a more explicit way. From the asymptotic behavior of i_{\pm} (2.96), we can obtain the form of $W_{\text{ex}}^{(i)}$ near z_i as

$$W_{\text{ex}}^{(i)} \sim \pm (q_i(x)d\tau^{(i)} + ip_i(x)d\sigma^{(i)}) \quad \text{as } z \rightarrow z_i. \quad (5.42)$$

Here $(\tau^{(i)}, \sigma^{(i)})$ is the local coordinate defined in (2.97), and $+$ or $-$ sign is chosen depending on which of the solutions i_{\pm} is small. Substituting (5.42) into the definition (5.41), we obtain a simple expression

$$N_i \equiv |\text{Re } p_i(x)|. \quad (5.43)$$

Since the phase around the puncture is governed by the local monodromy, it is natural that N_i can be expressed in terms of $p_i(x)$.

Before we make use of the concept of N_i in a more global context, let us derive two important properties of the EWKB $_{(i)}$'s which will be necessary for determining their configurations.

The first property will be termed the *non-contractibility*. It can be stated as follows:

“All the exact WKB curves which start and end at the same puncture are non-contractible.”

In other words, such curves must go around a different puncture at least once. The proof is simple. Recall that the Wronskians between small solutions should be nonzero if two punctures are connected by an exact WKB curve. If we apply this statement to the same puncture z_i connected by an EWKB curve, we would conclude that $\langle s_i, s_i \rangle$ is non-zero, which is clearly false. The only way to be consistent with the general assertion above is that the curve is non-contractible and the solution gets transformed by the non-trivial monodromy Ω as it goes around other punctures. In this case the Wronskian is of the form $\langle s_i, \Omega s_i \rangle$, which need not vanish.

The next property is concerned with the endpoints of the exact WKB curves. It can be stated as follows:

“ All but finitely many exact WKB curves terminate at punctures. ”

The proof can be given as follows. As in the case of the ordinary WKB curves, the possible endpoints are the zeros or the poles of $W_{\text{ex}}^{(i)}$. Concerning the former, the number of exact WKB curves flowing into a zero is always finite, as shown in figure 5.1. On the other hand, a pole can be the endpoint of infinitely many curves and thus plays a crucial role in the study of the analyticity of the Wronskians. Now there are three different types of poles for

$W_{\text{ex}}^{(i)}$. The first is a puncture, at which the vertex operator is inserted. The second type of a pole corresponds to the situation where the small eigenvector s_i develops a singularity at a position different from the puncture. Since we only consider the worldsheet without additional singularities as mentioned in section 2.3, such a singularity in s_i should not occur. The last type of divergence for $W_{\text{ex}}^{(i)}$ occurs when s_i develops a zero. Indeed, s_i in general has several zeros on the Riemann surface. However, such points cannot be the endpoints of the exact WKB curves for the following reason: At the zeros of s_i , the ratio s_i/b_i of the small and the big solutions must also vanish³⁴. But this contradicts the basic property of the exact WKB curve that such a ratio, determined by the exponential factor in (5.38), monotonically increases along the exact WKB curve as we move away from z_i . From these considerations, we find that apart from a finite number of curves which can flow into zeros of $W_{\text{ex}}^{(i)}$, the rest of the infinitely many exact WKB curves must end at the punctures.

The two properties we have proved above are extremely important for the following reason. They provide certain global restrictions for the EWKB curves for all values of the spectral parameter, about which we only know the local behaviors explicitly in the vicinity of the punctures. Below, they allow us to show that there are essentially two distinct classes of configurations for the exact WKB curves.

These two classes are distinguished by whether the number of lines N_i fully satisfy the triangle inequalities or not³⁵. When N_i 's satisfy the relations

$$N_i + N_j - N_k > 0, \quad (5.44)$$

for all possible combinations of distinct i, j, k , we refer to such a configuration as *symmetric*. It is easy to show that if (5.44) is satisfied the number of lines connecting z_i and z_j cannot be zero. As this holds for all the interconnecting lines, the three punctures must be piece-wise connected to each other as in the left figure of figure 5.2.

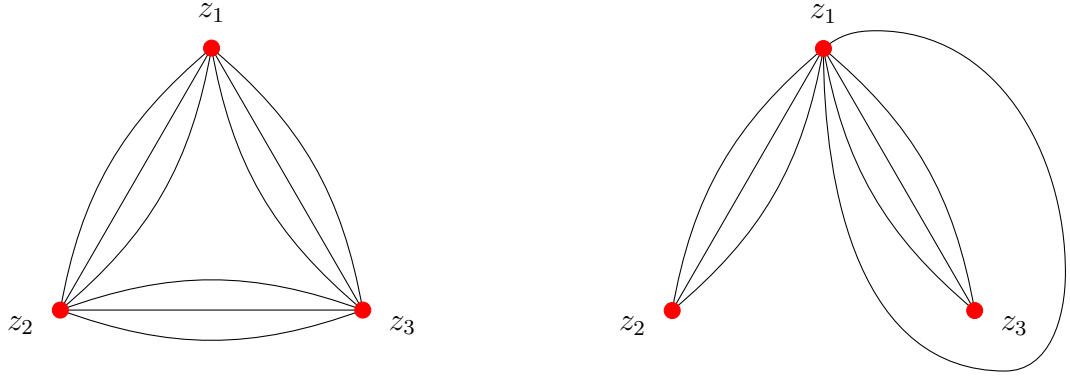
On the other hand, in the second case, which we shall call *asymmetric*, not all the triangle inequalities are satisfied. For example, one is violated like

$$N_2 + N_3 - N_1 < 0. \quad (5.45)$$

In this case, one can readily convince oneself that, while all the curves emanating from z_2 and z_3 end at z_1 , there must exist a non-contractible curve connecting z_1 to itself. This is depicted in the right figure of figure 5.2.

³⁴The big solution b_i cannot vanish at such points so as to ensure the normalization condition $\langle s_i, b_i \rangle = 1$.

³⁵In the case of the usual WKB curves, $W_{\text{ex}} \sim \sqrt{T(z)}dz$ and hence N_i is proportional to κ_i . Classification by the triangle inequalities for κ_i already appeared in [9].



(a) Symmetric case ($N_i + N_j - N_k > 0$) (b) Asymmetric case ($N_2 + N_3 - N_1 < 0$)

Figure 5.2: Two distinct classes for the connectivity of exact WKB curves. When all the triangle inequalities are satisfied (“symmetric” case), each exact WKB curve connects two different punctures. On the other hand, when some of the triangle inequalities are violated (“asymmetric” case), there must exist non-contractible curve(s) which starts and ends at the same puncture.

In this way, we can completely classify the configurations of the exact WKB curves from the local information $N_i = |\operatorname{Re} p_i(x)|$. Note that N_i depends on x . In fact it happens that as x changes a symmetric configuration can turn into an asymmetric configuration and vice versa. In an application of the present idea to the classical three-point function in Liouville theory [29], it was checked that such a transition must be taken into account in order to obtain the correct result. Below, we will see explicitly how the patterns of the configurations of the exact WKB curves analyzed above can be used to determine the zeros of the Wronskians.

5.3.3 Determination of the zeros of the Wronskians

As an example, let us focus on the factor

$$\sin\left(\frac{p_1 + p_2 + p_3}{2}\right), \quad (5.46)$$

and determine which Wronskians develop a zero when this factor vanishes. (The logic below applies to all the other cases straightforwardly.) From the relations (5.9)–(5.14), we find that the products of Wronskians that become zero are

$$\langle 1_+, 2_+ \rangle \langle 1_-, 2_- \rangle, \quad \langle 2_+, 3_+ \rangle \langle 2_-, 3_- \rangle, \quad \langle 3_+, 1_+ \rangle \langle 3_-, 1_- \rangle. \quad (5.47)$$

For convenience, let us define the following two sets of eigenvectors, namely the set $\mathcal{S}_+ \equiv \{1_+, 2_+, 3_+\}$ and the set $\mathcal{S}_- \equiv \{1_-, 2_-, 3_-\}$. An important feature of the quantities shown in (5.47) is that only the Wronskians of the eigenstates in the same group, \mathcal{S}_+ or \mathcal{S}_- , appear. This is in fact a general feature and holds also for other situations.

Now, let us present two theorems, which will be useful in the determination of the zeros. The first theorem is the following assertion, which we have already proved:

Theorem 1. When two punctures z_i and z_j are connected by an exact WKB curve, the Wronskian between the two small eigenvectors $\langle s_i, s_j \rangle$ is non-vanishing.

The second theorem classifies the possibilities of the patterns of the zeros and is stated as follows:

Theorem 2. There are only two distinct possibilities concerning the zeros of the Wronskians in (5.47): Either (a) all the Wronskians among the members of \mathcal{S}_+ are zero and those among \mathcal{S}_- are nonzero, or (b) all the Wronskians among \mathcal{S}_- are zero and those among \mathcal{S}_+ are nonzero.

The proof is as follows. Let us first note that in each product of two Wronskians appearing in (5.47), only one of them vanishes. In fact if both factors become zero simultaneously, the product develops a double zero, which contradicts the fact that the zeros of (5.46) are all simple zeros. This property implies that in the list given in (5.47), at least two of the individual Wronskians which actually vanish must be between the members belonging to the same set, which can be \mathcal{S}_+ or \mathcal{S}_- . Suppose they belong to \mathcal{S}_+ . Since $\langle i_+, j_+ \rangle = 0$ means that i_+ and j_+ are parallel to each other, vanishing of two such different Wronskians between the states of \mathcal{S}_+ implies that in fact all the three states in \mathcal{S}_+ are proportional to each other. Therefore the third Wronskian from the set \mathcal{S}_+ must also vanish. Obviously the same logic applies to the \mathcal{S}_- case. This proves the theorem.

We can now analyze the zeros of the Wronskians using these theorems. First consider the symmetric case. Since one of the states i_{\pm} must be a small solution, either \mathcal{S}_+ or \mathcal{S}_- must contain two small solutions. For a symmetric configuration, they must be connected by an exact WKB curve. Then by theorem 1 the Wronskian between them must be non-vanishing. Theorem 2 further asserts that all the Wronskians for the members of that set are non-vanishing, while the ones for elements of the other set all vanish.

Next, consider the asymmetric case. For simplicity, let us assume that $N_1 > N_2 + N_3$ is satisfied³⁶. In such a case, there exist exact WKB curves which start from z_1 , go around z_2 (or z_3), and return to z_1 . To make use of the existence of such a curve, consider the following Wronskians:

$$\langle 1_+, \Omega_2 1_+ \rangle, \quad \langle 1_-, \Omega_2 1_- \rangle. \quad (5.48)$$

³⁶Generalization to other cases is straightforward.

To compute them, we first note that 1_{\pm} can be expressed in terms of 2_{\pm} in the following manner

$$1_{\pm} = \langle 1_{\pm}, 2_{-} \rangle 2_{+} - \langle 1_{\pm}, 2_{+} \rangle 2_{-}. \quad (5.49)$$

Then, applying Ω_2 to (5.49) and substituting them to (5.48), we can express (5.48) in terms of the ordinary Wronskians as

$$\langle 1_{+}, \Omega_2 1_{+} \rangle = 2i \sin p_2 \langle 1_{+}, 2_{-} \rangle \langle 1_{+}, 2_{+} \rangle, \quad (5.50)$$

$$\langle 1_{-}, \Omega_2 1_{-} \rangle = 2i \sin p_2 \langle 1_{-}, 2_{-} \rangle \langle 1_{-}, 2_{+} \rangle. \quad (5.51)$$

Consider the case where 1_{+} is the small solution. Since $\Omega_2 1_{+}$ can be obtained by parallel-transporting 1_{+} along the exact WKB curve which starts and ends at z_1 , $\Omega_2 1_{+}$ must behave as the big solution around z_1 . Therefore, the Wronskian $\langle 1_{+}, \Omega_2 1_{+} \rangle$ is non-vanishing in this case. Then from (5.50) it follows that $\langle 1_{+}, 2_{+} \rangle$ must also be non-vanishing. Applying the theorem 2, we conclude that the Wronskians between the members of \mathcal{S}_{+} are non-vanishing and those of \mathcal{S}_{-} all vanish. In an entirely similar manner, when 1_{-} is the small eigenvector, we obtain the result where the roles of \mathcal{S}_{+} and \mathcal{S}_{-} are interchanged.

Performing similar analyses for the other cases, we obtain the general rules summarized below.

Rule 1: *Decomposition of the eigenvectors into two groups.*

When a factor of the form $\sin(\sum_i \epsilon_i p_i / 2)$ vanishes, the Wronskians which vanish are the ones among $\{1_{\epsilon_1}, 2_{\epsilon_2}, 3_{\epsilon_3}\}$ or the ones among $\{1_{-\epsilon_1}, 2_{-\epsilon_2}, 3_{-\epsilon_3}\}$.

Rule 2: *Symmetric case.*

When the configuration of the exact WKB curves is symmetric, the Wronskians from the group which contains two or more small solutions are nonzero whereas the Wronskians from the other group are zero.

Rule 3: *Asymmetric case.*

When the configuration of the exact WKB curves is asymmetric and N_i 's satisfy $N_i > N_j + N_k$, the Wronskians from the group which contains the smaller of the two solutions i_{\pm} are nonzero whereas the Wronskians from the other group are zero.

In the next subsection, we will utilize these rules to evaluate the individual Wronskians.

5.4 Individual Wronskian from the Wiener-Hopf decomposition

Making use of the data for the analyticity of the Wronskians obtained in the previous subsection, we now set up and solve a Riemann-Hilbert problem to decompose the product

of Wronskians and extract the individual Wronskians. The standard method for such a procedure is known as the Wiener-Hopf decomposition, which extracts from a complicated function a part regular on the upper half plane and the part regular on the lower half plane. The typical set up is as follows. Suppose $F(x)$ is a function which decreases sufficiently fast at infinity and can be written as a sum of two components $F(x) = F_{\uparrow}(x) + F_{\downarrow}(x)$, where $F_{\uparrow}(x)$ is regular on the upper half plane while $F_{\downarrow}(x)$ is regular on the lower half plane. Then, each component, in the region where it is regular, can be extracted from $F(x)$ as

$$F_{\uparrow}(x) = \int_{-\infty}^{\infty} \frac{dx'}{2\pi i} \frac{1}{x' - x} F(x') \quad (\text{Im } x > 0), \quad (5.52)$$

$$F_{\downarrow}(x) = - \int_{-\infty}^{\infty} \frac{dx'}{2\pi i} \frac{1}{x' - x} F(x') \quad (\text{Im } x < 0). \quad (5.53)$$

These equations can be easily proven by first substituting $F(x') = F_{\uparrow}(x') + F_{\downarrow}(x')$ on the right hand side and then closing the integration contour for $F_{\uparrow}(x')$ ($F_{\downarrow}(x')$) on the upper (lower) half plane. Now when the argument x is not in the region specified in (5.52) and (5.53), we need to analytically continue the above formulas. For instance, $F_{\uparrow}(x)$ in the region where $\text{Im } x < 0$ should be expressed as

$$F_{\uparrow}(x) = F(x) - F_{\downarrow}(x) = F(x) + \int_{-\infty}^{\infty} \frac{dx'}{2\pi i} \frac{1}{x' - x} F(x'). \quad (5.54)$$

Note that the first term $F(x)$ on the right hand side can be thought of as due to the integral along a small circle around $x' = x$.

To apply this method to the case of our interest, namely to the equations (5.9)–(5.14), we take the logarithm and represent them in a general form as

$$\begin{aligned} \ln \langle i_{\epsilon_i}, j_{\epsilon_j} \rangle + \ln \langle i_{-\epsilon_i}, j_{-\epsilon_i} \rangle &= \ln \sin \left(\frac{\epsilon_i p_i + \epsilon_j p_j + p_k}{2} \right) + \ln \sin \left(\frac{\epsilon_i p_i + \epsilon_j p_j - p_k}{2} \right) \\ &\quad - \ln \sin p_i - \ln \sin p_j. \end{aligned} \quad (5.55)$$

Here ϵ_i denotes a + or – sign. In this process, we have neglected the contributions of the form $\ln(-1)$, since they only contribute to the overall phase of the three-point functions. Our aim will be to express each of the terms on the left hand side of (5.55) in terms of some convolution integrals of the functions on the right hand side. To put it in another way, we wish to decompose each term on the right hand side into contributions coming from each term on the left hand side. Since the quasi-momentum $p_i(x)$ is defined on a Riemann surface with branch cuts, we need to generalize the Wiener-Hopf decomposition formula in an appropriate way, as discussed below.

5.4.1 Separation of the poles

Let us first decompose the terms of the form $-\ln \sin p_i$, which give rise to poles of the Wronskians. As shown in the previous section, which Wronskian develops a pole is determined purely by the sign of the real part of the quasi-momentum $q_i(x)$. Therefore, we should be able to decompose the quantity $-\ln \sin p_i$ by using a convolution integral along the curve defined by $\text{Re } q_i = 0$. For the ordinary Wiener-Hopf decomposition, the convolution kernel is given simply by $1/(x - x')$. In the present case, however, we have a two-sheeted Riemann surface and hence we must make sure that the kernel has the simple pole only when x and x' coincide on the same sheet. When they are on top of each other on different sheets, no singularity should occur. The appropriate kernel with this property is given by

$$\widehat{\mathcal{K}}_i(x'; x) \equiv \frac{1}{2(x' - x)} \left(\sqrt{\frac{(x - u_i)(x - \bar{u}_i)}{(x' - u_i)(x' - \bar{u}_i)}} + 1 \right). \quad (5.56)$$

When x and x' get close to each other but on different sheets, the square root factor tends to -1 canceling the $+1$ term and hence the kernel is indeed regular. Furthermore, in the limit that x' tends to ∞ , the kernel $\widehat{\mathcal{K}}_i(x'; x)$ decreases like $(x')^{-2}$, which is sufficiently fast for our purpose.

With such a convolution kernel, we can carry out the Wiener-Hopf decomposition in the usual way. Namely the term $-\ln \sin p_i(x)$ can be decomposed into the contributions of $\langle i_+, j_{\epsilon_j} \rangle(x)$ and $\langle i_-, j_{-\epsilon_j} \rangle(x)$ as

$$\langle i_+, j_{\epsilon_j} \rangle(x) \ni \oint_{\Gamma_{i_+}} \widehat{\mathcal{K}}_i * (-\ln \sin p_i), \quad (5.57)$$

$$\langle i_-, j_{-\epsilon_j} \rangle(x) \ni \oint_{\Gamma_{i_-}} \widehat{\mathcal{K}}_i * (-\ln \sin p_i), \quad (5.58)$$

where the convolution integral is defined as

$$\int A * B \equiv \int \frac{dx'}{2\pi i} A(x'; x) B(x'). \quad (5.59)$$

As for the contours of integration, Γ_{i_+} is defined by $\text{Re } q_i = 0$ and Γ_{i_-} stands for $-\Gamma_{i_+}$. The direction of the contour Γ_{i_+} is defined such that $\langle i_+, j_{\epsilon_j} \rangle(x)$ does not contain poles in the region to the left of the contour³⁷.

Now note that under the holomorphic involution $x \rightarrow \hat{\sigma}x$, the quasi-momentum $p_i(x)$ and the square-root contained in (5.56) simply flip sign. Making use of this property, we

³⁷A typical form of the contour is depicted in figure 7.4 in section 7, where we study explicit examples.

can re-express the convolution integrals (5.57) and (5.58) as integrals only on the first (or the upper) sheet.:

$$\langle i_+, j_{\epsilon_j} \rangle(x) \ni - \oint_{\Gamma_{i_+}^u} \mathcal{K}_i * \ln \sin p_i, \quad (5.60)$$

$$\langle i_-, j_{-\epsilon_j} \rangle(x) \ni - \oint_{\Gamma_{i_-}^u} \mathcal{K}_i * \ln \sin p_i. \quad (5.61)$$

Here, $\Gamma_{i_{\pm}}^u$ denotes the portion of $\Gamma_{i_{\pm}}$ on the upper-sheet of the spectral curve and the kernel $\mathcal{K}_i(x'; x)$ (without a hat) is defined by

$$\mathcal{K}_i(x'; x) \equiv \frac{1}{x' - x} \sqrt{\frac{(x - u_i)(x - \bar{u}_i)}{(x' - u_i)(x' - \bar{u}_i)}}. \quad (5.62)$$

Again we have neglected the factors of the form $\ln(-1)$ arising from the sign flip of $p_i(x)$, as they only modify the overall phase of the Wronskians and the three-point functions.

It is important to note that (5.57) and (5.58) are valid only when x is on the left hand side of the contours, just as in the case of the ordinary Wiener-Hopf decomposition. When the argument x is on the right hand side of the contour $\Gamma_{i_{\pm}}$, we must add $-\ln \sin p_i$ to (5.57) and (5.58), as explained in (5.54). Such effects can be taken into account also in (5.60) and (5.61), if x is on the upper sheet, by adding a small circle encircling $x' = x$ counterclockwise to the integration contours. In what follows, such contributions will be referred to as *contact terms*.

5.4.2 Separation of the zeros

Next we shall discuss the decomposition of the first two terms on the right hand side of (5.55), which are responsible for the zeros of the Wronskians. To perform the decomposition, again we need to determine the appropriate convolution kernel and the integration contour.

Let us first discuss the convolution kernel. As the terms of our focus depend on all the quasi-momenta $p_i(x)$'s, the appropriate convolution kernel must be a function on the Riemann surface which contains all the branch cuts of the $p_i(x)$'s. Such a kernel can be easily written down as a generalization of the expression (5.56) and is given by

$$\widehat{\mathcal{K}}_{\text{all}} \equiv \frac{1}{8(x' - x)} \prod_{i=1}^3 \left(\sqrt{\frac{(x - u_i)(x - \bar{u}_i)}{(x' - u_i)(x' - \bar{u}_i)}} + 1 \right). \quad (5.63)$$

Since there are two choices of sign for each square root factor on the right hand side of (5.63), $\widehat{\mathcal{K}}_{\text{all}}$ is properly defined on the eightfold cover of the complex plane. In what follows, we distinguish these eight sheets as $\{*, *, *\}$ -sheet, where the successive entry $*$

is either “ u ” denoting upper sheet or “ l ” denoting lower sheet, referring to the two sheets for $p_1(x)$, $p_2(x)$ and $p_3(x)$ respectively. It is clear that the kernel (5.63) has a pole with a residue $+1$ at $x' = x$ only when two-points are on the same sheet. Therefore it has a desired property for the Wiener-Hopf decomposition.

Let us next turn to the contour of integration. As discussed in the previous section, the zeros of the Wronskians are determined by the following two properties: (i) The connectivity of the exact WKB-curves and (ii) the relative magnitude of the eigenvectors i_{\pm} . Therefore, curves across which these two properties change can be the possible integration contours. Corresponding to the properties (i) and (ii) above, there are two types of integration contours; the curves defined by $\text{Re } q_i(x) = 0$ and the curves defined by $N_i = N_j + N_k$. An important point to bare in mind is that in general only some portions of these curves will be the proper integration contours, since in some cases the analyticity of the Wronskians does not change even when we cross these curves. In order to determine the correct integration contours explicitly, we need to apply the general rules derived in the previous section. However, as the form of the contours determined through such a procedure depends on the specific details of the choice of the external states, we will postpone such an analysis until section 7, where we work out some specific examples. Thus, in what follows we will denote the integration contours without specifying their explicit forms as $\mathcal{M}_{\pm\pm\pm}$, where $\mathcal{M}_{\epsilon_1\epsilon_2\epsilon_3}$ denotes the contour we use to determine the contribution of the factor $\sin(\sum_i \epsilon_i p_i)$ to $\langle i_{\epsilon_i}, j_{\epsilon_j} \rangle$. They are defined such that they flip the orientation if we flip the signs of three indices, for example $\mathcal{M}_{+++} = -\mathcal{M}_{---}$.

Employing the kernel and the contours given above, let us perform the decomposition of the product of Wronskians, taking that of $\langle 1_+, 2_+ \rangle$ and $\langle 1_-, 2_- \rangle$ as a representative example. Applying the Wiener-Hopf decomposition to the relation (5.55) with $i = 1, j = 2$ and $\epsilon_1 = +, \epsilon_2 = +$, we obtain

$$\langle 1_+, 2_+ \rangle \ni \oint_{\mathcal{M}_{+++}} \widehat{\mathcal{K}}_{\text{all}} * \ln \sin \left(\frac{p_1 + p_2 + p_3}{2} \right) + \oint_{\mathcal{M}_{+++}} \widehat{\mathcal{K}}_{\text{all}} * \ln \sin \left(\frac{p_1 + p_2 - p_3}{2} \right), \quad (5.64)$$

$$\langle 1_-, 2_- \rangle \ni \oint_{\mathcal{M}_{---}} \widehat{\mathcal{K}}_{\text{all}} * \ln \sin \left(\frac{p_1 + p_2 + p_3}{2} \right) + \oint_{\mathcal{M}_{---}} \widehat{\mathcal{K}}_{\text{all}} * \ln \sin \left(\frac{p_1 + p_2 - p_3}{2} \right). \quad (5.65)$$

As in the case of the ordinary Wiener-Hopf decomposition, the expressions (5.64) and (5.65) are valid only when x is located to the left of the integration contour. Additional terms, to be discussed shortly, are needed when x is on the other side of the contour.

Let us now show that the kernel $\widehat{\mathcal{K}}_{\text{all}}$ used in (5.64) and (5.65) can be effectively replaced by simpler combinations of the form $(\mathcal{K}_i + \mathcal{K}_j)/8$. To explain the idea, consider

the following integral as an example:

$$\oint_{\mathcal{M}_{+++}} \frac{dx'}{2\pi i} \widehat{\mathcal{K}}_{\text{all}}(x'; x) \ln \sin \left(\frac{p_1 + p_2 + p_3}{2} \right) (x'). \quad (5.66)$$

As the first step, we make a change of integration variable from x' to $\hat{\sigma}_3 x'$, where $\hat{\sigma}_i$ denotes the holomorphic involution with respect to p_i , namely the operation that exchanges the two sheets associated with p_i . Although this clearly leaves the value of the integral intact, the form of the integral changes. One can easily verify that the following transformation formulas for the integrand and the contours hold:

$$\ln \sin \left(\frac{p_1 + p_2 + p_3}{2} \right) (\hat{\sigma}_3 x') = \ln \sin \left(\frac{p_1 + p_2 - p_3}{2} \right) (x'), \quad (5.67)$$

$$\widehat{\mathcal{K}}_{\text{all}}(\hat{\sigma}_3 x'; x) = \widehat{\mathcal{K}}_{\text{all}}^{(3)}(x'; x), \quad (5.68)$$

$$\oint_{\mathcal{M}_{+++}} d(\hat{\sigma}_3 x') = \oint_{\mathcal{M}_{+-}} dx'. \quad (5.69)$$

In the second line (5.68), the ‘‘sign-flipped kernel’’ $\widehat{\mathcal{K}}_{\text{all}}^{(3)}$ is defined by

$$\widehat{\mathcal{K}}_{\text{all}}^{(3)} \equiv \frac{1}{8(x' - x)} \left(-\sqrt{\frac{(x - u_3)(x - \bar{u}_3)}{(x' - u_3)(x' - \bar{u}_3)}} + 1 \right) \prod_{\ell=1,2} \left(\sqrt{\frac{(x - u_\ell)(x - \bar{u}_\ell)}{(x' - u_\ell)(x' - \bar{u}_\ell)}} + 1 \right). \quad (5.70)$$

Making such transformations, we can re-express the integral (5.66) as

$$\oint_{\mathcal{M}_{+-}} \frac{dx'}{2\pi i} \widehat{\mathcal{K}}_{\text{all}}^{(3)}(x'; x) \ln \sin \left(\frac{p_1 + p_2 - p_3}{2} \right) (x'). \quad (5.71)$$

Performing similar analysis for all the possible sign-flips, we obtain 2^3 different expressions for (5.66). Then averaging over all the 2^3 expressions, we find that the final expressions are given in terms of the kernels \mathcal{K}_i as follows:

$$\begin{aligned} &\langle 1_+, 2_+ \rangle \ni \\ &\frac{1}{16} \left(\oint_{\mathcal{M}_{+++}} (\mathcal{K}_1 + \mathcal{K}_2) * \ln \sin \left(\frac{p_1 + p_2 + p_3}{2} \right) + \oint_{\mathcal{M}_{+-}} (\mathcal{K}_1 + \mathcal{K}_2) * \ln \sin \left(\frac{p_1 + p_2 - p_3}{2} \right) \right. \\ &\left. + \oint_{\mathcal{M}_{+--}} (\mathcal{K}_1 - \mathcal{K}_2) * \ln \sin \left(\frac{p_1 - p_2 + p_3}{2} \right) + \oint_{\mathcal{M}_{-++}} (-\mathcal{K}_1 + \mathcal{K}_2) * \ln \sin \left(\frac{-p_1 + p_2 + p_3}{2} \right) \right), \end{aligned} \quad (5.72)$$

$$\begin{aligned} &\langle 1_-, 2_- \rangle \ni \\ &\frac{1}{16} \left(\oint_{\mathcal{M}_{---}} (\mathcal{K}_1 + \mathcal{K}_2) * \ln \sin \left(\frac{p_1 + p_2 + p_3}{2} \right) + \oint_{\mathcal{M}_{--+}} (\mathcal{K}_1 + \mathcal{K}_2) * \ln \sin \left(\frac{p_1 + p_2 - p_3}{2} \right) \right. \\ &\left. + \oint_{\mathcal{M}_{-+-}} (\mathcal{K}_1 - \mathcal{K}_2) * \ln \sin \left(\frac{p_1 - p_2 + p_3}{2} \right) + \oint_{\mathcal{M}_{+--}} (-\mathcal{K}_1 + \mathcal{K}_2) * \ln \sin \left(\frac{-p_1 + p_2 + p_3}{2} \right) \right). \end{aligned} \quad (5.73)$$

Just as before, we neglected the contributions of the form $\ln(-1)$ as leading to pure phases. Also, the same remarks made below equations (5.64) and (5.65) on the position of x relative to the contour lines apply to the expressions (5.72) and (5.73) above.

Finally, for later convenience, let us further re-write the above expressions as integrals performed purely on the $\{u, u, u\}$ -sheet. Each contour $\mathcal{M}_{\epsilon_1 \epsilon_2 \epsilon_3}$ has parts on the eight different sheets denoted by $\mathcal{M}_{\epsilon_1 \epsilon_2 \epsilon_3}^{u, u, u}, \mathcal{M}_{\epsilon_1 \epsilon_2 \epsilon_3}^{u, u, l}$, etc., where the superscripts indicate the relevant sheet in an obvious way. Consider for example the first integral in (5.72) along the contour \mathcal{M}_{+++} . The form as given is for the portion \mathcal{M}_{+++}^{uuu} . For the portion denoted by \mathcal{M}_{+++}^{ulu} for example, if we wish to express its contribution in terms of an integral on the $\{u, u, u\}$ -sheet, we need to change the sign of \mathcal{K}_2 and p_2 . Then the integral becomes identical to that of the first term in the second line of (5.72), except along \mathcal{M}_{+-+}^{uuu} . In similar fashions we can re-express the contributions from the eight parts of \mathcal{M}_{+++} in terms of the integrals on the $\{u, u, u\}$ -sheet. After repeating the same procedure for the rest of the three terms in (5.72), one finds that the net effect is that each term of (5.72) is multiplied by a factor of eight, with each contour restricted to the $\{u, u, u\}$ -sheet. In this way we obtain the representations

$$\begin{aligned} \langle 1_+, 2_+ \rangle \ni & \\ \frac{1}{2} \left(\oint_{\mathcal{M}_{+++}^{uuu}} (\mathcal{K}_1 + \mathcal{K}_2) * \ln \sin \left(\frac{p_1 + p_2 + p_3}{2} \right) + \oint_{\mathcal{M}_{+++}^{uu-}} (\mathcal{K}_1 + \mathcal{K}_2) * \ln \sin \left(\frac{p_1 + p_2 - p_3}{2} \right) \right. & \\ \left. + \oint_{\mathcal{M}_{+-+}^{uuu}} (\mathcal{K}_1 - \mathcal{K}_2) * \ln \sin \left(\frac{p_1 - p_2 + p_3}{2} \right) + \oint_{\mathcal{M}_{+-+}^{uu-}} (-\mathcal{K}_1 + \mathcal{K}_2) * \ln \sin \left(\frac{-p_1 + p_2 + p_3}{2} \right) \right), & \end{aligned} \quad (5.74)$$

$$\begin{aligned} \langle 1_-, 2_- \rangle \ni & \\ \frac{1}{2} \left(\oint_{\mathcal{M}_{---}^{uuu}} (\mathcal{K}_1 + \mathcal{K}_2) * \ln \sin \left(\frac{p_1 + p_2 + p_3}{2} \right) + \oint_{\mathcal{M}_{---}^{uu+}} (\mathcal{K}_1 + \mathcal{K}_2) * \ln \sin \left(\frac{p_1 + p_2 - p_3}{2} \right) \right. & \\ \left. + \oint_{\mathcal{M}_{-+-}^{uuu}} (\mathcal{K}_1 - \mathcal{K}_2) * \ln \sin \left(\frac{p_1 - p_2 + p_3}{2} \right) + \oint_{\mathcal{M}_{-+-}^{uu-}} (-\mathcal{K}_1 + \mathcal{K}_2) * \ln \sin \left(\frac{-p_1 + p_2 + p_3}{2} \right) \right). & \end{aligned} \quad (5.75)$$

The results obtained in this subsection and the previous subsection are both expressed in terms of certain convolution integrals on the spectral curve. Thus, in what follows, we will denote their sum by $\mathbf{Conv}\langle i_{\pm}, j_{\pm} \rangle$.

Before ending this subsection, let us make one important remark. Although each convolution integral obtained so far is divergent at $x = \pm 1$, the divergence cancels³⁸ in the sum $\mathbf{Conv}\langle i_{\pm}, j_{\pm} \rangle$. Thus the contribution singular at $x = \pm 1$ must be separately taken into account as we will do in the next subsection.

³⁸One can confirm this by expanding the convolution integrals around $x = \pm 1$.

5.5 Singular part and constant part of the Wronskians

In addition to the main non-trivial parts determined by the Wiener-Hopf decomposition described above, there are two further contributions to the Wronskians. One is the contribution singular at $x = \pm 1$, coming from such structure in the connections used in ALP. The other is the possibility of adding a constant function on the spectral curve. In this subsection, we will determine these two contributions.

Let us first focus on terms singular at $x = 1$. To determine such terms, we will need the WKB expansions around $x = 1$ for all the Wronskians, not just the ones that were discussed in section 3.2, namely $\langle i_+, j_+ \rangle$ and $\langle i_-, j_- \rangle$. This is because of the following reason: Although the formulas we obtained for the contribution of the action and that of the wave function appear to contain Wronskians of the type $\langle i_+, j_+ \rangle$ and $\langle i_-, j_- \rangle$ only, we must understand their behavior when they are followed into the second sheet as well in order to know the analyticity property on the entire Riemann surface. As shown in (2.100), when we cross the branch cut associated with $p_i(x)$ into the lower sheet, the eigenfunctions i_+ and i_- behave like i_- and $-i_+$ on the upper sheet, respectively. Therefore the behavior of $\langle i_+, j_+ \rangle$ on the $\{u, l, *\}$ -sheet can be obtained from the behavior of $\langle i_+, j_- \rangle$ on the $\{u, u, *\}$ -sheet, etc.

Now the WKB expansions of the Wronskians of the type $\langle i_+, j_- \rangle$ can be obtained from those of $\langle i_+, j_+ \rangle$ by the use of the following Schouten identities:

$$\langle i_+, j_- \rangle \langle j_+, k_+ \rangle + \langle i_+, j_+ \rangle \langle j_-, k_+ \rangle + \langle i_+, k_+ \rangle \langle j_-, j_+ \rangle = 0. \quad (5.76)$$

Indeed these identities can be regarded as the equations for the six unknown Wronskians of the form $\langle i_+, j_- \rangle$. If we consider all the combinations of i, j and k in (5.76), we obtain three independent equations. Combining them with the equations (5.12)–(5.14) for the products of the Wronskians, we can completely determine $\langle i_+, j_- \rangle$'s in terms of $\langle i_+, j_+ \rangle$

in the following form:

$$\langle 1_+, 2_- \rangle = e^{-i(p_1+p_2-p_3)/2} \frac{\sin\left(\frac{p_1-p_2-p_3}{2}\right)}{\sin p_2} \frac{\langle 3_+, 1_+ \rangle}{\langle 2_+, 3_+ \rangle}, \quad (5.77)$$

$$\langle 1_-, 2_+ \rangle = e^{i(p_1+p_2-p_3)/2} \frac{\sin\left(\frac{p_1-p_2-p_3}{2}\right)}{\sin p_1} \frac{\langle 2_+, 3_+ \rangle}{\langle 3_+, 1_+ \rangle}, \quad (5.78)$$

$$\langle 2_+, 3_- \rangle = e^{-i(-p_1+p_2+p_3)/2} \frac{\sin\left(\frac{-p_1+p_2-p_3}{2}\right)}{\sin p_3} \frac{\langle 1_+, 2_+ \rangle}{\langle 3_+, 1_+ \rangle}, \quad (5.79)$$

$$\langle 2_-, 3_+ \rangle = e^{i(-p_1+p_2+p_3)/2} \frac{\sin\left(\frac{p_1+p_2-p_3}{2}\right)}{\sin p_2} \frac{\langle 3_+, 1_+ \rangle}{\langle 1_+, 2_+ \rangle}, \quad (5.80)$$

$$\langle 3_+, 1_- \rangle = e^{-i(p_1-p_2+p_3)/2} \frac{\sin\left(\frac{-p_1-p_2+p_3}{2}\right)}{\sin p_1} \frac{\langle 2_+, 3_+ \rangle}{\langle 1_+, 2_+ \rangle}, \quad (5.81)$$

$$\langle 3_-, 1_+ \rangle = e^{i(p_1-p_2+p_3)/2} \frac{\sin\left(\frac{-p_1+p_2+p_3}{2}\right)}{\sin p_3} \frac{\langle 1_+, 2_+ \rangle}{\langle 2_+, 3_+ \rangle}. \quad (5.82)$$

From these expressions, we can obtain the WKB-expansion for every Wronskian using the results for $\langle i_+, j_+ \rangle$.

The singular term of the Wronskians is given simply by the leading term in the WKB expansion. For instance, the singular terms for $\langle i_+, j_+ \rangle$ and $\langle i_-, j_- \rangle$ at $x = 1$ on the $\{u, u, u\}$ -sheet is determined from the expansion (3.37) and (3.38) as

$$\ln\langle 1_+, 2_+ \rangle \stackrel{x \sim 1}{\sim} \frac{2}{1-x} \int_{\ell_{21}} \sqrt{T} dz, \quad \ln\langle 1_-, 2_- \rangle \stackrel{x \sim 1}{\sim} \frac{2}{1-x} \int_{\ell_{12}} \sqrt{T} dz, \quad (5.83)$$

$$\ln\langle 2_+, 3_+ \rangle \stackrel{x \sim 1}{\sim} \frac{2}{1-x} \int_{\ell_{23}} \sqrt{T} dz, \quad \ln\langle 2_-, 3_- \rangle \stackrel{x \sim 1}{\sim} \frac{2}{1-x} \int_{\ell_{32}} \sqrt{T} dz, \quad (5.84)$$

$$\ln\langle 3_+, 1_+ \rangle \stackrel{x \sim 1}{\sim} \frac{2}{1-x} \int_{\ell_{31}} \sqrt{T} dz, \quad \ln\langle 3_-, 1_- \rangle \stackrel{x \sim 1}{\sim} \frac{2}{1-x} \int_{\ell_{13}} \sqrt{T} dz. \quad (5.85)$$

Then by using (5.77)–(5.82) we can determine the singular terms for $\langle i_+, j_- \rangle$ on the $\{u, u, u\}$ -sheet as

$$\ln\langle 1_+, 2_- \rangle \stackrel{x \sim 1}{\sim} \frac{2\pi i(\kappa_1 + \kappa_2 - \kappa_3)}{1-x} + \frac{2}{1-x} \int_{\ell_{23} + \ell_{31}} \sqrt{T} dz, \quad (5.86)$$

$$\ln\langle 1_-, 2_+ \rangle \stackrel{x \sim 1}{\sim} \frac{2\pi i(-\kappa_1 - \kappa_2 + \kappa_3)}{1-x} + \frac{2}{1-x} \int_{\ell_{13} + \ell_{32}} \sqrt{T} dz, \quad (5.87)$$

$$\ln\langle 2_+, 3_- \rangle \stackrel{x \sim 1}{\sim} \frac{2\pi i(-\kappa_1 + \kappa_2 + \kappa_3)}{1-x} + \frac{2}{1-x} \int_{\ell_{21} + \ell_{13}} \sqrt{T} dz, \quad (5.88)$$

$$\ln\langle 2_-, 3_+ \rangle \stackrel{x \sim 1}{\sim} \frac{2\pi i(\kappa_1 - \kappa_2 - \kappa_3)}{1-x} + \frac{2}{1-x} \int_{\ell_{31} + \ell_{12}} \sqrt{T} dz, \quad (5.89)$$

$$\ln\langle 3_+, 1_- \rangle \stackrel{x \sim 1}{\sim} \frac{2\pi i(\kappa_1 - \kappa_2 + \kappa_3)}{1-x} + \frac{2}{1-x} \int_{\ell_{12} + \ell_{23}} \sqrt{T} dz, \quad (5.90)$$

$$\ln\langle 3_-, 1_+ \rangle \stackrel{x \sim 1}{\sim} \frac{2\pi i(-\kappa_1 + \kappa_2 - \kappa_3)}{1-x} + \frac{2}{1-x} \int_{\ell_{32} + \ell_{21}} \sqrt{T} dz. \quad (5.91)$$

In order to determine the singular terms completely, we also need to understand the singular behavior on other sheets. As already described, this can be done by utilizing the fact that i_+ and i_- transform into i_- and $-i_+$ respectively as one crosses a branch cut associated to $p_i(x)$. For instance, applying this rule we can easily find that the singular term for $\langle 1_+, 2_+ \rangle$ must behave in the following way on each sheet:

$$\langle 1_+, 2_+ \rangle \stackrel{x \sim 1}{\sim} \frac{2}{1-x} \int_{\ell_{21}} \sqrt{T} dz \quad (\text{on the } \{u, u, *\}\text{-sheet}), \quad (5.92)$$

$$\langle 1_+, 2_+ \rangle \stackrel{x \sim 1}{\sim} \frac{2\pi i(\kappa_1 + \kappa_2 - \kappa_3)}{1-x} + \frac{2}{1-x} \int_{\ell_{23} + \ell_{31}} \sqrt{T} dz \quad (\text{on the } \{u, l, *\}\text{-sheet}), \quad (5.93)$$

$$\langle 1_+, 2_+ \rangle \stackrel{x \sim 1}{\sim} \frac{2\pi i(-\kappa_1 - \kappa_2 + \kappa_3)}{1-x} + \frac{2}{1-x} \int_{\ell_{13} + \ell_{32}} \sqrt{T} dz \quad (\text{on the } \{l, u, *\}\text{-sheet}), \quad (5.94)$$

$$\langle 1_+, 2_+ \rangle \stackrel{x \sim 1}{\sim} \frac{2}{1-x} \int_{\ell_{12}} \sqrt{T} dz \quad (\text{on the } \{l, l, *\}\text{-sheet}). \quad (5.95)$$

Combining all these results, it is possible to write down the expression on the entire Riemann surface which gives the correct singular behavior on the respective sheet. It is given by

$$\begin{aligned} \text{Sing}_+ [\langle 1_+, 2_+ \rangle] &= \frac{1}{1-x} \sqrt{\frac{(x-u_1)(x-\bar{u}_1)}{(1-u_1)(1-\bar{u}_1)}} \left(\pi i(\kappa_1 + \kappa_2 - \kappa_3) + 2 \int_{\ell_{12} + \ell_{23} + \ell_{31}} \sqrt{T} dz \right) \\ &+ \frac{1}{1-x} \sqrt{\frac{(x-u_2)(x-\bar{u}_2)}{(1-u_2)(1-\bar{u}_2)}} \left(\pi i(-\kappa_1 - \kappa_2 + \kappa_3) + 2 \int_{\ell_{23} + \ell_{31} + \ell_{12}} \sqrt{T} dz \right). \end{aligned} \quad (5.96)$$

Here and hereafter, we will use the notation $\text{Sing}_\pm [f(x)]$ to denote the singular term of $f(x)$ around $x = \pm 1$. In an entirely similar manner, we can determine the terms singular at $x = -1$ as

$$\begin{aligned} \text{Sing}_- [\langle 1_+, 2_+ \rangle] &= \frac{1}{1+x} \sqrt{\frac{(x-u_1)(x-\bar{u}_1)}{(1-u_1)(1-\bar{u}_1)}} \left(\pi i(-\kappa_1 - \kappa_2 + \kappa_3) + 2 \int_{\ell_{12} + \ell_{23} + \ell_{31}} \sqrt{\bar{T}} d\bar{z} \right) \\ &+ \frac{1}{1+x} \sqrt{\frac{(x-u_2)(x-\bar{u}_2)}{(1-u_2)(1-\bar{u}_2)}} \left(\pi i(\kappa_1 + \kappa_2 - \kappa_3) + 2 \int_{\ell_{23} + \ell_{31} + \ell_{12}} \sqrt{\bar{T}} d\bar{z} \right). \end{aligned} \quad (5.97)$$

Singular terms for other Wronskians at $x = \pm 1$ can be determined in a similar manner.

The remaining issue is the ambiguity of adding a constant function to the logarithm of the Wronskian. Such an ambiguity can be fixed by once more utilizing the property

that i_{\pm} that i_+ (i_-) transforms into i_- ($-i_+$) as it crosses the branch cut of p_i . This leads to the following constraint for the Wronskians

$$\langle i_+, j_+ \rangle(\hat{\sigma}_i \hat{\sigma}_j x) = \langle i_-, j_- \rangle(x). \quad (5.98)$$

It turns out that all the results obtained so far satisfy (5.98). Since this property gets lost upon adding a constant to the logarithm of the Wronskian, it shows that our results are already complete and we should not add any constant functions.

6 Complete three-point functions at strong coupling

Up to the last section, we have developed necessary methods and acquired the knowledge of the various parts that make up the three-point functions of our interest. Now we are ready to put them together and see that they combine in a non-trivial fashion to produce a rather remarkable answer.

First in subsection 6.1, we obtain the complete result for the S^3 part by putting together the contribution of the action and that of the vertex operators. These two contributions combine nicely to produce a simple expression in terms of integrals on the spectral curve. Then, adapting the methods developed for the S^3 part, we evaluate in subsection 6.2 the $EAdS_3$ part of the three-point function. Our focus will be on the differences between the S^3 and $EAdS_3$ contributions. Finally in subsection 6.3, we present the full answer by combining the contributions of the S^3 part and the $EAdS_3$ part. We will see that the structure of the final answer closely resembles that of the weak coupling result. Detailed comparison for certain specific cases will be performed in section 7.

6.1 The S^3 part

Before we begin the actual computations, let us summarize the structure of the contributions from the S^3 part to the logarithm of the three-point function, which we denote by F_{S^3} . As was already indicated in section 2.3, F_{S^3} consists of the contribution of the action and that of the vertex operators, namely

$$F_{S^3} = \mathcal{F}_{\text{action}} + \mathcal{F}_{\text{vertex}}. \quad (6.1)$$

Each contribution can be further split into several different pieces as

$$\mathcal{F}_{\text{action}} = \frac{\sqrt{\lambda}}{6} + \mathcal{A}_{\varpi} + \mathcal{A}_{\eta}, \quad \mathcal{F}_{\text{vertex}} = \mathcal{V}_{\text{kin}} + \mathcal{V}_{\text{dyn}} + \mathcal{V}_{\text{energy}}. \quad (6.2)$$

Among these terms, \mathcal{A}_{ϖ} , \mathcal{V}_{kin} and $\mathcal{V}_{\text{energy}}$ have already been evaluated respectively in (3.47), (4.61) and (4.63). Thus, our main task will be to compute \mathcal{A}_{η} and \mathcal{V}_{dyn} . As shown

in (3.48) and (4.62), \mathcal{A}_η is given by the normal ordered derivatives of the Wronskians, $:\partial_x \ln\langle i_+, j_+ \rangle:_{\pm}$, whereas \mathcal{V}_{dyn} is given by the Wronskians evaluated at $x = 0$ and $x = \infty$, $\ln\langle i_+, j_+ \rangle|_{\infty}$ and $\ln\langle i_-, j_- \rangle|_0$. From the discussion in section 5, we know the Wronskians are comprised of two different parts, the convolution-integral part $\text{Conv}[\ln\langle i_*, j_* \rangle]$ and the singular part $\text{Sing}_{\pm}[\ln\langle i_*, j_* \rangle]$. They both contribute to \mathcal{A}_η and \mathcal{V}_{dyn} . In what follows, we examine these two parts separately and evaluate their contributions to \mathcal{A}_η and \mathcal{V}_{dyn} .

6.1.1 Contributions from the convolution integrals

We begin with the computation of the convolution integrals. To illustrate the basic idea, let us study $\text{Conv}[\ln\langle 2_+, 1_+ \rangle]|_{\infty}$, $\text{Conv}[\ln\langle 2_-, 1_- \rangle]|_0$ and $:\partial_x \text{Conv}[\ln\langle 2_+, 1_+ \rangle]:_{\pm}$ as representative examples.

To compute the first two quantities, we need to know on which side of the integration contours the points $x = 0$ and $x = \infty$ are located. This is because the convolution integrals derived in subsection 5.4 are valid only when x is on the left hand side of the contours. When x is on the right hand side of the contours, we must include the contact terms, which originate from the integration around $x' = x$. Unfortunately, the form of the contours depend on the specific details of the solutions we use and hence we cannot give a general discussion. We will therefore postpone the discussion of the contact terms until we study several explicit examples in the next section.

Apart from such contact terms, $\text{Conv}[\langle 2_+, 1_+ \rangle]|_{\infty}$ and $\text{Conv}[\langle 2_-, 1_- \rangle]|_0$ can be obtained directly from (5.60), (5.61), (5.74) and (5.75) by setting the value of x in the convolution kernels $\mathcal{K}_i(x'; x)$ to be 0 and ∞ respectively.

Next, consider the evaluation of the normal-ordered derivative $:\partial_x \text{Conv}[\ln\langle 2_+, 1_+ \rangle]:_{\pm}$. This quantity does not receive contributions from the contact terms since the integration contours pass right through $x = \pm 1$ and we can compute $:\partial_x \text{Conv}[\ln\langle 2_+, 1_+ \rangle]:_{\pm}$ always on the left hand side of the contour. In addition, since the convolution integrals are nonsingular at $x = \pm 1$, as discussed at the end of section 5.4, the normal ordering is in fact unnecessary. Thus, $:\partial_x \text{Conv}[\ln\langle 2_+, 1_+ \rangle]:_{\pm}$ can be obtained from (5.60) and (5.74) by simply replacing $\mathcal{K}_i(x'; x)$ with their derivatives $\partial_x \mathcal{K}_i(x'; x)|_{x=\pm 1}$.

Applying similar analyses to other Wronskians and using the formulas (3.48) and (4.62), we can obtain the contributions of the convolution integrals to \mathcal{A}_η and \mathcal{V}_{dyn} , which

will be denoted by $\text{Conv}[\mathcal{A}_\eta]$ and $\text{Conv}[\mathcal{V}_{\text{dyn}}]$. They are given by

$$\begin{aligned}
\text{Conv}[\mathcal{A}_\eta] = & \sqrt{\lambda} \left[\int_{\mathcal{M}_{---}} \left\langle \kappa_i \partial_x \mathcal{K}_i|_+ - \kappa_i \partial_x \mathcal{K}_i|_- \right\rangle_{123} * \ln \sin \left(\frac{p_1 + p_2 + p_3}{2} \right) \right. \\
& + \int_{\mathcal{M}_{--+}} \left\langle \kappa_i \partial_x \mathcal{K}_i|_+ - \kappa_i \partial_x \mathcal{K}_i|_- \right\rangle_{12}^3 * \ln \sin \left(\frac{p_1 + p_2 - p_3}{2} \right) \\
& + \int_{\mathcal{M}_{+-}} \left\langle \kappa_i \partial_x \mathcal{K}_i|_+ - \kappa_i \partial_x \mathcal{K}_i|_- \right\rangle_{13}^2 * \ln \sin \left(\frac{p_1 - p_2 + p_3}{2} \right) \\
& + \int_{\mathcal{M}_{+--}} \left\langle \kappa_i \partial_x \mathcal{K}_i|_+ - \kappa_i \partial_x \mathcal{K}_i|_- \right\rangle_{23}^1 * \ln \sin \left(\frac{-p_1 + p_2 + p_3}{2} \right) \\
& \left. - 2 \sum_{j=1}^3 \int_{\Gamma_{j-}^u} (\kappa_j \partial_x \mathcal{K}_j|_+ - \kappa_j \partial_x \mathcal{K}_j|_-) * \ln \sin p_j \right], \tag{6.3}
\end{aligned}$$

$$\begin{aligned}
\text{Conv}[\mathcal{V}_{\text{dyn}}] = & \int_{\mathcal{M}_{---}} \left\langle S_\infty^i \mathcal{K}_i|_\infty + S_0^i \mathcal{K}_i|_0 \right\rangle_{123} * \ln \sin \left(\frac{p_1 + p_2 + p_3}{2} \right) \\
& + \int_{\mathcal{M}_{--+}} \left\langle S_\infty^i \mathcal{K}_i|_\infty + S_0^i \mathcal{K}_i|_0 \right\rangle_{12}^3 * \ln \sin \left(\frac{p_1 + p_2 - p_3}{2} \right) \\
& + \int_{\mathcal{M}_{+-}} \left\langle S_\infty^i \mathcal{K}_i|_\infty + S_0^i \mathcal{K}_i|_0 \right\rangle_{13}^2 * \ln \sin \left(\frac{p_1 - p_2 + p_3}{2} \right) \\
& + \int_{\mathcal{M}_{+--}} \left\langle S_\infty^i \mathcal{K}_i|_\infty + S_0^i \mathcal{K}_i|_0 \right\rangle_{23}^1 * \ln \sin \left(\frac{-p_1 + p_2 + p_3}{2} \right) \\
& - 2 \sum_{j=1}^3 \int_{\Gamma_{j-}^u} (S_\infty^j \mathcal{K}_j|_\infty + S_0^j \mathcal{K}_j|_0) * \ln \sin p_j. \tag{6.4}
\end{aligned}$$

To simplify the expressions, we have introduced the double bracket notation $\langle\langle \star \rangle\rangle$, to denote sum of three terms with designated combinations of signs, defined as

$$\langle\langle a_i \rangle\rangle_{123} = a_1 + a_2 + a_3, \quad \langle\langle a_i \rangle\rangle_{12}^3 = a_1 + a_2 - a_3, \quad \text{etc.}, \tag{6.5}$$

Also, we have employed the abbreviated symbols $\partial_x \mathcal{K}_i|_\pm$, $\mathcal{K}_i|_\infty$ and $\mathcal{K}_i|_0$, which are defined by

$$\partial_x \mathcal{K}_i|_\pm \equiv \partial_x \mathcal{K}_i(x'; x)|_{x=\pm 1}, \quad \mathcal{K}_i|_\infty \equiv \mathcal{K}_i(x'; \infty), \quad \mathcal{K}_i|_0 \equiv \mathcal{K}_i(x'; 0). \tag{6.6}$$

It turns out that the two contributions (6.3) and (6.4) combine to give a remarkably simple expression displayed below. This is due to the crucial relation of the form

$$\sqrt{\lambda} \kappa_i \partial_x \mathcal{K}_i|_+ - \sqrt{\lambda} \kappa_i \partial_x \mathcal{K}_i|_- + S_\infty^i \mathcal{K}_i|_\infty + S_0^i \mathcal{K}_i|_0 = z(x') \frac{dp_i(x')}{dx'}, \tag{6.7}$$

where $z(x)$ on the right hand side is the Zhukovsky variable, defined in (2.36). Although this equality can be verified by a direct computation using the explicit form of $p_i(x)$ for

the one-cut solutions given in (2.58), it is important to give a more intuitive and essential understanding. Note that the right hand side of (6.7) is proportional to the integrand of the filling fraction given in (2.35). Therefore when integrated over appropriate a -type cycles, it produces the corresponding conserved charges. In other words, it is characterized by the singularities associated with such charges. Now observe that the left hand side precisely consists of terms which provide such singularities. The first two terms are responsible for the singularities at $x = \pm 1$, while the last two terms contain the poles at $x = \infty$ and $x = 0$ associated with the charges S_∞^i and S_0^i respectively. Furthermore, it should be emphasized that the formula above *unifies* the contributions in two sense of the word. First, it unites the contributions from the action, represented by the first two terms, and those from the vertex operators, represented by the last two terms. Only when they are put together one can reproduce all the singularities of the right hand side. Second, the expression obtained on the right hand side is universal in that all the specific data shown on the left hand side, namely κ_i, S_∞^i and S_0^i , are contained in one quantity $p_i(x)$. As we shall discuss in section 6.2, this feature allows us to write down the same form of the result (except for an overall sign) given by the right hand side of (6.7) for the contributions from the $EAdS_3$ part, using the quasi-momentum for that part of the string.

Now, applying (6.7) we can rewrite the sum $\mathcal{T}_{\text{conv}} \equiv \text{Conv}[\mathcal{A}_\eta] + \text{Conv}[\mathcal{V}_{\text{dyn}}]$ into the following compact expression:

$$\begin{aligned}
\mathcal{T}_{\text{conv}} = & \int_{\mathcal{M}_{uuu-}} \frac{z(x)(dp_1 + dp_2 + dp_3)}{2\pi i} \ln \sin \left(\frac{p_1 + p_2 + p_3}{2} \right) \\
& + \int_{\mathcal{M}_{uuu+}} \frac{z(x)(dp_1 + dp_2 - dp_3)}{2\pi i} \ln \sin \left(\frac{p_1 + p_2 - p_3}{2} \right) \\
& + \int_{\mathcal{M}_{uu+-}} \frac{z(x)(dp_1 - dp_2 + dp_3)}{2\pi i} \ln \sin \left(\frac{p_1 - p_2 + p_3}{2} \right) \\
& + \int_{\mathcal{M}_{u+--}} \frac{z(x)(-dp_1 + dp_2 + dp_3)}{2\pi i} \ln \sin \left(\frac{-p_1 + p_2 + p_3}{2} \right) \\
& - 2 \sum_{j=1}^3 \int_{\Gamma_{j-}^u} \frac{z(x) dp_j}{2\pi i} \ln \sin p_j + \text{Contact}. \tag{6.8}
\end{aligned}$$

In the last line, we included the possible contributions from the contact terms, denoted by Contact .

6.1.2 Contributions from the singular part of the Wronskians

We now turn to the computation of the singular part $\text{Sing}_\pm[\ln\langle i_*, j_* \rangle]$. By substituting the expressions for the singular part of the Wronskians, such as (5.96) and (5.97), into

the formulas (3.48) and (4.62), we can evaluate the contributions of the singular part in a straightforward manner. From this calculation, we find that a part of the terms contribute only to the overall phase of the three-point functions. For instance, the first and the third term in (5.96), which are proportional to $\pm\pi i(\kappa_1 + \kappa_2 - \kappa_3)$, will only yield an overall phase owing to the factor of πi . Just as before, we will ignore such contributions in this work. Then the contributions of $\text{Sing}_+[\ln\langle i_*, j_* \rangle]$ to \mathcal{A}_η and \mathcal{V}_{dyn} , denoted by $\text{Sing}_+[\mathcal{A}_\eta]$ and $\text{Sing}_+[\mathcal{V}_{\text{dyn}}]$, are obtained as

$$\begin{aligned} \text{Sing}_+[\mathcal{A}_\eta] = \sqrt{\lambda} & \left[\left\langle \left\langle \kappa_i : \partial_x \mathcal{K}_i(1; x) :_+ - \kappa_i \partial_x \mathcal{K}_i(1; x) |_- \right\rangle \right\rangle_{12}^3 \int_{\ell_{21}} \varpi \right. \\ & + \left\langle \left\langle \kappa_i : \partial_x \mathcal{K}_i(1; x) :_+ - \kappa_i \partial_x \mathcal{K}_i(1; x) |_- \right\rangle \right\rangle_{23}^1 \int_{\ell_{23}} \varpi \\ & \left. + \left\langle \left\langle \kappa_i : \partial_x \mathcal{K}_i(1; x) :_+ - \kappa_i \partial_x \mathcal{K}_i(1; x) |_- \right\rangle \right\rangle_{13}^2 \int_{\ell_{31}} \varpi \right], \end{aligned} \quad (6.9)$$

and

$$\begin{aligned} \text{Sing}_+[\mathcal{V}_{\text{dyn}}] = & \left[\left\langle \left\langle S_\infty^i \mathcal{K}_i |_\infty + S_0^i \mathcal{K}_i |_0 \right\rangle \right\rangle_{12}^3 \int_{\ell_{21}} \varpi + \left\langle \left\langle S_\infty^i \mathcal{K}_i |_\infty + S_0^i \mathcal{K}_i |_0 \right\rangle \right\rangle_{23}^1 \int_{\ell_{23}} \varpi \right. \\ & \left. + \left\langle \left\langle S_\infty^i \mathcal{K}_i |_\infty + S_0^i \mathcal{K}_i |_0 \right\rangle \right\rangle_{13}^2 \int_{\ell_{31}} \varpi \right] \Big|_{x'=+1}. \end{aligned} \quad (6.10)$$

Note that in the present case, in contrast to the case of $:\partial_x \text{Conv}[\ln\langle i_*, j_* \rangle] :_\pm$ discussed previously, the normal ordering in $:\partial_x \mathcal{K}_i(1; x) :_+$ is necessary since $\partial_x \mathcal{K}_i(1; x)$ is singular at $x = 1$. In an entirely similar manner, the contributions of $\text{Sing}_-[\ln\langle i_*, j_* \rangle]$ to \mathcal{A}_η and \mathcal{V}_{dyn} , denoted by $\text{Sing}_-[\mathcal{A}_\eta]$ and $\text{Sing}_-[\mathcal{V}_{\text{dyn}}]$, are computed as

$$\begin{aligned} \text{Sing}_-[\mathcal{A}_\eta] = -\sqrt{\lambda} & \left[\left\langle \left\langle \kappa_i \partial_x \mathcal{K}_i(-1; x) |_+ - \kappa_i : \partial_x \mathcal{K}_i(-1; x) :_- \right\rangle \right\rangle_{12}^3 \int_{\ell_{21}} \bar{\varpi} \right. \\ & + \left\langle \left\langle \kappa_i \partial_x \mathcal{K}_i(-1; x) |_+ - \kappa_i : \partial_x \mathcal{K}_i(-1; x) :_- \right\rangle \right\rangle_{23}^1 \int_{\ell_{23}} \bar{\varpi} \\ & \left. + \left\langle \left\langle \kappa_i \partial_x \mathcal{K}_i(-1; x) |_+ - \kappa_i : \partial_x \mathcal{K}_i(-1; x) :_- \right\rangle \right\rangle_{13}^2 \int_{\ell_{31}} \bar{\varpi} \right], \end{aligned} \quad (6.11)$$

and

$$\begin{aligned} \text{Sing}_-[\mathcal{V}_{\text{dyn}}] = - & \left[\left\langle \left\langle S_\infty^i \mathcal{K}_i |_\infty + S_0^i \mathcal{K}_i |_0 \right\rangle \right\rangle_{12}^3 \int_{\ell_{21}} \bar{\varpi} + \left\langle \left\langle S_\infty^i \mathcal{K}_i |_\infty + S_0^i \mathcal{K}_i |_0 \right\rangle \right\rangle_{23}^1 \int_{\ell_{23}} \bar{\varpi} \right. \\ & \left. + \left\langle \left\langle S_\infty^i \mathcal{K}_i |_\infty + S_0^i \mathcal{K}_i |_0 \right\rangle \right\rangle_{13}^2 \int_{\ell_{31}} \bar{\varpi} \right] \Big|_{x'=-1}. \end{aligned} \quad (6.12)$$

Now just as we did for $\text{Conv}[\mathcal{A}_\eta] + \text{Conv}[\mathcal{V}_{\text{dyn}}]$, we can make use of the relation (6.7)

to rewrite the sum $\text{Sing}_\pm[\mathcal{A}_\eta] + \text{Sing}_\pm[\mathcal{V}_{\text{dyn}}]$ into much simpler forms. The results are

$$\begin{aligned} \text{Sing}_+[\mathcal{A}_\eta] + \text{Sing}_+[\mathcal{V}_{\text{dyn}}] &= :z(x) \left(\frac{dp_1}{dx} + \frac{dp_2}{dx} - \frac{dp_3}{dx} \right) :_+ \int_{\ell_{21}} \varpi \\ &\quad + :z(x) \left(\frac{dp_1}{dx} - \frac{dp_2}{dx} + \frac{dp_3}{dx} \right) :_+ \int_{\ell_{31}} \varpi \\ &\quad + :z(x) \left(-\frac{dp_1}{dx} + \frac{dp_2}{dx} + \frac{dp_3}{dx} \right) :_+ \int_{\ell_{23}} \varpi, \end{aligned} \quad (6.13)$$

and

$$\begin{aligned} \text{Sing}_-[\mathcal{A}_\eta] + \text{Sing}_-[\mathcal{V}_{\text{dyn}}] &= - :z(x) \left(\frac{dp_1}{dx} + \frac{dp_2}{dx} - \frac{dp_3}{dx} \right) :_- \int_{\ell_{21}} \bar{\varpi} \\ &\quad - :z(x) \left(\frac{dp_1}{dx} - \frac{dp_2}{dx} + \frac{dp_3}{dx} \right) :_- \int_{\ell_{31}} \bar{\varpi} \\ &\quad - :z(x) \left(-\frac{dp_1}{dx} + \frac{dp_2}{dx} + \frac{dp_3}{dx} \right) :_- \int_{\ell_{23}} \bar{\varpi}. \end{aligned} \quad (6.14)$$

The expressions $:z(x) dp_i/dx :_\pm$ in (6.13) and (6.14) above can be evaluated using the explicit form of the quasi-momentum, given in (2.58), as³⁹

$$:z(x) \frac{dp_i}{dx} :_+ = -2\pi\kappa_i - \pi\kappa_i\Lambda_i, \quad :z(x) \frac{dp_i}{dx} :_- = 2\pi\kappa_i + \pi\kappa_i\bar{\Lambda}_i. \quad (6.15)$$

This provides fairly explicit forms for the expressions $\text{Sing}_\pm[\mathcal{A}_\eta] + \text{Sing}_\pm[\mathcal{V}_{\text{dyn}}]$.

6.1.3 Result for the S^3 part

We can now combine the results obtained so far and obtain the net contribution of the S^3 part. Recall that the general structure of the S^3 part of the three-point functions we have computed is of the form

$$\begin{aligned} F_{S^3} &= \frac{\sqrt{\lambda}}{6} + 2\sqrt{\lambda} \sum_{i=1}^3 \kappa_i^2 \ln \epsilon_i + \mathcal{A}_\varpi + \mathcal{V}_{\text{kin}} + \text{Conv}[\mathcal{A}_\eta] + \text{Conv}[\mathcal{V}_{\text{dyn}}] \\ &\quad + \text{Sing}_+[\mathcal{A}_\eta] + \text{Sing}_+[\mathcal{V}_{\text{dyn}}] + \text{Sing}_-[\mathcal{A}_\eta] + \text{Sing}_-[\mathcal{V}_{\text{dyn}}]. \end{aligned} \quad (6.16)$$

Among the various terms shown above, those which can be expressed in terms of the contour integrals of ϖ or $\bar{\varpi}$ can be combined and evaluated using the explicit form of $:z dp_i/dx :_\pm$ given in (6.15). The result is

$$\begin{aligned} \mathcal{T}_{\text{sing}} &\equiv \mathcal{A}_\varpi + \text{Sing}_+[\mathcal{A}_\eta] + \text{Sing}_+[\mathcal{V}_{\text{dyn}}] + \text{Sing}_-[\mathcal{A}_\eta] + \text{Sing}_-[\mathcal{V}_{\text{dyn}}] \\ &= -\frac{\sqrt{\lambda}}{2} \left[(\kappa_1 + \kappa_2 - \kappa_3) \int_{\ell_{21}} (\varpi + \bar{\varpi}) + (\kappa_1 - \kappa_2 + \kappa_3) \int_{\ell_{31}} (\varpi + \bar{\varpi}) \right. \\ &\quad \left. + (-\kappa_1 + \kappa_2 + \kappa_3) \int_{\ell_{23}} (\varpi + \bar{\varpi}) \right]. \end{aligned} \quad (6.17)$$

³⁹Definitions of Λ_i and $\bar{\Lambda}_i$ are given in (3.20) and (3.31).

Since ϖ and $\bar{\varpi}$ behave near the punctures as

$$\varpi \rightarrow \frac{\kappa_i}{z - z_i}, \quad \bar{\varpi} \rightarrow \frac{\kappa_i}{\bar{z} - \bar{z}_i}, \quad (z \rightarrow z_i) \quad \text{for } i = 1, \bar{2}, 3, \quad (6.18)$$

the expression (6.17) diverges in the following fashion as the regularization parameters ϵ_i 's tend to zero:

$$\mathcal{T}_{\text{sing}} \rightarrow -2\sqrt{\lambda} \sum_{i=1}^3 \kappa_i^2 \ln \epsilon_i = -\mathcal{V}_{\text{energy}}. \quad (6.19)$$

Notice, however, that this divergence is precisely canceled by the second term of (6.16). Therefore, the quantity (6.16) as a whole is finite in the limit $\epsilon_i \rightarrow 0$. This is as expected for correctly normalized three-point functions.

Let us summarize the final result for the logarithm of the three-point functions coming from the S^3 part. It can be written in the form

$$F_{S^3} = \frac{\sqrt{\lambda}}{6} + \mathcal{V}_{\text{energy}} + \mathcal{T}_{\text{sing}} + \mathcal{V}_{\text{kin}} + \mathcal{T}_{\text{conv}}, \quad (6.20)$$

where \mathcal{V}_{kin} is the kinematical factor depending only on the normalization vectors given in (4.61), $\mathcal{T}_{\text{conv}}$ is the sum of the contributions from the convolution integrals (6.8), and $\mathcal{T}_{\text{sing}}$, which is given in (6.17), represents the sum of \mathcal{A}_{ϖ} defined in (3.47) and the contributions from the singular parts of the Wronskians.

6.2 The $EAdS_3$ part

We now discuss the contributions from the $EAdS_3$ part. Since the logic of the evaluation is almost entirely similar, we will not repeat the long analysis we performed for the S^3 part. In fact it suffices to explain which part of the analysis for the S^3 part can be ‘‘copied’’ and which part has to be modified.

6.2.1 Contribution from the action

Let us begin with the contribution from the action integral. Since $EAdS_3$ and S^3 are formally quite similar, the computation of the action integral can be performed in exactly the same manner. There is, however, a simple but crucial difference. It is the overall sign of the integral. For $EAdS_3$, the counterpart of the matrix \mathbb{Y} shown in (2.14) is given by

$$\mathbb{X} \equiv \begin{pmatrix} X_+ & X \\ X_- & \bar{X} \end{pmatrix}, \quad (6.21)$$

where

$$X_{\pm} \equiv X^{-1} \pm X^4, \quad X \equiv X^1 + iX^2, \quad \bar{X} \equiv X^1 - iX^2. \quad (6.22)$$

The right current is then defined as

$$\hat{j} \equiv \mathbb{X}^{-1} d\mathbb{X} = \hat{j}_z dz + \hat{j}_{\bar{z}} d\bar{z}. \quad (6.23)$$

Now compare the expressions of the stress tensors and the action integrals for S^3 and $EAdS_3$, expressed in terms of the respective right current. They are given by

$$T(z) \equiv T_{AdS}(z) = \frac{1}{2} \text{tr}(\hat{j}_z \hat{j}_z) = \kappa^2, \quad T_S(z) = -\frac{1}{2} \text{tr}(j_z j_z) = -\kappa^2, \quad (6.24)$$

$$S_{EAdS_3} = \frac{\sqrt{\lambda}}{2\pi} \int d^2z \text{tr}(\hat{j}_z \hat{j}_{\bar{z}}), \quad S_{S^3} = -\frac{\sqrt{\lambda}}{2\pi} \int d^2z \text{tr}(j_z j_{\bar{z}}). \quad (6.25)$$

This shows that while we have the equality $\text{tr}(\hat{j}_z \hat{j}_z) = \text{tr}(j_z j_z) = \kappa^2$, the signs in front of the action integrals are opposite. Therefore all the results for the action integral are formally the same as those for the S^3 case, but with opposite signs. This will lead to various cancellations with the contributions from the S^3 part, as we shall see shortly.

6.2.2 Contribution from the wave function

As for the evaluation of the contribution from the wave function, the basic logic of the formalism developed in section 4 for the S^3 still applies. However, there are a few important modifications, as we shall explain below.

As discussed in our previous work [11], in the case of a string in $EAdS_3$ the global symmetry group is $\text{SL}(2, \mathbb{C})_R \times \text{SL}(2, \mathbb{C})_L$ and hence the the raising operators with respect to which we define the highest weight state are the left and the right special conformal transformations given by

$$V_R^{\text{sc}} = \begin{pmatrix} 1 & 0 \\ \beta_R & 1 \end{pmatrix}, \quad V_L^{\text{sc}} = \begin{pmatrix} 1 & \beta_L \\ 0 & 1 \end{pmatrix}, \quad (6.26)$$

where β_R and β_L are constants. Applying our general argument for the determination of the polarization spinors, we readily find

$$(V_R^{\text{sc}})^t n^{\text{diag}} = n^{\text{diag}}, \quad n^{\text{diag}} = \begin{pmatrix} 1 \\ 0 \end{pmatrix}, \quad (6.27)$$

$$(V_L^{\text{sc}})^t \tilde{n}^{\text{diag}} = \tilde{n}^{\text{diag}}, \quad \tilde{n}^{\text{diag}} = \begin{pmatrix} 0 \\ 1 \end{pmatrix}. \quad (6.28)$$

It should be noted that, compared to the S^3 case given in (4.23), n^{diag} here for the right sector is the same as \tilde{n}^Z for the left sector there and similarly \tilde{n} for the left sector in the present case is identical to n^Z for the right sector for the S^3 case. Now the algebraic manipulations for the construction of the wave functions are the same as for the S^3 case up to the computation of the factor $e^{i\Delta\phi}$. Therefore, for the right sector, we get the same

result for the Z -type operator in the left sector, given in (4.58). For example at z_1 we have

$$e^{i\Delta\phi_{R,1}} = a_1^{-2} = \frac{\langle 1_+, 2_+ \rangle \langle 3_+, 1_+ \rangle}{\langle 2_+, 3_+ \rangle} \Big|_{\infty} \frac{\langle n_2, n_3 \rangle}{\langle n_1, n_2 \rangle \langle n_3, n_1 \rangle} \quad (6.29)$$

This is the *inverse* of the result for S^3 obtained in (4.51) with i_- replaced by i_+ . The result for the left sector is similar. What this means is that the wave function for the $EAdS_3$ is obtained from the one for the S^3 case by (i) reversing the sign of the powers and (ii) exchanging i_+ and i_- . Abusing the same notations for the polarization spinors and the eigenvectors as in the S^3 case, we get

$$\Psi_R^{EAdS_3} = \prod_{i \neq j \neq k} \left(\frac{\langle n_i, n_j \rangle}{\langle i_+, j_+ \rangle} \Big|_{\infty} \right)^{-(R_i + R_j - R_k)}, \quad (6.30)$$

$$\Psi_L^{EAdS_3} = \prod_{i \neq j \neq k} \left(\frac{\langle \tilde{n}_i, \tilde{n}_j \rangle}{\langle \tilde{i}_-, \tilde{j}_- \rangle} \Big|_0 \right)^{-(L_i + L_j - L_k)}, \quad (6.31)$$

where R_i and L_i here are the combinations of the conformal dimension Δ_i and the spin S_i given by

$$R_i = \frac{1}{2} (\Delta_i - S_i), \quad L_i = \frac{1}{2} (\Delta_i + S_i). \quad (6.32)$$

This reversal of power relative to the S^3 case is what is desired. Effectively it is equivalent to employing $e^{+iS\phi}$ as the form of the wave function, which is what we adopted in the previous work [11] for the three-point function of the GKP string in $EAdS_3$ and lead to the power structure given in (6.30) and (6.31). As we shall show below, correctness of this power structure becomes obvious when we relate the Wronskian $\langle n_i, n_j \rangle$ to the difference of the coordinates x_i and x_j , where x_i is the position of the i -th vertex operator on the boundary of $EAdS_3$.

Recall that the embedding coordinates of $EAdS_3$ are taken to be X^μ ($\mu = -1, 1, 2, 4$), which is a vector of $SO(1, 3)$ with signature $(-, +, +, +)$, while the Poincaré coordinates are given by $z = 1/(X^{-1} + X^4)$, $x^r = zX^r$, ($r = 1, 2$), with which $X^{-1} - X^4$ is expressed as $z + (\vec{x}^2/z)$. Consider approaching a point on the boundary $z = 0$ with finite values of x^r . Then the term z in $X^{-1} - X^4$ becomes negligible compared to \vec{x}^2/z and X^μ approaches a null vector, with large components. Such a vector can be parametrized, up to an overall scale, by the boundary coordinates $\vec{x} = (x^1, x^2)$ as

$$X^{-1} = \frac{1}{2}(1 + \vec{x}^2), \quad X^4 = \frac{1}{2}(1 - \vec{x}^2), \quad (X^1, X^2) = \vec{x}, \quad (6.33)$$

$$\vec{x}^2 = x^r \eta_{rs} x^s = x^r x_r, \quad \eta_{rs} = (+, +), \quad r, s = 1, 2. \quad (6.34)$$

As usual, one can map X^μ to the matrix $X^\mu \hat{\Sigma}_\mu$, with $\hat{\Sigma}_\mu = (1, \sigma_1, \sigma_2, \sigma_3)$, which transforms from left under $SL(2, C)$ and from right under $SL(2, C)^*$. Then, it is well-known that for

a null vector X^μ the matrix elements of $X^\mu \hat{\Sigma}_\mu$ can be written as a product of spinors (or twistors) as

$$(X^\mu \hat{\Sigma}_\mu)_{\alpha\dot{\alpha}} = \begin{pmatrix} 1 & x \\ \bar{x} & \bar{x}^2 \end{pmatrix} = (\sigma_1 \tilde{n})_\alpha n_{\dot{\alpha}}, \quad (6.35)$$

where

$$x \equiv x^1 + ix^2, \quad \bar{x} \equiv x^1 - ix^2, \quad (6.36)$$

$$n = \begin{pmatrix} 1 \\ x \end{pmatrix}, \quad \tilde{n} = \begin{pmatrix} \bar{x} \\ 1 \end{pmatrix}. \quad (6.37)$$

These spinors can be identified precisely as the polarization spinors characterizing a vertex operator which is placed at \vec{x} on the boundary for the following reasons. First they transform in the correct way: Under the global transformation $X^\mu \hat{\Sigma}_\mu \rightarrow V_L(X^\mu \hat{\Sigma}_\mu)V_R$, we have $(\sigma_1 \tilde{n})_\alpha \rightarrow (V_L \sigma_1 \tilde{n})_\alpha$ and $n_{\dot{\alpha}} \rightarrow (n V_R)_{\dot{\alpha}}$. This is equivalent to $\tilde{n} \rightarrow V_L^t \tilde{n}$ and $n \rightarrow V_R^t n$, which are the right transformation laws. Second, these spinors coincide with the polarization spinors given in (6.27) and (6.28) when we bring the point \vec{x} to the origin of the boundary by the translation by the vector $-\vec{x}$. This is effected by the right and the left translation matrices given by

$$V_R^{\text{tr}}(-x) = \begin{pmatrix} 1 & -x \\ 0 & 1 \end{pmatrix}, \quad V_L^{\text{tr}}(-\bar{x}) = \begin{pmatrix} 1 & 0 \\ -\bar{x} & 1 \end{pmatrix}. \quad (6.38)$$

Then we get

$$(V_R^{\text{tr}})^t(-x)n = \begin{pmatrix} 1 \\ 0 \end{pmatrix}, \quad (V_L^{\text{tr}})^t(-\bar{x})\tilde{n} = \begin{pmatrix} 0 \\ 1 \end{pmatrix}. \quad (6.39)$$

Therefore n and \tilde{n} can be identified with the polarization spinors for the vertex operator at \vec{x} on the boundary. Now let n' and \tilde{n}' be similar polarization spinors corresponding to a vertex operator at \vec{x}' on the boundary. Then we immediately get

$$\langle n, n' \rangle = x' - x, \quad \langle \tilde{n}, \tilde{n}' \rangle = \bar{x}' - \bar{x}, \quad (6.40)$$

$$\langle n, n' \rangle \langle \tilde{n}, \tilde{n}' \rangle = (x' - x)(\bar{x}' - \bar{x}) = (x' - x)^2. \quad (6.41)$$

In this way, for the $EAdS_3$ the Wronskians formed by the polarization spinors produce the difference of the boundary position vectors. Therefore the relevant part of the wave function becomes

$$\begin{aligned} & \prod_{\{i,j,k\}} \langle n_i, n_j \rangle^{-(R_i+R_j-R_k)} \langle \tilde{n}_i, \tilde{n}_j \rangle^{-(L_i+L_j-L_k)} \\ & = \prod_{\{i,j,k\}} (x_i - x_j)^{-(R_i+R_j-R_k)} (\bar{x}_i - \bar{x}_j)^{-(L_i+L_j-L_k)}. \end{aligned} \quad (6.42)$$

In particular, for the case of spinless configurations that we are considering, this becomes

$$\prod_{\{i,j,k\}} \frac{1}{|x_i - x_j|^{\Delta_i + \Delta_j - \Delta_k}}, \quad (6.43)$$

which exhibits the familiar coordinate dependence for the three-point function in such a case.

6.2.3 Total contribution from the $EAdS_3$ part

As we have seen, the structure of the contribution from the $EAdS_3$ part is essentially the same as that from the S^3 case, except for the important reversal of signs in the powers in the contributing factor (or the terms contributing to the the logarithm of the three-point coupling.) This change of sign occurred both for the action and for the wave function. As we compute the basic Wronskians in exactly the same way as before and use them to compute the contributions to the logarithm of the three-point function from the action part and the wave function part, we again obtain the expression of the form of the left hand side of (6.7), with the overall sign reversed. Therefore, we can use the identity (6.7) again to obtain the result $-z(x')d\hat{p}_i(x')/dx'$, where \hat{p}_i denotes the quasi-momentum for the $EAdS_3$ part of the string. One can check that in fact this rule of correspondence, namely $p_i(x) \rightarrow \hat{p}_i(x)$ and the reversal of sign for the convolution integrals, applies to all the contributions. Thus, combining all the results for the AdS part, the contribution to the logarithm of the three-point function is given by the following expression:

$$F_{EAdS_3} = -\frac{\sqrt{\lambda}}{6} + \hat{\mathcal{V}}_{\text{energy}} + \hat{\mathcal{T}}_{\text{sing}} + \hat{\mathcal{V}}_{\text{kin}} + \hat{\mathcal{T}}_{\text{conv}}. \quad (6.44)$$

Here, $\hat{\mathcal{V}}_{\text{energy}}$ and $\hat{\mathcal{T}}_{\text{sing}}$ are equal to $-\mathcal{V}_{\text{energy}}$ and $-\mathcal{T}_{\text{sing}}$ respectively, $\hat{\mathcal{V}}_{\text{kin}}$ is the kinematical factor given in (6.43), and $\hat{\mathcal{T}}_{\text{conv}}$ is the convolution integrals obtained from the unhatted counterpart for the S^3 case with the substitution rule described above.

6.3 Complete expression for the three-point function

We are finally ready to put together the contributions from the S^3 part summarized in (6.20) and those from the $EAdS_3$ part given in (6.44) and present the full answer for the three-point function. As we have already discussed, the divergent terms cancel with each other for the S^3 part and the $EAdS_3$ part separately. On the other hand, the constant terms proportional to $\sqrt{\lambda}/6$ cancel between S^3 and $EAdS_3$ contributions. Thus we are left with the kinematical factors and the contributions from the convolution integrals which are of the same structure except for the overall sign. Therefore, factoring the kinematical

structure as

$$\begin{aligned}
\langle \mathcal{V}_1 \mathcal{V}_2 \mathcal{V}_3 \rangle &= \frac{1}{N} \frac{C_{123}}{|x_1 - x_2|^{\Delta_1 + \Delta_2 - \Delta_3} |x_2 - x_3|^{\Delta_2 + \Delta_3 - \Delta_1} |x_3 - x_1|^{\Delta_3 + \Delta_1 - \Delta_2}} \\
&\times \langle n_1, n_2 \rangle^{R_1 + R_2 - R_3} \langle n_2, n_3 \rangle^{R_2 + R_3 - R_1} \langle n_3, n_1 \rangle^{R_3 + R_1 - R_2} \\
&\times \langle \tilde{n}_1, \tilde{n}_2 \rangle^{L_1 + L_2 - L_3} \langle \tilde{n}_2, \tilde{n}_3 \rangle^{L_2 + L_3 - L_1} \langle \tilde{n}_3, \tilde{n}_1 \rangle^{L_3 + L_1 - L_2},
\end{aligned} \tag{6.45}$$

the logarithm of the structure constant C_{123} is finally given by

$$\begin{aligned}
\ln C_{123} &= \\
&\int_{\mathcal{M}_{-+-}^{uuu}} \frac{z(x)(dp_1 + dp_2 + dp_3)}{2\pi i} \ln \sin \left(\frac{p_1 + p_2 + p_3}{2} \right) + \int_{\mathcal{M}_{--+}^{uuu}} \frac{z(x)(dp_1 + dp_2 - dp_3)}{2\pi i} \ln \sin \left(\frac{p_1 + p_2 - p_3}{2} \right) \\
&+ \int_{\mathcal{M}_{+-+}^{uuu}} \frac{z(x)(dp_1 - dp_2 + dp_3)}{2\pi i} \ln \sin \left(\frac{p_1 - p_2 + p_3}{2} \right) + \int_{\mathcal{M}_{+--}^{uuu}} \frac{z(x)(-dp_1 + dp_2 + dp_3)}{2\pi i} \ln \sin \left(\frac{-p_1 + p_2 + p_3}{2} \right) \\
&- \int_{\mathcal{K}_{-+-}^{uuu}} \frac{z(x)(d\hat{p}_1 + d\hat{p}_2 + d\hat{p}_3)}{2\pi i} \ln \sin \left(\frac{\hat{p}_1 + \hat{p}_2 + \hat{p}_3}{2} \right) - \int_{\mathcal{K}_{--+}^{uuu}} \frac{z(x)(d\hat{p}_1 + d\hat{p}_2 - d\hat{p}_3)}{2\pi i} \ln \sin \left(\frac{\hat{p}_1 + \hat{p}_2 - \hat{p}_3}{2} \right) \\
&- \int_{\mathcal{K}_{+-+}^{uuu}} \frac{z(x)(d\hat{p}_1 - d\hat{p}_2 + d\hat{p}_3)}{2\pi i} \ln \sin \left(\frac{\hat{p}_1 - \hat{p}_2 + \hat{p}_3}{2} \right) - \int_{\mathcal{K}_{+--}^{uuu}} \frac{z(x)(-d\hat{p}_1 + d\hat{p}_2 + d\hat{p}_3)}{2\pi i} \ln \sin \left(\frac{-\hat{p}_1 + \hat{p}_2 + \hat{p}_3}{2} \right) \\
&- 2 \sum_{j=1}^3 \int_{\Gamma_{j-}^u} \frac{z(x) dp_j}{2\pi i} \ln \sin p_j + 2 \sum_{j=1}^3 \int_{\hat{\Gamma}_{j-}^u} \frac{z(x) d\hat{p}_j}{2\pi i} \ln \sin \hat{p}_j + \text{Contact},
\end{aligned} \tag{6.46}$$

where **Contact** stands for the contribution from the contact terms. We find it truly remarkable that, in spite of the complexity of both the analysis and the intermediate expressions, the final answer takes such a simple form. Moreover, it exhibits essential similarity to the form of the weak coupling result [4–7] even before taking any further limits. In the next section, we shall evaluate the structure constant (6.46) more explicitly, including the quantity **Contact**, for several important examples and compare with the weak coupling results more closely.

7 Examples and comparison with the weak coupling result

The results obtained in the previous section are quite general and applicable to three-point functions of arbitrary one-cut solutions on $EAdS_3 \times S^3$. In this section we focus on several explicit examples, make some basic checks and discuss the relation with the results at weak coupling.

In subsection 7.1, we first explain the basic set-up, which will be used throughout this section. Then, in subsection 7.2, we study the correlation functions of three BPS operators and see that the contributions from the S^3 part and the $EAdS_3$ part completely cancel out in this case. The results thus obtained fully agree with the results obtained in the gauge theory. In subsection 7.3, we study the behavior of the three-point function

under the limit where the charge of one of the operators becomes negligibly small while the other two operators become identical. We confirm that the result reduces to that of the two-point function, as expected. Next, in subsection 7.4, we study three-point functions of one non-BPS and two BPS operators, which were studied on the gauge theory side in [4]. We will focus on certain explicit examples and show that the full three-point functions can be expressed in terms of simple integrals which resemble the semi-classical limit of the results at weak coupling [4–7]. Then, in subsection 7.5, we discuss the Frolov-Tseytlin limit of such three-point functions. In this limit, the integrands in the final expression approximately agree with the ones in the weak coupling, whereas the integration contours are rather different. Lastly, we discuss the possible origin and the implication of this mismatch.

7.1 Basic set-up

Before starting the detailed analysis, let us clarify the basic set-ups to be used in this section.

The three-point functions studied extensively on the gauge theory side are those of the following three types of operators (see also Table 2.):

$$\mathcal{O}_1 = \text{tr} (Z^{l_1-M_1} X^{M_1}) + \dots, \quad \mathcal{O}_2 = \text{tr} (\bar{Z}^{l_2-M_2} \bar{X}^{M_2}) + \dots, \quad \mathcal{O}_3 = \text{tr} (Z^{l_3-M_3} \bar{X}^{M_3}) + \dots.$$

As explained in section 4.3.4, such three-point functions vanish unless the conservation laws⁴⁰ for the charges, (4.64), are satisfied. Due to these conservation laws, one cannot in general take the operators to be simple BPS states, such as $\text{tr} (Z^l)$ or $\text{tr} (\bar{Z}^l)$, which are the highest-weight vectors of the global $\text{SU}(2)_R \times \text{SU}(2)_L$ symmetry. Instead, we need to use descendants of the global symmetry to satisfy the conservation laws when we study three-point functions involving BPS operators [4, 27]. While this can be done without problems on the gauge theory side, it leads to certain difficulty on the string theory side. This is because all the classical solutions of string are known to (or believed to) correspond to some highest-weight states. To circumvent this difficulty, below we will utilize the global transformations to make all three operators to be built on different “vacua”. On the string theory side, this corresponds to taking the polarization vectors of the three operators, n_i ’s and \tilde{n}_i ’s, to be all distinct. Then no conservation laws will be imposed and we can safely take the limit where some of the operators become BPS while keeping them to be of highest-weight. Since the correlation functions involving descendants can be obtained from the correlation functions involving the highest-weight states by simple group theoretical manipulations, knowledge of the three-point functions for the highest

⁴⁰As we have shown in section 4, such conservation laws can be derived also on the string theory side.

weight states is sufficient. In addition, replacing the highest-weight operator with its descendant only modifies the kinematical factor, \mathcal{V}_{kin} , of our result and the dynamical parts of three-point functions, which are main subjects of study in this section, will not be affected.

After making the global transformations, the operators \mathcal{O}_1 , \mathcal{O}_2 and \mathcal{O}_3 can be treated almost on the same footing. However, there is an important difference between \mathcal{O}_3 and the other two in string theory: As explained in section 4.3.4, the quasi-momenta for the operators \mathcal{O}_1 and \mathcal{O}_2 contain branch cuts in the $|\text{Re } x| > 1$ region, whereas the quasi-momentum for the operator \mathcal{O}_3 contains a branch cut in the $|\text{Re } x| < 1$ region. This difference is important in the analysis to follow, since the position of the branch cuts affects the contours for the convolution integrals.

7.2 Case of three BPS operators

Let us first study the correlation functions of three BPS operators. In order to apply the general formula for the three-point functions of one-cut solutions obtained in the previous section, we need the explicit forms of $p(x)$ and $q(x)$ for the BPS operators, which in particular determine the integration contours. Within the bosonic sector, the characteristic feature of a BPS state is that, as it should correspond to a supergravity mode, it is “point-like”, meaning that its two-point function is σ -independent. In the language of the spectral curve, it means the absence of a branch cut, since a branch cut corresponds to a non-trivial string mode with σ -dependence.

Now in fixing the forms of $p(x)$ and $q(x)$, there is a subtle problem with the configuration without a branch cut. In the case of one-cut solutions corresponding to non-BPS operators, the constant parts of $p(x)$ and $q(x)$ are fixed in such a way that they vanish at the branch points. Obviously, for configurations without a branch cut, this prescription cannot be applied. One natural remedy would be to start with a non-BPS solution, apply the usual method above to fix the constants and then shrink the cut to obtain a BPS solution. This idea, however, still does not cure the problem since the resultant $p(x)$ and $q(x)$ depend on the points on the spectral curve at which we shrink the branch cut. The existence of such an ambiguity possibly implies that the semi-classical three-point functions are affected by the presence of infinitesimal branch cuts. Although such an assertion sounds counter-intuitive, it is not totally inconceivable since similar effects were already observed in the study of “heavy-heavy-light” three-point functions⁴¹ in [30].

Below we shall fix the ambiguity by employing a prescription which is quite natural from the viewpoint of the correspondence with the spin chain on the gauge theory side.

⁴¹In [30], such effects were called *back reactions*.

The prescription is to shrink the branch cuts either at $x = 0$ or at $x = \infty$ in producing BPS operators. This choice is based on the following fact: In gauge theory, adding a small number of Bethe roots at $x = 0$ or $x = \infty$ correspond to performing a small global transformation and keeps the operator to be BPS, whereas adding a small number of Bethe roots at generic points on the spectral curve creates nontrivial magnon excitations and makes the operator non-BPS.

Having identified the classical solutions corresponding to BPS operators, let us now determine the integration contours. First we focus on the S^3 -part of three-point functions. As discussed in section 4.3.4, for \mathcal{O}_1 and \mathcal{O}_2 , $p_i(x)$ and $q_i(x)$ can have branch cuts only in the the $|\operatorname{Re} x| > 1$ region and hence we take the infinitesimal branch cut to be placed at $x = \infty$. Then from the general form of the one-cut solution given in (2.58) and (2.59), we get

$$p_i(x) = -2\pi\kappa_i \left(\frac{1}{x-1} + \frac{1}{x+1} \right), \quad q_i(x) = -2\pi\kappa_i \left(\frac{1}{x-1} - \frac{1}{x+1} \right), \quad (7.1)$$

which vanish at $x = \infty$, as desired. On the other hand, for \mathcal{O}_3 , since the branch cuts can only be in the $|\operatorname{Re} x| < 1$ region, we place an infinitesimal branch cut at $x = 0$. Then from (2.58) and (2.59) we get

$$p_3(x) = -2\pi\kappa_3 \left(\frac{x}{x-1} - \frac{x}{x+1} \right) = -2\pi\kappa_3 \left(\frac{1}{x-1} + \frac{1}{x+1} \right) \quad (7.2)$$

$$q_3(x) = -2\pi\kappa_3 \left(\frac{x}{x-1} + \frac{x}{x+1} \right). \quad (7.3)$$

These expressions vanish at $x = 0$.

As discussed in detail in section 5, the contours for the convolution integrals consist of two types of curves. The first type are those defined by $\operatorname{Re} q_i(x) = 0$, across which the relative magnitude of i_+ and i_- changes. They determine the integration contours Γ_{i-}^u defined in section 5.4 and are depicted in figure 7.1. Note that in the present case, the contours Γ_{1-}^u and Γ_{2-}^u coincide since $q_1(x) = q_2(x)$. The second type are the curves defined by $N_i = N_j + N_k$, across which the connectivity of the exact WKB curves changes. Now for a BPS operator, $N_i = |\operatorname{Re} p_i(x)|$ is given by a common function $|\operatorname{Re} ((x+1)^{-1} + (x-1)^{-1})|$ times the factor $-2\pi\kappa_i$, as shown above. Since κ_i 's satisfy the triangular inequalities, this means that $N_i = N_j + N_k$ cannot be satisfied. Hence the second type of curves are absent and the integration contours are determined solely by the first type of curves.

With this knowledge, we can now apply the general rules given at the end of section 5.3 to determine the integration contours $\mathcal{M}_{\pm\pm\pm}^{uuu}$. As an example, consider the contour \mathcal{M}_{---}^{uuu} , which is used for the convolution integral involving $\sin \frac{1}{2}(-p_1(x) - p_2(x) - p_3(x))$. From the Rule 1, either Wronskians among $\mathcal{S}_- = \{1_-, 2_-, 3_-\}$ vanish or those among

$\mathcal{S}_+ = \{1_+, 2_+, 3_+\}$ vanish. Then we must apply Rule 2, since the triangle inequalities are satisfied in the present case. It states that if two of the members of \mathcal{S}_- (resp. \mathcal{S}_+) are small solutions, then the Wronskians for the members of \mathcal{S}_+ (resp. \mathcal{S}_-) vanish. Now consider the curve Γ_{1-}^u . From its definition, it is along $\text{Re } q_1(x) = 0$ with the direction such that to the left of this curve 1_- is the small solution. The curve Γ_{2-}^u is identical, as we already remarked. These curves are depicted in the left figure of figure 7.1, together with the states which are small in the three regions separated by these curves. Together with the rules mentioned above, we see explicitly that the analyticity of Wronskians change across such curves and hence we can identify $\Gamma_{1-}^u (= \Gamma_{2-}^u)$ as the contour \mathcal{M}_{---}^{uuu} . Similarly, the curve Γ_{3-}^u , identified as \mathcal{M}_{+--}^{uuu} , is shown in the right figure of figure 7.1. In this way, we find the contours $\mathcal{M}_{\pm\pm\pm}^{uuu}$ to be given by

$$\begin{aligned} \mathcal{M}_{---}^{uuu} &= \Gamma_{1-}^u (= \Gamma_{2-}^u), & \mathcal{M}_{+--}^{uuu} &= \Gamma_{3-}^u, \\ \mathcal{M}_{-+-}^{uuu} &= \Gamma_{3-}^u, & \mathcal{M}_{--+}^{uuu} &= \Gamma_{1-}^u (= \Gamma_{2-}^u). \end{aligned} \tag{7.4}$$

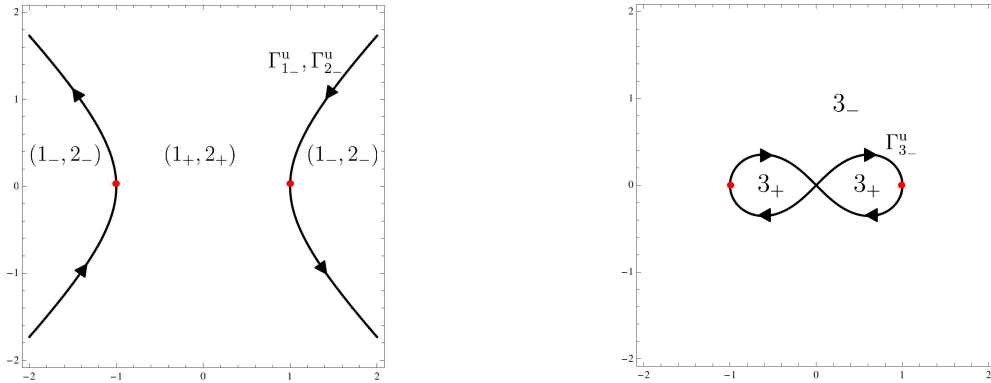


Figure 7.1: The contours Γ_{i-}^u , defined by $\text{Re } q_i = 0$. In each region, we showed which of the eigenvectors is the small solution.

Let us next consider the effects of the contact terms. As argued in section 6, such contribution must be taken into account when $x = 0$ ($x = \infty$) is on the left (right) hand side of the integration contours. The effect is most conveniently done by adding a small circle around $x = 0$ ($x = \infty$) to the contour for each integration in (6.8). However, in the case of BPS operators, the integration contours terminate right at $x = 0$ or $x = \infty$. Therefore we need to first regularize them by putting a small branch cut slightly away from $x = 0$ or $x = \infty$ and then take the limit where the branch cut shrinks to $x = 0$ or $x = \infty$. An example of such a procedure is depicted in figure 7.2. Since the sine-functions in the convolution integrals (6.8) turn out to vanish only on the real axis in the case of BPS operators, we can further deform the contours into those on the unit circle. As a

result, we find that the S^3 -part of the three-point function is given by

$$\begin{aligned} & \oint_U \frac{z(dp_1 + dp_2 + dp_3)}{2\pi i} \ln \sin \left(\frac{p_1 + p_2 + p_3}{2} \right) + \oint_U \frac{z(dp_1 + dp_2 - dp_3)}{2\pi i} \ln \sin \left(\frac{p_1 + p_2 - p_3}{2} \right) \\ & + \oint_U \frac{z(dp_1 - dp_2 + dp_3)}{2\pi i} \ln \sin \left(\frac{p_1 - p_2 + p_3}{2} \right) + \oint_U \frac{z(-dp_1 + dp_2 + dp_3)}{2\pi i} \ln \sin \left(\frac{-p_1 + p_2 + p_3}{2} \right) \\ & - 2 \sum_{j=1}^3 \int_U \frac{z dp_j}{2\pi i} \ln \sin p_j, \end{aligned}$$

where U denotes the contour which goes around the unit circle clockwise.

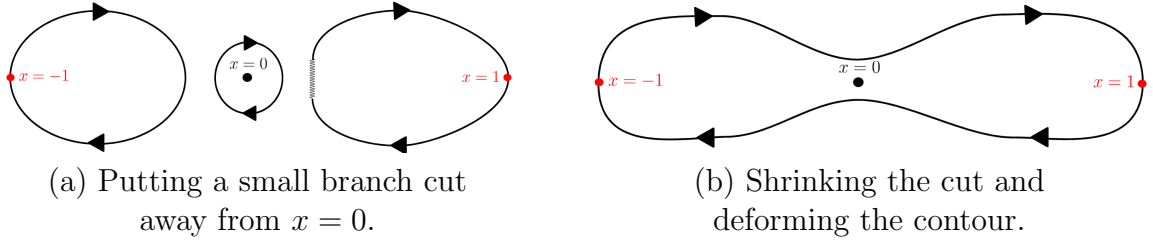


Figure 7.2: An example of the contour deformation. The contour depicted in (b) can be further deformed into the contour on the unit circle.

Next consider the $EAdS_3$ -part of the three-point function. The quasi-momenta and the quasi-energies for the operators without spin in AdS are given in [8] by⁴²

$$\hat{p}_i(x) = -2\pi\kappa_i \left(\frac{1}{x-1} + \frac{1}{x+1} \right), \quad \hat{q}_i(x) = -2\pi\kappa_i \left(\frac{1}{x-1} - \frac{1}{x+1} - 1 \right). \quad (7.5)$$

Then, performing a similar analysis as in the case of S^3 -part, we find that the result is again given by the integrals along the unit circle. As the quasi-momenta $p_i(x)$ for the S^3 -part and the ones $\hat{p}_i(x)$ for the $EAdS_3$ -part coincide in the case of BPS operators, we see from the general formula (6.46) that the contributions from these two parts cancel each other completely. Therefore, the three-point function for three BPS operators is given purely by the kinematical factors as

$$\begin{aligned} \langle \mathcal{V}_1 \mathcal{V}_2 \mathcal{V}_3 \rangle &= \frac{1}{|x_1 - x_2|^{\Delta_1 + \Delta_2 - \Delta_3} |x_2 - x_3|^{\Delta_2 + \Delta_3 - \Delta_1} |x_3 - x_1|^{\Delta_3 + \Delta_1 - \Delta_2}} \\ &\times \langle n_1, n_2 \rangle^{R_1 + R_2 - R_3} \langle n_2, n_3 \rangle^{R_2 + R_3 - R_1} \langle n_3, n_1 \rangle^{R_3 + R_1 - R_2} \\ &\times \langle \tilde{n}_1, \tilde{n}_2 \rangle^{L_1 + L_2 - L_3} \langle \tilde{n}_2, \tilde{n}_3 \rangle^{L_2 + L_3 - L_1} \langle \tilde{n}_3, \tilde{n}_1 \rangle^{L_3 + L_1 - L_2}, \end{aligned} \quad (7.6)$$

This is consistent with the result in the gauge theory that the three-point functions of BPS operators are tree-level exact and have no dependence on the 't Hooft coupling constant λ .

⁴²The spectral parameter x used in (7.5) is related to the spectral parameter ξ used in [8] by $\xi = (x-1)/(x+1)$.

7.3 Limit producing two-point function

Having seen that the BPS three-point functions are correctly reproduced from our general formula, let us next discuss the limit where the three-point functions are expected to reduce to two-point functions. As an example, we take two of the operators \mathcal{O}_1 and \mathcal{O}_2 to have identical quasi-momenta and quasi-energy, while \mathcal{O}_3 is a BPS operator with vanishingly small charge⁴³.

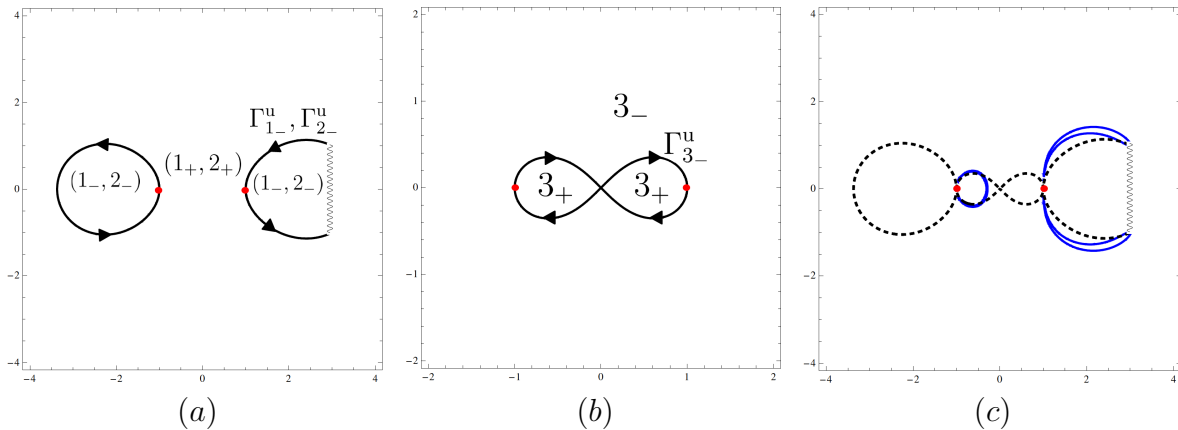


Figure 7.3: The curves which determine the integration contours in the limit where three-point functions reduce to two-point functions. In the left and the middle figures, the contours Γ_{i-}^u , determined by $\text{Re } q_i(x) = 0$ are depicted. The segment represented by a wavy line is the branch cut. In the rightmost figure, the curve defined by $N_3 = N_1 + N_2$ is drawn in blue. For convenience, we redisplayed the curves in figures (a) and (b) as dotted lines.

To understand what happens in such a limit, let us draw the two types of curves, namely $\text{Re } q_i = 0$ and $N_i = N_j + N_k$. The first type of curves are depicted in the first and the second figures of figure 7.3. As for the second type, the only curve we need to consider is the curve given by $N_3 = N_1 + N_2$. This is because the inequalities $N_1 + N_3 \geq N_2$ and $N_2 + N_3 \geq N_1$ are always satisfied since $N_1 = N_2$ in the present case. When the operator \mathcal{O}_3 is sufficiently small, the curve defined by $N_3 = N_1 + N_2$ almost vanishes and we can practically ignore the effects of such a curve. Thus the integration contours are given purely by $\text{Re } q_1 = \text{Re } q_2 = 0$. Applying the rules given in the previous section and taking into account the contact terms, we find that the convolution integrals for the S^3 -part are

⁴³Although the case considered here appears similar to the one studied in the gauge theory [30] with \mathcal{O}_3 taken to be small but nonvanishing, there is a difference: In [30], \mathcal{O}_1 and \mathcal{O}_2 must have slightly different quasi-momenta in the presence of \mathcal{O}_3 , due to the conservation law for the magnons. In the present case, however, as we performed the global transformation, no conservation law is imposed and we can take \mathcal{O}_1 and \mathcal{O}_2 to have identical quasi-momenta.

given by

$$\begin{aligned}
& \int_{\Gamma_{1_-}^u + \mathcal{C}_\infty} \frac{z(dp_1 + dp_2 + dp_3)}{2\pi i} \ln \sin \left(\frac{p_1 + p_2 + p_3}{2} \right) + \int_{\Gamma_{1_-}^u + \mathcal{C}_\infty} \frac{z(dp_1 + dp_2 - dp_3)}{2\pi i} \ln \sin \left(\frac{p_1 + p_2 - p_3}{2} \right) \\
& + \int_{\Gamma_{3_-}^u + \mathcal{C}_0} \frac{z(dp_1 - dp_2 + dp_3)}{2\pi i} \ln \sin \left(\frac{p_1 - p_2 + p_3}{2} \right) + \int_{\Gamma_{3_-}^u} \frac{z(-dp_1 + dp_2 + dp_3)}{2\pi i} \ln \sin \left(\frac{-p_1 + p_2 + p_3}{2} \right) \\
& - 2 \sum_{j=1}^2 \int_{\Gamma_{j_-}^u + \mathcal{C}_\infty} \frac{z dp_j}{2\pi i} \ln \sin p_j - 2 \int_{\Gamma_{3_-}^u + \mathcal{C}_0} \frac{z dp_3}{2\pi i} \ln \sin p_3, \tag{7.7}
\end{aligned}$$

where \mathcal{C}_∞ is the contour encircling $x = \infty$ counterclockwise and \mathcal{C}_0 is the contour encircling $x = 0$ clockwise. Setting $p_1 = p_2$ and $p_3 = 0$ in this formula, we see that in this limit all the terms in (7.7) completely cancel out with each other. Similar cancellation occurs also for the $EAdS_3$ -part. Therefore the structure constant C_{123} of the three-point function in this limit becomes unity and the result correctly reproduces the correctly normalized two-point function given by

$$\frac{\langle n_1, n_2 \rangle^{2R} \langle \tilde{n}_1, \tilde{n}_2 \rangle^{2L}}{|x_1 - x_2|^{2\Delta}}. \tag{7.8}$$

Here, Δ , R and L are, respectively, the conformal dimension, the (absolute values of the) right and the left global charges, which are common to \mathcal{O}_1 and \mathcal{O}_2 .

7.4 Case of one non-BPS and two BPS operators

Having checked that our formula correctly reproduces the known results in simple limits, let us now study more nontrivial examples. In this subsection, we take up the three-point functions of one non-BPS and two BPS operators, which were studied on the gauge-theory side in [4]. As in [4], we take \mathcal{O}_2 to be non-BPS and \mathcal{O}_1 and \mathcal{O}_3 to be BPS. In this case, the typical forms of the curves corresponding to $\text{Re } q_i = 0$ and $N_i = N_j + N_k$, are given in figure 7.4.

To perform a more detailed analysis, we need to specify the properties of the operators more explicitly, since the precise form of the integration contours depend on such details. As we wish to analyze the so-called Frolov-Tseytlin limit and make a comparison with the results in the gauge theory in the next subsection, we will take as a representative example the following set of operators carrying large conformal dimensions:

$$\begin{aligned}
\mathcal{O}_1 & : \text{BPS}, \quad 2\pi\kappa_1 = 2500, \\
\mathcal{O}_2 & : \text{non-BPS}, \quad 2\pi\kappa_2 = 3250, \\
& p(u) - p(\infty^+) = -16\pi, \quad p(0^+) - p(\infty^+) = -2\pi, \\
\mathcal{O}_3 & : \text{BPS}, \quad 2\pi\kappa_3 = 3000.
\end{aligned} \tag{7.9}$$

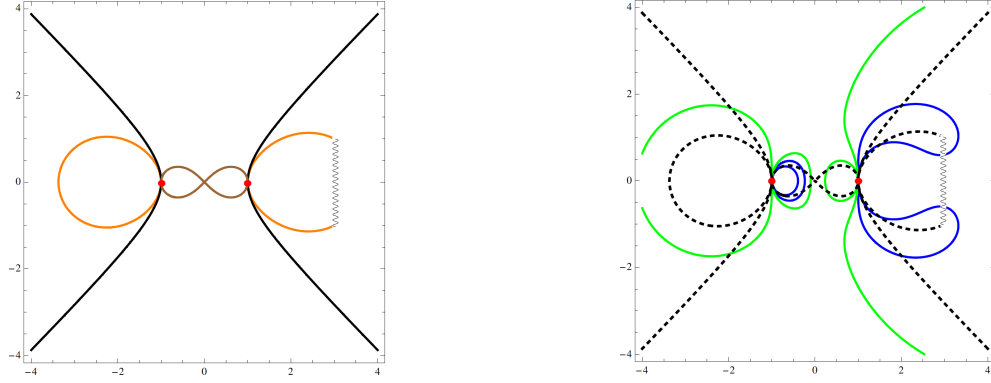


Figure 7.4: Typical configuration of the curves produced by the conditions $\text{Re } q_i = 0$ and $N_i = N_j + N_k$, for the three-point functions of one non-BPS operator and two BPS operators. In the left figure, $\text{Re } q_1 = 0$, $\text{Re } q_2 = 0$ and $\text{Re } q_3 = 0$ are drawn respectively in black, orange and brown. In the right figure, $N_1 = N_2 + N_3$ is drawn in blue and $N_2 = N_1 + N_3$ is drawn in green.

Here u denotes the position of an end of the branch cut for the non-BPS operator \mathcal{O}_2 . For these operators, the curves defined by $\text{Re } q_i = 0$ and those defined by $N_i = N_j + N_k$ are depicted respectively in figure 7.5 and figure 7.6.

As in the case of the three BPS operators, we must now apply the general rules of section 5 to determine the integration contours. As an example, consider the contour \mathcal{M}_{---}^{uuu} in the region where $|\text{Re } x| \gg 1$. Focus first on the left figure of figure 7.5. Compared to the typical configuration shown in the left figure of figure 7.4, the curve determined by $\text{Re } q_3 = 0$ (shown in brown in figure 7.4) is depicted here as a point in the middle since we are considering the region where $|\text{Re } x| \gg 1$. Since the inside of the shrunken region is where 3_+ is small, we have 3_- as the small solution everywhere in this figure. From the direction of the curves Γ_{1-}^u and Γ_{2-}^u , we can easily tell which of the states 1_\pm and 2_\pm are the small solutions in each of the region separated by these curves.

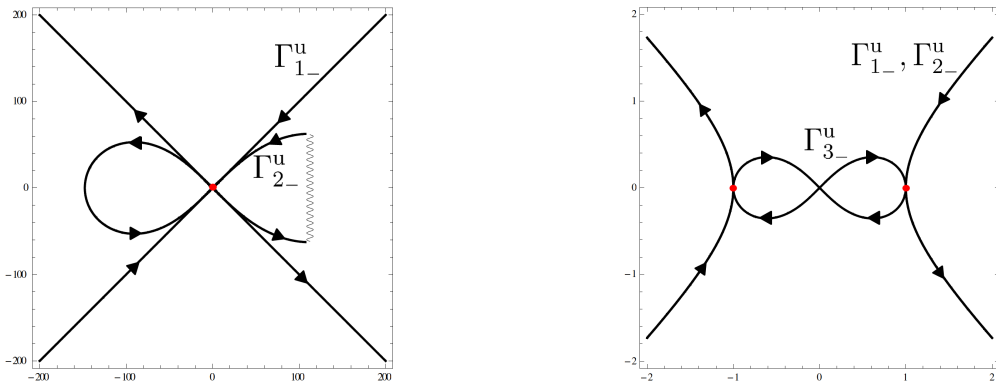


Figure 7.5: The contours Γ_{i-}^u , defined by $\text{Re } q_i = 0$. The left figure shows the configuration of contours in the $|x| \gg 1$ region, whereas the right figure depicts the configuration of contours in the $|x| < 1$ region.

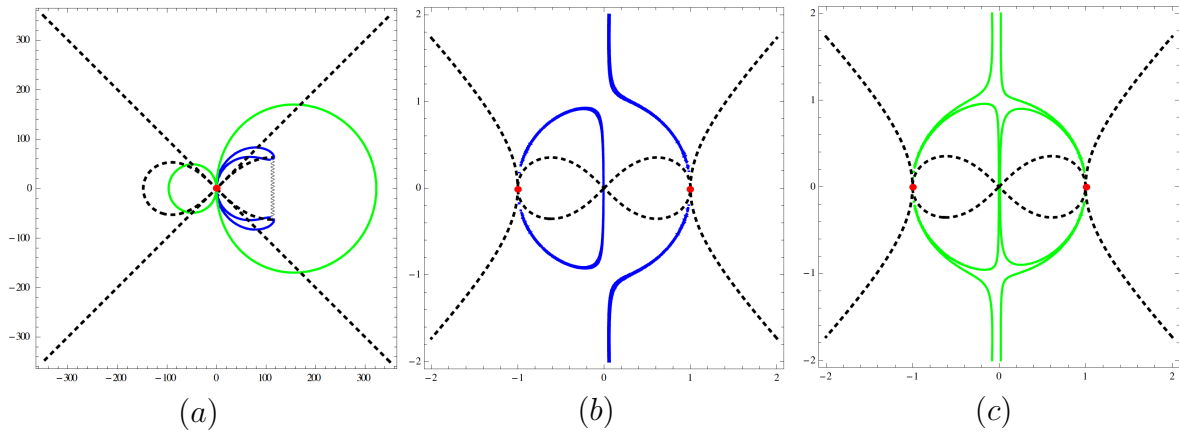


Figure 7.6: The curves defined by $N_i = N_j + N_k$. The figure (a) shows the configuration of curves in $|x| \gg 1$ region whereas the figure (b) shows the configuration of $N_1 = N_2 + N_3$ in $|x| < 1$ region and the figure (c) shows the configuration of $N_2 = N_1 + N_3$ in $|x| < 1$ region. In the present case, the curve $N_3 = N_1 + N_2$ does not exist.

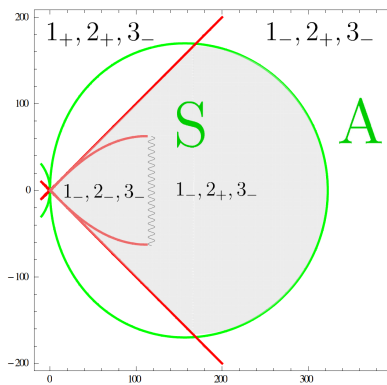


Figure 7.7: Magnified view of a part of the figure (a) of figure 7.6, with data necessary for determining the contour of integration. In each region separated by lines and/or the cut (wavy line), the set of “small” eigenvectors are indicated. The green circle separates the symmetric (S) and the asymmetric (A) regions, to which different rules of analysis apply. The result is that across the boundary of the shaded area, the analyticity of the Wronskian changes. For details of the analysis using this figure, see the explanation in the main text.

Now, in distinction to the case of three BPS operators, we must also take into account the possible change of the analyticity of the Wronskians as we cross the lines defined by $N_i = N_j + N_k$. Thus, we must analyze relevant curves drawn in figure 7.6 (a), where the one in green corresponds to $N_2 = N_1 + N_3$ and the one in blue represents $N_1 = N_2 + N_3$. Across these lines the configuration changes from symmetric to asymmetric. Accordingly, the rule to find the non-vanishing set of Wronskians changes from Rule 2 to Rule 3. Let us focus on the green curve, which is re-drawn in figure 7.7, with additional information. It turns out that the configuration is symmetric inside the green circles and asymmetric outside, indicated by the letters S and A respectively. Now in the region outside of the arc of the large green circle bordered by the lines representing Γ_{1-}^u , shown in figure 7.7 by the red straight lines, $1_-, 2_+, 3_-$ are the small solutions, as indicated in the figure. As this is the asymmetric region we apply the Rules 1 and 3 and conclude that the Wronskians among the states $\{1_+, 2_+, 3_+\}$ are non-vanishing. As we cross the arc into the shaded region inside of the green circle where the configuration is symmetric, still $1_-, 2_+, 3_-$ are the small solutions but now we must apply the Rules 1 and 2. Then we learn that the Wronskians among the states $\{1_-, 2_-, 3_-\}$ are non-vanishing instead. In other words, the analyticity property of the Wronskians change across this portion of the green curve and hence it serves as a part of the contour for the convolution integral. This explains the portion of the contour along the arc of the large circle shown in the left-most figure in figure 7.8. Now consider what happens when this contour meets the Γ_{1-}^u line. Across this line, the small solution changes from 1_- to 1_+ . Thus when we cross this line from inside the large circle, the set of small solutions change from $1_-, 2_+$ and 3_- to $1_+, 2_+$ and 3_- as shown in figure 7.7. As we are still in the symmetric region, the Rules 1 and 2 apply and hence we learn that set of non-vanishing Wronskians change across this line. Therefore this portion must constitute a part of the contour. This explains the straight red line starting from the the point of intersection with the large circle. In this fashion, we can uniquely obtain the integration contour \mathcal{M}_{---}^{uuu} , shown in the leftmost figure of figure 7.8, across which the analyticity property of the Wronskians change. All the other contours $\mathcal{M}_{\pm\pm\pm}^{uuu}$ can also be determined in an entirely similar manner, the result of which are depicted in figure 7.8 and figure 7.9.

The contours shown in figure 7.8 and figure 7.9 can be simplified by continuous deformation as long as we do not make them pass through the singularities of the integrands. We can determine the positions of the singularities numerically and find that most of the singularities lie on the real axis. Avoiding them, we can deform each contour into a sum of the contour along the unit circle and the one which is far from the unit circle. The

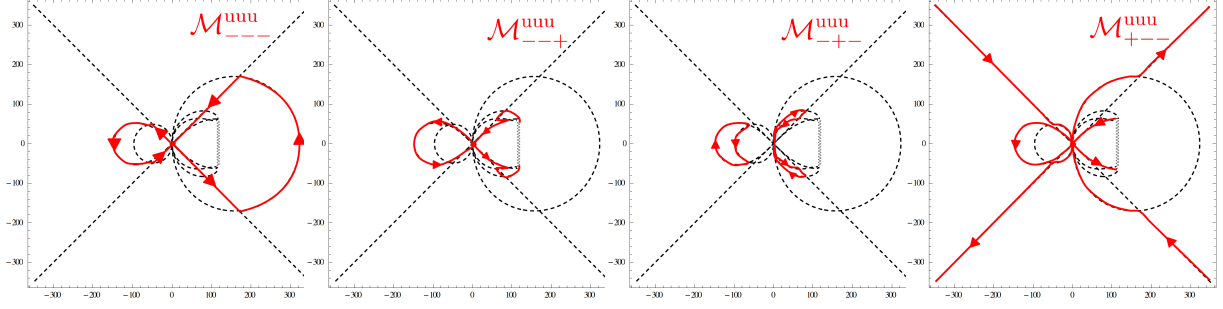


Figure 7.8: The integration contours $\mathcal{M}_{\pm\pm\pm}^{uuu}$ in the region $|x| \gg 1$. From left to right, \mathcal{M}_{----}^{uuu} , \mathcal{M}_{--+-}^{uuu} , \mathcal{M}_{-+-+}^{uuu} and \mathcal{M}_{+---}^{uuu} .

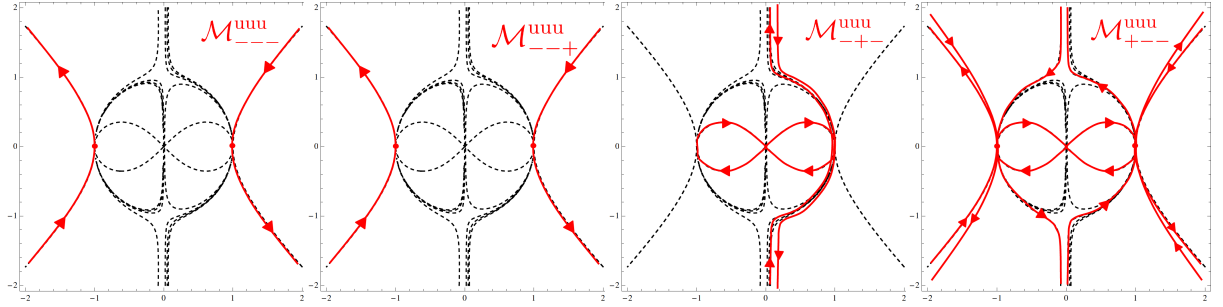


Figure 7.9: The integration contours $\mathcal{M}_{\pm\pm\pm}^{uuu}$ in the region $|x| < 1$. From left to right, \mathcal{M}_{----}^{uuu} , \mathcal{M}_{--+-}^{uuu} , \mathcal{M}_{-+-+}^{uuu} and \mathcal{M}_{+---}^{uuu} .

results of this deformation are summarized as

$$\begin{aligned}
 \mathcal{M}_{----}^{uuu} &\mapsto (\mathcal{M}_{----}^{uuu})' + U, & \mathcal{M}_{--+-}^{uuu} &\mapsto (\Gamma_{2-}^u)' + U, \\
 \mathcal{M}_{-+-+}^{uuu} &\mapsto (\mathcal{M}_{-+-+}^{uuu})' + U, & \mathcal{M}_{+---}^{uuu} &\mapsto (\Gamma_{2-}^u)' + U, \\
 \Gamma_{1-}^u &\mapsto U, & \Gamma_{2-}^u &\mapsto (\Gamma_{2-}^u)' + U, & \Gamma_{3-}^u &\mapsto U,
 \end{aligned} \tag{7.10}$$

where, as before, U denotes the unit circle and the primed contours are as depicted in figure 7.10.

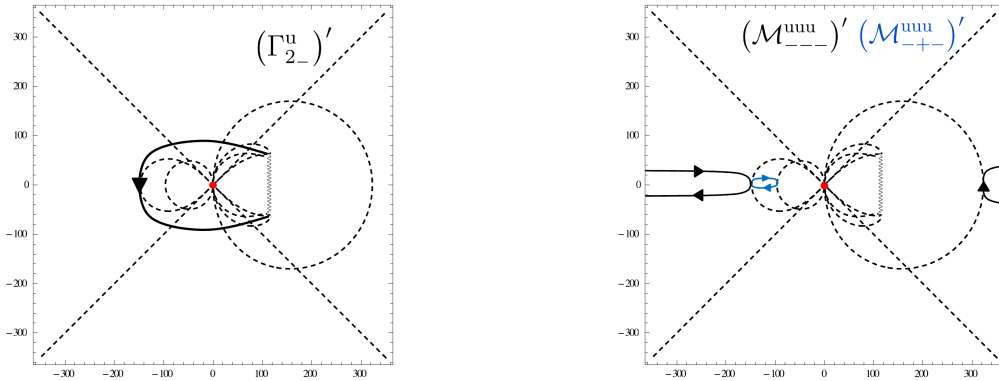


Figure 7.10: The contours obtained after the deformation. On the left figure, we depicted $(\Gamma_{2-}^u)'$. On the right figure, we depicted $(\mathcal{M}_{----}^{uuu})'$ in black and $(\mathcal{M}_{-+-+}^{uuu})'$ in blue.

Let us make a remark on the separation of the integration contours into the unit circle

and the large contours. It is intriguingly reminiscent of the expressions for the one-loop correction to the spectrum of a classical string [31]. In that context, the integration along the unit circle is interpreted as giving the dressing phase and the finite size corrections. Since our results do not include one-loop corrections, it is not at all clear whether our results can be interpreted in a similar way. However, the apparent structural similarity calls for further study.

7.5 Frolov-Tseytlin limit and comparison with the weak coupling result

7.5.1 Frolov-Tseytlin limit of the three-point function

We are now ready to discuss the Frolov-Tseytlin limit of the three-point function and compare it with the weak coupling result. Let us briefly recall how such a limit arises. As shown in [32], the dynamics of the fluctuations around a fast-rotating string on S^3 can be mapped to the dynamics of the Landau-Lifshitz model, which arises as a coherent state description of the XXX spin chain. In such a situation, the angular momentum J of the S^3 rotation can be taken to be so large that the ratio $\sqrt{\lambda}/J$ becomes vanishingly small, even when λ is large. For the spectral problem, it has been demonstrated that such a limit is quite useful in comparing the strong coupling result with the weak coupling counterpart. We would like to see if it applies also to the three point functions. For this purpose, we need to know how such a limit is taken at the level of the quasi-momenta. Since the $SO(4)$ charges of the external states are proportional to κ_i , the appropriate limit is to scale all the κ_i to infinity while keeping the mode numbers $\oint_{b_i} dp$ finite. As already indicated, we have chosen the example in the previous subsection to be such that we can readily take such a limit.

Upon taking the Frolov-Tseytlin limit, two simplifications occur in our formula. First, since the branch points are far away from the unit circle, we can approximate $p_2(x)$ on the unit circle by a quasi-momentum for a BPS operator, namely

$$p_2(x) \simeq p_2^{\text{BPS}}(x) = -2\pi\kappa_2 \left(\frac{1}{x-1} + \frac{1}{x+1} \right). \quad (7.11)$$

Now recall that the contribution from the $EAdS_3$ part is such that it precisely canceled the S^3 part in the case of the three BPS operators. Since the $EAdS_3$ part is unchanged for the present case, again the same exact cancellation takes place as far as the integrals over the unit circles are concerned. Therefore we can drop such integrals and obtain

$$\begin{aligned}
& \int_{(\mathcal{M}_{--}^{uu})'+\mathcal{C}_\infty} \frac{z(dp_1 + dp_2 + dp_3)}{2\pi i} \ln \sin \left(\frac{p_1 + p_2 + p_3}{2} \right) + \int_{(\Gamma_{2-}^u)'+\mathcal{C}_\infty} \frac{z(dp_1 + dp_2 - dp_3)}{2\pi i} \ln \sin \left(\frac{p_1 + p_2 - p_3}{2} \right) \\
& + \int_{(\mathcal{M}_{+-}^{uu})'+\mathcal{C}_\infty} \frac{z(dp_1 - dp_2 + dp_3)}{2\pi i} \ln \sin \left(\frac{p_1 - p_2 + p_3}{2} \right) + \int_{(\Gamma_{2-}^u)'+\mathcal{C}_\infty} \frac{z(-dp_1 + dp_2 + dp_3)}{2\pi i} \ln \sin \left(\frac{-p_1 + p_2 + p_3}{2} \right) \\
& - 2 \int_{(\Gamma_{2-}^u)'+\mathcal{C}_\infty} \frac{z dp_2}{2\pi i} \ln \sin p_2, \tag{7.12}
\end{aligned}$$

Second simplification occurs because on the large contours the integration variable x is of order κ_i . This is precisely the situation where we can approximate the quasi-momenta of the classical strings by the corresponding quantities for the spin-chains. Indeed, as explained in [12], the quasi-momentum for the string can be identified with that of the Landau-Lifshitz model, which describes the spin-chain on the gauge theory side in the above limit. More precisely, we can use the following identification of the quasi-momenta on the large contour:

$$p^{\text{string}}(x) \simeq p^{\text{spin}}(z(x)). \tag{7.13}$$

The use of the Zhukovsky variable $z(x)$ on the right hand side is motivated by the fact that in the all-loop asymptotic Bethe ansatz equation [33, 34], the rapidity of the spin-chain on the gauge theory side is identified with the Zhukovsky variable on the string theory side. In the present situation, however, since $z(x) \simeq x$ for large x , the quasi-momenta in (7.12) can be replaced simply with the quasi-momenta for the corresponding spin-chain states at the same value of x .

With such a replacement, the expression (7.12) already appears rather similar to the weak-coupling result. To make the resemblance more conspicuous, we can regard the integral of $\sin((-p_1 + p_2 + p_3)/2)$ along $(\Gamma_{2-}^u)'$ on the upper sheet as the integral of $\sin((p_1 + p_2 - p_3)/2)$ along the reversed contour on the lower sheet for p_2 , which we denote by $(\Gamma_{2-}^l)'$. Combining this with the integral of $\sin((p_1 + p_2 - p_3)/2)$ along $(\Gamma_{2-}^u)'$ already present and defining $(\Gamma_{2-})'$ to be the sum of $(\Gamma_{2-}^u)'$ and $(\Gamma_{2-}^l)'$, we can write (7.12) as

$$\int_{(\Gamma_{2-})'+\mathcal{C}_\infty} \frac{z(dp_1 + dp_2 - dp_3)}{2\pi i} \ln \sin \left(\frac{p_1 + p_2 - p_3}{2} \right) - \int_{(\Gamma_{2-})'+\mathcal{C}_\infty} \frac{z dp_2}{2\pi i} \ln \sin p_2 + \text{Mismatch}, \tag{7.14}$$

where **Mismatch** is given by

$$\begin{aligned}
\text{Mismatch} &= \int_{(\mathcal{M}_{--}^{uu})'+\mathcal{C}_\infty} \frac{z(dp_1 + dp_2 + dp_3)}{2\pi i} \ln \sin \left(\frac{p_1 + p_2 + p_3}{2} \right) \\
&+ \int_{(\mathcal{M}_{+-}^{uu})'+\mathcal{C}_\infty} \frac{z(dp_1 - dp_2 + dp_3)}{2\pi i} \ln \sin \left(\frac{p_1 - p_2 + p_3}{2} \right). \tag{7.15}
\end{aligned}$$

Now the corresponding weak-coupling result obtained in [4] can be re-cast into the following form by the use of integration by parts,

$$\int_{-\mathcal{A}_2} \frac{z \left(dp_1^{\text{spin}} + dp_2^{\text{spin}} - dp_3^{\text{spin}} \right)}{2\pi i} \ln \sin \left(\frac{p_1^{\text{spin}} + p_2^{\text{spin}} - p_3^{\text{spin}}}{2} \right) - \int_{-\mathcal{A}_2} \frac{z dp_2^{\text{spin}}}{2\pi i} \ln \sin p_2^{\text{spin}}, \quad (7.16)$$

where \mathcal{A}_2 is the contour which encircles the branch cut of p_2 counterclockwise. Comparing (7.14) and (7.16), one notes the following: (i) The terms denoted by **Mismatch** in the strong coupling result are not present in the weak coupling expression. (ii) The integrands of the rest of the terms are precisely of the same form as for the weak coupling result, but the contours of integrations are different. This makes a difference in the answer since in deforming the contours from those for the strong coupling to those for the weak coupling picks up non-vanishing contributions from the singularities of the integrands. Concerning the three-point functions, there is no firm argument that the Frolov-Tseytlin limit must be universal for all the observables. Therefore the discrepancies that we found above do not immediately imply the breakdown of the duality. However, it is certainly of importance to clarify the origin of these differences. As a part of the possible understanding, below we shall offer a natural mechanism which can change the contours of integration.

7.5.2 A mechanism for modifying the contours

The mechanism that we wish to point out is based on the possibility of having extra singularities on the worldsheet. To see this, let us first recall that in the derivation of the important rules which determine the analyticity of the Wronskians, we have made an important assumption that the only singularities on the worldsheet of the solutions of the ALP occur at the positions of the vertex insertion points. This in turn means that if there exist extra singularities this assumption breaks down and affects the rules for determining the contours of the convolution integrals⁴⁴. Depending on the number and the positions of the extra singularities, the contours can be modified in various ways and it might be possible to obtain the contour which appear in the weak coupling result.

Now we can provide some arguments which indicate that indeed the existence of additional singularities is not uncommon. First, recall that the usual finite gap method is capable of constructing solutions which correspond to the saddle point configurations for two-point functions. As such they contain only two singularities, normally placed at $\tau = \pm\infty$ in the cylinder coordinates. In such a formalism designed to deal with two-point functions, description of three-point solutions would require additional singularities. In

⁴⁴A similar mechanism of changing the integration contour by the extra singularities is discussed in the context of the so-called ODE/IM correspondence [35].

our treatment, due to the inability to construct genuine three-point saddle solutions, we describe the effect of the three vertex operators separately except for imposing the global monodromy condition that reflects the essence of their interaction. However, as already emphasized in our previous work [11], if we wish to deal properly with the three- and higher- point functions using algebraic curve setup for a theory with infinite degrees of freedom, one should actually start from the infinite gap solutions and then consider the limits where the infinite number of cuts on the spectral curve degenerate to zero size. This process is rather non-trivial and it should be possible to produce some extra singularities on the worldsheet. Although we cannot demonstrate this phenomenon explicitly for the three-point solution, we know that already at the level of two-point solution such a mechanism exists, as discussed in some detail in section 2.2.2. There we saw explicitly that a “one-cut” solution obtained from a multi-cut solution in a certain degeneration limit can produce extra singularities without affecting the infinite number of conserved charges carried by the solution. It is certainly expected that such a mechanism would exist also in the case of higher-point solutions. An interesting question is which of the saddle points, those with extra singularities or those without, describe the correlator of the gauge-theory operators. In any case, further studies are definitely needed to clarify this issue.

8 Discussions

In this paper, we have succeeded in computing the three-point functions at strong coupling of certain non-BPS states with large charges corresponding to the composite operators in the $SU(2)$ sector of the $\mathcal{N} = 4$ super Yang-Mills theory. As we have already given a summary of the main result in section 1.1, we shall not repeat it here. Instead, below we would like to give some comments and indicate some important issues to be clarified in the future.

One conspicuous feature of our result is that even for rather general external states the integrands of the integrals expressing the structure constant exhibit structures quite similar to the corresponding result at weak coupling. This is quite non-trivial since the weak coupling result in the relevant semi-classical regime is obtained from the determinant formula for the inner product of the Bethe states, which is so different from the method employed for strong coupling. This suggests that we should seek better understanding by reformulating the weak coupling computation in a more “physical” way. As a step toward such a goal, an attempt was made in [36], where the inner product of the Bethe states is re-expressed in terms of an integral over the separated dynamical variables. As the notion of the wave function is clearly visible in this formulation, it may give a hint for

the common feature of the strong and the weak coupling regimes, if an efficient method to identify the semi-classical saddle point can be developed.

In contrast to the similarity of the integrands, there is a rather clear difference in the contours of the integrals expressing the three-point coupling in the weak and the strong coupling computations. This is not just a quantitative difference but rather a qualitative one. Reflecting the fact that the determinant formula deals with the Bethe roots, the contour of integration in the weak coupling case is around a cut formed by the condensation of such Bethe roots. Information of such a cut is contained in the quasi-momentum $p(x)$. On the other hand, the principal quantity which determines the integration contour is the real part of the quasi-energy $q(x)$, which is conjugate to the worldsheet time τ . Apparently, this notion is not present in the weak coupling formulation. Together with the possible extra singularities on the worldsheet discussed in section 7.5.2, the question of the contour requires better understanding.

There are a couple of further interesting questions that one should study concerning our result. One is about the limit of our formula where one of the operators is much smaller than the other two. Such three-point functions were first studied on the string-theory side in [37–39] assuming that the light operator does not change the saddle-point configuration of the other two operators. However, a systematic study on the gauge-theory side [30] reveals that the light operator in some cases modifies the saddle-point substantially. By examining the limit of our formula, it would be possible to understand in detail when and how such a “back-reaction” occurs. Another important problem is to understand the physical meaning of the integration along the unit circle in our formula and clarify if it can be interpreted as the contribution from the dressing phase and the finite size correction as in the case of the one-loop spectrum of a classical string [31].

Finally, let us go back once again to the rather simple structure of the integrand we found, similar to the weak coupling result. The simplicity of such a result suggests that there should perhaps be a better more intrinsic formulation for computing the three-point functions. In the existing literature, including this work, the calculation of the three-point function in the strong coupling regime is divided into the computation of the contribution of the action part and that of the vertex operator (wave function) part. As we have seen in section 6, in the process of putting these separate contributions together there occurs a substantial simplification, besides the usual cancellation of divergences. This strongly indicates that such a separation is not essential and one should rather seek relations which reflect the structure of the entire three-point function based on some dynamical symmetry of the theory including the integrable structure. This is of utmost importance since the true understanding of the AdS/CFT duality lies not just in the comparison of the calculations of various physical quantities in the strong and the weak coupling

regimes itself but rather in identifying the common principle behind such computations and agreements.

To make the above remark somewhat more concrete, let us recall that the most important ingredient in the computation performed in this paper at strong coupling is the global consistency relations for the monodromy of the solutions of the auxiliary linear problem around three vertex insertion points. Together with the analyticity property in the spectral parameter, the important quantity $\langle i_{\pm}, j_{\pm} \rangle$, which relates the behavior of the solutions around different insertion points, is extracted and serves as the building block for the three-point coupling. On the other hand, in the weak coupling computations so far performed, the computation of the three-point coupling is reduced to those of the inner products of the Bethe states and their combinations. Although this is an efficient method, it is based basically on the picture of the two-point function and not on some principle which governs the entire three-point function. Therefore we believe that an extremely important problem is to find some functional equations (or differential equations) satisfied by the three-point function, from which one can determine the coupling constant more or less directly. We hope to discuss this type of formulation elsewhere.

Acknowledgment

We would like to thank Y. Jiang, I. Kostov, D. Serban and P. Vieira for discussions. S.K. would like to acknowledge the hospitality of the Perimeter Institute for Theoretical Physics, where part of this work was done. The research of Y.K. is supported in part by the Grant-in-Aid for Scientific Research (B) No. 25287049, while that of S.K. is supported in part by JSPS Research Fellowship for Young Scientists, from the Japan Ministry of Education, Culture, Sports, Science and Technology.

A Details on the one-cut solutions

In this appendix, we will provide some further details on the one-cut solutions.

A.1 Parameters of one-cut solutions in terms of the position of the cut

In section 2.2 we have given generic expressions for the parameters which characterize the one-cut solutions in terms of the integrals involving $p(x)$ and $q(x)$. If we now use the explicit forms of $p(x)$ and $q(x)$ given in (2.58) and (2.59), one can evaluate the parameters ν_i , m_i and θ_0 in terms of the position of the cut specified by u . The results take several different forms depending on the region where the cut is located. It is convenient to

express them in universal forms by introducing two additional sign factors η_1 and $\eta_{0,1}$. Together with the factor ϵ already introduced in (2.60), we give their definitions in the following table:

Table 3. Sign factors to distinguish between the positions of the cut.

	$\text{Re } u < -1$	$-1 < \text{Re } u < 0$	$0 < \text{Re } u < 1$	$1 < \text{Re } u$
ϵ	+	-	-	+
η_1	+	+	+	-
$\eta_{0,1}$	+	+	-	+

Then, ν_1 and ν_2 are obtained as

$$\nu_1 = \kappa \left[-\frac{\eta_1 + \eta_{0,1}|u|}{|u-1|} + \epsilon \frac{\eta_1 - \eta_{0,1}|u|}{|u+1|} \right], \quad (\text{A.1})$$

$$\nu_2 = \kappa \left[\frac{\eta_1 - \eta_{0,1}|u|}{|u-1|} - \epsilon \frac{\eta_1 + \eta_{0,1}|u|}{|u+1|} \right] = \epsilon \nu_1(u \rightarrow -u). \quad (\text{A.2})$$

As for m_i , we can immediately obtain them from ν_i by the substitution $\epsilon \rightarrow -\epsilon$, because, as seen in (2.58) and (2.59), this interchanges $q(x)$ and $p(x)$:

$$m_1 = \nu_1(\epsilon \rightarrow -\epsilon), \quad (\text{A.3})$$

$$m_2 = \nu_2(\epsilon \rightarrow -\epsilon). \quad (\text{A.4})$$

Now $\cos^2(\theta_0/2)$ and $\sin^2(\theta_0/2)$ can be deduced from the Virasoro condition (2.70) as

$$\cos^2 \frac{\theta_0}{2} = \frac{|u| - \eta_1 \eta_{0,1} \text{Re } u}{2|u|}, \quad \sin^2 \frac{\theta_0}{2} = \frac{|u| + \eta_1 \eta_{0,1} \text{Re } u}{2|u|}. \quad (\text{A.5})$$

The right and the left charges are obtained from (2.30) and (2.31) to be

$$R = -\frac{\kappa \sqrt{\lambda} \eta_1}{2} \left(\frac{\text{Re } u - 1}{|u-1|} + \epsilon \frac{\text{Re } u + 1}{|u+1|} \right), \quad (\text{A.6})$$

$$L = \frac{\kappa \sqrt{\lambda} \eta_{0,1}}{2|u|} \left(\frac{|u|^2 - \text{Re } u}{|u-1|} + \epsilon \frac{|u|^2 + \text{Re } u}{|u+1|} \right). \quad (\text{A.7})$$

From the definition of R and L as the Noether charges, they must be expressed in terms of the parameters ν_i and θ_0 in a universal manner independent of the position of the cut. Indeed by using the formulas already obtained for the parameters and the charges in terms of u , we can check the universal expressions

$$\frac{R}{\sqrt{\lambda}} = \frac{1}{2} \left(-\nu_1 \cos^2 \frac{\theta_0}{2} + \nu_2 \sin^2 \frac{\theta_0}{2} \right), \quad (\text{A.8})$$

$$\frac{L}{\sqrt{\lambda}} = \frac{1}{2} \left(-\nu_1 \cos^2 \frac{\theta_0}{2} - \nu_2 \sin^2 \frac{\theta_0}{2} \right). \quad (\text{A.9})$$

Finally, let us discuss the signs and the relative magnitudes of the parameters and the charges. The signs and the relative magnitude of ν_i depend on u . From the formulas for ν_i we can check that

$$|\operatorname{Re} u| > 1 : \quad \nu_2 < \nu_1 < 0, \quad (\text{A.10})$$

$$|\operatorname{Re} u| < 1 : \quad \nu_1 < 0 < \nu_2, (|\nu_1| < \nu_2). \quad (\text{A.11})$$

As for the angles, we always have

$$\cos^2 \frac{\theta_0}{2} > \sin^2 \frac{\theta_0}{2}. \quad (\text{A.12})$$

The signs of R and L can be checked to be always positive. (R for the case $|\operatorname{Re} u| > 1$ and L for the case $|\operatorname{Re} u| < 1$ are somewhat non-trivial to check.)

The relative magnitude of R and L can be deduced easily from the difference

$$\frac{1}{\sqrt{\lambda}}(R - L) = 2\nu_2 \sin^2 \frac{\theta_0}{2}. \quad (\text{A.13})$$

As the sign of ν_2 has already been obtained in (A.10) and (A.11), we immediately get

$$R < L \quad \text{for} \quad |\operatorname{Re} u| > 1, \quad (\text{A.14})$$

$$R > L \quad \text{for} \quad |\operatorname{Re} u| < 1. \quad (\text{A.15})$$

A.2 Pohlmeyer reduction for one-cut solutions

Let us next consider the variables appearing in the Pohlmeyer reduction, ρ , $\tilde{\rho}$ and γ for one-cut solutions. From their definitions, we can express them in terms of the parameters of the one-cut solution as

$$\cos 2\gamma = \frac{\nu_1^2 - m_1^2}{4\kappa^2} = \frac{\nu_2^2 - m_2^2}{4\kappa^2}, \quad (\text{A.16})$$

$$\rho = \frac{1}{8} \cos \frac{\theta_0}{2} \sin \frac{\theta_0}{2} ((\nu_1 + m_1)^2 - (\nu_2 + m_2)^2), \quad (\text{A.17})$$

$$\tilde{\rho} = \frac{1}{8} \cos \frac{\theta_0}{2} \sin \frac{\theta_0}{2} ((\nu_1 - m_1)^2 - (\nu_2 - m_2)^2), \quad (\text{A.18})$$

where we used $z = \tau + i\sigma$ coordinate when we compute these quantities⁴⁵.

Using the results in the previous subsection, we can re-express (A.16), (A.17) and (A.18) in terms of the branch points u and \bar{u} . They are given by

$$\cos 2\gamma = \epsilon \frac{|u|^2 - 1}{|u^2 - 1|}, \quad \sin 2\gamma = \frac{2\operatorname{Im} u}{|u^2 - 1|}, \quad (\text{A.19})$$

$$\rho = -\kappa^2 \frac{\operatorname{Im} u}{|u - 1|^2}, \quad \tilde{\rho} = \kappa^2 \frac{\operatorname{Im} u}{|u + 1|^2}. \quad (\text{A.20})$$

⁴⁵Note that γ is invariant under the coordinate change $z \rightarrow z' = f(z)$, whereas ρ and $\tilde{\rho}$ transform respectively as $\rho \rightarrow \rho' = \rho/(\partial f)^2$ and $\tilde{\rho} \rightarrow \tilde{\rho}' = \tilde{\rho}/(\bar{\partial} f)^2$.

The ALP in the Pohlmeyer gauge can be solved in a similar manner and the result is given in (2.98) and (2.99).

In the case of three-point functions, we can compute these quantities separately for each puncture as

$$\gamma_i = \frac{1}{2} \arcsin \left(\frac{2 \operatorname{Im} u_i}{|u_i^2 - 1|} \right), \quad (\text{A.21})$$

$$\rho_i = -\kappa^2 \frac{\operatorname{Im} u_i}{|u_i - 1|^2}, \quad (\text{A.22})$$

$$\tilde{\rho}_i = \kappa^2 \frac{\operatorname{Im} u_i}{|u_i + 1|^2}. \quad (\text{A.23})$$

They will be used in the computation of three-point functions.

A.3 Computation of various integrals

Using the above results, let us compute various integrals which appear in **Local** and **Double** in section 3. Around a puncture, one can approximate the behavior of the world-sheet by that of the two-point functions. Thus, when three string states are semi-classically described 1-cut solutions, we expect the following asymptotic behavior of the one-forms:

$$\lambda \stackrel{z \rightarrow z_i}{\sim} \kappa_i dw_i, \quad \omega \stackrel{z \rightarrow z_i}{\sim} -\frac{\kappa_i \cos 2\gamma_i}{2} d\bar{w}_i + \frac{2\rho_i^2}{\kappa_i^3} dw_i, \quad (\text{A.24})$$

where w_i is the local coordinate $w_i \equiv \tau^{(i)} + i\sigma^{(i)}$ around the puncture z_i .

Using (A.24), one can evaluate various integrals. First, the contour integrals of λ and ω along \mathcal{C}_i 's are given by

$$\oint_{\mathcal{C}_i} \lambda = 2\pi i \kappa_i, \quad \oint_{\mathcal{C}_i} \omega = 2\pi i \left(\frac{\kappa_i \cos 2\gamma_i}{2} + \frac{2\rho_i^2}{\kappa_i^3} \right) \quad i = 1, \bar{2}, 3. \quad (\text{A.25})$$

On the other hand, the double contour integral, which appears in **Double** can be computed as follows:

$$\begin{aligned} \oint_{\mathcal{C}_i} \omega \int_{z_i^*}^z \lambda &= \int_{\sigma=0}^{\sigma=2\pi} \left(-\frac{\kappa_i \cos 2\gamma_i}{2} d\bar{w}_i + \frac{2\rho_i^2}{\kappa_i^3} dw_i \right) \int_{\sigma'=0}^{\sigma'=\sigma} \kappa_i dw'_i \\ &= -\int_0^{2\pi} d\sigma \left(\frac{\kappa_i \cos 2\gamma_i}{2} + \frac{2\rho_i^2}{\kappa_i^3} \right) \kappa_i \sigma \\ &= -2\pi^2 \left(\frac{\kappa_i \cos 2\gamma_i}{2} + \frac{2\rho_i^2}{\kappa_i^3} \right) \kappa_i. \end{aligned} \quad (\text{A.26})$$

These results are used in section 3.1 to explicitly evaluate **Local** and **Double**.

B Pohlmeyer reduction

In this appendix, we will give some details of the Pohlmeyer reduction for the string on S^3 .

In terms of the embedding coordinate Y_I ($I = 1, \dots, 4$), S^3 is realized as a hypersurface in R^4 satisfying $\sum_I Y_I^2 = 1$. The basic idea of the Pohlmeyer reduction is to describe the dynamics of the string in terms of a *moving frame* in R^4 consisting of four basis vectors $\{Y_I, \partial Y_I, \bar{\partial} Y_I, N_I\}$, which satisfy the following properties:

$$N^I N_I = 1, \quad N^I Y_I = N^I \partial Y_I = N^I \bar{\partial} Y_I = 0. \quad (\text{B.1})$$

Then, using the equation of motion, $\partial \bar{\partial} Y^I + (\partial Y^J \bar{\partial} Y_J) Y^I = 0$ and the Virasoro constraints, $\partial Y^I \partial Y_I = -T(z)$ and $\bar{\partial} Y^I \bar{\partial} Y_I = -\bar{T}(\bar{z})$, we can express the derivatives of these basis vectors, $\partial N^I, \partial^2 Y^I$, etc. again in terms of the basis vectors:

$$\partial N^I = \frac{2\rho}{T \sin^2 2\gamma} \partial Y^I + \frac{2 \cos 2\gamma \rho}{\sqrt{T\bar{T}} \sin^2 2\gamma} \bar{\partial} Y^I, \quad (\text{B.2})$$

$$\bar{\partial} N^I = \frac{2\rho}{\bar{T} \sin^2 2\gamma} \bar{\partial} Y^I + \frac{2 \cos 2\gamma \tilde{\rho}}{\sqrt{T\bar{T}} \sin^2 2\gamma} \partial Y^I, \quad (\text{B.3})$$

$$\partial^2 Y = T Y^I + \frac{\partial \ln (T\bar{T} \sin^2 2\gamma)}{2} \partial Y^I + \sqrt{\frac{\bar{T}}{T}} \frac{2\partial\gamma}{\sin 2\gamma} \bar{\partial} Y^I + 2\rho N^I, \quad (\text{B.4})$$

$$\bar{\partial}^2 Y = \bar{T} Y^I + \frac{\bar{\partial} \ln (T\bar{T} \sin^2 2\gamma)}{2} \bar{\partial} Y^I + \sqrt{\frac{T}{\bar{T}}} \frac{2\bar{\partial}\gamma}{\sin 2\gamma} \partial Y^I + 2\tilde{\rho} N^I, \quad (\text{B.5})$$

$$\partial \bar{\partial} Y = -\sqrt{T\bar{T}} \cos 2\gamma Y, \quad (\text{B.6})$$

where $\rho, \tilde{\rho}$ and γ are defined by

$$\partial Y^I \bar{\partial} Y_I = \sqrt{T\bar{T}} \cos 2\gamma, \quad \rho \equiv \frac{1}{2} N^I \partial^2 Y_I, \quad \tilde{\rho} \equiv \frac{1}{2} N^I \bar{\partial}^2 Y_I. \quad (\text{B.7})$$

Using the equation of motion, one can also show that γ, ρ and $\tilde{\rho}$ satisfy the generalized sin-Gordon equation, which is given in (2.44).

Let us next derive a flat connection associated with the system of equations (B.2)–(B.6). For this purpose, it is convenient to introduce the following orthonormal basis:

$$q_1 \equiv Y, \quad q_2 \equiv -\frac{i}{\sin 2\gamma} \left[\frac{e^{i\gamma}}{\sqrt{T}} \partial Y + \frac{e^{-i\gamma}}{\sqrt{\bar{T}}} \bar{\partial} Y \right], \quad (\text{B.8})$$

$$q_3 \equiv \frac{i}{\sin 2\gamma} \left[\frac{e^{i\gamma}}{\sqrt{\bar{T}}} \bar{\partial} Y + \frac{e^{-i\gamma}}{\sqrt{T}} \partial Y \right], \quad q_4 \equiv N, \quad (\text{B.9})$$

which satisfy the following normalization conditions:

$$q_1^2 = q_4^2 = 1, \quad q_2 q_3 = -2. \quad (\text{B.10})$$

With these orthonormal vectors, (B.2)–(B.6) can be re-expressed as the following set of equations,

$$\partial q_1 = \frac{\sqrt{T}}{2} [e^{i\gamma} q_2 + e^{-i\gamma} q_3], \quad (\text{B.11})$$

$$\partial q_2 = e^{-i\gamma} \sqrt{T} q_1 + i\partial\gamma q_2 - \frac{2i\rho}{\sqrt{T} \sin 2\gamma} e^{i\gamma} q_4, \quad (\text{B.12})$$

$$\partial q_3 = e^{i\gamma} \sqrt{T} q_1 - i\partial\gamma q_3 + \frac{2i\rho}{\sqrt{T} \sin 2\gamma} e^{-i\gamma} q_4, \quad (\text{B.13})$$

$$\partial q_4 = \frac{i\rho e^{-i\gamma}}{\sqrt{T} \sin 2\gamma} q_2 - \frac{i\rho e^{i\gamma}}{\sqrt{T} \sin 2\gamma} q_3, \quad (\text{B.14})$$

$$\bar{\partial} q_1 = -\frac{\sqrt{T}}{2} [e^{-i\gamma} q_2 + e^{i\gamma} q_3], \quad (\text{B.15})$$

$$\bar{\partial} q_2 = -e^{i\gamma} \sqrt{T} q_1 - i\bar{\partial}\gamma q_2 - \frac{2i\tilde{\rho}}{\sqrt{T} \sin 2\gamma} e^{-i\gamma} q_4, \quad (\text{B.16})$$

$$\bar{\partial} q_3 = -e^{-i\gamma} \sqrt{T} q_1 + i\bar{\partial}\gamma q_3 + \frac{2i\tilde{\rho}}{\sqrt{T} \sin 2\gamma} e^{i\gamma} q_4, \quad (\text{B.17})$$

$$\bar{\partial} q_4 = \frac{i\tilde{\rho} e^{i\gamma}}{\sqrt{T} \sin 2\gamma} q_2 + \frac{i\tilde{\rho} e^{-i\gamma}}{\sqrt{T} \sin 2\gamma} q_3. \quad (\text{B.18})$$

By expressing the basis in a matrix form,

$$W \equiv \frac{1}{2} \begin{pmatrix} q_1 + iq_4 & q_2 \\ q_3 & q_1 - iq_4 \end{pmatrix}, \quad (\text{B.19})$$

we can convert the above equations into the following form:

$$\partial W + B_z^L W + W B_z^R = 0, \quad \bar{\partial} W + B_{\bar{z}}^L W + W B_{\bar{z}}^R = 0, \quad (\text{B.20})$$

where $B_{z,\bar{z}}^{L,R}$ are matrices defined by

$$B_z^L \equiv \begin{pmatrix} -\frac{i\partial\gamma}{2} & \frac{\rho e^{i\gamma}}{\sqrt{T} \sin 2\gamma} - \frac{\sqrt{T}}{2} e^{-i\gamma} \\ \frac{\rho e^{-i\gamma}}{\sqrt{T} \sin 2\gamma} - \frac{\sqrt{T}}{2} e^{i\gamma} & \frac{i\partial\gamma}{2} \end{pmatrix}, \quad (\text{B.21})$$

$$B_z^R \equiv \begin{pmatrix} \frac{i\partial\gamma}{2} & -\frac{\rho e^{i\gamma}}{\sqrt{T} \sin 2\gamma} - \frac{\sqrt{T}}{2} e^{-i\gamma} \\ -\frac{\rho e^{-i\gamma}}{\sqrt{T} \sin 2\gamma} - \frac{\sqrt{T}}{2} e^{i\gamma} & -\frac{i\partial\gamma}{2} \end{pmatrix}, \quad (\text{B.22})$$

$$B_{\bar{z}}^L \equiv \begin{pmatrix} \frac{i\bar{\partial}\gamma}{2} & \frac{\tilde{\rho} e^{-i\gamma}}{\sqrt{T} \sin 2\gamma} + \frac{\sqrt{T}}{2} e^{i\gamma} \\ \frac{\tilde{\rho} e^{i\gamma}}{\sqrt{T} \sin 2\gamma} + \frac{\sqrt{T}}{2} e^{-i\gamma} & -\frac{i\bar{\partial}\gamma}{2} \end{pmatrix}, \quad (\text{B.23})$$

$$B_{\bar{z}}^R \equiv \begin{pmatrix} -\frac{i\bar{\partial}\gamma}{2} & -\frac{\tilde{\rho} e^{-i\gamma}}{\sqrt{T} \sin 2\gamma} + \frac{\sqrt{T}}{2} e^{i\gamma} \\ -\frac{\tilde{\rho} e^{i\gamma}}{\sqrt{T} \sin 2\gamma} + \frac{\sqrt{T}}{2} e^{-i\gamma} & \frac{i\bar{\partial}\gamma}{2} \end{pmatrix}. \quad (\text{B.24})$$

(B.20) is equivalent to the flatness conditions of the connections B^L and B^R ,

$$\partial B_{\bar{z}}^L - \bar{\partial} B_z^L + [B_z^L, B_{\bar{z}}^L] = 0, \quad \partial B_{\bar{z}}^R - \bar{\partial} B_z^R + [B_z^R, B_{\bar{z}}^R] = 0. \quad (\text{B.25})$$

Owing to the classical integrability of the string sigma model, we can “deform” the above connection without spoiling the flatness by introducing a spectral parameter $\zeta = (1 - x)/(1 + x)$ as

$$B_z(\zeta) \equiv \frac{\Phi_z}{\zeta} + A_z, \quad B_{\bar{z}}(\zeta) \equiv \zeta \Phi_{\bar{z}} + A_{\bar{z}}. \quad (\text{B.26})$$

Φ 's and A 's are defined by⁴⁶

$$\Phi_z \equiv \begin{pmatrix} 0 & -\frac{\sqrt{T}}{2} e^{-i\gamma} \\ -\frac{\sqrt{T}}{2} e^{i\gamma} & 0 \end{pmatrix}, \quad \Phi_{\bar{z}} \equiv \begin{pmatrix} 0 & \frac{\sqrt{T}}{2} e^{i\gamma} \\ \frac{\sqrt{T}}{2} e^{-i\gamma} & 0 \end{pmatrix}, \quad (\text{B.27})$$

$$A_z \equiv \begin{pmatrix} -\frac{i\partial\gamma}{2} & \frac{\rho e^{i\gamma}}{\sqrt{T} \sin 2\gamma} \\ \frac{\rho e^{-i\gamma}}{\sqrt{T} \sin 2\gamma} & \frac{i\partial\gamma}{2} \end{pmatrix}, \quad A_{\bar{z}} \equiv \begin{pmatrix} \frac{i\bar{\partial}\gamma}{2} & \frac{\bar{\rho} e^{-i\gamma}}{\sqrt{T} \sin 2\gamma} \\ \frac{\bar{\rho} e^{i\gamma}}{\sqrt{T} \sin 2\gamma} & -\frac{i\bar{\partial}\gamma}{2} \end{pmatrix}. \quad (\text{B.28})$$

The deformed connection (B.26) evaluated at $\zeta = 1$ or $\zeta = -1$ is related to the original connection $B^{L,R}$ in the following way:

$$B^L = B(\zeta = 1), \quad (B^R)^t = \sigma_2 B(\zeta = -1) \sigma_2. \quad (\text{B.29})$$

Furthermore (B.26) is related to the usual left/right connection by an appropriate gauge transformation as will be shown in Appendix C.

C Relation between the Pohlmeyer reduction and the sigma model formulation

In this appendix, we explain how the Pohlmeyer reduction and the sigma model formulation are related.

C.1 Reconstruction formula for the Pohlmeyer reduction

In section 2.2 we presented the simple formulas (2.65) and (2.66) which reconstruct the solution \mathbb{Y} of the equations of motion from the eigenfunctions of the ALP in the sigma model formulation. We now describe a similar formula for the Pohlmeyer reduction and by comparing such reconstruction formulas we can relate the two formulations. Consider the left and the right ALP associated with the Pohlmeyer reduction,

$$(d + B^L) \psi^L = 0, \quad (d + B^R) \psi^R = 0, \quad (\text{C.1})$$

⁴⁶(B.26) is equivalent in form to the SL(2)-Hitchin system. However, the boundary conditions we impose around the punctures are different from the ones used in the usual analysis of the Hitchin system.

and let $\psi_1^{L,R}$ and $\psi_2^{L,R}$ be two linearly independent solutions satisfying the normalization conditions

$$\det(\psi_1^L, \psi_2^L) = 1, \quad \det(\psi_1^R, \psi_2^R) = 1. \quad (\text{C.2})$$

Then, similarly to the sigma model case, the embedding coordinates \mathbb{Y} can be reconstructed by the formula

$$\mathbb{Y} = q_1 = \begin{pmatrix} Z_1 & Z_2 \\ -\bar{Z}_2 & \bar{Z}_1 \end{pmatrix} = (\Psi^L)^t \Psi^R, \quad (\text{C.3})$$

where $\Psi^{L,R}$ are 2×2 matrices with a unit determinant, defined by

$$\Psi^L \equiv (\psi_1^L, \psi_2^L), \quad \Psi^R \equiv (\psi_1^R, \psi_2^R). \quad (\text{C.4})$$

Concerning the property under the global symmetry transformations, we should note the following. Since the Pohlmeyer connections B^L and B^R in the equation (C.1) are invariant, Ψ^L and Ψ^R must also be invariant under such transformations acting from left. However, as for transformations from right, they may transform non-trivially. In fact, as we shall see shortly, they must transform covariantly from right so that the solutions of the ALP for the Pohlmeyer and the sigma model formulations are connected consistently by a gauge transformation.

Furthermore, one can check that the quantities q_2 and q_3 , which consist of the derivatives of \mathbb{Y} , can be reconstructed as

$$q_2 = (\Psi^L)^t \begin{pmatrix} 0 & 2 \\ 0 & 0 \end{pmatrix} \Psi^R, \quad q_3 = (\Psi^L)^t \begin{pmatrix} 0 & 0 \\ 2 & 0 \end{pmatrix} \Psi^R. \quad (\text{C.5})$$

From these formulas the derivatives of \mathbb{Y} can be obtained as

$$\partial\mathbb{Y} = \frac{\sqrt{T}}{2} [e^{i\gamma} q_2 + e^{-i\gamma} q_3], \quad \bar{\partial}\mathbb{Y} = -\frac{\sqrt{\bar{T}}}{2} [e^{-i\gamma} q_2 + e^{i\gamma} q_3]. \quad (\text{C.6})$$

Note that, in distinction to the case of the sigma model, the reconstruction formulas for the Pohlmeyer reduction does not use the eigenvectors of the monodromy matrices, namely $\hat{\psi}_\pm$. The solutions $\psi_i^{L,R}$ used are simply two linearly independent solutions to the ALP, which are not necessarily the eigenvectors of Ω .

C.2 Relation between the connections and the eigenvectors

We now discuss the relation between the connections and the eigenvectors of the the Pohlmeyer reduction and those of the sigma model.

First consider the relation to the right connection of the sigma model. From the formulas for $\partial\mathbb{Y}$ and $\bar{\partial}\mathbb{Y}$ given in (C.6), we can form the right connection j as

$$j_z = \sqrt{T} (\Psi^R)^{-1} \begin{pmatrix} 0 & e^{i\gamma} \\ e^{-i\gamma} & 0 \end{pmatrix} \Psi^R, \quad j_{\bar{z}} = -\sqrt{T} (\Psi^R)^{-1} \begin{pmatrix} 0 & e^{-i\gamma} \\ e^{i\gamma} & 0 \end{pmatrix} \Psi^R. \quad (\text{C.7})$$

Then, comparing (C.7) with (B.26)–(B.28), we find that the following gauge transformation connects the flat connections of the two formulations:

$$\frac{1}{1-x} j_z = \mathcal{G}^{-1} B_z(\zeta) \mathcal{G} + \mathcal{G}^{-1} \partial \mathcal{G}, \quad (\text{C.8})$$

$$\frac{1}{1+x} j_{\bar{z}} = \mathcal{G}^{-1} B_{\bar{z}}(\zeta) \mathcal{G} + \mathcal{G}^{-1} \bar{\partial} \mathcal{G}, \quad (\text{C.9})$$

where

$$\mathcal{G} = i\sigma_2 \Psi^R. \quad (\text{C.10})$$

The eigenvectors ψ_{\pm} of the sigma model formulation and those of the Pohlmeyer reduction, denoted by $\hat{\psi}_{\pm}$, are related as

$$\psi_{\pm} = \mathcal{G}^{-1} \hat{\psi}_{\pm}. \quad (\text{C.11})$$

Note that the factor of i in (C.10) is needed to reproduce the correct normalization condition $\langle \psi_+, \psi_- \rangle = 1$. Under the global $SU(2)_R$ transformation U_R , ψ_{\pm} transform as $\psi_{\pm} \rightarrow U_R^{-1} \psi_{\pm}$. From the above formulas (C.10) and (C.11) we see that this corresponds to the transformation $\Psi^R \rightarrow \Psi^R U_R$, as remarked previously.

In an exactly similar manner, we can construct the left current l 's by

$$l_z = \sqrt{T} (\Psi^L)^t \begin{pmatrix} 0 & e^{i\gamma} \\ e^{-i\gamma} & 0 \end{pmatrix} [(\Psi^L)^t]^{-1}, \quad l_{\bar{z}} = -\sqrt{T} (\Psi^L)^t \begin{pmatrix} 0 & e^{-i\gamma} \\ e^{i\gamma} & 0 \end{pmatrix} [(\Psi^L)^t]^{-1}, \quad (\text{C.12})$$

Comparing (C.12) with (B.26)–(B.28), we find that the following gauge transformation connects the two connections:

$$\frac{x}{1-x} l_z = \tilde{\mathcal{G}}^{-1} B_z(\zeta) \tilde{\mathcal{G}} + \tilde{\mathcal{G}}^{-1} \partial \tilde{\mathcal{G}}, \quad (\text{C.13})$$

$$-\frac{x}{1+x} l_{\bar{z}} = \tilde{\mathcal{G}}^{-1} B_{\bar{z}}(\zeta) \tilde{\mathcal{G}} + \tilde{\mathcal{G}}^{-1} \bar{\partial} \tilde{\mathcal{G}}, \quad (\text{C.14})$$

where

$$\tilde{\mathcal{G}} = [(\Psi^L)^t (-i\sigma_2)]^{-1} = i\Psi^L \sigma_2. \quad (\text{C.15})$$

The eigenvectors are related as

$$\tilde{\psi}_{\pm} = \tilde{\mathcal{G}}^{-1} \hat{\psi}_{\pm}. \quad (\text{C.16})$$

Using (C.11) and (C.16), one can show the equivalence between the reconstruction formulas (2.65), (2.66) and (C.3).

D Details of the WKB expansion

In this appendix, we explain the details of the WKB expansion for the solutions to the ALP. We will describe two approaches, each of which has its own merit. First in subsection D.1, we will perform a direct expansion in the small parameter ζ , which is useful for clarifying the general structure of the expansion. This method, however, turned out to be not quite suitable for deriving the explicit formulas for the expansion of the Wronskians. Therefore, in subsection D.2, we take a slightly different approach based on the Born series expansion. This allows us to derive the expressions for the Wronskians up to the $O(\zeta^1)$ terms with relative ease, with the results given in (3.37), (3.38), (3.40) and (3.41).

D.1 Direct expansion of the solutions to the ALP

In this subsection, we will perform a direct expansion of the ALP in the ‘‘diagonal gauge’’ introduced in section 3.2. In this gauge the ALP equations become

$$\left(\partial + \frac{1}{\zeta}\Phi_z^d + A_z^d\right)\hat{\psi}^d = 0, \quad (\bar{\partial} + \zeta\Phi_{\bar{z}}^d + A_{\bar{z}}^d)\hat{\psi}^d = 0. \quad (\text{D.1})$$

Denoting the components of $\hat{\psi}^d$ as

$$\hat{\psi}^d \equiv \begin{pmatrix} \psi^{(1)} \\ \psi^{(2)} \end{pmatrix}, \quad (\text{D.2})$$

and substituting the expressions for Φ_z^d, A_z^d , etc. given in (3.35), the ALP equations above take the form

$$\partial\psi^{(1)} + \frac{\sqrt{T}}{2\zeta}\psi^{(1)} - \frac{\rho}{\sqrt{T}}\cot 2\gamma\psi^{(1)} + i\left(\frac{\rho}{\sqrt{T}} - \partial\gamma\right)\psi^{(2)} = 0, \quad (\text{D.3})$$

$$\partial\psi^{(2)} - \frac{\sqrt{T}}{2\zeta}\psi^{(2)} + \frac{\rho}{\sqrt{T}}\cot 2\gamma\psi^{(2)} - i\left(\frac{\rho}{\sqrt{T}} + \partial\gamma\right)\psi^{(1)} = 0, \quad (\text{D.4})$$

and

$$\bar{\partial}\psi^{(1)} - \zeta\frac{\sqrt{T}\cos 2\gamma}{2}\psi^{(1)} - \frac{\tilde{\rho}}{\sqrt{T}\sin 2\gamma}\psi^{(1)} + i\frac{\sqrt{T}\sin 2\gamma}{2}\psi^{(2)} = 0, \quad (\text{D.5})$$

$$\bar{\partial}\psi^{(2)} + \zeta\frac{\sqrt{T}\cos 2\gamma}{2}\psi^{(2)} + \frac{\tilde{\rho}}{\sqrt{T}\sin 2\gamma}\psi^{(2)} - i\frac{\sqrt{T}\sin 2\gamma}{2}\psi^{(1)} = 0. \quad (\text{D.6})$$

Let us examine the first two equations (D.3) and (D.4). To perform the WKB expansion, it is useful to introduce a coordinate w defined by

$$dw = \sqrt{T}dz. \quad (\text{D.7})$$

By this coordinate transformation we can absorb the factor \sqrt{T} and bring the equations to the simplified form

$$\partial_w \psi^{(1)} + \frac{1}{2\zeta} \psi^{(1)} - \frac{\rho}{T} \cot 2\gamma \psi^{(1)} + i \left(\frac{\rho}{T} - \partial_w \gamma \right) \psi^{(2)} = 0, \quad (\text{D.8})$$

$$\partial_w \psi^{(2)} - \frac{1}{2\zeta} \psi^{(2)} + \frac{\rho}{T} \cot 2\gamma \psi^{(2)} - i \left(\frac{\rho}{T} + \partial_w \gamma \right) \psi^{(1)} = 0. \quad (\text{D.9})$$

Let us express $\psi^{(2)}$ in terms of $\psi^{(1)}$ using (D.8). We get

$$\psi^{(2)} = -i \left(\frac{\rho}{T} - \partial_w \gamma \right)^{-1} \left[\partial_w \psi^{(1)} + \left(\frac{1}{2\zeta} - \frac{\rho}{T} \cos 2\gamma \right) \psi^{(1)} \right]. \quad (\text{D.10})$$

Substituting (D.10) into (D.9), we obtain a second order differential equation for $\psi^{(1)}$ of the form

$$\partial_w^2 \psi^{(1)} - \partial_w \ln \left(\frac{\rho}{T} - \partial_w \gamma \right) \partial_w \psi^{(1)} - A \psi^{(1)} = 0, \quad (\text{D.11})$$

where A is given by

$$A = \left(\frac{1}{2\zeta} - \frac{\rho}{T} \cot 2\gamma \right)^2 + \partial_w \left(\frac{\rho}{T} \cot 2\gamma \right) + \partial_w \ln \left(\frac{\rho}{T} - \partial_w \gamma \right) \left(\frac{1}{2\zeta} - \frac{\rho}{T} \cot 2\gamma \right) + (\partial_w \gamma)^2 - \left(\frac{\rho}{T} \right)^2. \quad (\text{D.12})$$

We now make the WKB expansion of $\psi^{(1)}$ in powers of ζ in the form,

$$\psi^{(1)} = \sqrt{\frac{\rho}{T} - \partial_w \gamma} \exp \left[\frac{W_{-1}}{\zeta} + W_0 + \zeta W_1 + \dots \right], \quad (\text{D.13})$$

and substitute it into (D.11). Then, at order ζ^{-2} , we get the equation

$$(\partial_w W_{-1})^2 = \frac{1}{4}, \quad (\text{D.14})$$

with the solutions given by $\partial_w W_{-1} = \pm 1/2$. At the next order, we get the equation

$$\partial_w^2 W_{-1} + 2\partial_w W_{-1} \partial_w W_0 = \frac{1}{2} \partial_w \ln \left(\frac{\rho}{T} - \partial_w \gamma \right) - \frac{\rho}{T} \cot 2\gamma. \quad (\text{D.15})$$

From this $\partial_w W_0$ is determined as

$$\partial_w W_0 = \pm \left[\frac{1}{2} \partial_w \ln \left(\frac{\rho}{T} - \partial_w \gamma \right) - \frac{\rho}{T} \cot 2\gamma \right], \quad (\text{D.16})$$

where the plus sign is for $\partial_w W_{-1} = +1/2$ and the minus sign is for $\partial_w W_{-1} = -1/2$. Similarly, we can determine $\partial_w W_1$ as

$$\begin{aligned} \partial_w W_1 = \pm & \left[(\partial_w \gamma)^2 - \left(\frac{\rho}{T} \right)^2 + \partial_w \left(\frac{\rho}{T} \cot 2\gamma \right) - \frac{1}{2} \partial_w^2 \ln \left(\frac{\rho}{T} - \partial_w \gamma \right) \right] \\ & - \frac{1}{2} \partial_w^2 \ln \left(\frac{\rho}{T} - \partial_w \gamma \right), \end{aligned} \quad (\text{D.17})$$

where the choice of the sign should be the same as in (D.16). Continuing in this fashion using (D.5) and (D.6), we can determine $\bar{\partial}W_{-1}$, $\bar{\partial}W_0$ and $\bar{\partial}W_1$ to be

$$\begin{aligned}\bar{\partial}W_{-1} &= 0, & \bar{\partial}W_0 &= \pm \left[\frac{1}{2} \bar{\partial} \ln \left(\frac{\rho}{T} - \partial_w \gamma \right) - \frac{\tilde{\rho}}{\sqrt{T} \sin 2\gamma} \right], \\ \bar{\partial}W_1 &= \pm \left[\frac{\eta}{2} - \frac{1}{2} \bar{\partial} \partial_w \ln \left(\frac{\rho}{T} - \partial_w \gamma \right) \right] - \frac{1}{2} \bar{\partial} \partial_w \ln \left(\frac{\rho}{T} - \partial_w \gamma \right).\end{aligned}\tag{D.18}$$

The results obtained above can be reorganized into a compact form. In fact we can write the expansion (D.13) as

$$\psi^{(1)} = \exp [W_{\text{odd}} + W_{\text{even}}],\tag{D.19}$$

where W_{odd} (resp. W_{even}) denotes terms which (do not) change sign under the sign-flip of $\partial_w W_{-1}$. Then, by substituting (D.19) into (D.11) and extracting the terms odd under the above flip of sign, we can obtain the following simple equation expressing W_{even} in terms of W_{odd} :

$$W_{\text{even}} = -\frac{1}{2} \ln \partial_w W_{\text{odd}}.\tag{D.20}$$

As is clear from the analysis above, the WKB expansion of W_{odd} is given in terms of the integrals of certain functions of the worldsheet variables, such as γ , ρ and $\tilde{\rho}$. On the other hand, the even part W_{even} , which depends only on the derivatives of W_{odd} , is expressed purely in terms of the local values of the worldsheet variables. With such classifications, we can recast the WKB expansion of the two linearly independent solutions of the ALP into the following form:

$$\hat{\psi}^d = \begin{pmatrix} f_{\pm}^{(1)} \\ f_{\pm}^{(2)} \end{pmatrix} \exp \left(\pm \int_{z_0}^z W_{\text{WKB}}(z, \bar{z}; \zeta) \right).\tag{D.21}$$

Here we renamed W_{odd} to W_{WKB} and the functions $f_{\pm}^{(1)}$ and $f_{\pm}^{(2)}$ are defined in terms of W_{WKB}^z by

$$f_{\pm}^{(1)} \equiv k_{\text{WKB}} = \sqrt{\frac{\rho - \sqrt{T} \partial \gamma}{T W_{\text{WKB}}^z}},\tag{D.22}$$

$$f_{\pm}^{(2)} \equiv \frac{-i}{\sqrt{W_{\text{WKB}}^z}} \left[\pm W_{\text{WKB}}^z + \left(\frac{\sqrt{T}}{2\zeta} - \frac{\rho \cos 2\gamma}{\sqrt{T}} + \frac{\partial \ln k_{\text{WKB}}}{2} \right) \right].\tag{D.23}$$

D.2 Born series expansion of the Wronskians

In this subsection, we will derive the explicit form of the expansion for the Wronskians up to $O(\zeta^1)$ using the Born series method, which turned out to be more convenient compared

to the direct expansion described above. In particular, with this method it is much easier to take into account the normalization conditions of the eigenvectors i_{\pm} given in (2.96). Although the method has been described in Appendix B of [22], we will spell out the details of the derivation since several additional considerations are necessary in our case.

To illustrate the basic idea, let us take the Wronskian $\langle 2_+, 1_+ \rangle$ as an example and discuss its expansion. To compute $\langle 2_+, 1_+ \rangle$, we need to parallel-transport the eigenvector 1_+ , which is defined originally in the neighborhood of z_1 , to the neighborhood of z_2 using the flat connection and compute the Wronskian with 2_+ . In the diagonal gauge, this procedure can be implemented in the following way:

$$\langle \hat{2}_+^d, \hat{1}_+^d \rangle = \langle \hat{2}_+^d(z_2^*), \text{P exp} \left[- \int_0^1 dt \left(\frac{1}{\zeta} H_0(t) + V(t) \right) \right] \hat{1}_+^d(z_1^*) \rangle. \quad (\text{D.24})$$

In this expression t parametrizes the curve joining z_1^* (at $t = 0$) and z_2^* (at $t = 1$) and H_0 and V are defined in terms of the connection in the diagonal gauge, given in (3.35), as

$$H_0(t) \equiv \tilde{\Phi}_z \dot{z}, \quad V(t) \equiv \tilde{A}_z \dot{z} + \tilde{A}_{\bar{z}} \dot{\bar{z}} + \zeta \tilde{\Phi}_{\bar{z}} \dot{\bar{z}}, \quad (\text{D.25})$$

with \dot{z} and $\dot{\bar{z}}$ standing for dz/dt and $d\bar{z}/dt$ respectively. The equation (D.24) is similar in form to the transition amplitude in quantum mechanics, where $H_0(t)/\zeta$ is the unperturbed Hamiltonian and $V(t)$ is the time-dependent perturbation. Therefore we can derive the expansion of (D.24) by applying the familiar Born series expansion.

As the first step toward this goal, let us determine the expansion of the ‘‘initial states’’, $\hat{1}_+^d(z_1^*)$ and $\hat{2}_+^d(z_2^*)$. As explained in section 2.3, the eigenvectors can be well-approximated near the puncture by those of the corresponding two-point functions. Thus, the expansion of the initial states can be obtained from the explicit form of $\hat{i}_{\pm}^{2\text{pt}}$ given in (2.98) and (2.99) as

$$\hat{1}_+^d(z_1^*) \sim \hat{1}_+^{2\text{pt},d} = \begin{pmatrix} O(\zeta^1) \\ 1 + O(\zeta^2) \end{pmatrix}, \quad \hat{2}_+^d(z_2^*) \sim \hat{2}_+^{2\text{pt},d} = \begin{pmatrix} 1 + O(\zeta^2) \\ O(\zeta^1) \end{pmatrix}. \quad (\text{D.26})$$

Let us now study the leading terms (*i.e.* the $O(V^0)$ terms) in the Born series expansion of (D.24). They can be expressed as

$$1_+^{(2)}(z_1^*) 2_+^{(1)}(z_2^*) \langle \mathbf{e}_2 | e^{-\int_0^1 H_0 dt / \zeta} | \mathbf{e}_2 \rangle - 1_+^{(1)}(z_1^*) 2_+^{(2)}(z_2^*) \langle \mathbf{e}_1 | e^{-\int_0^1 H_0 dt / \zeta} | \mathbf{e}_1 \rangle, \quad (\text{D.27})$$

where $|\mathbf{e}_1\rangle$ and $|\mathbf{e}_2\rangle$ stand for the unit vectors

$$|\mathbf{e}_1\rangle = \begin{pmatrix} 1 \\ 0 \end{pmatrix}, \quad |\mathbf{e}_2\rangle = \begin{pmatrix} 0 \\ 1 \end{pmatrix}, \quad (\text{D.28})$$

and $i_{\pm}^{(1)}$ and $i_{\pm}^{(2)}$ are the upper and the lower component of \hat{i}_{\pm}^d respectively, which can be expressed as

$$\hat{i}_{\pm}^d = i_{\pm}^{(1)} |\mathbf{e}_1\rangle + i_{\pm}^{(2)} |\mathbf{e}_2\rangle. \quad (\text{D.29})$$

Using (D.26), we can evaluate the expression (D.27) explicitly as

$$(1 + O(\zeta^2)) \exp\left(\int_{\ell_{12}} \frac{1}{\zeta} \varpi\right) - O(\zeta^2) \exp\left(-\int_{\ell_{12}} \frac{1}{\zeta} \varpi\right), \quad (\text{D.30})$$

where ℓ_{12} is the contour that connects z_1^* and z_2^* , defined in section 3.1. Note that the second term in (D.30), which has an overall $O(\zeta^2)$ factor can be safely neglected only when $\text{Re}\left(\int_{\ell_{12}} \varpi/\zeta\right)$ is positive so that the exponential $\exp\left(-\int_{\ell_{12}} \varpi/\zeta\right)$ becomes vanishingly small. The positivity of $\text{Re}\left(\int_{\ell_{12}} \varpi/\zeta\right)$ is guaranteed when the following two conditions are satisfied:

1. The eigenvectors, 1_+ and 2_+ , are small solutions.
2. z_1 and z_2 are connected by a *WKB curve* $z(s)$ defined to be satisfying the condition

$$\text{Im}\left(\sqrt{T} \frac{dz}{ds}\right) = 0, \quad (\text{D.31})$$

where s parameterizes the curves.

This can be deduced in the following way: First, from the definition (D.31), one can show that the real part of the integral $\int \varpi/\zeta$ monotonically increases or decreases along the WKB curve. Second, when 1_+ and 2_+ are both small solutions, $\text{Re}\left(\int \varpi/\zeta\right)$ increases as we *move away from* z_1 in the vicinity of z_1 while it increases as we *approach* z_2 in the vicinity of z_2 . From these two observations, one can conclude that $\text{Re}\left(\int_{\ell_{12}} \varpi/\zeta\right)$ is positive when both of the eigenvectors are small and the punctures are connected by a WKB curve. Actually, in practice the second condition above is inessential. This is because all the punctures are always connected with each other by WKB curves, except at discrete values of $\text{Arg}(\zeta)$, due to the triangular inequalities, $\Delta_i < \Delta_j + \Delta_k$ (or equivalently $\kappa_i < \kappa_j + \kappa_k$), which hold in all the cases we study in this paper.

Let us now move on to the study of the $O(V^1)$ contributions. When 1_+ and 2_+ are small solutions, the $O(V^1)$ terms in the Born series expansion are given by

$$\begin{aligned} & -1_+^{(2)}(z_1^*) 2_+^{(1)}(z_2^*) \int_0^1 dt_1 \langle \mathbf{e}_2 | e^{-\int_{t_1}^1 H_0 dt/\zeta} V(t_1) e^{-\int_0^{t_1} H_0 dt/\zeta} | \mathbf{e}_2 \rangle \\ & -1_+^{(1)}(z_1^*) 2_+^{(2)}(z_2^*) \int_0^1 dt_1 \langle \mathbf{e}_2 | e^{-\int_{t_1}^1 H_0 dt/\zeta} V(t_1) e^{-\int_0^{t_1} H_0 dt/\zeta} | \mathbf{e}_1 \rangle \\ & +1_+^{(2)}(z_1^*) 2_+^{(2)}(z_2^*) \int_0^1 dt_1 \langle \mathbf{e}_1 | e^{-\int_{t_1}^1 H_0 dt/\zeta} V(t_1) e^{-\int_0^{t_1} H_0 dt/\zeta} | \mathbf{e}_2 \rangle. \end{aligned} \quad (\text{D.32})$$

Note that we have omitted the terms of the form, $\langle \mathbf{e}_1 | * | \mathbf{e}_1 \rangle$, since they are proportional to the factor $\exp\left(\int_{\ell_{12}} \varpi/\zeta\right)$, which, as discussed above, is exponentially small when 1_+

and 2_+ are small solutions. Since $|\mathbf{e}_1\rangle$ and $|\mathbf{e}_2\rangle$ are the eigenvectors of H_0 , we can evaluate (D.32) as

$$\begin{aligned}
& -1_+^{(2)}(z_1^*)2_+^{(1)}(z_2^*)e^{\int_{\ell_{12}} \varpi/(2\zeta)} \int_0^1 dt_1 \langle \mathbf{e}_2 | V(t_1) | \mathbf{e}_2 \rangle \\
& -1_+^{(1)}(z_1^*)2_+^{(1)}(z_2^*)e^{\int_{\ell_{12}} \varpi/(2\zeta)} \int_0^1 dt_1 \langle \mathbf{e}_2 | V(t_1) | \mathbf{e}_1 \rangle e^{-\int_0^{t_1} \varpi/\zeta} \\
& +1_+^{(2)}(z_1^*)2_+^{(2)}(z_2^*)e^{\int_{\ell_{12}} \varpi/(2\zeta)} \int_0^1 dt_1 \langle \mathbf{e}_1 | V(t_1) | \mathbf{e}_2 \rangle e^{-\int_{t_1}^1 \varpi/\zeta}.
\end{aligned} \tag{D.33}$$

In the limit $\zeta \rightarrow 0$, the integral over t_1 in the second term will be exponentially suppressed by the factor $\exp\left(-2\int_0^{t_1} \varpi/\zeta\right)$, except when the interval is short, *i.e.* $0 < t_1 < O(\zeta^1)$. Thus, to $O(\zeta^1)$, one can take ϖ in $\int_0^{t_1} \varpi/\zeta$ to be constant and replace $V(t_1)$ with $V(0)$. We can thus approximate the second term in (D.33) as

$$-\zeta 1_+^{(1)}(z_1^*)2_+^{(1)}(z_2^*)e^{\int_{\ell_{12}} \varpi/(2\zeta)} \langle \mathbf{e}_2 | V(0) | \mathbf{e}_1 \rangle \left(\sqrt{T(z_1^*)} \dot{z}(t=0) \right)^{-1}. \tag{D.34}$$

Since the factor $1_+^{(1)}(z_1^*)$ is of $O(\zeta^1)$, (D.34) as a whole is of $O(\zeta^2)$ and thus can be neglected to the order of our approximation. Similarly, one can also show that the third term of (D.33) is of $O(\zeta^2)$. Thus, up to $O(\zeta^1)$, the contribution comes only from the first term proportional to

$$-e^{\int_{\ell_{12}} \varpi/(2\zeta)} \int_0^1 dt_1 \langle \mathbf{e}_2 | V(t_1) | \mathbf{e}_2 \rangle. \tag{D.35}$$

Lastly let us examine the $O(V^2)$ terms. The only term which contributes at $O(\zeta^1)$ is

$$1_+^{(2)}(z_1^*)2_+^{(1)}(z_2^*) \int_0^1 dt_2 \int_0^{t_2} dt_1 \langle \mathbf{e}_2 | e^{-\int_{t_2}^1 H_0 dt/\zeta} V(t_2) e^{-\int_{t_1}^{t_2} H_0 dt/\zeta} V(t_1) e^{-\int_0^{t_1} H_0 dt/\zeta} | \mathbf{e}_2 \rangle. \tag{D.36}$$

Inserting the identity $1 = |\mathbf{e}_1\rangle\langle \mathbf{e}_1| + |\mathbf{e}_2\rangle\langle \mathbf{e}_2|$, this quantity can be computed as

$$\begin{aligned}
& 1_+^{(2)}(z_1^*)2_+^{(1)}(z_2^*)e^{\int_{\ell_{12}} \varpi/(2\zeta)} \left(\frac{1}{2} \left[\int_0^1 dt_1 \langle \mathbf{e}_2 | V(t_1) | \mathbf{e}_2 \rangle \right]^2 \right. \\
& \left. + \int_0^1 dt_1 \int_0^{t_1} dt_2 e^{-\int_{t_2}^{t_1} \varpi/\zeta} \langle \mathbf{e}_2 | V(t_1) | \mathbf{e}_1 \rangle \langle \mathbf{e}_1 | V(t_2) | \mathbf{e}_2 \rangle \right).
\end{aligned} \tag{D.37}$$

As in the discussion of the $O(V^1)$ terms, we can take ϖ in $\int_{t_2}^{t_1} \varpi/\zeta$ to be constant and replace $V(t_2)$ with $V(t_1)$ in the second term of (D.37), thanks to the suppression factor $\exp\left(-\int_{t_1}^{t_2} \varpi/\zeta\right)$. Then (D.37) can be evaluated as

$$e^{\int_{\ell_{12}} \varpi/(2\zeta)} \left(\frac{1}{2} \left[\int_0^1 dt_1 \langle \mathbf{e}_2 | V(t_1) | \mathbf{e}_2 \rangle \right]^2 + \zeta \int_0^1 dt_1 \frac{\langle \mathbf{e}_2 | V(t_1) | \mathbf{e}_1 \rangle \langle \mathbf{e}_1 | V(t_1) | \mathbf{e}_2 \rangle}{\dot{z}\sqrt{T}} \right). \tag{D.38}$$

Putting together the expressions (D.30), (D.35) and (D.38), we find that the result can be grouped into an exponential in the following way:

$$\langle 2_+, 1_+ \rangle \sim \exp \left(\frac{1}{2\zeta} \int_{\ell_{12}} \varpi - \int_0^1 dt \langle \mathbf{e}_2 | V(t) | \mathbf{e}_2 \rangle + \zeta \int_0^1 dt_1 \frac{\langle \mathbf{e}_2 | V(t) | \mathbf{e}_1 \rangle \langle \mathbf{e}_1 | V(t) | \mathbf{e}_2 \rangle}{\dot{z} \sqrt{T}} \right). \quad (\text{D.39})$$

Thus we have obtained the expansion of $\langle 2_+, 1_+ \rangle$ to be given by

$$\langle 2_+, 1_+ \rangle = \exp \left(-\frac{1}{2\zeta} \int_{\ell_{21}} \varpi - \int_{\ell_{21}} \alpha - \frac{\zeta}{2} \int_{\ell_{21}} \eta + O(\zeta^2) \right), \quad (\text{D.40})$$

where the one-form α is given by

$$\alpha = -\frac{\rho}{\sqrt{T}} \cot 2\gamma dz - \frac{\tilde{\rho}}{\sqrt{\bar{T}} \sin 2\gamma} d\bar{z}. \quad (\text{D.41})$$

The expansion of other Wronskians can be worked out in a similar manner leading to (3.37) and (3.38). Furthermore, we can apply the same argument to the expansion around $\zeta = \infty$ and obtain (3.40) and (3.41), where the one-form $\tilde{\alpha}$ appearing in the $O(\zeta^0)$ term is given by

$$\tilde{\alpha} = -\frac{\rho}{\sqrt{T} \sin 2\gamma} dz - \frac{\tilde{\rho}}{\sqrt{\bar{T}}} \cot 2\gamma d\bar{z}. \quad (\text{D.42})$$

References

- [1] J.M. Maldacena, “The large-N limit of superconformal field theories and supergravity”, *Adv. Theor. Math. Phys.* **2** (1998) 231, [arXiv:hep-th/9711200](#).
- [2] S.S. Gubser, I.R. Klebanov and A.M. Polyakov, “Gauge theory correlators from non-critical string theory”, *Phys. Lett.* **B 428** (1998) 105, [arXiv:hep-th/9802109](#).
- [3] E. Witten, “Anti-de Sitter space and holography”, *Adv. Theor. Math. Phys.* **2** (1998) 253, [arXiv:hep-th/9802150](#).
- [4] N. Gromov, A. Sever and P. Vieira, “Tailoring Three-Point Functions and Integrability III. Classical Tunneling,” *JHEP* **1207**, 044 (2012) [arXiv:1111.2349](#).
- [5] I. Kostov, “Classical Limit of the Three-Point Function from Integrability,” *Phys. Rev. Lett.* **108**, 261604 (2012) [arXiv:1203.6180](#).
- [6] I. Kostov, “Three-point function of semiclassical states at weak coupling,” *J. Phys.* **A 45**, 494018 (2012) [arXiv:1205.4412](#).

- [7] D. Serban, “A note on the eigenvectors of long-range spin chains and their scalar products,” JHEP **1301**, 012 (2013) [arXiv:1203.5842](#).
- [8] R. A. Janik and A. Wereszczynski, “Correlation functions of three heavy operators - the AdS contribution,” JHEP **1112**, 095 (2011), [arXiv:1109.6262](#).
- [9] Y. Kazama and S. Komatsu, “On holographic three point functions for GKP strings from integrability,” JHEP **1201**, 110 (2012) [arXiv:1110.3949](#).
- [10] S. S. Gubser, I. R. Klebanov and A. M. Polyakov, “A Semiclassical limit of the gauge / string correspondence,” Nucl. Phys. B **636**, 99 (2002) [hep-th/0204051](#).
- [11] Y. Kazama and S. Komatsu, “Wave functions and correlation functions for GKP strings from integrability”, JHEP **1209**, 022 (2012) [arXiv:1205.6060](#)
- [12] V. A. Kazakov, A. Marshakov, J. A. Minahan and K. Zarembo, “Classical/quantum integrability in AdS/CFT,” JHEP **0405**, 024 (2004), [hep-th/0402207](#).
- [13] N. Dorey and B. Vicedo, “On the dynamics of finite-gap solutions in classical string theory,” JHEP **0607**, 014 (2006) [hep-th/0601194](#).
- [14] N. Dorey and B. Vicedo, “A Symplectic Structure for String Theory on Integrable Backgrounds,” JHEP **0703**, 045 (2007) [hep-th/0606287](#).
- [15] B. Vicedo, “The method of finite-gap integration in classical and semi-classical string theory,” J. Phys. A **44**, 124002 (2011).
- [16] E. K. Sklyanin, “Separation of variables - new trends,” Prog. Theor. Phys. Suppl. **118**, 35 (1995), [solv-int/9504001](#).
- [17] I. Bena, J. Polchinski and R. Roiban, “Hidden symmetries of the $AdS_5 \times S^5$ superstring,” Phys. Rev. D **69**, 046002 (2004), [hep-th/0305116](#).
- [18] K. Pohlmeyer, “Integrable Hamiltonian Systems and Interactions Through Quadratic Constraints,” Commun. Math. Phys. **46**, 207 (1976).
- [19] H. J. De Vega and N. G. Sanchez, “Exact integrability of strings in D-Dimensional De Sitter space-time,” Phys. Rev. D **47**, 3394 (1993).
- [20] B. Vicedo, “Semiclassical Quantisation of Finite-Gap Strings,” JHEP **0806**, 086 (2008) [arXiv:0803.1605](#).
- [21] H. M. Farkas and I. Kra, “Riemann surfaces,” Springer New York, 1992.
- [22] J. Caetano and J. Toledo, “ χ -Systems for Correlation Functions”, [arXiv:1208.4548](#)

- [23] D. Gaiotto, G. W. Moore and A. Neitzke, “Wall-crossing, Hitchin Systems, and the WKB Approximation”, [arXiv:0907.3987](#).
- [24] L. F. Alday and J. Maldacena, “Null polygonal Wilson loops and minimal surfaces in Anti-de-Sitter space,” JHEP **0911**, 082 (2009) [arXiv:0904.0663](#).
- [25] L. F. Alday, D. Gaiotto and J. Maldacena, “Thermodynamic Bubble Ansatz,” JHEP **1109**, 032 (2011) [arXiv:0911.4708](#).
- [26] L.F. Alday, J. Maldacena, A. Sever and P. Vieira, “Y-system for Scattering Amplitudes”, J.Phys. **A 43** (2010) 485401, [arXiv:1002.2459](#).
- [27] J. Escobedo, N. Gromov, A. Sever and P. Vieira, “Tailoring Three-Point Functions and Integrability,” JHEP **1109**, 028 (2011), [arXiv:1012.2475](#).
- [28] V E Korepin, N M Bogoliubov and A G Izergin, “Quantum inverse scattering method and correlation functions,” Cambridge University Press (1993)
- [29] D. Honda and S. Komatsu, “Classical Liouville Three-point Functions from Riemann-Hilbert Analysis,” [arXiv:1311.2888](#).
- [30] J. Escobedo, N. Gromov, A. Sever and P. Vieira, “Tailoring Three-Point Functions and Integrability II. Weak/strong coupling match,” JHEP **1109**, 029 (2011) [arXiv:1104.5501](#).
- [31] N. Gromov and P. Vieira, “The $AdS_5 \times S^5$ superstring quantum spectrum from the algebraic curve,” Nucl. Phys. B **789**, 175 (2008) [hep-th/0703191](#).
- [32] M. Kruczenski, “Spin chains and string theory,” Phys. Rev. Lett. **93**, 161602 (2004) [hep-th/0311203](#).
- [33] N. Beisert, V. Dippel and M. Staudacher, “A Novel long range spin chain and planar N=4 super Yang-Mills,” JHEP **0407**, 075 (2004) [hep-th/0405001](#).
- [34] N. Beisert, “The $SU(2|2)$ dynamic S-matrix,” Adv. Theor. Math. Phys. **12**, 945 (2008) [hep-th/0511082](#).
- [35] V. V. Bazhanov, S. L. Lukyanov and A. B. Zamolodchikov, “Higher level eigenvalues of Q operators and Schroedinger equation,” Adv. Theor. Math. Phys. **7**, 711 (2004) [hep-th/0307108](#).
- [36] Y. Kazama, S. Komatsu and T. Nishimura, “A new integral representation for the scalar products of Bethe states for the XXX spin chain,” JHEP **1309**, 013 (2013) [arXiv:1304.5011](#).

- [37] K. Zarembo, “Holographic three-point functions of semiclassical states”, JHEP **09** (2010) 030, [arXiv:1008.1059](#).
- [38] M.S. Costa, R. Monteiro, J.E. Santos and D. Zoakos, “On three-point correlation functions in the gauge/gravity duality”, JHEP **11** (2010) 141, [arXiv:1008.1070](#).
- [39] R. Roiban and A.A. Tseytlin, “On semiclassical computation of 3-point functions of closed string vertex operators in $AdS_5 \times S^5$ ”, Phys.Rev. **D 82** (2010) 106011, [arXiv:1008.4921](#).